



HAL
open science

Optimal design of flexible, operable and sustainable processes under uncertainty : biorefinery applications

Alessandro Di Pretoro

► **To cite this version:**

Alessandro Di Pretoro. Optimal design of flexible, operable and sustainable processes under uncertainty : biorefinery applications. Chemical and Process Engineering. Institut National Polytechnique de Toulouse - INPT; Politecnico di Milano, 2020. English. NNT : 2020INPT0073 . tel-04237404

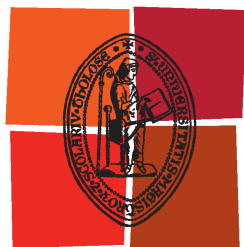
HAL Id: tel-04237404

<https://theses.hal.science/tel-04237404>

Submitted on 11 Oct 2023

HAL is a multi-disciplinary open access archive for the deposit and dissemination of scientific research documents, whether they are published or not. The documents may come from teaching and research institutions in France or abroad, or from public or private research centers.

L'archive ouverte pluridisciplinaire **HAL**, est destinée au dépôt et à la diffusion de documents scientifiques de niveau recherche, publiés ou non, émanant des établissements d'enseignement et de recherche français ou étrangers, des laboratoires publics ou privés.



Université
de Toulouse

THÈSE

En vue de l'obtention du

DOCTORAT DE L'UNIVERSITÉ DE TOULOUSE

Délivré par :

Institut National Polytechnique de Toulouse (Toulouse INP)

Discipline ou spécialité :

Génie des Procédés et de l'Environnement

Présentée et soutenue par :

M. ALESSANDRO DI PRETORO

le mercredi 30 septembre 2020

Titre :

Optimal design of flexible, operable and sustainable processes under uncertainty: Biorefinery applications

Ecole doctorale :

Mécanique, Energétique, Génie civil, Procédés (MEGeP)

Unité de recherche :

Laboratoire de Génie Chimique (LGC)

Directeur(s) de Thèse :

M. LUDOVIC MONTASTRUC

M. FLAVIO MANENTI

Rapporteurs :

MME ANA PAULA BARBOSA POVOA, INSTITUTO SUPERIOR TECNICO LISBONNE

M. SIGURD SKOGESTAD, NORWEGIAN UNI OF SCE AND TECHN TRONDHEIM

Membre(s) du jury :

M. XAVIER JOULIA, TOULOUSE INP, Président

M. ANTONIO ESPUNA, UNIVERSITAT POLITECNICA DE CATALUNYA, Membre

M. FLAVIO MANENTI, POLITECNICO DE MILAN, Membre

M. LUDOVIC MONTASTRUC, TOULOUSE INP, Membre



**POLITECNICO
MILANO 1863**

Philosophiæ Doctor in Industrial Chemistry and Chemical Engineering

Department of Chemistry, Materials and Chemical Engineering

“Giulio Natta”

**OPTIMAL DESIGN OF FLEXIBLE, OPERABLE AND
SUSTAINABLE PROCESSES UNDER UNCERTAINTY:
BIOREFINERY APPLICATIONS**

Doctoral dissertation of: Alessandro DI PRETORO
ID 922269

Supervisors :

Prof. Flavio MANENTI (Politecnico di Milano)

Prof. Ludovic MONTASTRUC (INP de Toulouse)

PhD School Coordinator :

Prof. Alessio FRASSOLDATI (Politecnico di Milano)

Cycle XXXIII

*"The wind does not break a tree
that can bend."*

SUKUMA PROVERB

Résumé

La démarche conventionnelle pour la conception des procédés est une procédure bien établie dans le domaine du génie des procédés qui utilise des méthodes d'optimisation multi-objectifs visant à exploiter au mieux les différents degrés des libertés. Cependant, l'optimalité de la solution obtenue avec cette procédure est uniquement valable pour les conditions opératoires nominales et ne prend pas en compte les fluctuations externes.

L'objectif de cette thèse est la prise en compte de la flexibilité à chaque étape de la démarche de conception des procédés. Pour illustrer notre propos un cas d'étude concernant une opération de séparation ABE/W (Acétone-Butanol-Éthanol/Eau) dans une bioraffinerie a été choisie.

Après une recherche bibliographique détaillée sur la flexibilité et sur les indicateurs précédemment proposés par d'autres auteurs, les indices de flexibilité déterministes et stochastiques ont été comparés sur la base d'un cas de distillation simple selon une procédure rigoureuse. L'analyse de flexibilité a été couplée à l'évaluation économique ce qui se traduit par un diagramme «coûts d'investissement additionnels vs. flexibilité» permettant à l'ingénieur de prendre une décision.

L'analyse de flexibilité a ensuite été appliquée aux opérations unitaires multi-étagée. La procédure conventionnelle pour la définition du nombre optimal d'étages d'équilibre pour n'importe quelle opération multi-étagée (e.g. évaporateurs multiple effets, absorbeurs, colonnes à distiller, etc.) repose sur l'optimisation du coût annuel total (OPEX et CAPEX). Cependant, cette optimisation est réalisée par rapport aux conditions opératoires nominales; cela signifie que, pour compenser une fluctuation, le système de contrôle doit gérer les utilités externes (e.g. débit vapeur, taux de reflux etc.) avec un impact considérable sur les coûts énergétiques. Même si les CAPEX sont fixés pour un design donné, la valeur des OPEX peut en fait changer dans un certain intervalle en fonction de la probabilité de déviation des paramètres incertains. Une nouvelle procédure basée sur la moyenne des OPEX dans le domaine d'incertitude a donc été définie pour trouver le nombre optimal d'étages d'équilibre (CAPEX) sous incertitude.

Un critère additionnel associé à l'impact environnemental du procédé a alors été introduit. Une unité flexible implique en fait une demande énergétique inférieure pour le système, c'est-à-dire un impact environnemental beaucoup moins important. L'empreinte carbone a été utilisée pour quantifier l'impact environnemental et ajoutée aux autres critères. De cette façon, l'évaluation du meilleur compromis entre le surdimensionnement des équipements (i.e. investissement) et la demande d'utilités externes (i.e. coûts opératoires) nécessaires pour compenser les perturbations a été possible.

Notre analyse s'est ensuite focalisée sur les applications à la bioraffinerie. Le cas d'étude sélectionné concerne un procédé de séparation de bioraffinerie, à savoir un

train de distillation en aval d'un procédé de fermentation ABE (Acétone-Butanol-Éthanol) après une extraction préliminaire de l'eau. Ce mélange a été choisi pour l'intérêt actuel porté sur les biocombustibles et pour la possibilité d'analyser comment les non-idéalités influencent le procédé dans la perspective de la flexibilité. De plus, les fluctuations dans la nature de la charge d'alimentation liées à la saisonnalité des matières premières sont bien connues et la rentabilité des bioprocessus est strictement associée aux performances de la section de purification. C'est pourquoi cet exemple semble particulièrement adéquat pour une analyse de flexibilité.

Contrairement aux cas d'étude précédents qui purifiaient des mélanges simples d'hydrocarbures, quand les courants à distiller contiennent de l'eau et des alcools, les frontières de faisabilité du procédé doivent être analysées en détail du fait de la présence d'azéotropes. Les courbes de résidu ont été exploitées par rapport aux différentes spécifications selon une procédure bien définie afin de générer dans le domaine des compositions les limites de faisabilité physique sous des conditions opératoires incertaines. La démarche pour une colonne simple a été aussi généralisée à des trains de colonnes ainsi qu'à des configurations intensifiées équivalentes comme la colonne à paroi séparatrice (Dividing Wall Column, DWC).

Le domaine de faisabilité thermodynamique ayant été déterminée, pour que le procédé soit rentable, une récupération efficace du butanol et de l'acétone est nécessaire. À cette fin, différentes configurations de train de distillation ont été conçues et comparées en prenant en compte simultanément les objectifs de flexibilité et d'évaluation économique. L'analyse a été réalisée à la fois avec des indices de flexibilité déterministes et stochastiques et la meilleure solution de design a été identifiée.

Pendant les trains de distillation sans intégration énergétique sont considérés à ce jour comme une solution obsolète pour la purification des mélanges multiconstituant. Il convient ainsi de les remplacer par des procédés intensifiés qui permettent de réduire à la fois les coûts d'investissement et les coûts opératoires. À cette fin, une procédure de design d'une colonne à paroi séparatrice (DWC) pour les mêmes spécifications est proposée sur la base d'une méthode à chemin réalisable. Une analyse de flexibilité a ensuite été réalisée sur la DWC pour mettre en évidence les avantages et les inconvénients de l'utilisation d'un procédé intensifié. Le design optimal de la DWC a été effectuée en prenant en compte les besoins associés à la flexibilité et les surcoûts correspondants par rapport au train de colonnes conventionnel.

Enfin, pour avoir une vision d'ensemble des indices de flexibilité, la dynamique des procédés a été analysée. Si la dynamique est prise en compte, les résultats de l'analyse de flexibilité, et donc le surdimensionnement nécessaire, dépendent de la configuration choisie pour le contrôle. Un nouveau index de «switchabilité» a été défini sur la base de la corrélation entre les performances du système en régimes permanent et dynamique du point de vue de la flexibilité.

La définition rigoureuse de cet index a été associée à une stratégie de contrôle prédictif (MPC) pour un système simple mais elle peut aussi être utilisée pour différentes stratégies de contrôle afin de les comparer. Pour décrire ce dernier cas le même exemple de colonne de distillation utilisé pour la comparaison des indices statiques a été simulé avec DynSim[®] en utilisant des régulateurs PID pour mettre en évidence l'influence des transitoires.

Le résultat final de ce travail de thèse est donc la définition d'une approche globale pour une conception multiobjectif des opérations unitaires sous des conditions opératoires incertaines et l'analyse de problématiques associées. Les critères retenus pour le design sont la rentabilité, la flexibilité, la contrôlabilité et l'impact environnemental.

Abstract

The conventional process design procedure is a well-established standard in process engineering and implies the fulfillment of the residual degrees of freedom by means of optimizations based on several possible criteria. However, the optimality of the solution obtained by this procedure is strictly related to nominal operating conditions and doesn't account for external perturbations.

The purpose of this PhD thesis work is then to include flexibility in every step of the process design procedure. An ABE/W (Acetone-Butanol-Ethanol/Water) biorefinery separation case study has been selected for this purpose.

After a detailed literature research about flexibility and the associated indicators already proposed by other authors, both deterministic and stochastic indexes were found and compared each other on a simple distillation column case study according to a thorough procedure. The flexibility assessment was then coupled with the economic one and an "additional investment costs vs flexibility" diagram was outlined in order to allow the decision maker a more conscious decision based on both those indicators.

The flexibility analysis was then extended and studied in deep on equilibrium-staged operations. The usual design procedure to assess the optimal number of equilibrium stages in a whatever multi-staged operation (e.g. multiple-effect evaporators, absorbers, distillation columns, etc.) is based indeed on a Total Annualized Costs (OPEX and CAPEX) cost optimization. However, this optimization is carried out with respect to nominal operating conditions; this means that, when perturbations occur, the control system compensates to those disturbances by managing the external duties (e.g. steam, reflux ratio etc.) considerably affecting energy costs. Although CAPEX is fixed once the design is carried out, OPEX value may vary over a certain range reflecting the uncertain variables deviation likelihood. A new procedure based on an OPEX averaged over a the uncertain domain was outlined to define the optimal number of trays (CAPEX) under uncertainty.

An additional criterion related to the process sustainability was then introduced. A flexible unit design indeed reflects into a lower system energy demand, i.e. a considerably lower environmental impact. Thus the carbon footprint indicator was used to integrate the design procedure and to include sustainability among the design criteria. This way it has been possible to assess the best compromise between units oversizing (i.e. investment costs) and external duty demand (OPERating EXPenses) to compensate operating conditions perturbations.

Then the analysis shifted to the biorefinery application. The selected case study refers to a biorefinery separation process, namely a distillation train downstream an ABE (Acetone-Butanol-Ethanol) fermentation process after a preliminary dewatering operation. This mixture was selected both because of the renewed interest in biofuels and because of the possibility to discuss how mixture

non-idealities affect the process from a flexibility perspective. Moreover it is well-known that biomasses feedstock nature fluctuates according to their seasonality and the profitability of bioprocesses is strictly related to the good performances of the purification section. Thus this example looked particularly suitable for such a flexibility assessment case study worth to be analyzed even for practical applications.

Differently from the former case studies aimed to separate relatively simple hydrocarbon mixtures, when both water and alcohols are involved in a distillation process the operation feasibility boundaries should be better investigated due to the presence of azeotropic species.

Residue Curve Mapping was then exploited for different kinds of separation specifications through a well-defined procedure used to generate the thermodynamic feasibility boundaries under uncertain operating conditions. The procedure for a single column was extended to distillation trains as well as equivalent integrated configurations such as the Dividing Wall Column (DWC).

Once thermodynamic boundaries have been outlined, the several possible distillation train configurations aimed to purify the ABE mixture components were simulated and compared from a flexibility and economic viewpoint at once. The analysis was carried out both with deterministic and stochastic flexibility indexes and the optimal design choice was successfully identified.

However distillation trains with no energy integration are considered an outdated solution for multicomponent mixtures purification. They have been indeed replaced by integrated solutions resulting in both lower investments and lower operating costs. A Dividing Wall Column was then designed with respect to the same process specifications with a feasible-paths based algorithm. A flexibility assessment was then performed on the DWC as well highlighting both benefits and drawbacks of the employment of a process intensifying design solution. The optimal DWC design was then discussed by considering flexibility needs and oversizing costs compared to the classical distillation train configuration.

All calculations and simulations performed so far were nonetheless related to steady state conditions. In order to have a more complete overview of flexibility indexes process dynamics was investigated as well. When taking into account process dynamics the flexibility assessment results and thus the required equipment oversizing necessarily depend on the control configuration. A new «switchability» index has been defined by correlating the dynamic and steady state performances under a flexibility point of view. The proper definition of this index was referred to a Model Predictive Control configuration for a simple system but it can be used for any kind of control loop configurations in order to compare them. To describe this latter case study the same distillation column involved in the steady state indexes comparison was simulated in DynSim[®] dynamic process simulator with PID controllers in order to highlight the influence of dynamics.

The final outcome of this thesis work is then the definition of a comprehensive

approach for multicriteria design of unit operations in general under uncertain operating conditions and the investigation of the associated criticalities. Those criteria are respectively economics, flexibility, controllability and sustainability.

Estratto

La procedura tradizionale per la progettazione di processi chimici costituisce uno standard ben consolidato nell'ingegneria di processo e solitamente richiede la saturazione di alcuni gradi di libertà residui tramite un'ottimizzazione basata su vari criteri. Tuttavia, la soluzione che si ottiene tramite questa procedura può dirsi "ottimale" unicamente in relazione alle condizioni operative nominali e non tiene conto delle possibili perturbazioni esterne.

Lo scopo di questo lavoro di dottorato è quindi quello di includere la flessibilità in ogni tappa della procedura di progettazione. A tal proposito è stato scelto di utilizzare come caso di studio un processo di bioraffineria relativo alla separazione di una miscela ABE/W (Acetone-Butanolo-Etanololo/Acqua) nei suoi componenti puri.

In seguito ad una ricerca bibliografica dettagliata sulla flessibilità e sui vari indicatori proposti precedentemente da altri autori, indici di flessibilità sia di tipo deterministico che stocastico sono stati trovati e messi a confronto sulla base di un semplice caso di distillazione di miscela ideale.

L'analisi di flessibilità è stata quindi combinata con la valutazione economica permettendo la costruzione di un diagramma "costi aggiuntivi vs. flessibilità" che permette al progettista di effettuare una scelta di design più consapevole basata sugli indicatori precedentemente discussi.

In seguito, l'analisi di flessibilità è stata estesa ed analizzata in dettaglio in merito al problema relativo al numero ottimale di stadi di equilibrio in caso di incertezza nelle operazioni multi-stadio. La procedura tradizionale per la scelta del numero di stadi di equilibrio in questo tipo di operazioni (e.g. evaporazione a multiplo effetto, assorbimento, distillazione etc.) è basata infatti su un'ottimizzazione dei Costi Totali Annui (CAPEX ed OPEX). Tuttavia questa ottimizzazione viene realizzata in base alle condizioni operative nominali. Questo significa che, nel caso di perturbazioni, il sistema di controllo deve compensare i disturbi esterni con la gestione delle utenze (e.g. vapore al ribollitore, rapporto di reflusso etc.) influenzando notevolmente i costi relativi ai consumi energetici. Sebbene i costi di investimento per un design definito siano già fissati, i costi operativi possono variare in un intervallo che rispecchia la probabilità delle deviazioni dei parametri incerti. Una nuova procedura basata sulla media degli OPEX pesata sulla distribuzione di probabilità nell'intervallo di incertezza è stata quindi delineata in modo da definire il numero ottimale di stadi di equilibrio (e quindi i CAPEX) in caso di condizioni operative incerte.

Un ulteriore criterio associato alla sostenibilità del processo è stato dunque introdotto. Un design flessibile si riflette infatti in una minor domanda di energia, ovvero un impatto ambientale considerevolmente inferiore. Pertanto l'impronta di carbonio è stata presa in considerazione per integrare la procedura di design ed includere la sostenibilità tra i criteri di progettazione. In tal modo è stato possibile

trovare il miglior compromesso tra sovradimensionamento delle apparecchiature (costi di investimento) e consumo di utenza esterna (costi operativi) al fine di compensare la perturbazione delle condizioni operative.

L'analisi si è quindi spostata sulle applicazioni relative ai processi di bioraffineria. Il case study scelto fa riferimento ad un'operazione di separazione di bioraffineria, nello specifico ad un treno di colonne di distillazione a valle di un processo di fermentazione ABE (Acetone-Butanolo-Etanol) in seguito ad una rimozione preliminare del contenuto d'acqua.

Questa miscela è stata scelta sia per il rinnovato interesse nei biocombustibili sia perché permette di discutere in dettaglio come le non-idealità della miscela incidono sul processo dal punto di vista della flessibilità. Inoltre è noto che la natura della materia prima biomassa fluttua durante l'anno con l'alternarsi delle stagioni e la redditività dei bio-processi è strettamente legata alle buone prestazioni della sezione di purificazione. Per tutte queste ragioni, tale esempio è sembrato particolarmente adatto per questo tipo di analisi di flessibilità che merita di essere analizzata anche in termini di applicazioni pratiche.

A differenza dei casi precedenti, il cui fine era la separazione di miscele idrocarburiche relativamente semplici, quando acqua ed alcoli sono coinvolti nello stesso processo di distillazione la regione di fattibilità dell'operazione dev'essere delineata con maggiore accuratezza a causa della presenza degli azeotropi.

Per svariati valori delle specifiche di separazione sono state utilizzate le curve di residuo (RCM) tramite una procedura dettagliata al fine di generare i limiti di fattibilità termodinamica in condizioni operative incerte. La procedura per una singola colonna di distillazione è stata quindi estesa ai treni di colonne ed alle configurazioni integrate equivalenti come la colonna a parete separatrice (DWC).

Una volta definiti i limiti termodinamici, le differenti configurazioni del treno di distillazione per la purificazione dei componenti nella miscela ABE sono state simulate e confrontate tra loro per flessibilità e costi al contempo. L'analisi è stata realizzata sia con indici di flessibilità deterministici che stocastici e la scelta progettuale ottimale è stata identificata con successo.

Tuttavia i treni di colonne di distillazione sono considerati un'opzione tecnologica superata per la purificazione di miscele multicomponente. Essi sono stati infatti rimpiazzati da soluzioni integrate che permettono sia costi di investimento che costi operativi inferiori. Una colonna a parete separatrice (DWC) è stata quindi progettata al fine di ottenere le stesse specifiche di processo tramite un algoritmo basato sui cammini fattibili. È stata dunque condotta un'analisi di flessibilità sulla DWC e messi in risalto sia i benefici che gli inconvenienti dell'impiego di una soluzione di processo intensificata. Il design ottimale della DWC è stato quindi discusso tenendo conto sia dei bisogni di flessibilità e dei costi di sovradimensionamento e confrontato con la classica configurazione del treno di colonne.

Tutti i calcoli e le simulazioni fatte finora tuttavia fanno unicamente riferimento alle condizioni stazionarie. Al fine di avere una prospettiva più completa degli

indici di flessibilità è stata quindi studiata la dinamica di processo. Quando si prende in considerazione anche la dinamica di un processo i risultati dell'analisi di flessibilità e quindi il sovradimensionamento delle apparecchiature dipendono necessariamente dalla configurazione del sistema di controllo. Un nuovo indice di "switchabilità" è stato quindi definito correlando le prestazioni in dinamico ed in stazionario dal punto di vista della flessibilità. La definizione più appropriata di questo indice è stata riferita ad una strategia di Model Predictive Control per un sistema semplice ma può essere adattata a qualsiasi tipo di loop di controllo al fine di confrontarli. Per descrivere quest'ultimo caso è stata simulata la stessa colonna di distillazione trattata nel confronto degli indici stazionari tramite il simulatore di processo dinamico DynSim[®] con controllori di tipo PID al fine di evidenziare gli effetti legati ai transitori.

Il risultato finale di questo lavoro di tesi è quindi la definizione di un approccio globale per la progettazione e l'ottimizzazione multicriterio di operazioni unitarie in generale in condizioni operative incerte e l'analisi delle criticità ad esso associate. I criteri presi in considerazione sono stati rispettivamente l'aspetto economico, la flessibilità, la controllabilità e la sostenibilità.

Contents

I	Introduction	24
1	Why this research study	25
2	The European collaboration	26
3	The thesis structure	27
II	Flexibility Indexes	35
1	Introduction: a measure of flexibility	37
2	The debutanizer case study	46
3	Flexibility analysis	48
3.1	Deterministic indexes: F_{SG} and RI	48
3.2	Stochastic indexes: SF and F_V	56
4	Conclusion	69
A	List of acronyms and symbols	71
B	Capital costs estimations	73
B.1	Purchase equipment cost in base conditions	73
B.2	Bare module cost	73
C	Probability distributions	75
C.1	Normal distribution function	75
C.2	Laplace distribution function	77
III	Thermodynamic Feasibility Assessment	81
1	Introduction	84
2	Methodology	85
3	Case study	88
4	The binary systems	89
4.1	Homogeneous azeotrope	89
4.2	Heterogeneous azeotrope	92
5	The multicomponent systems	95
5.1	Ternary system	96
5.2	Quaternary system	97
5.3	Systems with more than four components	101
6	Distillation trains and Dividing Wall Column	102
7	Conclusions	106
A	List of acronyms and symbols	107
B	Thermodynamic model	109

IV	Optimal Design: Optimal Number of Equilibrium Stages	114
1	Introduction	117
2	The uncertainty characterization	119
3	Flexible design procedure	122
4	Multiple-effect evaporator	123
4.1	Optimal Design under Nominal Operating Conditions	125
4.2	Flexible Design	126
5	Distillation column	129
5.1	Optimal Design under Nominal Operating Conditions	129
5.2	Flexible Design	131
6	Environmental impact	134
7	Conclusions	138
A	List of acronyms and symbols	140
B	Capital and operating expenses estimations	142
B.1	Purchase equipment cost in base conditions	142
B.2	Bare module cost	142
B.3	External heat duty cost	143
C	Global Warming Potential calculations	144
V	Optimal Design: Sequence of Operations	150
1	Introduction	153
1.1	Conventional vs flexible design procedure	153
1.2	Multicomponent mixtures separation	156
2	Flexibility operational definition and flexibility indexes	157
3	The biorefinery case study	161
4	Thermodynamic flexibility analysis	163
4.1	RCMs overview	163
4.2	Thermodynamic model	165
4.3	Thermodynamic feasibility assessment	166
5	Economic assessment and optimal design under uncertain conditions	167
6	Conclusions	173
A	List of acronyms and symbols	175
B	Capital costs estimations	177
B.1	Purchase equipment cost in base conditions	177
B.2	Bare module cost	177
VI	Process intensification	182
1	Introduction: DWC design state of the art	185
2	The ABE mixture case study	189
3	DWC equivalent layouts	191
4	DWC design algorithm	192

5	Results	197
6	Conclusions	199
A	List of acronyms and symbols	201
B	Thermodynamic model	203
C	Capital costs estimations	204
C.1	Purchase equipment cost in base conditions	204
C.2	Bare module cost	204
D	Global Warming Potential calculations	206
VII	Process intensification under Uncertainty	214
1	Introduction	216
2	The ABE mixture case study	219
3	DWC design	221
4	Results	223
4.1	Flexibility assessment	223
4.2	Environmental Assessment	226
5	Conclusions	229
A	List of acronyms and symbols	231
B	Thermodynamic model	233
C	Capital costs estimations	234
C.1	Purchase equipment cost in base conditions	234
C.2	Bare module cost	234
D	Global Warming Potential calculations	236
VIII	Switchability	242
1	Introduction	245
2	Index definition	248
3	Dynamic CSTR case study	251
4	Distillation column case study	257
4.1	Flexible design	260
4.2	Economic assessment	264
5	Conclusions	267
A	List of acronyms and symbols	269
B	Capital costs estimations	271
B.1	Purchase equipment cost in base conditions	271
B.2	Bare module cost	271
IX	Conclusions and perspectives	277
1	Conclusions	278
2	Perspectives	283

X Acknowledgements

285

List of Figures

1.1	Thesis conceptual map	28
2.1	Feasibility domain - F_{SG} [2]	38
2.2	Feasibility domain - F_{SG} vs RI [3]	40
2.3	Feasibility domain - F_{SG} vs SF [6]	41
2.4	Feasibility domain - F_V [9]	43
2.5	Debutanizer column layout	46
2.6	Heat transfer areas (F_{SG})	49
2.7	Column max & min diameters (F_{SG})	50
2.8	Equipment bare module cost (F_{SG})	52
2.9	Capital costs comparison (F_{SG})	53
2.10	Heat transfer areas (RI)	55
2.11	Column max & min diameters (RI)	55
2.12	Equipment bare module cost (RI)	57
2.13	Capital costs comparison (RI)	57
2.14	Condenser SF : Normal PDF	59
2.15	Condenser SF : Laplace PDF	59
2.16	3D SF analysis domain	60
2.17	SF results Normal PDF	61
2.18	SF results Laplace PDF	62
2.19	SF optimal sizing NDF	62
2.20	SF optimal sizing LDF	63
2.21	$\frac{dC}{C}$ vs. SF Derivatives ratio	65
2.22	F_V probability distribution function	65
2.23	2D F_V analysis	66
2.24	3D F_V analysis domain - operating conditions	67
2.25	F_V analysis economic results	67
2.26	F_V analysis optimal sizing	68
2.27	1D NDF and its CDF	75
2.28	2D NDF	76
2.29	1D Laplace DF and its CDF	77
2.30	2D Laplace DF	78
3.1	Open evaporation process	86
3.2	RCMs examples (■ <i>stable</i> , ● <i>saddle</i> , ★ <i>unstable</i>)	87
3.3	Ethanol–Water equilibrium diagrams (▼ <i>bottom</i> , ◆ <i>feed</i> , ▲ <i>distillate</i>)	91
3.4	n-Butanol–Water equilibrium diagrams (▼ <i>bottom</i> , ◆ <i>feed</i> , ▲ <i>distillate</i>)	93
3.5	Standard distillation column vs distillation column with decanter	94
3.6	Butanol recovery ratio in the bottom stream	95
3.7	Distillation RCM on ternary diagrams	98
3.8	Distillation RCM on quaternary diagrams lateral (left) and top (right) view	100

3.9	Infinitely staged indirect distillation train (left) and DWC (right)	103
3.10	Distillation RCM for distillation train and DWC	105
4.1	Uncertainty characterization	121
4.2	Cocurrent multiple-effect evaporator	124
4.3	Multiple effect TAC under nominal operating conditions	126
4.4	External duty under uncertain operating conditions	127
4.5	Multiple effect TAC under uncertain operating conditions (Beta PDF)	129
4.6	Distillation TAC under nominal operating conditions	130
4.7	Reboiler duty under uncertain operating conditions	132
4.8	Distillation TAC under uncertain operating conditions (Beta PDF)	133
4.9	CO_2 average emissions	135
4.10	CO_2 emissions - sensitivity	137
5.1	Conventional design procedure	154
5.2	Flexible design procedure	155
5.3	Distillation train configurations for two components recovery	158
5.4	Flexibility index (F_{SG}) vs Resilience Index (RI)[7]	159
5.5	Stochastic Flexibility (SF) assessment of a heat exchanger[7]	160
5.6	RCMs on a ternary diagram	165
5.7	Feasibility boundaries assessment via residue curve maps	168
5.8	Indirect vs midsplit feasibility (Green: feasible, Blue: unfeasible)	170
5.9	Total annualized costs vs. partial flowrates perturbations	171
5.10	First column reboiler heat transfer surface	171
5.11	Deterministic indexes economic comparison	172
5.12	Additional costs vs. stochastic flexibility	173
6.1	Distillation train vs DWC	190
6.2	DWC equivalent configurations	191
6.3	DWC design algorithm	193
6.4	TAC minimum search domain and algorithm path	195
6.5	ABE case study configurations	197
6.6	TAC vs Number of stages	198
6.7	Indirect configuration vs DWC	199
7.1	Conventional vs intensified distillation	216
7.2	Flexibility index (F_{SG}) vs Resilience Index (RI)[23]	218
7.3	Two-column model (Petlyuk)	222
7.4	DWC total costs vs uncertain domain	223
7.5	Additional costs vs Flexibility (F_{SG})	224
7.6	Additional costs vs Flexibility (RI)	225
7.7	GWP vs F_{SG}	227
7.8	GWP vs RI	227
8.1	Relevant vs negligible overshoot in process control	245
8.2	Feasible domain dynamic behaviour	250
8.3	Non-isothermal CSTR reactor layout	251

8.4	Closed-loop dynamic response	254
8.5	Jacket heat transfer surface area	255
8.6	Switchability vs design plot	256
8.7	Debutanizer control configurations	258
8.8	Reboiler heat transfer surface area	261
8.9	Condenser heat transfer surface area	262
8.10	Column minimum and maximum diameter	263
8.11	Additional investment costs vs flexibility	265
8.12	Combined switchability and economic assessment chart	266
9.1	New design procedure	279

List of Tables

2.1	Flexibility studies in literature	45
2.2	Feed conditions and composition	46
2.3	Design parameters	47
2.4	Uncertain parameters θ^k	47
2.5	Flexibility analysis results: F_{SG}	50
2.6	Critical vertices	51
2.7	Allowed disturbances loads	54
2.8	Flexibility analysis results: RI	54
2.9	Steady state flexibility indexes comparison	70
2.10	Equipment cost in base conditions parameters	73
2.11	Bare module parameters	74
3.1	Analytical results for 5 components RCMs	101
4.1	Nominal Operating Conditions	125
4.2	Feed properties and distillation nominal operating conditions	130
4.3	Equipment cost in base conditions parameters	142
4.4	Bare module parameters	143
5.1	Feed composition and physical properties	162
5.2	Distillation train optimal design	169
5.3	Equipment cost in base conditions parameters	177
5.4	Bare module parameters	178
6.1	Feed properties	190
6.2	Process specifications	190
6.4	NRTL Binary interaction parameters	203
6.5	Equipment cost in base conditions parameters	204
6.6	Bare module parameters	205
7.1	Feed properties	219
7.3	Equipment cost in base conditions parameters	234
7.4	Bare module parameters	235
8.1	CSTR process parameters	252
8.2	Composition controller tuning parameters	253
8.3	Design data and process specifications	257
8.4	Uncertain variables and expected deviations	259
8.5	Uncertain parameters critical deviations (positive + or negative -)	261
8.6	Equipment cost in base conditions parameters	271
8.7	Bare module parameters	272

Part I. Introduction

1 Why this research study

This PhD thesis work was conceived with the purpose to answer one main question: how process performances such as feasibility, profitability, sustainability etc., are affected when the operating conditions vary with respect to the nominal ones according which the process was designed and optimized ?

In the light of several studies published in literature during the last decades concerning the design under uncertainty, the goal of this thesis work can be rephrased as the need to include flexibility in the process design procedure. In particular, in this study we will account for the so-called aleatory uncertainty since the uncertain values are related to process parameters deviations and not to the process model inaccuracies (epistemic uncertainty).

In order to better investigate the flexibility impact on the process design procedure, a suitable case study should be then selected. The interest was focused in particular to current practical applications and needs in process industry.

Over the last years sustainability has become by far the topic of major concern in the chemical industry domain. The energy challenge is the key point of the environmental friendly policies adopted by all the most developed and industrialized countries worldwide. For this purpose indeed several research programmes, such as Horizon 2020, have been funded by the European Union and other institutions for the EU member states. As regards this decarbonisation policy, the International Energy Agency defines renewables as the centre of the transition to a less carbon-intensive and more sustainable energy system [1].

For all those reasons bio-processes have seen a considerably renewed interest during the last decades. However, in order to be competitive with the petrochemical industry and to replace part of it as soon as possible, the bio-processes need to be able soon to cover a substantial part of the market demand and to be flexible with respect to the market needs and the raw material properties. The conventional optimal design procedure used in general for chemical processes deserves indeed a more detailed analysis and discussion before being applied to bio-processes due to the intrinsic fluctuating nature of the feedstock involved across the year's seasons.

For this purpose an Acetone-Butanol-Ethanol/Water (ABE/W) separation case study has been arranged. The ABE process, which was the most spread industrial scale fermentation process during the first half of the 20th century, is based on well-established technology solutions. The ABE/W stream to be treated comes from an upstream microbial fermentation process characterized by product inhibition [2] and the recovery of at least the most valuable products, i.e. n-butanol and acetone, is necessary for the profitability of the process. After a preliminary dewatering operation, usually liquid-liquid extraction or pervaporation, the ABE/W remaining products can be separated by means of different distillation configurations.

The distillation process design for the butanol and acetone recovery will be then the mainline of the flexibility problem applications in this PhD thesis work. It will be involved in the thermodynamic feasibility boundaries assessment via Residue Curve Maps (RCMs), in the optimal distillation train design under uncertainty and finally in the optimal design and flexibility assessment of process intensifying solutions, that is a Dividing Wall Column unit.

2 The European collaboration

In order to satisfy all the needs of such a complex roadmap through the flexible design procedure, a collaboration between the Institut National Polytechnique de Toulouse and the Politecnico di Milano institutions was set up with the purpose of combining the skills in process simulation and design on one side and in process dynamic simulation and control on the other side. This flexibility oriented research for biorefinery operations is a new research field for both the research groups worth to be better investigated by means of the available resources.

This joint PhD thesis was then carried out in the main site (INP de Toulouse) during the entire first year as well as for the second semester of the 2nd and 3rd years of the PhD within the PSI (Procédés et Systèmes Industriels) research group at the Laboratoire de Génie Chimique under the supervision of Prof. Ludovic Montastruc and Prof. Xavier Joulia. On the other hand the stay in the host university (Politecnico di Milano) took place during the first semester of both 2nd and 3rd years of the thesis within the SuPER (Sustainable Process Engineering Research) team under the supervision of Prof. Flavio Manenti.

The purpose of this European joint PhD thesis project was also to enhance and reinforce the collaboration between two of the most active research teams working in the Computer Aided Process Engineering (CAPE) community and to confirm the importance of combining different perspectives and skills at an international level to make the research outcome more fruitful and robust from multiple points of view.

Specifically, the thesis tasks were distributed during the different stays as follows:

- 1st year:
 - Laboratoire de Génie Chimique:
 - * Flexibility indexes review and distillation train design;
- 2nd year:
 - Politecnico di Milano
 - * Dynamic flexibility analysis and switchability assessment;
 - Laboratoire de Génie Chimique

- * Thermodynamic flexibility assessment via Residue Curve Mapping and DWC literature review;
- 3rd year:
 - Politecnico di Milano
 - * Operating costs under uncertain conditions, economic - flexibility - environmentally based optimal number of equilibrium stages;
 - Laboratoire de Génie Chimique
 - * Dividing Wall Column design, flexibility assessment and manuscript writing.

3 The thesis structure

As already introduced in the first paragraph, the main goal of this research work is the analysis from a flexibility perspective of the various process design procedure steps. Actually, some indicators able to define a few system properties from a flexibility point of view have already been proposed in literature but without a thoroughly defined methodology for the process design procedure. Based on the previous premises, a conceptual map describing the PhD thesis structure has been outlined as shown in Figure 1.1.

Given a separation problem, the very first step of the process design procedure is the feasibility assessment. Among the possible unit operations, the most suitable for the separation to be carried out can be identified and its feasibility needs to be assessed. Another possible alternative could be to carry out the feasibility analysis for a set of suitable separation and, given its outcome, define the best operation afterwards. Finally, the most suitable operation can be nonetheless defined after the following steps of the design procedure. The cost to pay for this delayed decision is the computational effort required to perform the other phases of the design procedure for all the possible alternatives before selecting the best one. In particular, the later the separation process is defined the higher the calculations to be performed will be.

Each process has a set of dedicated tools that can be used for the feasibility analysis. In case the selected operation is distillation, such as for the ABE/W downstream processing case study, the computational tool employed for the feasibility boundaries evaluation is the Residue Curve Mapping.

On the one hand, for zeotropic mixtures the feasibility assessment is rather trivial since, given the process specifications and that the number of equilibrium stages is higher than the minimum value N_{min} , a reflux ratio allowing for the sharp split of the components always exists. On the other hand, for an azeotropic mixture, a much more detailed feasibility study is required since non-idealities could lead to the impossibility to separate one of the components at the desired

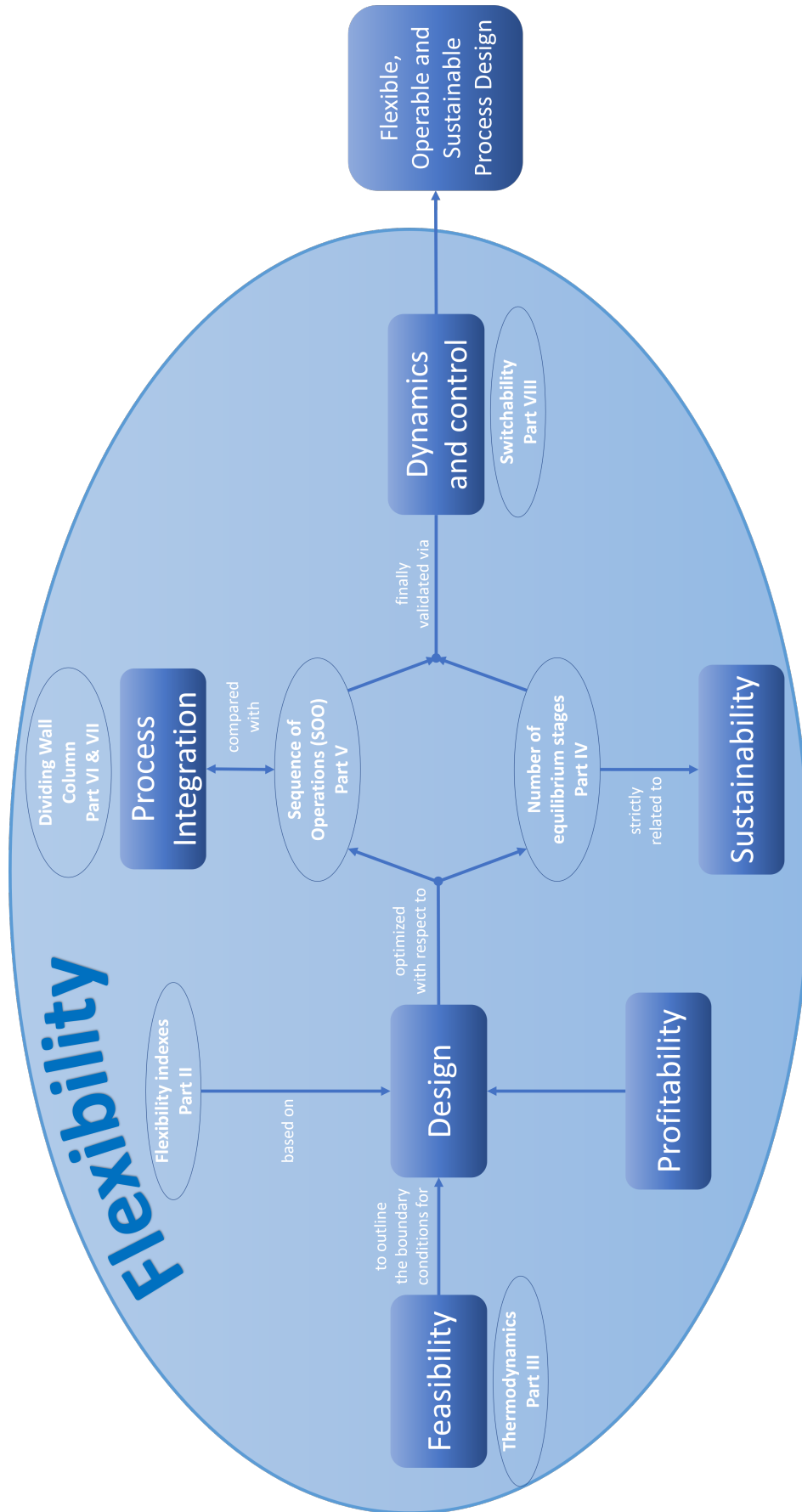


Fig. 1.1: Thesis conceptual map

purity specification. Therefore, the very first task of a flexible design procedure is the outline of the thermodynamically feasible domain boundaries. The theoretical background of residue curves is widely known and well-established and the related applications are usually presented with respect to a single distillation column with two composition constraints [3].

In this thesis work, starting from the same physical laws, the procedure has been extended to distillation trains and the recovery ratio has been introduced as secondary specifications by means of the combination of the ABE/W mixture components into binary, ternary and quaternary applications. Moreover, due to their thermodynamic equivalence [4], the distillation train application is valid for the Dividing Wall Column unit as well.

Once the feasible domain has been thoroughly defined, the unit design phase, usually including equipment sizing and economic assessment, could be then carried out by including uncertainty about the operating conditions. However, in order to account for flexibility during the design phase, a flexibility indicator should be defined in order to make possible its quantification.

After a detailed literature research, several flexibility indexes have been found in literature. The majority of them and the most commonly used were proposed during the last decades of the 20th century. In particular, the most spread flexibility index is by far the Swaney and Grossmann [5] index defined in 1983 as the maximum fraction of the expected deviation of all the uncertain variables at once that can be accommodated by the system. Another widespread indicator is the Resilience Index that was proposed by Saboo and Morari [6] in the same year and that assesses the largest total disturbance load, independent of the direction of the disturbance, that a system is able to withstand without becoming unfeasible. Both those indexes evaluate a geometrical property of the feasible domain and do not account for the deviation likelihood. That's why they can be defined as deterministic flexibility indexes.

On the other hand, flexibility indexes that accounts for the deviation probability distribution function can be found as well. They are defined as stochastic flexibility indexes and they provide a more accurate flexibility estimation at the cost of the information required about the deviation nature and likelihood. The most popular is the stochastic flexibility index proposed by Pistikopoulos and Mazzuchi [7] in 1990 defined as the integral of the deviation probability distribution function over the feasible domain. Other indexes such as the volumetric flexibility proposed by Lai and Hui in 2008 [8] can be reconducted to a particular case of the stochastic index.

Those four indexes have been compared on a simple debutanizer case study in order to analyze in detail their behaviour and the main pros and cons in using each of them. In any case, all those indicators do not account for process dynamics and can be classified as steady state flexibility indexes. For this reason, as later discussed in detail, the last chapter of this manuscript is devoted to the definition

of an indicator accounting for the process dynamics under a flexibility perspective.

Once the index analysis has been completed, further properties of the optimal design under uncertainty have been investigated. First of all, when talking about optimal design in process engineering, we usually refer to two main areas:

- the saturation of the residual unit degrees of freedom by means of an economic/environmental optimization;
- optimal sequence of operation (SOO) in case of several units to be arranged.

In particular, for multi-stage operations, such as distillation, the residual degree of freedom to be satisfied via Total Annual Costs optimization is the number of equilibrium stages. The conventional design procedure is based on the best external duty (OPEX) and number of stages (CAPEX) compromise from an economic point of view.

However, this procedure neglects two important aspects. First of all the number of equilibrium stages is optimized accounting for nominal operating conditions only. This means that, in case perturbation occurs, its higher profitability with respect to the alternative design could be seriously compromised.

Second this economic evaluation makes no difference between 1 \$ of CAPEX and 1 \$ of OPEX. Although from an economic perspective this assumption can be reliable, operating expenses are usually associated to the system external duties demand, i.e. energy consumption. This means that, from a sustainability point of view, for a given amount of Total Costs, it would be much better to have a predominant cost distribution towards the CAPEX.

In brief, for a given design, external perturbations are managed by the external duties, i.e. higher operating costs. Therefore, a process configuration with a higher number of equilibrium stages, i.e. initial investments, could not only provide a more profitable solution under uncertain operating conditions, but would as well result in a higher process sustainability due to the lower energy demand with corresponding lower environmental impact. In order to analyze in deep the sustainability aspects under uncertain conditions during the design phase, both a desalination case study via multiple-effect evaporation and a phenol-cyclohexane distillation case studies have been set up. The operating expenses, i.e. the energy demand, at each number of equilibrium stages are averaged on the operating condition likelihood function over the uncertain domain.

To provide a more general result, the deviation nature has been described by using probability distribution functions with different properties in order to assess the impact of the PDF on the final outcome.

After that, the analysis has focused on the other part of the design optimization concerning the sequence of operations. The ABE/W mixture case study was used to introduce the analysis of the optimal distillation train. Multicomponent mixtures indeed can be separated into their single components by means of multiple distillation columns arranged in series or parallel. In particular, since both

molar fractions and recovery ratios are fixed for n-butanol and acetone in order to ensure the profitability of the entire process, at least two column in series are required.

For the ABE/W separation case study then the three main conventional distillation train configurations, namely direct, indirect and midsplit, have been designed and compared under nominal operating conditions. After that, the flexibility analysis for the same three configurations has been carried out and coupled with the equipment sizing and economic assessment in order to identify the additional costs required for a

flexibility target and to compare the different sequence of operations under uncertain conditions.

The indirect configuration resulted the most profitable in both cases due to the possibility to purify first the high butanol content in the feed and to send to the second column a considerably lower flowrate to process with an improved acetone relative content.

Without energy integration, the train of distillation columns is nevertheless considered an outdated design solution for multicomponent mixtures purification. During the last decades, in the light of the energy transition, the analysis of more cost and energy effective processes has been the focus of the process engineering research.

Process intensification can be mainly divided into two main areas [9]:

- process-intensifying equipment such as novel reactors, and intensive mixing, heat-transfer and mass-transfer devices;
- process-intensifying methods, such as new or hybrid separations, integration of reaction and separation, heat exchange, or phase transition (in so-called multifunctional reactors), techniques using alternative energy sources (light, ultrasound, etc.), and new process-control methods (like intentional unsteady-state operation).

In case of multicomponent mixtures separation the most established process-intensifying unit is the Dividing Wall Column. It consists of the arrangement of the Petlyuk configuration inside a single column shell and among the non-standard distillation column configurations it was studied in deep since it is the only large-scale process intensification case where both capital and operating costs as well as the required installation space can be drastically reduced [10].

The Dividing Wall Column unit for the ABE/W mixture separation has then been designed according to a new feasible-paths based procedure. The result thus obtained meets the requirements concerning both the higher profitability and the higher sustainability of about 30% with respect to the distillation train.

However, as usual, this better performances are strictly related to a designed optimized with respect to the nominal operating conditions. It would be interesting then to assess how the performance gap between the intensified configuration

and the conventional one is affected when external disturbances are likely to occur. For this reason, a combined economic-flexibility-environmental assessment has been carried out for different DWC number of equilibrium stages to compare to each other as well as to the indirect train configuration. The analysis revealed that beyond a certain deviation magnitude, a DWC with a higher number of equilibrium stages could result more profitable and less energy demanding than the optimal solution under nominal operating conditions. Moreover, there exists a breakeven flexibility index above which the conventional distillation train performs better than the process intensifying solution both from economic and environmental perspective due to the possibility to manage two more external duties and to limit the effect of the perturbation to the first distillation column aimed at separating butanol.

Therefore the outcome of the DWC design accounting for uncertain operating conditions did not provide an univocally defined optimal solution but more optimality ranges corresponding to different design alternatives locally meeting the minimum Total Annual Costs and CO_2 emissions goals.

However, the flexibility assessments carried out in these steps of the process design procedure were all referred to the steady state conditions only. The last task of this PhD thesis work has been then the definition of an indicator accounting for the process dynamics under a flexibility perspective. The fact that an operation is feasible both under nominal and under perturbed operating conditions doesn't imply indeed that it is also feasible at each point of the transition trajectory between these two states [11].

Based on the dynamic flexibility index proposed by Dimitriadis and Pistikopoulos in 1995 [12] a new switchability index SI can be defined in order to assess the dynamic performances of a process from a flexibility perspective with respect to the steady state one. This index can be defined as the ratio between the same flexibility index assessed accounting for dynamics and at steady state conditions. Since the steady state feasible domain is an upper boundary of the dynamic one, SI will be included within the range $[0, 1]$. A switchability index close to zero then means that process dynamics is really constraining from a flexibility perspective and it should be accounted when performing the system design under uncertainty. Otherwise the flexibility index for a given design could be considerably overestimated or, vice versa, the investment costs for a given flexibility requirement could be underestimated. On the other hand, a switchability index close to 1 indicates that the dynamic flexibility performances of a process design do not considerably differ from the steady state one and accounting for dynamics during the design phase could be a worthless effort.

The analysis of process dynamics can't be decoupled from the employed control configuration, that's why the switchability index defined this way necessarily depends on the process control layout. By means of a non-isothermal reactor case study, a first evaluation of this index is carried out with respect to a Model Pre-

dictive Control strategy. An equipment oversizing vs dynamic flexibility trend can be then outlined to assess the additional investment costs related to the process variables values during the transient.

Beside assessing the index value itself, the most suitable use of the switchability index is related to the different control strategies, configurations and parameters tuning comparison. For this purpose then the PID control strategy has been tested on the same case study according to the two most common tuning methods and finally the MPC, PID with Ziegler-Nichols and PID with Tyreus-Luyben configurations have been compared from a switchability point of view.

Since feedback controllers are still the most common applications in process industry, they are worth a more accurate analysis. The dynamic simulation of the same debutanizer case study used for the flexibility indexes comparison has been then carried out with two different control structures, namely reflux/boil-up (LV) and distillate/boil-up (DV), and its dynamic flexibility assessment has been performed. The distillation column sizing and the economic assessment were carried out and, even in this case, it is possible to compare the two control strategies from a switchability perspective via the proposed index and to identify two different flexibility intervals where one control configuration results in lower investments with respect to the other and vice versa.

In conclusion, the purpose of this first thesis chapter is then to introduce all the questions raised during the PhD thesis progressing and the arguments behind the procedure that has been followed in order to provide them some answers. The detailed discussion of each topic and the corresponding numerical results will be commented in deep in each of the following chapters.

The thesis structure allows to read independently each of the publications of which this manuscript consists since they are self-sustaining. However, it is suggested to read the feasibility assessment and the flexibility indexes literature review and comparison before the others.

In any case, Figure 1.1 can help to follow the logical scheme of this study and to find the pages corresponding to each publication.

References

- [1] IEA Bioenergy Annual Report 2018 retrieved at <https://www.ieabioenergy.com/wp-content/uploads/2019/04/IEA-Bioenergy-Annual-Report-2018.pdf>
- [2] Garcia, V., Pääkkilä, J., Ojamo, H., Muurinen, E., Keiski, R., 2011. Challenges in biobutanol production: How to improve the efficiency ?; *Renewable and Sustainable Energy Reviews*, 15, 964-980.
- [3] Petlyuk, F.B., 2004. *Distillation Theory and its Application to Optimal Design of Separation Units*. Cambridge University Press
- [4] Ramapriya, G.M., Tawarmalani, M., Agrawal, R., 2014. Thermal coupling links to liquid-only transfer streams: A path for new dividing wall columns. *AIChE Journal* 60, 2949–2961. <https://doi.org/10.1002/aic.14468>
- [5] Swaney, R.E., Grossmann, I.E., 1985. An index for operational flexibility in chemical process design. Part I: Formulation and theory. *AIChE J.* 31, 621–630. <https://doi.org/10.1002/aic.690310412>
- [6] Saboo, A.K., Morari, M., Woodcock, D., 1985. Design of Resilient Processing Plants .8. a Resilience Index for Heat-Exchanger Networks. *Chem. Eng. Sci.* 40, 1553–1565. [https://doi.org/10.1016/0009-2509\(85\)80097-X](https://doi.org/10.1016/0009-2509(85)80097-X)
- [7] Pistikopoulos, E.N., Mazzuchi, T.A., 1990. A Novel Flexibility Analysis Approach for Processes with Stochastic Parameters. *Comput. Chem. Eng.* 14, 991–1000. [https://doi.org/10.1016/0098-1354\(90\)87055-T](https://doi.org/10.1016/0098-1354(90)87055-T)
- [8] Lai, S.M., Hui, C.-W., 2008. Process Flexibility for Multivariable Systems. *Ind. Eng. Chem. Res.* 47, 4170–4183. <https://doi.org/10.1021/ie070183z>
- [9] Stankiewicz, A.I. and Moulijn, J.A. (2000) *Process Intensification: Transforming Chemical Engineering*. *Chemical Engineering Progress*, 96, 22-34.
- [10] Schultz, M.A., Stewart, D.G., Harris, J.M., Rosenblum, S.P., Shakur, M.S., O'Brien, D.E., 2002. Reduce costs with dividing-wall columns. *Chemical Engineering Progress* 98, 64–71
- [11] Luo, A.C.J., 2008. A theory for flow switchability in discontinuous dynamical systems. *Nonlinear Analysis: Hybrid Systems* 2, 1030–1061. <https://doi.org/10.1016/j.nahs.2008.07.003>
- [12] Dimitriadis V. D., Pistikopoulos E. N., 1995, Flexibility Analysis of Dynamic Systems, *Industrial & Engineering Chemistry Research*, 34.12, 4451–62.

Part II. Flexibility Indexes

Flexibility analysis of a distillation column: indexes comparison and economic assessment

Alessandro Di Pretoro^{a,b}, Ludovic Montastruc^a, Flavio Manenti^b, Xavier Joulia^a

^aLaboratoire de Génie Chimique, Université de Toulouse, CNRS/INP/UPS, Toulouse, France

^bPolitecnico di Milano, Dipartimento di Chimica, Materiali e Ingegneria Chimica «Giulio Natta», Piazza Leonardo da Vinci 32, 20133 Milano, Italy.

Abstract

The worldwide shared definition of “optimal design” refers to the cheapest and simplest design able to perform the required job; most of the time this definition is strictly related to given operating conditions, i.e. the input variables are seldom subjected to considerable variations.

However, in process engineering, plenty of cases don't fit this definition due to the uncertain nature of the feedstock needed to be processed. Therefore, if a system is likely to undergo several and substantial perturbations, an a priori flexibility assessment can be crucial for the good performance of the operation.

In chemical engineering the leading separation process is distillation. Hence the first purpose of this paper is to define a procedure and compare the different flexibility indexes found in literature in order to perform a simple distillation column flexibility assessment.

The second goal of this paper is to couple the flexibility and economic aspects related to the distillation column investment costs and again to compare the different indexes economic behaviours.

Highlights:

1. In process engineering, flexibility can be defined as the ability of a process to accommodate a set of uncertain parameters.
2. From a design point of view we can definitely conclude that the most suitable flexibility index for the particular analyzed system is a function of the expected deviation nature.
3. From an economic perspective, the introduction of the Capital costs vs. Flexibility relationship and its relative plots let the decision maker, i.e. the engineering, take a more informed decision whatever the adopted flexibility index.

Keywords: flexibility, index, distillation, design, economics.

1 Introduction: a measure of flexibility

Flexibility analysis is a step of process design procedure that is often skipped. Sometimes a sensitivity analysis is performed with features similar to the flexibility one but in general they don't overlap.

The standard procedure for chemical plants design consists of the assessment of the optimal design according to the economic and operational aspects. Nevertheless this optimal design is strictly related to the operating conditions, i.e. perturbations, when present, can seriously turn the tables. In these cases an a priori flexibility analysis could be of critical importance to assess in which range of operating conditions a system design is effectively better performant than another one.

The word flexibility commonly refers to the ability to change in order to cope with variable circumstances both in a passive and an active sense; to be more detailed, in process engineering, flexibility can be defined as the ability of a process to accommodate a set of uncertain parameters [1]. This concept looks easily understandable but actually the definition standalone says nothing about how we can deal with it. Thus we need an operational definition and to know what flexibility means through the way it could be measured.

The very first publication about the definition of a flexibility index is provided by Swaney and Grossmann in 1985 [2] and soon after Morari et al. [3] proposed another possible index to quantify the flexibility of a process design (called in this case "resiliency"). Moreover there exists an additional paper by both Grossmann and Morari [4] where the flexibility related problems and solution are thoroughly analyzed with a pioneering methodology.

The Swaney and Grossmann flexibility index (F_{SG}) mathematically states as follow:

Given that:

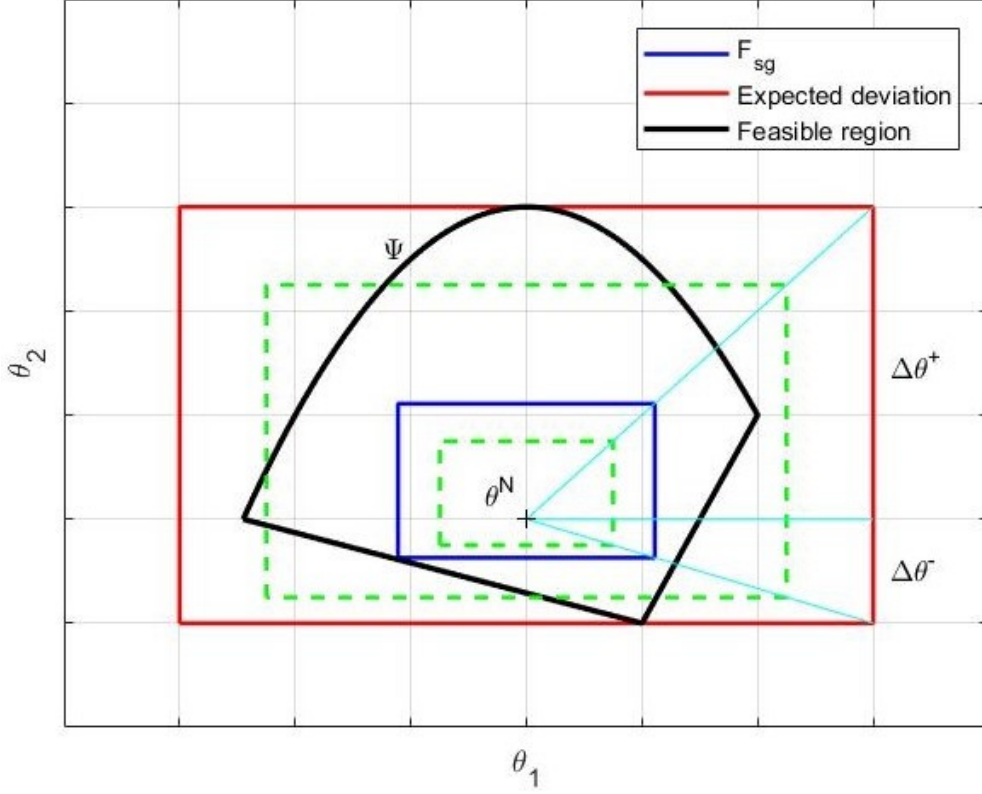
- θ^N : nominal values of uncertain parameters (base point);
- $\Delta\theta^+$, $\Delta\theta^-$: expected deviations for each parameter;
- d : design variables associated to the equipment capacities;
- z : control variables.

The flexibility index, for a given design d , is the solution of the problem:

$$F_{SG} = \max \delta \quad (1.1)$$

$$s.t. \max_{\theta \in T(\delta)} \min_z \max_{j \in J} f_j(d, z, \theta) \leq 0 \quad (1.2)$$

If $F=1$, the deviations $\Delta\theta^+$ and $\Delta\theta^-$ can be accommodated. In order to have a clearer idea of what these statement means we can help ourselves with the plot in Figure 2.1.

Fig. 2.1: Feasibility domain - F_{SG} [2]

The curve $\Psi(d, \theta)$ is the so called feasibility domain defined by the constraints. Constraints can be physical, legal, operational, economic etc. and in general a deeper study about the way this region is outlined and the conditions to be satisfied, as well as the degrees of freedom analysis, is needed. This step precedes the flexibility analysis since the domain shape is strictly related to the nature of the case study.

As shown by the optimization problem, the flexibility index defined as above (1.1, 1.2), is the maximum fraction of the expected deviation δ that can be accommodated by the system; it graphically represents the minimum among the maximum fractions of the hyperrectangle sides' lengths that is bounded by the feasible zone.

Moreover, for constraints jointly quasi convex in z and $1D$ quasi convex in θ the problem can be decomposed into two level optimization problem:

$$F_{SG} = \min_k \delta^k \quad (1.3)$$

$$\delta^k = \max_z \delta \quad (1.4)$$

$$f_j(d, z, \theta^k) \leq 0 \quad j \in J \quad (1.5)$$

$$\theta^k = \theta^N + \delta \cdot \Delta\theta^k \quad (1.6)$$

and the solution lies at a vertex of the hyperrectangle allowing us to solve the optimization problem by evaluating the feasibility of the design at each vertex. In this way, it can be noted that the explicit solution of the min-max problem can be circumvented; on the other hand certain types of non-convex domains may lead to nonvertex solutions[5].

Before the introduction of the flexibility study, to move from feasibility study towards the design phase, we just need to know whether the project is feasible under the nominal operating conditions or not, but once we deal with flexibility the qualitative answer yes/no is not sufficient anymore. We need to quantify “how much” the project is feasible and the independent variables ranges enclosing the possible operating conditions.

As anticipated at the beginning, the same year Morari et al. proposed a “resiliency index” defined as the capability to easily recover or adjust to misfortune or change, that is more or less the passive alter ego of the capability to adapt to new, different or changing requirements, i.e. flexibility.

This index is based on the same premises of the F_{SG} , i.e. even in this case the very first step to perform is the definition of the feasibility domain. Then the resiliency index RI is defined as the largest total disturbance load, independent of the direction of the disturbance, a system is able to withstand without becoming infeasible.

It mathematically stands as:

$$RI = \min_i \{|l_i^{max}|\} \quad (1.7)$$

$$s.t. \{ \max_j f_j(\theta) \leq 0, \forall l : \sum_i |l_i| \leq RI \} \quad (1.8)$$

this corresponds to inscribing the largest possible polytope inside the feasible region defined by the inequalities here above. The RI is then equal to the distance between a vertex V of the polytope and the nominal operating point 0 as shown in Figure 2.2.

The main advantage of the RI compared to the F_{SG} is that it requires a lower computational effort; this can be easily figured out in the case of an n-dimensional problem where a vertex analysis has to be performed: in the hyperrectangle case we have 2^n vertices to calculate while in the polytope case we have just $2n$ of them.

Moreover, the disturbance region measured in the first case might be practically more interesting because it expresses directly the disturbance load allowed in the direction of each parameter independently on the others.

For the same reason, since the hyperrectangles sides have to be parallel to the axes even if this configuration doesn't allow the biggest possible rectangle, the F_{SG} index results to be very conservative and significantly underestimate the actual flexibility of the system.

This representation of the feasible and expected possible zones does not reflect

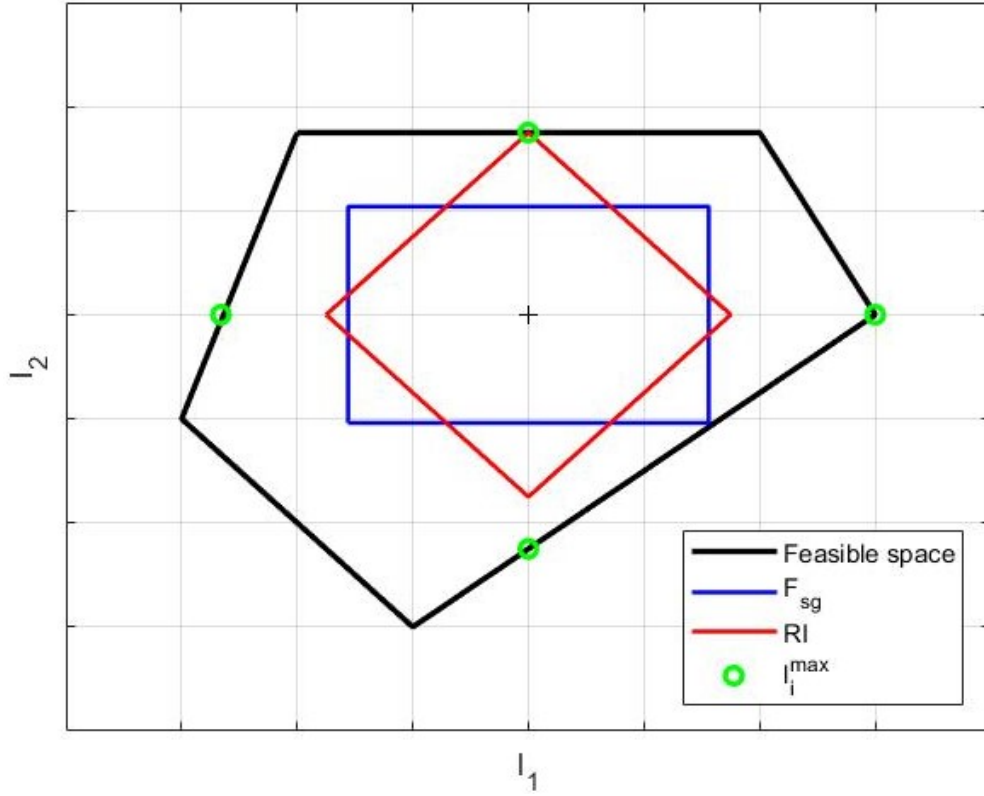


Fig. 2.2: Feasibility domain - F_{SG} vs RI [3]

thoroughly the real world since not all the possible operating conditions are equally probable; hence this kind of analysis results in rather conservative estimates. In many real world applications, however, data are usually available that allow a better definition of uncertainty in a statistical sense.

For this reason a novel flexibility analysis approach for processes with stochastic parameters was then proposed in 1990 by Pistikopoulos and Mazzuchi [6]. It's shown that the flexibility index can correspond to a multivariate cumulative distribution function transforming the original constraint space to the space of stochastically dependent flexibility function by means of the analytical properties of the flexibility problem.

Given the feasibility region constraints inequalities as:

$$\Psi(d, \theta) \leq 0 \quad (1.9)$$

the equality defines the boundary of the feasible zone.

The stochastic flexibility index SF can be defined as:

$$SF = Pr\{\Psi(d, \theta) \leq 0\} = \int_{\{\theta: \Psi(d, \theta) \leq 0\}} \dots \int P_D(\theta) \cdot d\theta \quad (1.10)$$

where P_D is the joint distribution function of the uncertain parameters θ .

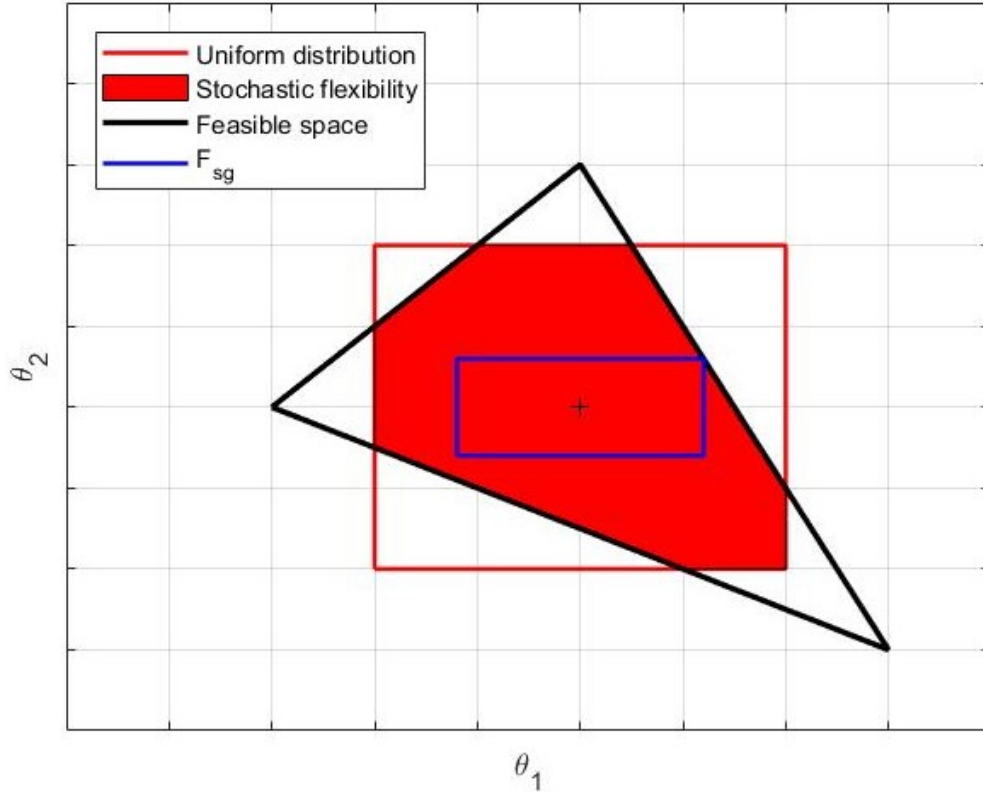


Fig. 2.3: Feasibility domain - F_{SG} vs SF [6]

The comparison between the stochastic flexibility index SF and the Swaney & Grossmann is better shown in Figure 2.3.

With this methodology we can calculate a weighted estimation of flexibility. Thus, if something is unlikely to happen and our system cannot withstand this operating conditions, it only slightly affects the final value of the flexibility index providing a measurement less conservative and more adherent to reality.

Obviously, the other side of the coin is the strict dependency of this index on the availability of probability distribution data, that is if no data are available this methodology is clearly unusable.

An additional problem to be solved was pointed out in 1995 by Dimitriadis and Pistikopoulos [7] and it consists in the evaluation of flexibility taking into account the dynamics of the studied system. This topic was already pointed out by Grossmann and Morari [4] few years before but Pistikopoulos is the very first one to define a specific index namely Dynamic Flexibility (DF) that takes into account the evolution of the system. Actually the definition itself of DF is not so different since it is a modification of the previous index F_{SG} . However, its introduction allows the study of a system taking into account its control loops and their tuning, therefore from an operational point of view its introduction is of critical importance.

The Dynamic Flexibility problem is introduced here below for literature coverage reasons. Nevertheless this index will not be taken into account in the flexibility

analysis proposed in the next section both because no other dynamic flexibility indexes to compare it with have been found in literature and because the analysis refers to steady state conditions.

The definition of the Dynamic Flexibility follows the path of the F_{SG} considering the uncertain and control parameters namely θ and z as a function of time, therefore the dynamic flexibility index evaluation problem becomes:

$$DF(d) = \max \delta \quad (1.11)$$

$$s.t. \chi(d) = \max_{\theta(t) \in T(\delta, t)} \min_{z(t) \in Z(t)} \max_{j \in J, t \in [0, H]} f_j(d, x(t), z(t), \theta(t), t) \leq 0 \quad (1.12)$$

$$s.t. h(d, x(t), z(t), \theta(t), t) = 0 \quad (1.13)$$

$$x(0) = x^0 \quad (1.14)$$

$$\delta \geq 0 \quad (1.15)$$

$$T(\delta, t) = \{\theta(t) | \theta^N(t) - \delta \cdot \Delta\theta^-(t) \leq \theta(t) \leq \theta^N(t) + \delta \cdot \Delta\theta^+(t)\} \quad (1.16)$$

$$Z(t) = \{z(t) | z^L(t) \leq z(t) \leq z^U(t)\} \quad (1.17)$$

Qualitatively, the dynamic flexibility index, DF, represents the largest scaled deviation of the uncertain parameter profile that the design can tolerate while remaining feasible within the horizon considered.

The dynamic flexibility index problem is a two-stage, semi-infinite, dynamic optimization problem with an infinite number of decision variables. Therefore, in order to solve it, an ad hoc methodology to reduce the dimension of the problem has to be implemented.

Finally, the most recent flexibility index found in literature is provided by Hui and Lai [8, 9]. It has the aim to overcome the problems related to previous indexes, i.e. the requirement of nominal point and the consideration of the critical uncertainty only (causing an underestimation) for F_{SG} and RI, as well as the availability of the probability distribution of all uncertain parameters at the design stage for the SF. This new flexibility metric is much easier to use and does not need a lot of computational effort or available data and it is defined as follow.

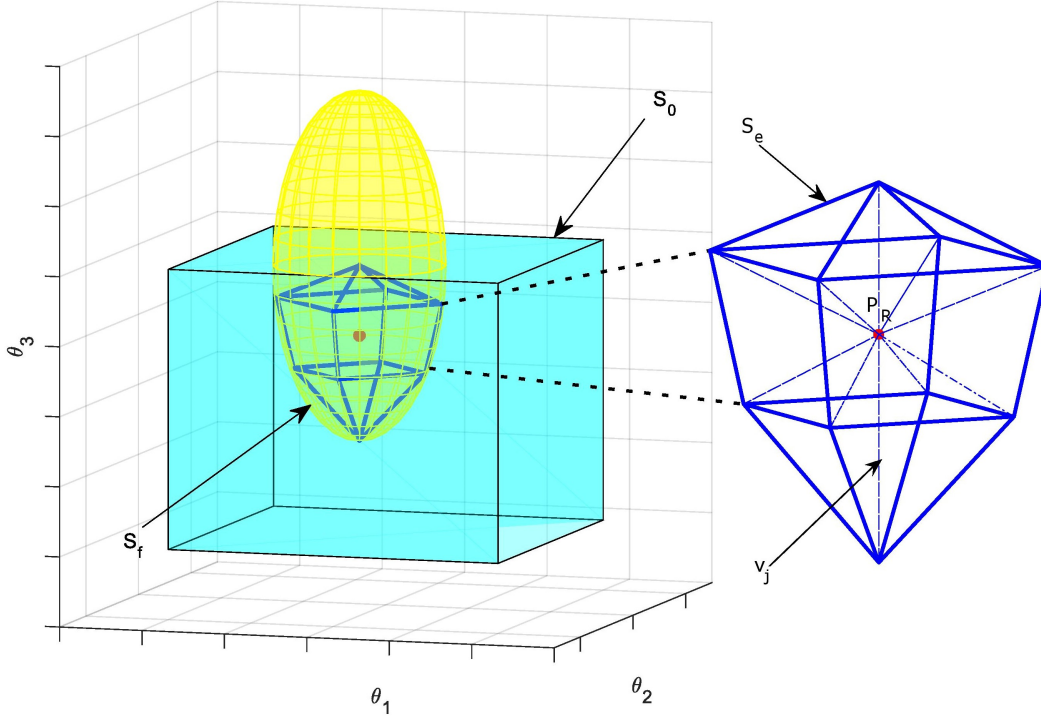
Let V_0 be the volume defined by the uncertain parameters:

$$V_0 = \prod_{i=1}^N (\theta_{iU} - \theta_{iL}) \quad (1.18)$$

and V_f the feasible volume defined as the intersection of the constrained volume and V_0 .

Then the flexibility index F_V is defined as the ratio between the feasible space and the uncertain space:

$$F_V = \frac{V_f}{V_0} \quad (1.19)$$

Fig. 2.4: Feasibility domain - F_V [9]

However, S_f is usually irregular in shape and its volume (V_f) determination is not straightforward. To estimate V_f , a constructed space (S_e , the region outlined by the thick solid line), whose volume determination is less difficult, can be inscribed inside S_f . With a careful selection of the shape of S_e , its volume (V_e) can be used as a close estimate of V_f .

As illustrated in Figure 2.4, S_e can be constructed by first picking a reference point (P_R), which is not necessarily the nominal point, within S_f . Auxiliary vectors v_j with selected directions can be radiated from P_R . The interception points (P_j) of v_j and the feasible space boundary are obtained. The S_e can then be constructed by joining these P_j points according to their positions in space. Since different S_e can be generated by different auxiliary vector direction selection schemes, estimation accuracy of V_f and F_V will depend on the selection scheme employed. The general formulation for the auxiliary vectors' positions in a 3D space is as follows:

$$\max_{x_j, y_j, z_j} V_e(x_j, y_j, z_j) \quad (1.20)$$

$$f_k(\theta_{ij}) \leq 0 \text{ and } 0 \leq x_j, y_j, z_j \leq 1 \quad (1.21)$$

$$s.t. \theta_{i,j} = v_{ij} i_j \Delta_{ij} + \theta_i^R, \Delta_{ij} = \begin{cases} \Delta^+ \cdot \theta_i & (v_{ij} \geq 0) \\ |\Delta^- \cdot \theta_i| & (v_{ij} < 0) \end{cases} \quad i = x, y, z \quad (1.22)$$

However, whether the feasibility domain is well defined and the constraints equations are known, there's no need to approximate anymore since we can get the exact value of the S_f volume through a multiple integral at the cost of a higher computational effort.

An additional remark is worth to be done: the volumetric flexibility index takes into account no perturbation outside the uncertain space and treat every point as equally possible. Therefore, given its definition, we can write it as:

$$F_v = \frac{V_f}{V_0} = \frac{1}{V_0} \int_{V_f} d\theta = \int_{V_f} \frac{1}{V_0} d\theta \quad (1.23)$$

that is the same definition as the stochastic flexibility index for a probability step function. A practical application of this analogy between SF and F_V will be shown in the following chapters.

Finally, on one hand we can say that several flexibility indexes have been found in literature but, on the other hand, except the steady state debutanizer case study proposed by Hoch et al. (1995)[10] (F_{SG}), no case studies about distillation have been provided (cf. Table 2.1). Most of the systems found in literature subjected to flexibility analysis have linear constraints or at least a quasi convex feasibility domain; whether a higher complexity can be detected, the flexibility analysis has been conducted with the simple F_{SG} that, due to its straightforward application, results to be the index used in the vast majority cases. However, the behaviour of less used and more complex indexes is worth to be studied in deeper and for a wider range of systems as well; therefore, a complete flexibility analysis of a distillation column, inspired by the aforementioned debutanizer example [10], is proposed here below with all the four steady state indexes. An accurate results comparison and economic assessment will follow.

Case study	Authors	Index
Pump and pipe	Grossmann & Morari 1983[4]	F_{SG}
	Swaney & Grossmann Part I 1985[2]	F_{SG}
	Floudas et al. 2001[11]	F_{SG}
	Lai & Hui 2008[9]	F_V
Refrigeration cycle	Swaney & Grossmann Part II 1985[12]	F_{SG}
Reactor-recycle	Swaney & Grossmann Part II 1985[12]	F_{SG}
Heat exchanger network	Grossmann & Morari 1983[4]	F_{SG}
	Swaney & Grossmann Part II 1985[12]	F_{SG}
	Saboo & Morari 1985[3]	RI
	Pistikopoulos & Mazzuchi 1990[6]	SF
	Dimitriadis & Pistikopoulos 1995[7]	DF
	Floudas et al. 2001[11]	F_{SG}
	Lai & Hui 2008[9]	F_V
Storage tank dynamic system	Dimitriadis & Pistikopoulos 1995[7]	DF
	Wu & Chang 2017[13]	DF
Debutanizer	Hoch, Eliceche et Grossmann 1995[10]	F_{SG}
	Hoch & Eliceche 1996[1]	F_{SG}
Reactor + cooler	Floudas et al. 2001[11]	F_{SG}
Chemical process with recycle	Floudas et al. 2001[11]	F_{SG}
Solar-driven membrane distillation desalination (SMDD) process	Wu & Chang 2017[13]	DF
Benzene chlorination reaction system	Huang et al. 2017[14]	DF
Batch reactor system	Huang et al. 2017[14]	DF

Tab. 2.1: Flexibility studies in literature

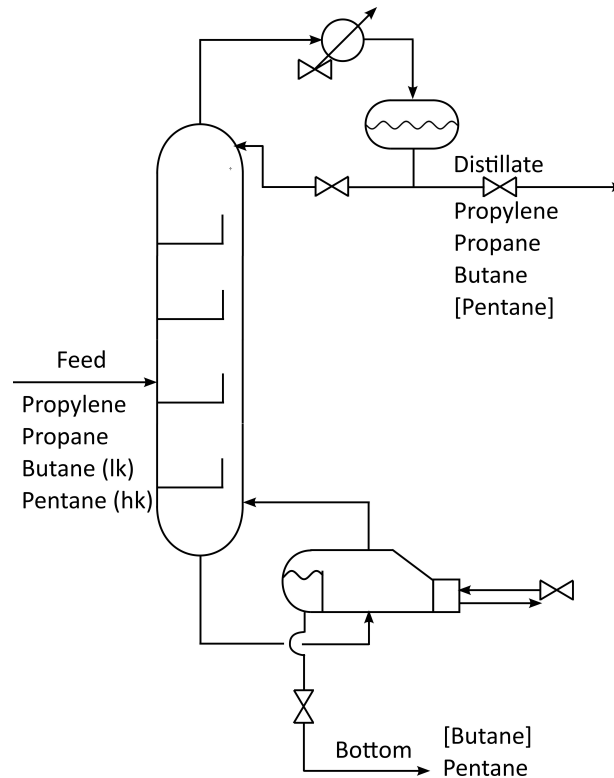


Fig. 2.5: Debutanizer column layout

2 The debutanizer case study

In order to better understand the distillation related application of these indexes, the simple debutanizer case study proposed by Hoch et al. [10], with few modifications, has been analyzed in detail.

In short, the system is made up of a standard distillation column, i.e. total condenser, no intermediate feeds/withdrawals and partial reboiler (Figure 2.5). The feed stream is defined by the composition and conditions shown in Table 2.2 while the given design parameters are listed in Table 2.3.

Partial molar flowrates	Value	Unit
Propylene	0.055	<i>mol/s</i>
Propane	0.053	<i>mol/s</i>
Butane (lk)	6.863	<i>mol/s</i>
Pentane (hk)	2.743	<i>mol/s</i>
Temperature	Bubble	<i>K</i>
Pressure	$15 \cdot 10^5$	<i>Pa</i>

Tab. 2.2: Feed conditions and composition

Desing variables	Symbol	Value	Unit
d			
Rectification stages	N_r	9	1
Stripping stages	N_s	10	1
Column diameter	D_{col}	0.634	m
Condenser area	A_{cond}	40.00	m^2
Reboiler area	A_{reb}	26.83	m^2
Top pressure	P_{top}	$4 \cdot 10^5$	Pa

Tab. 2.3: Design parameters

Parameter	Symbol	Value	Expected deviation	Unit
θ		θ^N	$\Delta\theta^{k\pm}$	
Butane flowrate	F_4	6.863	$\pm 10\%$ ± 0.686	mol/s
Pentane flowrate	F_5	2.743	$\pm 10\%$ ± 0.274	mol/s
Condenser heat transfer coefficient	U_{cond}	473.77	$\pm 10\%$ ± 47.377	$W/m^2/K$
Inlet cooling water temperature	T_w	20	$\pm 10\%$ ± 2	$^\circ C$
Reboiler heat transfer coefficient	U_{reb}	552.90	$\pm 10\%$ ± 55.29	$W/m^2/K$
Max vapor velocity	G_f	0.38	$\pm 10\%$ ± 0.038	m/s
Min vapor velocity	G_w	0.13	$\pm 10\%$ ± 0.013	m/s

Tab. 2.4: Uncertain parameters θ^k

Finally the uncertain parameters are reported in Table 2.4, their expected variation ranges $\Delta\theta^{k\pm}$ are the same in either positive or negative direction and equal to 10% of their nominal value as suggested in the paper. The feed variations are related to the nature of the upstream process, the performances of the heat exchangers to the tubes fouling, the water temperature to the seasonality and finally the flooding and weeping velocity are function of the trays technology and status.

The specifications are given by the paper as three inequality constraints, namely:

- Maximum molar fraction of butane in the bottom product = 0.01786;
- Maximum molar fraction of pentane in the distillate = 0.025;
- Minimum pentane recovery in the bottom = 0.97.

In this paper the two most restrictive equality relationships have been selected to fulfill the two remaining degrees of freedom:

- Molar fraction of butane in the bottom product = 0.01786;
- Pentane recovery in the bottom = 0.97.

The controlled variables are respectively the reflux and distillate flowrates.

3 Flexibility analysis

Flexibility analysis can be performed either during the design phase or for an already existing equipment (or plant). In the next chapters flexibility will be both assessed for the debutanizer column as shown in the previous paragraph and for a distillation column to be designed; the results will be then compared.

Moreover, the analysis will be conducted separately for the deterministic and stochastic indexes in order to highlight analogies and differences.

3.1 Deterministic indexes: F_{SG} and RI

First of all, in order to evaluate the Swaney & Grossmann flexibility index F_{SG} , we need to estimate the variation ranges of the uncertain variables as shown in Table 4, called from here on out “expected deviations”.

Since the system is rather simple (i.e. convex feasibility domain), for the moment there’s no need of outlining the whole feasible space as discussed in the first section; the vertex analysis, by increasing the parameters variation percentages until the expected values and keeping constant the ratios between them, can be then easily and effectively performed. Since there are 7 changing parameters, the hyperrectangle has 7 dimensions that means $2^7 = 128$ vertices should be theoretically calculated for each simulation but, thanks to the possibility to decouple some independent parameters, the computational effort can be substantially reduced.

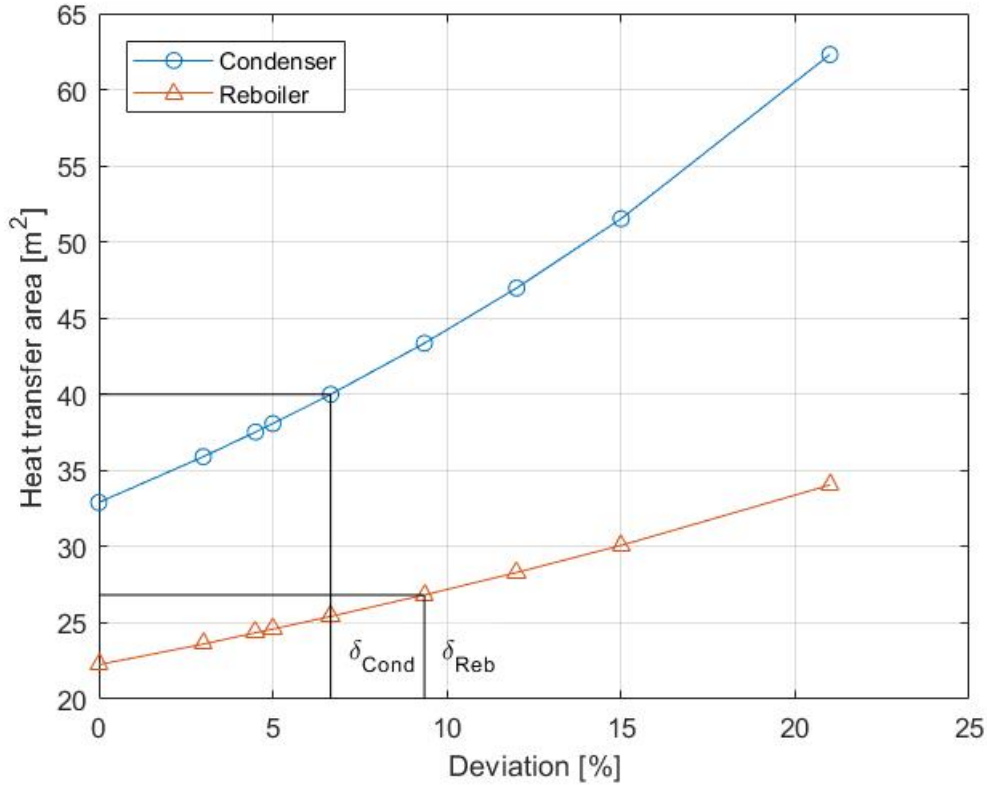


Fig. 2.6: Heat transfer areas (F_{SG})

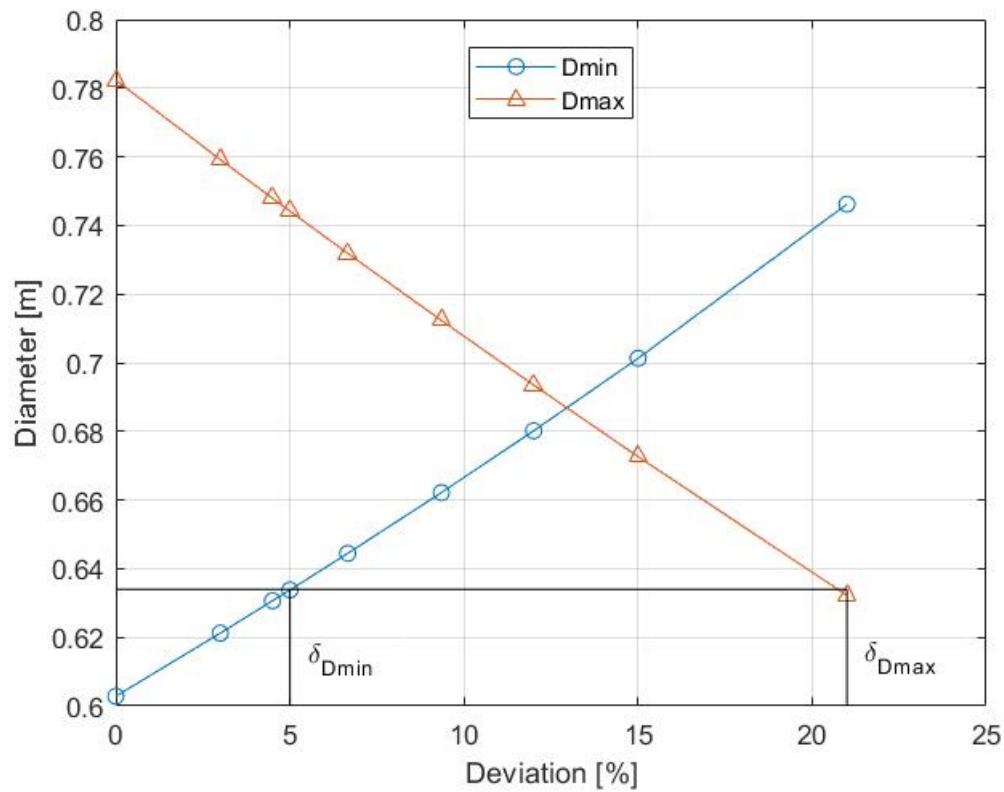
The complete flexibility analysis results and the corresponding plots are shown respectively in Table 2.5 and Figures 2.6 and 2.7, the debutanizer related values are indicated.

The resulting Swaney & Grossmann flexibility index for this case study is then given by:

$$F_{SG} = \frac{\text{allowed deviation}}{\text{expected deviation}} = \frac{5\%}{10\%} = 0.5 \quad (3.1)$$

The bottleneck of flexibility is given by the column minimum diameter equal to 0.634 m, i.e. by the flooding conditions. However, the analysis has been carried out for all the other design parameters standalone as well. The condenser results to be the second most constraining variable, while the reboiler the third one; for a value between 12 and 15% of the allowed deviation we can notice that the maximum diameter becomes lower than the minimum one causing the column design to be impossible with a single diameter column. This last phenomenon occurs because flexibility indexes refer both to positive and negative perturbations causing the range of diameter values able to ensure operable conditions to become smaller for higher flexibility requirements.

The conditions that cause the hyperrectangle to exceed the feasibility domain boundaries, i.e. which vertex is tangent one, for each design variable are reported

Fig. 2.7: Column max & min diameters (F_{SG})

Deviation [%]	Condenser area [m^2]	Reboiler area [m^2]	Minimum diameter max [m]	Maximum diameter min [m]
0.00	32.91	22.26	0.603	0.782
5.00	38.08	24.59	<u>0.634</u>	0.744
6.66	<u>40.00</u>	25.43	0.644	0.732
9.35	43.35	<u>26.83</u>	0.662	0.712
15.00	51.53	30.09	0.701	0.673
21.00	62.30	34.05	0.746	<u>0.632</u>

Tab. 2.5: Flexibility analysis results: F_{SG}

Parameter vs design	Condenser area	Reboiler area	Minimum diameter	Maximum diameter
Butane flowrate	+	+	+	-
Pentane flowrate	+	+	+	-
U_{Cond}	-	/	/	/
T_w	+	/	/	/
U_{Reb}	/	-	/	/
G_f	/	/	-	/
G_w	/	/	/	+

Tab. 2.6: Critical vertices

in Table 2.6; “+” and “-” indicate respectively a positive or negative deviation of the uncertain parameter while “/” indicates that the parameter does not affect the constraining design variable.

For the “Condenser area”, “Reboiler area” and “Minimum column diameter” critical conditions are achieved because of overfed column and underperforming equipment while for the maximum diameter, i.e. weeping conditions, criticalities are present in case of underfeeding as expected according to the physics of the problem.

Beside the design and sizing, an economic assessment has been performed as well. The purpose is to couple flexibility and investment costs in order to make the best decision during the design phase and avoid the plant underperform; operational costs have not been taken into account since they’re uniquely determined due to the fact that we’re not changing the number of trays. For more detail about equipment costs correlations cf. Appendix B.

The capital costs trends (normalized to the lowest value) as function of F_{SG} flexibility are plotted for each equipment in Figure 2.8. All of them increase as flexibility increases (according with their size). The most expensive equipment is the Kettle reboiler that has a much more accurate technology than the other heat exchangers and that works under pressure, while the column is relatively cheap because of its small diameter.

In Figure 2.9 three series of percentage data as function of flexibility have been plotted; they refer namely to:

- $\frac{dC}{C_0}$: the additional investment referred to a column designed in nominal operating conditions, i.e. 0 % flexibility (Blue trend);
- $\frac{dC}{C_{eff}}$: the cost differences with respect to the case study column design (Red trend);

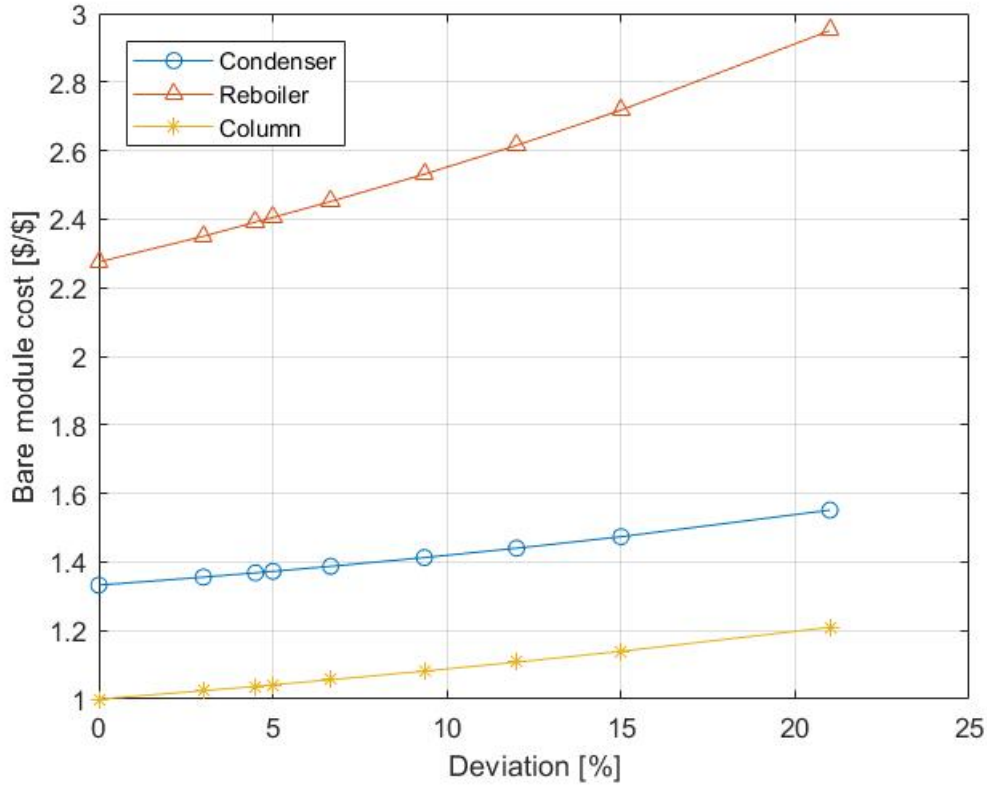


Fig. 2.8: Equipment bare module cost (F_{SG})

- $\frac{dC}{C_{real}}$: the effective cost differences if the case study column is already available (Yellow trend).

We can notice first that the trends are more or less linear; moreover, we can also point out that part of the investment (about 3%) could have been saved if the reboiler was properly designed, from a flexibility point of view, since its overdesign is practically useless considering the bottleneck of 5.00 % given by the column diameter.

Differently from the F_{SG} index, the resilience index defines the largest total disturbance load a system is able to withstand independently of the direction of the disturbance.

It was originally defined for heat exchangers networks, therefore some modifications are needed in order to adapt it to every type of system. First of all the Resilience Index has a dimension that usually is an “heat” related value (kW, K etc.); in this case, in order to make the comparison with the other indexes possible and because of the several perturbations we have to cope with, each one with its different dimension, the percentage deviation value will be used. Then, since we’re dealing with a simple system (i.e. quasi-convex domain), we’re sure we’re going to solve a so called “Class 1 problem”, i.e. the standard vertex analysis procedure can be performed successfully.

The complete Resilience analysis results are shown in Tables 2.7 and 2.8 and

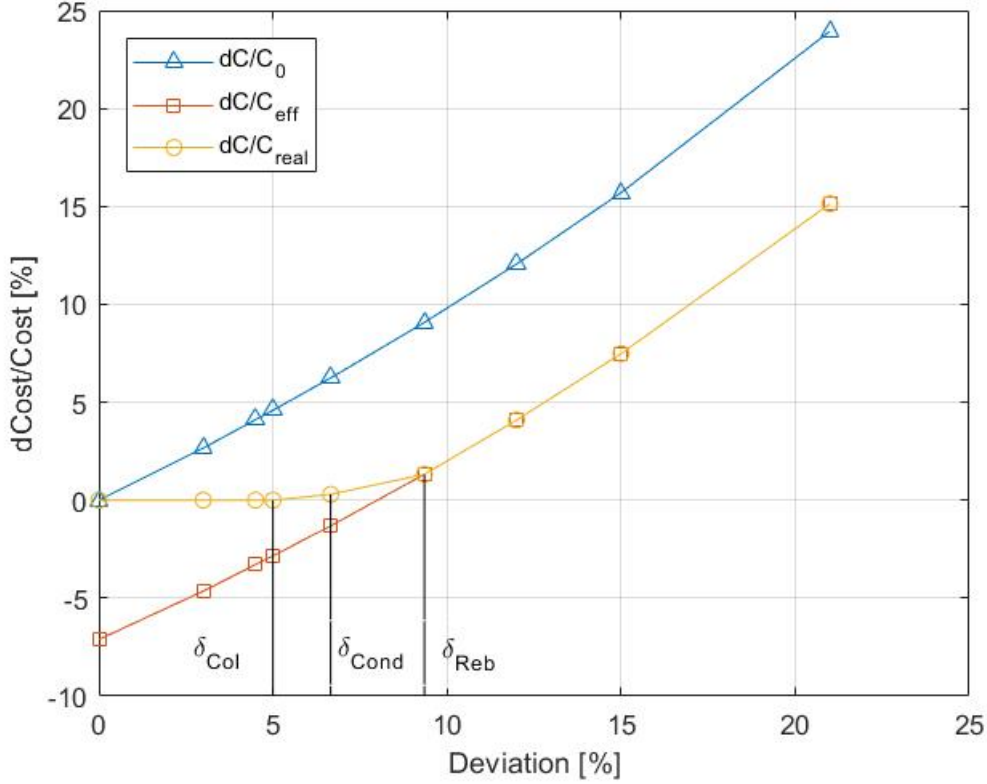


Fig. 2.9: Capital costs comparison (F_{SG})

Figures 2.10 and 2.11.

The resulting Resilience Index (RI) for this case study is then given by:

$$RI = \min_i \{|l_i^{max}|\} = 9.64 \quad (3.2)$$

First of all we can notice that there are no problems even if the intervals are only half-bounded because we're looking for the minimum of the maximum withstood perturbations. The ∞ values don't mean that we really calculated results for infinite percentage values of parameter deviation, but it means that the withstood percentage perturbation is large enough not to affect the flexibility analysis or enough to fulfill all the physically possible (not only expected) deviation range in that direction.

Then we can focus our attention on the limiting design factor that is, as for F_{SG} index, the column diameter whose corresponding parameter is the flooding velocity. The Resilience Index calculated this way has an higher value than the F_{SG} since we perturbate only one parameter at time leaving unchanged the others. Vice versa, in order to attain a given flexibility value, a smaller oversizing than F_{SG} case is needed.

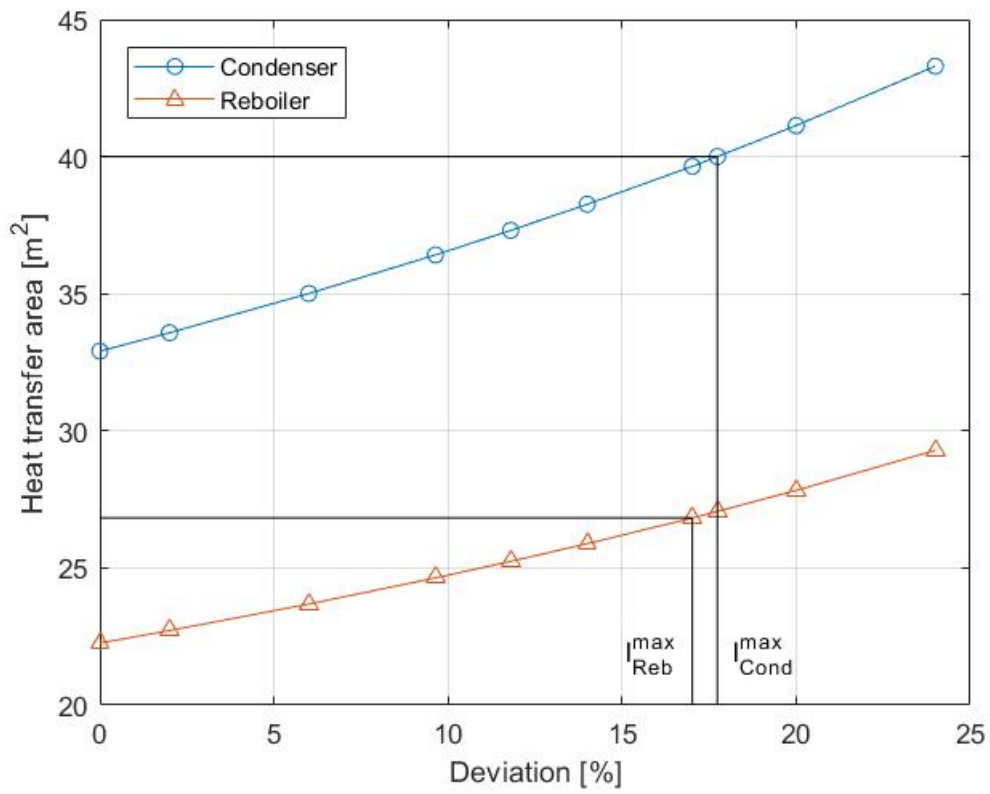
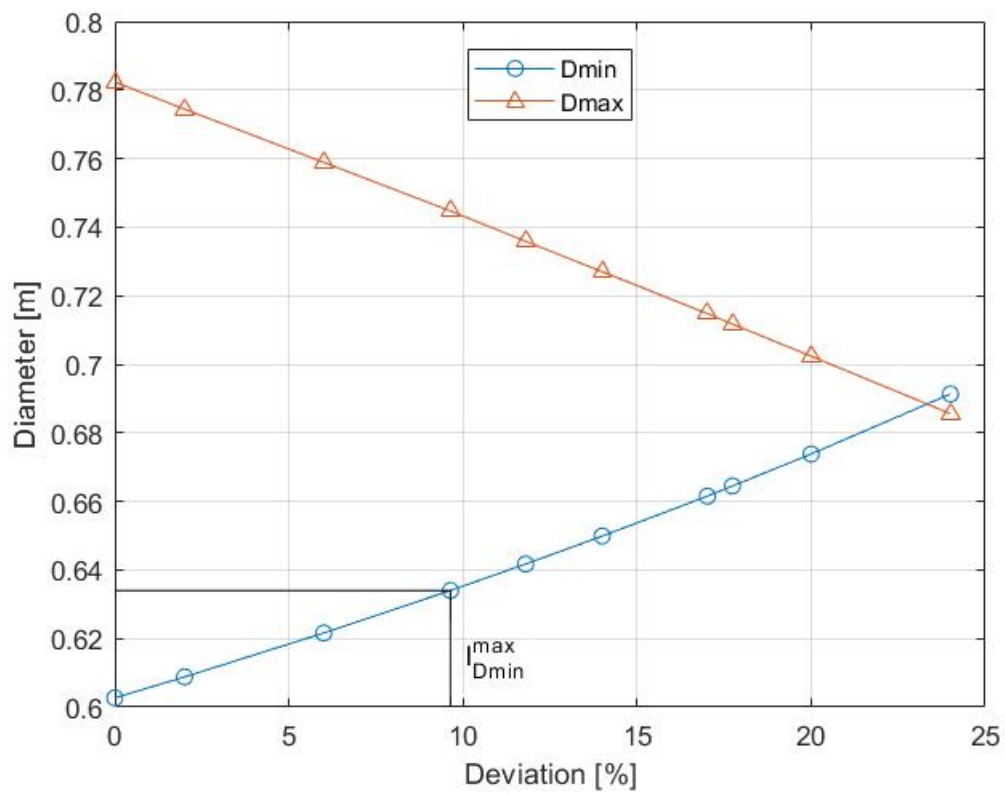
Even the crossover of the minimum and maximum diameter values, i.e. the completely infeasible conditions with a single diameter column, was more conser-

Parameter	Maximum deviation [%] l_i^{max+}	Minimum deviation [%] l_i^{max-}	Limiting constraint
Butane flowrate	11.80	∞	D_{min}
Pentane flowrate	81.00	∞	D_{min}
Inlet cooling water temperature	18.28	∞	A_{cond}
Condenser heat transfer coefficient	∞	17.74	A_{cond}
Reboiler heat transfer coefficient	∞	17.02	A_{reb}
Max vapor velocity	∞	9.64	D_{min}
Min vapor velocity	52.18	∞	D_{max}

Tab. 2.7: Allowed disturbances loads

Deviation [%]	Condenser area [m^2]	Reboiler area [m^2]	Minimum diameter max [m]	Maximum diameter min [m]
0.00	32.91	22.26	0.603	0.782
9.64	36.42	24.64	<u>0.634</u>	0.745
17.02	39.65	<u>26.82</u>	0.662	0,715
17.74	<u>40.00</u>	27.06	0.665	0.712
24.00	43.30	29.29	0.691	0.686

Tab. 2.8: Flexibility analysis results: RI

Fig. 2.10: Heat transfer areas (RI)Fig. 2.11: Column max & min diameters (RI)

vative in the F_{SG} analysis where it was about 13% (cf. Figure 2.7), while in the RI this condition is attained for a 24% (cf. Figure 2.11) flexibility more or less.

Moreover, it is worth noticing that, beside the column diameter, the second most constraining variable is the reboiler while for the F_{SG} analysis was the condenser. This is the most representative difference between the two indexes because the variables acting on the condenser are U_{cond} and T_w in both cases but, while in the RI analysis they are perturbed one at a time, in Swaney and Grossmann analysis they change all at once causing the equipment affected by an higher number of uncertain parameters (in this case the condenser) to be more critical.

As well as the Swaney & Grossmann index costs analysis, the capital costs trends (normalized to the lowest value) as function of RI flexibility are plotted for each equipment in Figure 2.12. All of them increase as flexibility increases (according with their size). The most expensive equipment is the Kettle reboiler that has a much more accurate technology than the other heat exchangers and that works under pressure, while the column is relatively cheap because of its small diameter.

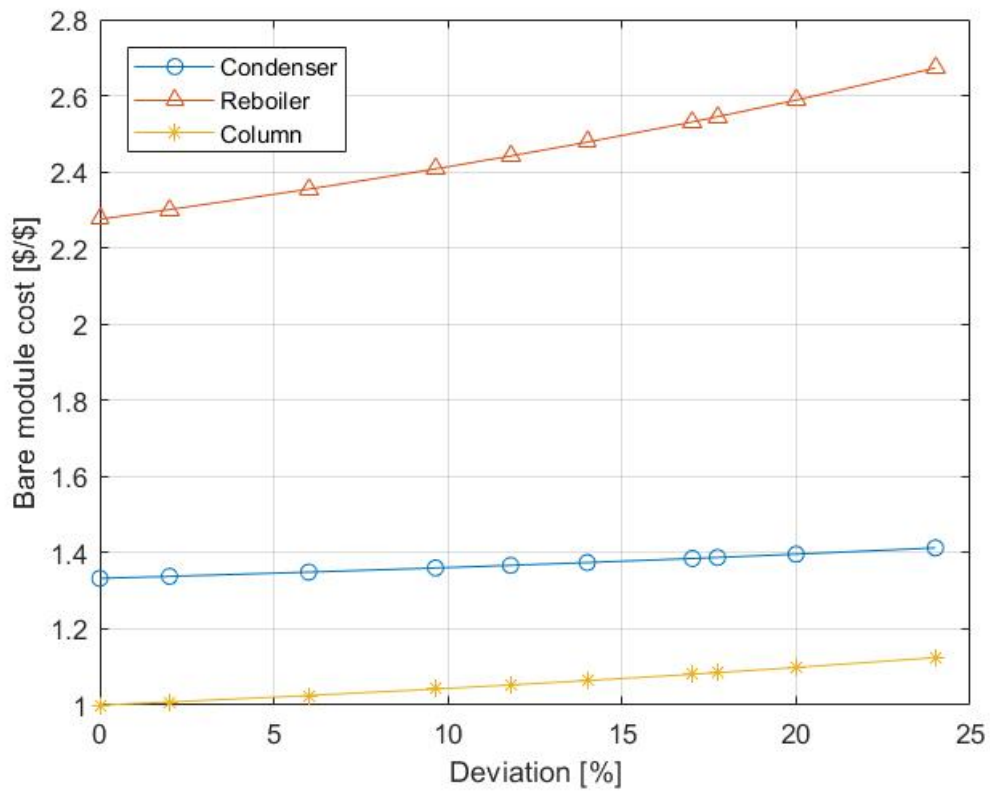
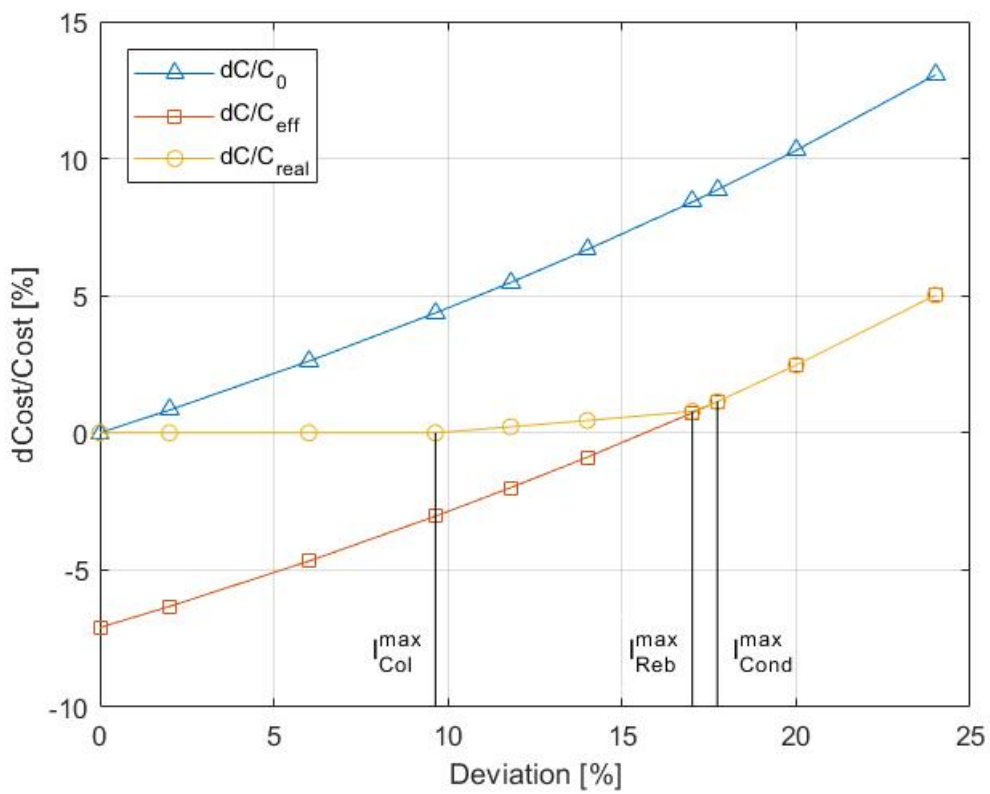
In Figure 2.13 the three series of percentage data as function of Resilience Index analogous to those in Figure 2.9 are reported.

Even in this case the trends are more linear, the differences between F_{SG} and RI indexes economic analysis reflects the differences highlighted in the equipment design analysis as well as the analogies, i.e. for a given flexibility value the capital cost is lower if we consider the Resilience Index flexibility. Obviously it doesn't mean that we can save money just by changing the index we use, it only means that by selecting a different index we are measuring different performances; so for each process the more suitable the index is the more accurate the economic analysis will be, where with the word "suitable" refers to the performances demanded to cope with the possible disturbances.

The Swaney and Grossmann flexibility measures the ability of the system to withstand an overall parameters deviation of $F_{SG} \cdot \Delta\theta^{k\pm\%}$, the Resilience Index measures the case of a single variable, it doesn't mind which one, deviation of $RI\%$, therefore, in order to find the most suitable index, we need to evaluate which of the two kinds of deviation our system is more likely to undergo to. This idea of "disturbance likelihood" leads us then to the stochastic characterization of the flexibility indexes discussed in the following section for the same debutanizer case study.

3.2 Stochastic indexes: SF and F_V

When we move from a deterministic point of view to a stochastic one we have to transform the idea of perturbation expected or not, defined by a well bounded deviation range, into a continuous function describing how much expected the deviation is. To do this we need to use a probability distribution function relating

Fig. 2.12: Equipment bare module cost (*RI*)Fig. 2.13: Capital costs comparison (*RI*)

a probability value to each condition “x”, i.e. the independent variable(s) (cf. Appendix C for more details).

The probability density function are usually parametric functions, the probability of the independent variable falling within a particular range of values is given by the integral of this variable’s PDF over that range. The probability density function is nonnegative everywhere and its integral over the entire space is equal to one.

Before going any further with the application of these principles to our debutanizer case study, a few observations about the chosen PDF and its properties will be remarked here below.

First of all, in order to univocally define the PDFs we need to set the parameters; the selected values are :

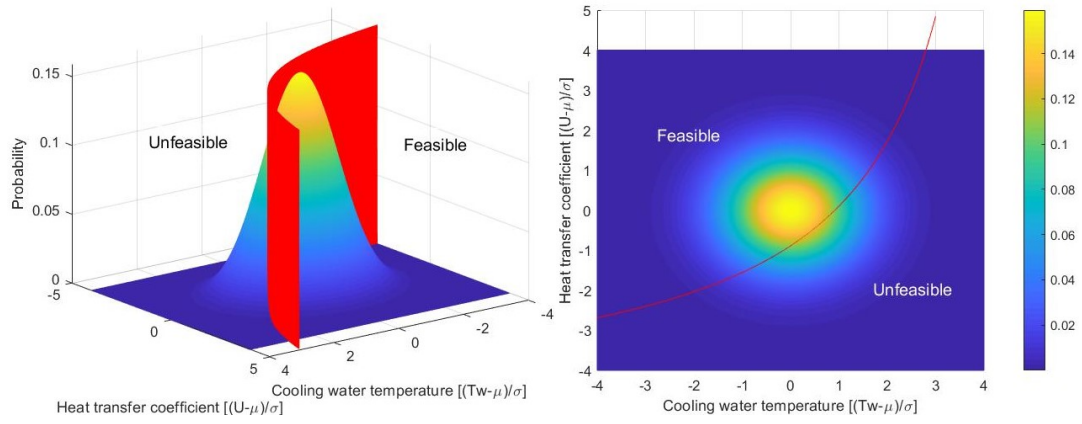
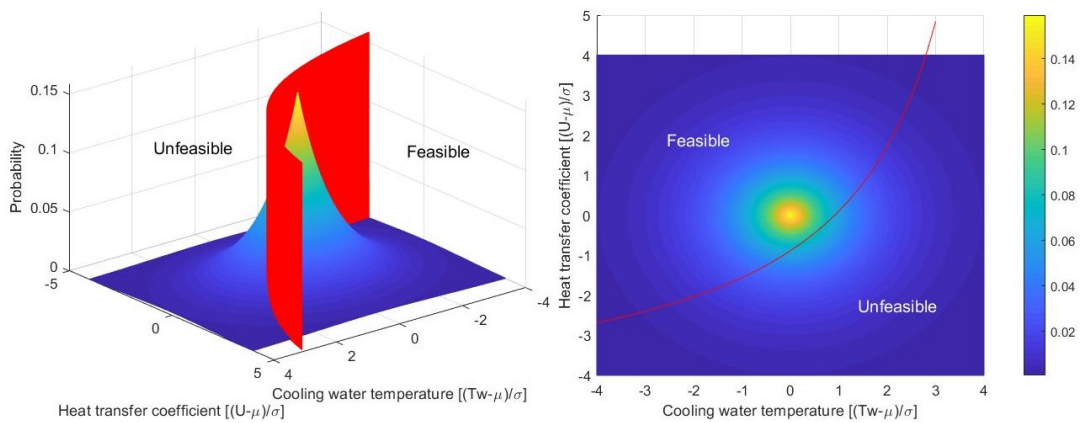
- μ = operating conditions for each variable;
- σ or $b = 20\%$ of μ for each variable.

For this case study a 20 % variance has been selected since it is about the maximum allowed individual deviation for the variables taken into account in the stochastic flexibility analysis. This choice makes the analysis sensible enough to appreciate the features of the coupling of flexibility and economics, that is the main goal of the paper. A very small σ value would result in a useless flexibility analysis since almost all possible perturbations would be withstood; on the other hand a higher σ value has poor reliability since variables uncertainty range would be too wide and a significant stochastic flexibility value would be never attained. Therefore 20 % results a good compromise allowing an analysis more sensible and unbiased by excessive optimism, keeping us as conservative as needed.

We have then to choose which type of PDFs would better describe the system under analysis. Probability reflects the state of the information therefore, since we actually have no data about the probability functions of our parameters deviations, the most general PDF possible should be used in order to have the more unbiased possible results. The condition of “general validity” is satisfied by the gaussian or normal probability distribution. It is symmetrical with respect to its mean and the 99.73% of cumulative probability falls in the range $[-3\sigma, +3\sigma]$.

For the sake of completeness, in order to prove that the results of the stochastic flexibility analysis are not qualitatively PDF dependent, it will be conducted with a different probability distribution function as well, i.e. the Laplace one. This distribution satisfies, in a sense, the same requirements needed by the system description, that is:

- the maximum probability is attained at the operating conditions;
- the probability value is not dependent on the deviation direction.

Fig. 2.14: Condenser SF : Normal PDFFig. 2.15: Condenser SF : Laplace PDF

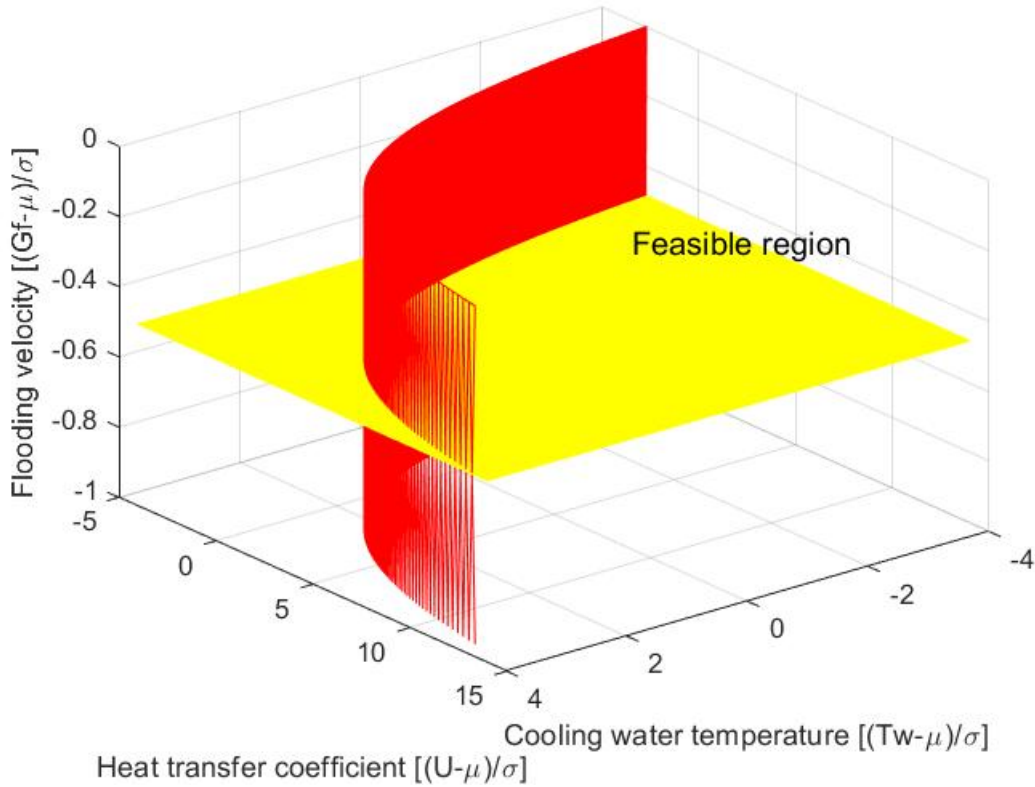


Fig. 2.16: 3D SF analysis domain

For further details about Normal and Laplace probability distribution functions cf. Appendix C.

In order to have a visual approach with the stochastic flexibility index meaning, a 2D analysis for the condenser perturbation has been performed first (Figures 2.14 and 2.15). Then, once dealt with it, the analysis is shifted to higher dimensions; it is nonetheless worth remarking that the analysis methodology is independent on the dimension of the problem. As we can notice, the two selected parameters, i.e. heat transfer coefficient and cooling water temperature, act on the same design variable, i.e. heat exchanger transfer area. Therefore a single constraint representing the heat balance is present.

However, since we don't want to perform the flexibility analysis of a heat exchanger, on one hand we need to increase the dimension of our problem on the other hand we don't want the computational effort to be too high. To match these two purposes we could, for instance, add the most constraining parameter (according to the previous flexibility analysis), i.e. the flooding velocity. This way we have a 3D domain with a variable (G_f) related to the column design (D_{min}) and the other two (T_w and U_{cond}) acting on the same design variable (A_{cond}) (Figure 2.16); the independence of the third parameter on the other two can be immediately noticed since the yellow plane, i.e. flooding constraint, is parallel to the $T_w \times U_{cond}$ plane.

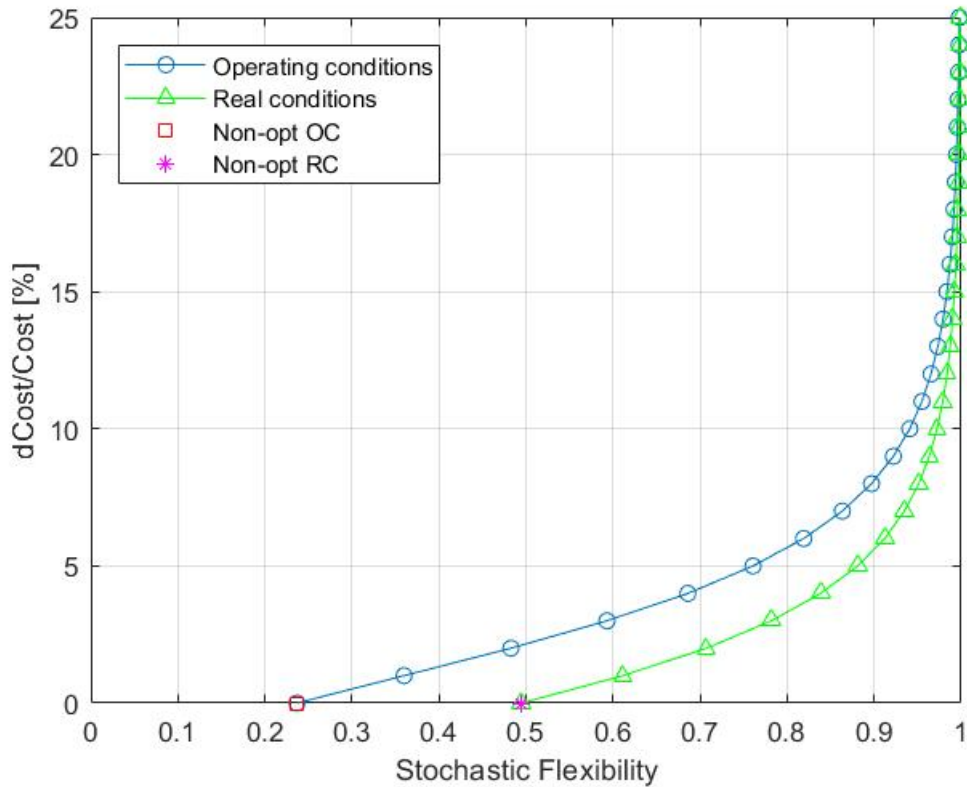


Fig. 2.17: SF results Normal PDF

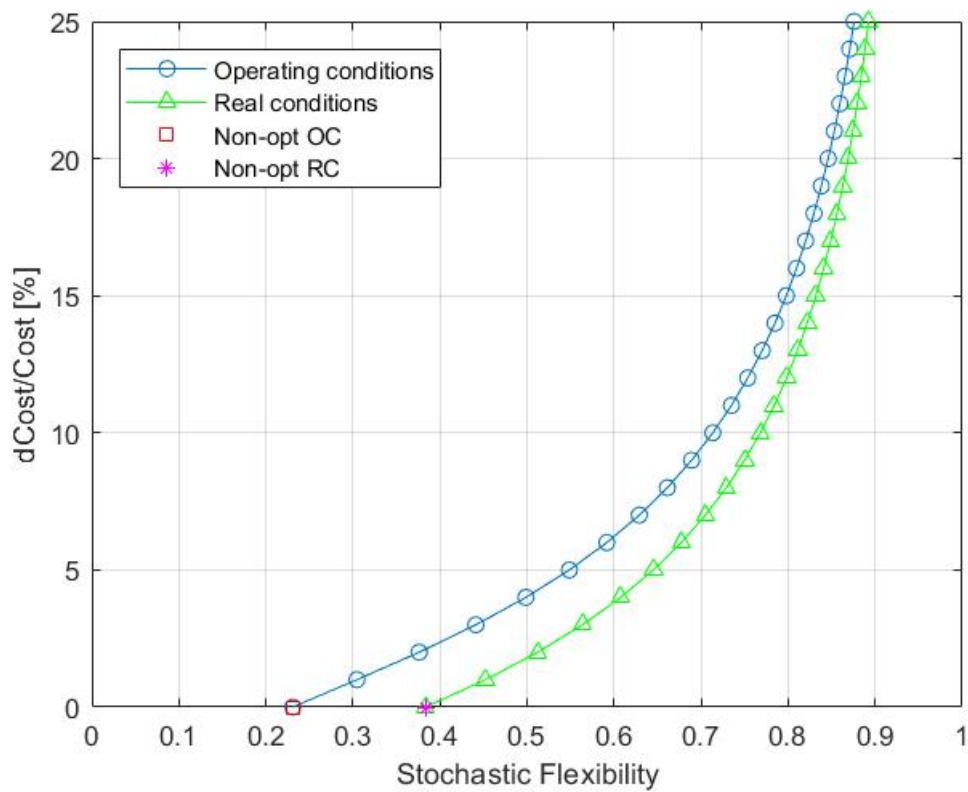
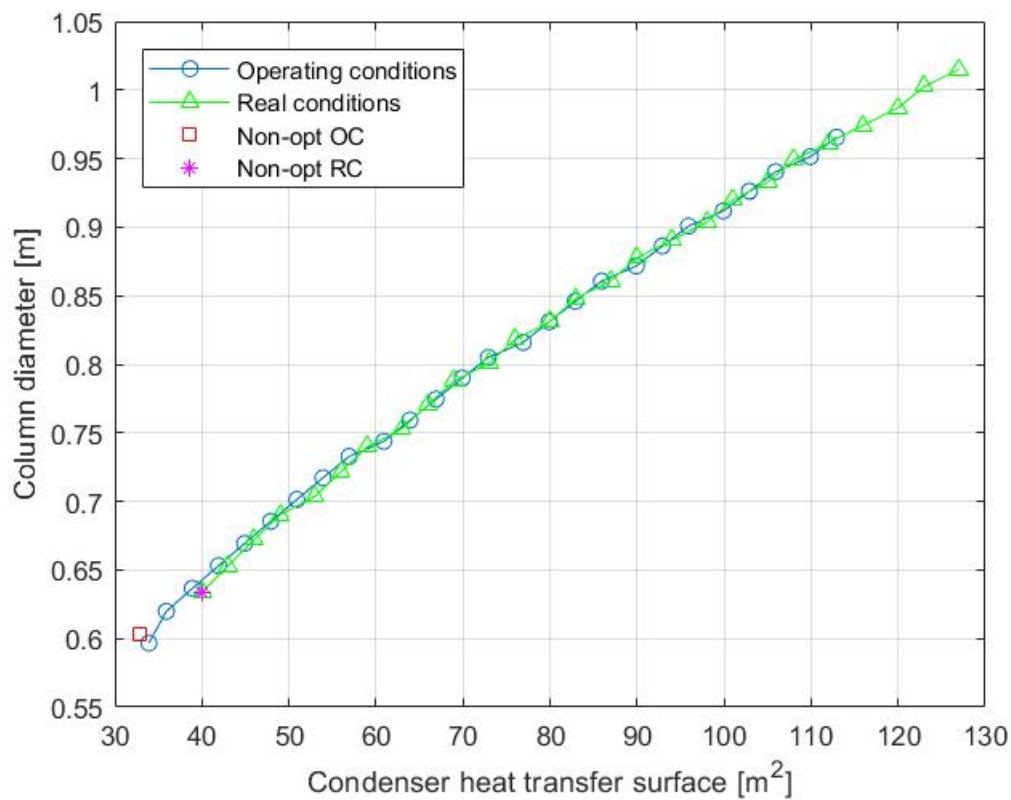
An additional difference between this index and the previous ones we've got to deal with is that, even if a given design defines univocally a stochastic flexibility value, a given stochastic flexibility value does not define univocally a system design. The two constraints can be shifted in several configuration keeping constant the value of the integral function indeed. Therefore we'll refer as the "x" stochastic flexibility value design to the optimal configuration that attains that value, where optimal simply means cheaper. This need of economic optimization directly links flexibility with design and economic aspects whose trends will be anticipated with respect to the sizing ones.

The results of the stochastic flexibility analysis for each 1% cost increase are reported in Figures 2.17 and 2.18, the optimal design variables in Figures 2.19 and 2.20.

First of all it's worth highlighting that, differently from previous flexibility indexes, the stochastic one has a non-zero value at operating conditions design.

Moreover the optimal design according to flexibility could be different from the operating conditions design or the economically optimal design.

An additional difference between SF and F_{SG} or RI is that its trend is highly non-linear if expressed as function of the equipment's size, that means that for big oversized equipment the flexibility increase due to a further oversizing is only slightly appreciable. The relative optimal oversizing trend between the condenser

Fig. 2.18: *SF* results Laplace PDFFig. 2.19: *SF* optimal sizing NDF

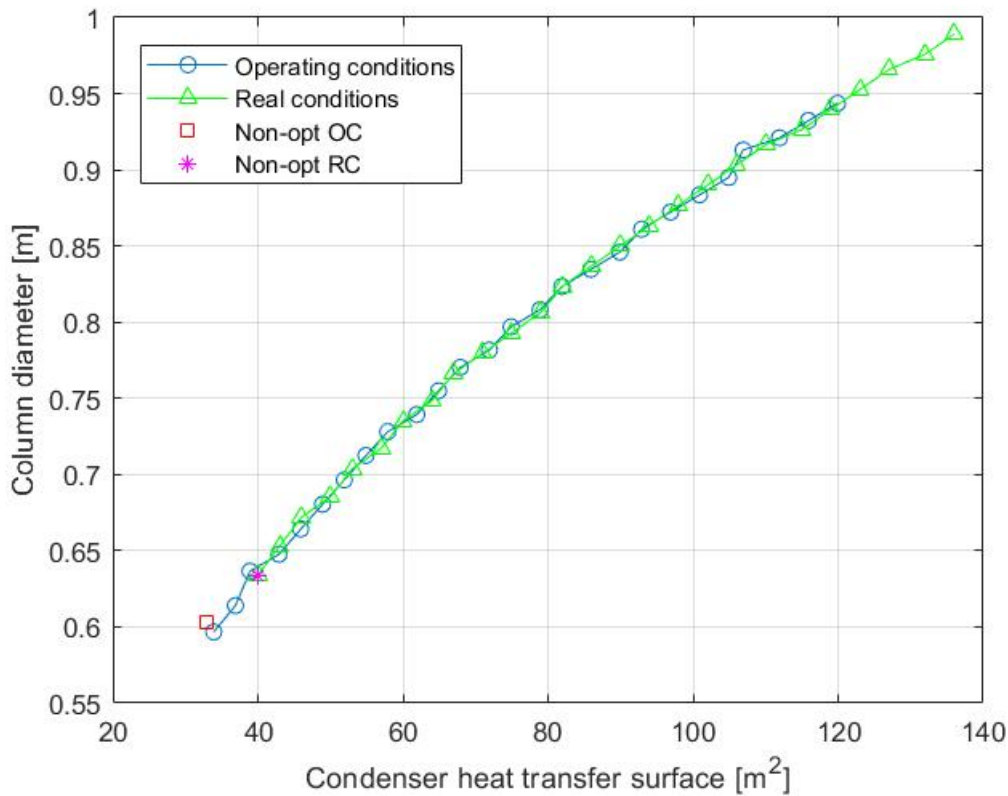


Fig. 2.20: SF optimal sizing LDF

and the column keeps being nonetheless almost linear and furthermore it follows the same line independently on the starting design condition as expected.

Finally if we compare the two different distributions results we can immediately notice that they reflect the nature of the distributions themselves. Laplace distribution converges more slowly than the Normal one, therefore the related SF approaches the value 1 only for a bigger oversizing. Nonetheless their trends are qualitatively as similar as the PDF are.

The same sizing related remarks are valid if we talk about costs since they're directly related.

For two different equipment design the starting points of the $\frac{dC}{C}$ vs. SF lines are different but, after a while, the ending branches of the two curves overlap each other approaching the asymptote.

Additional costs are higher for the Laplace distribution case than Normal distribution, as expected, because the deviation likelihood is slightly higher even far from the operating conditions.

Differently from F_{SG} and RI , costs increase as function of stochastic flexibility index shows a non-linear trend, this means that once a certain point of the curve has been passed the ratio between the increase in flexibility and costs starts declining fast.

The main purpose of Process System Engineering is to enhance the decision

making capability of the chemical engineer, therefore we'd like to identify the "certain point" after whom it's not worth keeping spending money in overdesign. The range of convenient oversizing is visible to the unaided eye: the first part of the curve gives a high flexibility increase with a small additional costs but the probability of the deviations that cannot be withstood is still relevant; on the other hand the last part, even withstanding almost the whole possible deviations, needs a consistent oversizing (i.e. additional costs) to be achieved. Finally we can then conclude that the middle range of the curve is a good compromise between high flexibility and affordable additional cost.

The thorough procedure we propose to assess the optimal range is based on the curve properties: tangent lines have almost the same slope (i.e. derivative) at the beginning and at the end of the curve while it considerably changes within the interval we're interested in.

The procedure then consists in plotting the ratio between the derivative calculated at each point and the derivative calculated at the previous one as illustrated in Figure 2.21 for the case of NDF and operating conditions.

This way, given the $\frac{dC}{C}$ vs. SF plot only, we can obtain a new plot whose trend shows a maximum corresponding to the value $SF = 0.9409$, i.e. 10% of additional cost.

However even the other values near there can be considered good conditions for a flexibility based design, more important than the optimal value itself is to avoid the conditions corresponding to very first and very last part of the plot.

The chronologically last flexibility index proposed in scientific literature is the volumetric flexibility index F_V . It is defined as the feasible fraction of the uncertain space, that is a line for 1D case, a surface for 2D case, a volume for 3D case and a hypervolume for higher dimensions.

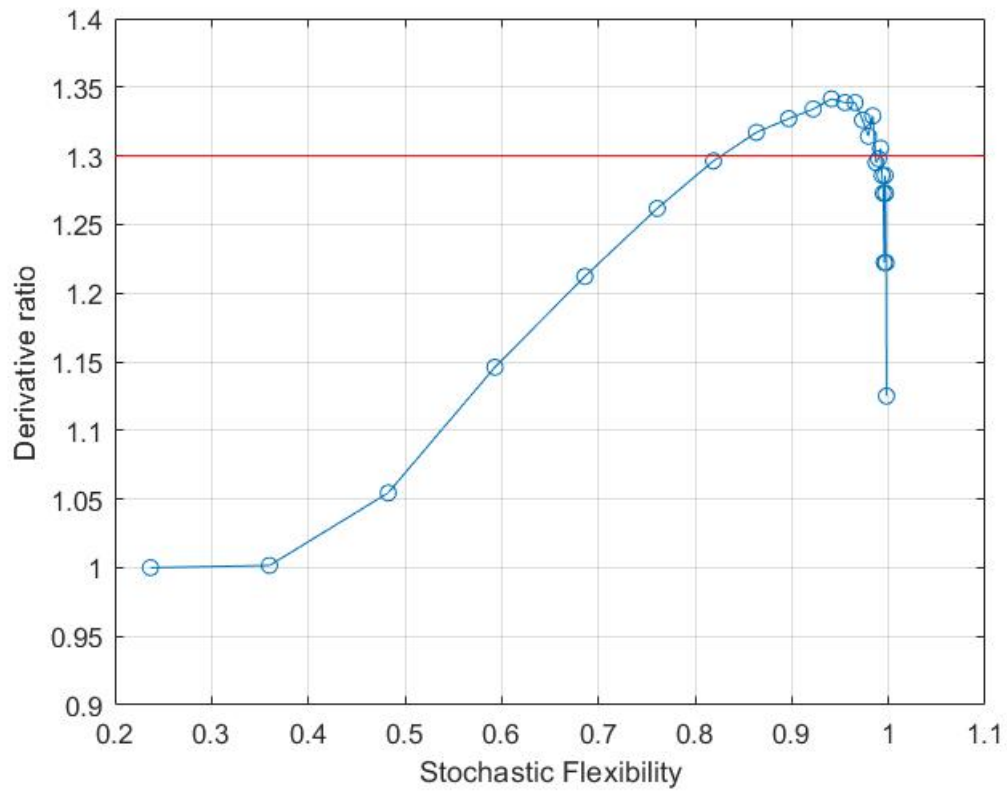
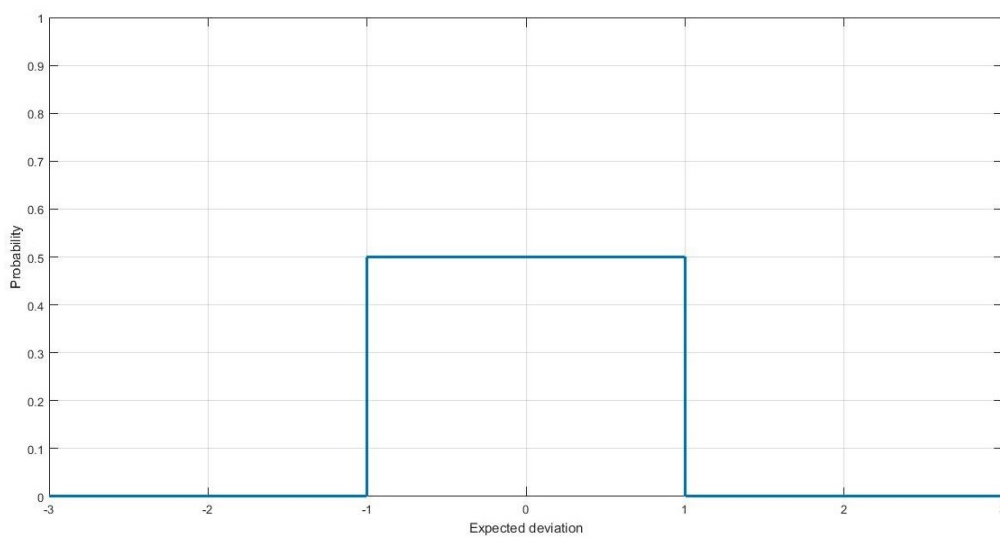
The reason why the volumetric flexibility index is included among the stochastic indexes is that it can be also thought as a SF index particular case whose deviation probability function is described by a step function (Figure 2.22) defined as:

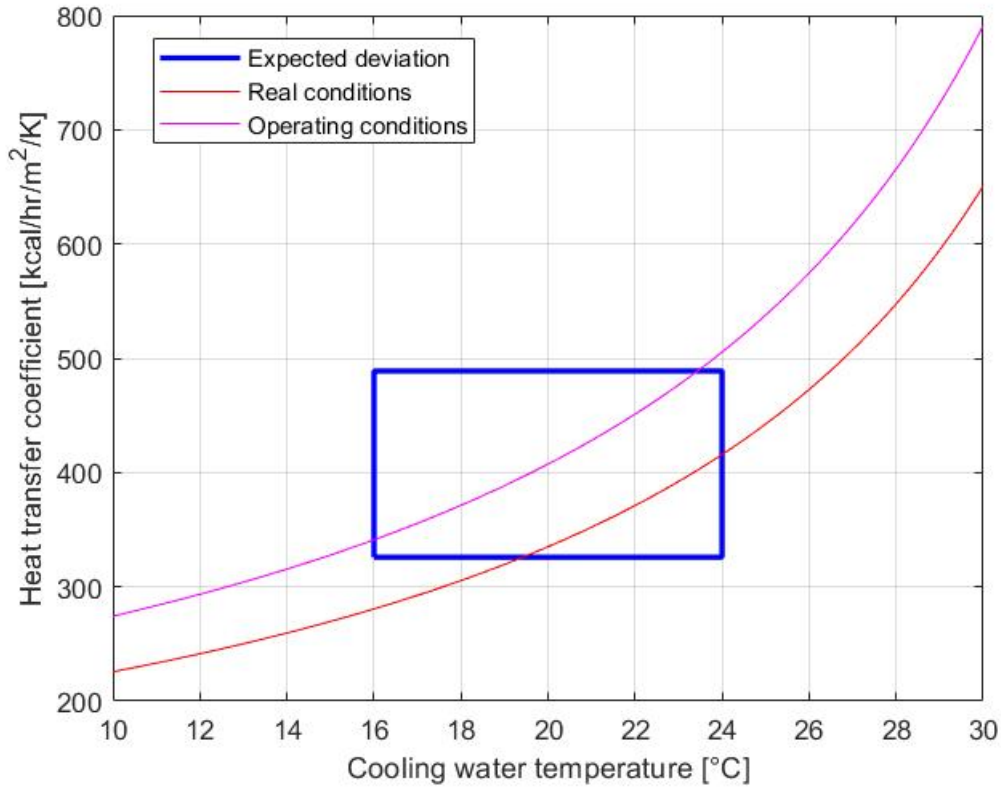
$$\begin{cases} \frac{1}{\prod_{i=1}^N (\theta_{iU} - \theta_{iL})} & \text{if } |x_i| < \Delta\theta_i^\pm \\ 0 & \text{if } |x_i| > \Delta\theta_i^\pm \end{cases} \quad (3.3)$$

therefore the same SF analysis rules and remarks can be applied.

Thus, in order to perform this kind of analysis, two parameters have to be set: the nominal point to the operating conditions and the expected deviation value to 20%.

For this index as well a 2D analysis for the condenser perturbation has been performed first (Figure 2.23) and then, once dealt with it, the analysis is shifted to higher dimensions. The same SF analysis remarks apply, i.e. the analysis methodology is independent on the dimension of the problem, the two selected parameters act on the same design variable, i.e. heat exchanger transfer area,

Fig. 2.21: $\frac{dC}{C}$ vs. SF Derivatives ratioFig. 2.22: F_V probability distribution function

Fig. 2.23: 2D F_V analysis

therefore a single constraint representing the heat balance is present.

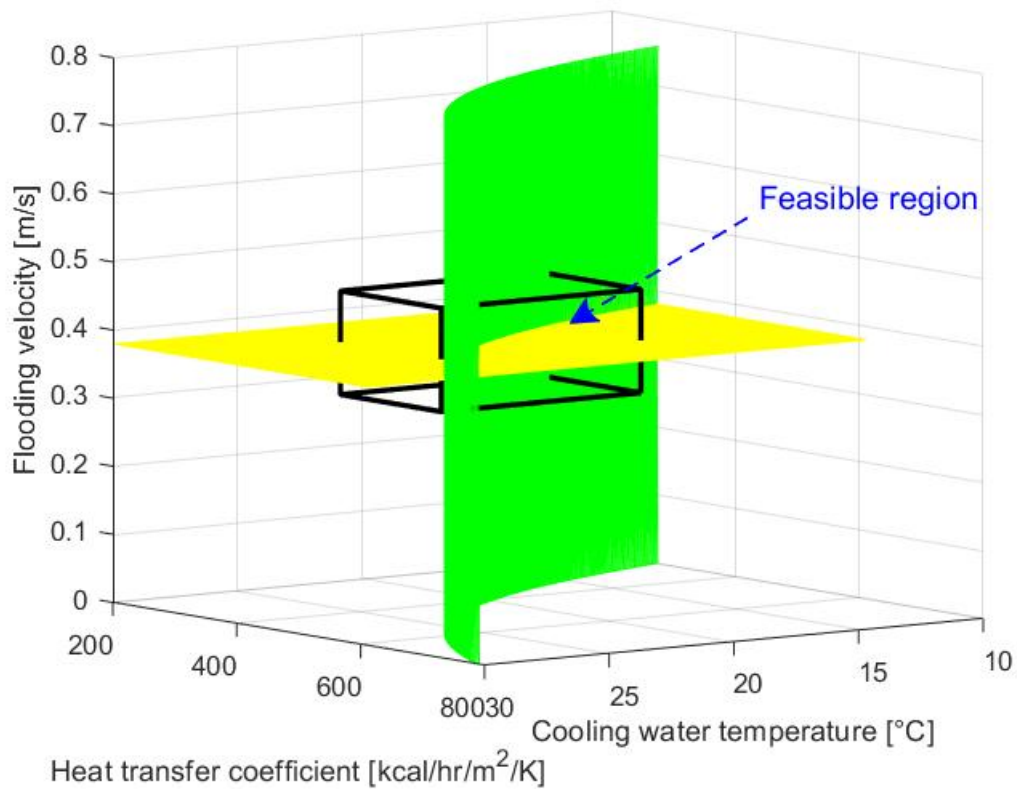
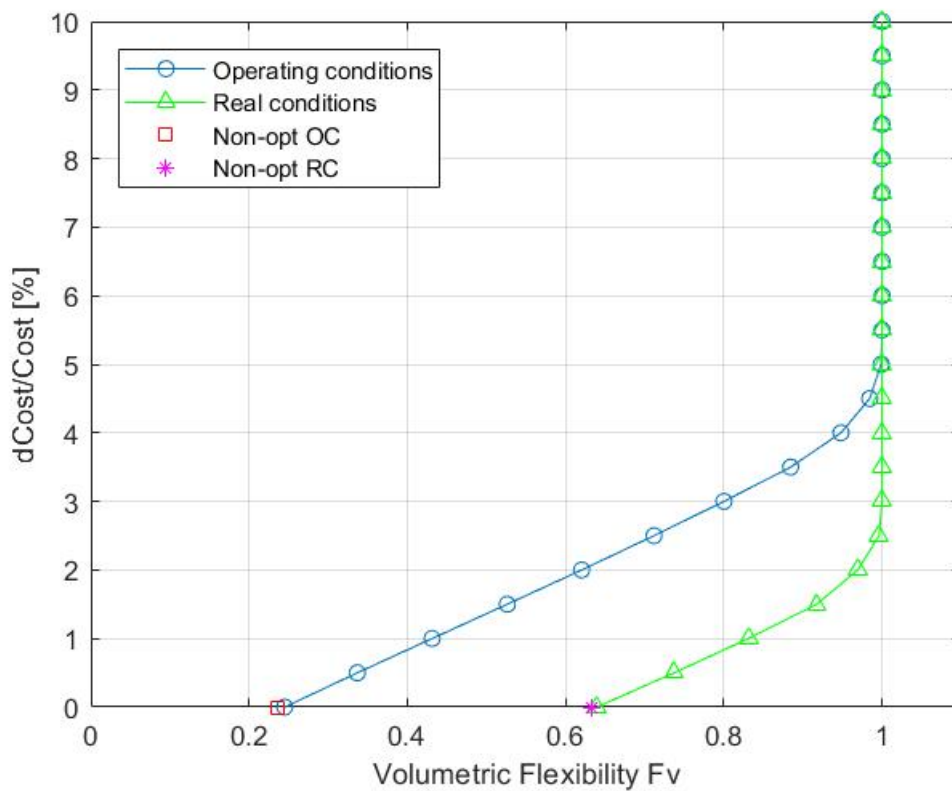
The results of this 2D case study are $F_V = 0.4714$ for operating conditions and $F_V = 0.8584$ for real conditions.

For the F_V index the analysis has been shifted in the same SF 3D domain (Figure 2.24). The flooding velocity has then been included in the analysis; since it is the most constraining parameter, it reduces significantly the feasibility of the system. The triple integral required by the SF index actually becomes a volume integral since the probability distribution is constant on each interval where it is defined; due to the complexity of PDF to be integrated in stochastic flexibility analysis, the computational effort for the F_V analysis prove much lower (seconds vs. minutes).

Even in this case a given volumetric flexibility value does not define univocally a system design, therefore the “x” volumetric flexibility value design refers to the optimal, i.e. cheapest, configuration that attains that value.

The results of the volumetric flexibility analysis for each 0.5 % cost increase are shown in Figures 2.25 and 2.26.

On one hand we have the analogies with the SF that are non-zero values at operating conditions, optimal sizing independent on the starting conditions and asymptote at $F_V = 1$. On the other hand we’ve got to notice that the trends of the F_V analysis results are rather peculiar and very distinctive of this kind of index.

Fig. 2.24: 3D F_V analysis domain - operating conditionsFig. 2.25: F_V analysis economic results

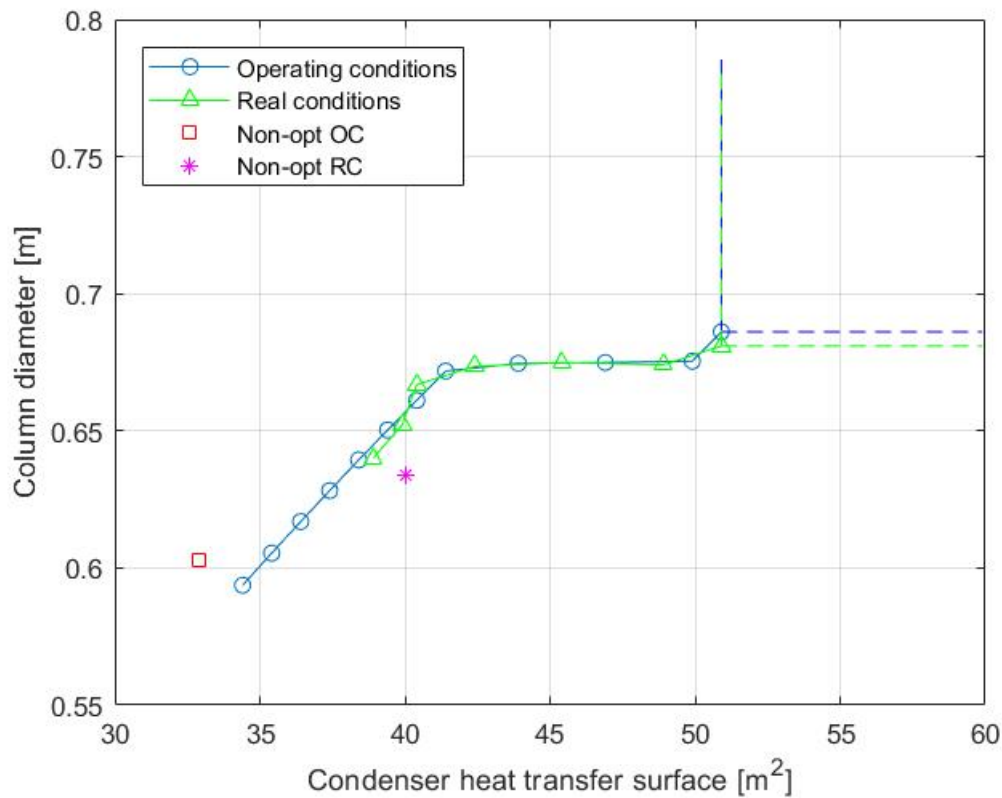


Fig. 2.26: F_V analysis optimal sizing

In Figure 2.26 we can mainly distinguish three zones:

1. Linear trend: in the very first overdesign part both the column diameter and condenser area affect the flexibility of the system, therefore the optimal design strategy is to split the investment according to the proportion expressed by the slope of the line.
2. Horizontal (or vertical) trend: after a while the flooding constraint is almost outside the uncertain parallelepiped. The only thing to do is then to shift the condenser constraint until it exits the parallelepiped as well. In the end a little adjustment of both the design variables is observed and the value $F_V = 1$ is finally attained.
3. Overpayment zone: after the $F_V = 1$ value has been achieved the whole uncertain domain is contained within the feasible boundaries therefore any additional oversizing is, considering flexibility, practically useless. The $A_{cond} = 50.90 \text{ m}^2$ and $D_{col} = 0.686 \text{ m}$ condition corresponds definitely the maximum achievable flexibility.

In the end it is worth remarking that the shape of the oversizing curve is strictly related to the system features and to the expected deviations, the flexibility analysis procedure has nonetheless general validity.

The cost related remarks are the direct consequence of the combination of sizes related ones. The increase in investment costs as function of volumetric flexibility shows an almost linear trend. Since the equivalent probability distribution has a constant value, the F_V index tendency results more similar to the F_{SG} and RI indexes one, even if the domain considerations, the way we compute its value and the properties of the oversizing curves practically make it analogous to the SF index.

In the end we can conclude that a 5.5% additional cost (w.r.t. operating conditions) is definitely the maximum investment worth to be done according to a flexibility improvement purpose.

4 Conclusion

After these four flexibility analysis an indexes comparison is necessary to summarize and comment the relationships between all the results.

First of all we can mainly distinguish two typologies of indexes according to their approach towards the feasible domain: the indexes assessing the minimum of the maximum performance and the ones giving a global assessment within the uncertain or feasible domain.

The F_{SG} and RI indexes are generally more conservative, they're based on n-D hyperpolygons that can be inscribed within the feasible domain, where n is the dimension of the uncertain zone (i.e. the number of possibly perturbed parameters). The first one is more suitable if the expected perturbation involves several variables at the same time, the second one for bigger variations referred to single variables. However, they're both very conservative (specially F_{SG}) since the described geometrical objects can only scale up or down but their structure is not flexible at all, it doesn't coast the domain, it just stops whether one point is tangent. This way two completely different systems could have the same flexibility index value just because they allow the same perturbation intensity for the most constraining parameter only; on the other hand given a certain starting design, a flexibility index defines univocally the system configuration.

On the other hand we have more optimistic indexes with non-null value at operating conditions that require integration to be calculated: SF and F_V . Even in this case one of them refers to an expected deviation while the other one needs an a priori knowledge or estimation of perturbation likelihood. F_V results are similar to the linear ones until the index achieves its maximum value of 1 after whom every kind of oversizing is useless; on the other hand the SF index is very sensitive and smart, it takes into account all the possible deviations proportionally to their likelihood, showing an hyperbolic trend in oversizing/cost vs. flexibility plots that reflects well the real capability of the system to better withstand small and likely deviations than big and unlikely ones. Several configurations may have the same SF or F_V index value since they assess a global system property, not the

	Pros/Cons	F_{SG}	RI	SF	F_V
Need for data	Expected deviation	-	+	+	-
	Feasibility region outline	-/+	-/+	-	-
	Probability distribution			-	
	Bounded domain	-/+	-/+	+	+
Computational effort	Vertex analysis	+	+	-	-
	Computational effort	++	+	4+	++
Results accuracy	Conservative	-	-/+	+	+
	Accuracy	-	-/+	+	-/+

Tab. 2.9: Steady state flexibility indexes comparison

most constraining one; therefore during the flexibility assessment we could need to solve an optimization problem according to the analysis purpose.

In the end it's worth remarking that the value of F_{SG} and F_V strictly depends on the expected deviations, nevertheless F_{SG} can be generalized and compared to the whole feasible domain as shown while F_V cannot.

Then, from a design point of view we can definitely conclude that the most suitable flexibility index for the particular analyzed system is a function of the expected deviation nature.

An advice of general validity is to perform the flexibility analysis using more than one index, combining this way their advantages; for instance the first two indexes are quite easy to compute while the ones requiring an integral calculation have a higher computational effort demand. Thus we can perform the flexibility analysis with F_{SG} or RI first in order to identify the most constraining variables in order to be able to reduce the dimension of the problem and perform the SF or F_V analysis on a smaller domain. Obviously this is a good procedure if some parameters perturbations affect variables whose constraints are very loose; if the order of magnitude of all the F_{SG_i} or RI_i is almost the same, this preliminary analysis is of little help since we cannot be sure that the most constraining variable for one index will be the most constraining for the other indexes as well unless much less relevant deviations are allowed with respect to the others.

In order to compare the four indexes more immediately, the Table 2.9 resuming all their main features has been outlined.

On the other hand, from an economic perspective, the introduction of the Capital costs vs. Flexibility relationship and its relative plots let the decision maker, i.e. the engineering, take a more informed decision whatever the adopted flexibility index. Moreover, it clearly shows how an a priori flexibility analysis during the design phase could have allowed to save part of the investment keeping unchanged the flexibility performance of the system.

A List of acronyms and symbols

Symbol	Definition	Unit
A	Characteristic dimension	m^n
A_{cond}	Condenser heat transfer area	m^2
C_{BM}	Equipment bare module cost	\$
C_p^0	Purchase equipment cost in base conditions	\$
CDF	Cumulative distribution function	Function
d	Design variables	/
D_{col}	Column diameter	m
D_{min}	Minimum column diameter	m
DF	Dynamic flexibility index	1
f_j	Inequality constraint	Function
F_4	Butane partial flowrate	mol/s
F_5	Pentane partial flowrate	mol/s
F_{BM}	Bare module factor	1
F_M	Material factor	1
F_P	Pressure factor	1
F_q	Column trays factor	1
F_{SG}	Swaney & Grossmann flexibility index	1
F_V	Lai & Hui flexibility index	1
G_f	Flooding velocity	m/s
G_w	Weeping velocity	m/s
h	Equality constraint	Function
$l_i^{max\pm}, l_i^\pm$	(Maximum) i-th direction disturbance load	1
LDF	Laplace distribution function	Function
$M\&S$	Marshall & Swift cost index	1
N, N_r, N_s	Overall, rectifying and stripping stages	1
NDF	Normal distribution function	Function
P	Pressure	Pa
Pr	Probability	1
PDF	Probability distribution function	Function

RI	Resilience index	1
S_e	Polygonal feasible space approximation	/
S_f	Feasible space	/
SF	Stochastic flexibility index	1
T	F_{SG} n-D hyperrectangle	/
T_w	Inlet cooling water temperature	°C
U_{cond}	Condenser heat transfer coefficient	$W/m^2/K$
U_{reb}	Reboiler heat transfer coefficient	$W/m^2/K$
V_0	F_V uncertain volume	/
V_e	Polygonal feasible volume approximation	/
V_f	Feasible volume	/
z	Control variables	/
Z	Control variables space	/
z^U, z^L	Control variables upper and lower limits	/

Greek letters	Definition	Unit
δ	Hyperrectangle vs. expected deviation ratio	1
δ^k	K-th rectangle ratio	1
θ^k	Uncertain parameters values	/
θ^N	Nominal conditions	/
$\Delta\theta^{k\pm}$	Expected deviation	1
θ_{iU}, θ_{iL}	F_V upper and lower expected deviation	1
μ	PDF mean value	1
σ	PDF variance	1
χ	Most restrictive dynamic constraint	Function
Ψ	Feasible space	/

Equipment	Typology	K_1	K_2	K_3	A
Heat exchanger	Fixed tubes	4.3247	-0.3030	0.1634	Heat transfer area [m^2]
	Kettle	4.4646	-0.5277	0.3955	Heat transfer area [m^2]
Columns (vessel)	Packed/tray	3.4974	0.4485	0.1074	Volume [m^3]
Trays	Sieved	2.9949	0.4465	0.3961	Cross sectional area [m^2]

Tab. 2.10: Equipment cost in base conditions parameters

B Capital costs estimations

In order to evaluate the investment cost required for the whole system or make any kind of economic consideration and comparison, we need to estimate the costs of every single equipment.

For this purpose the Guthrie-Ulrich-Navarrete correlations described in the next paragraphs will be used [15, 16, 17, 18].

B.1 Purchase equipment cost in base conditions

The purchase equipment cost in base conditions is obtained by means of the following equation:

$$\log_{10}(C_P^0[\$]) = K_1 + K_2 \cdot \log_{10}(A) + K_3 \cdot [\log_{10}(A)]^2 \quad (\text{B.1})$$

where A is the characteristic dimension and the K_i coefficients are relative to the equipment typology (cf. Table 2.10).

The provided coefficients refer to the year 2001 and to a M&S index equal to 1110. In order to update the costs value to the year 2016 we'll refer to a M&S index equal to 1245.2 by means of the correlation:

$$C_{P,2}^0 = \frac{M\&S_2}{M\&S_1} \cdot C_{P,1}^0 \quad (\text{B.2})$$

B.2 Bare module cost

The equipment bare module cost can be calculated according to the following correlation:

$$C_{BM} = C_P^0 \cdot F_{BM} \quad (\text{B.3})$$

Equipment	Typology	B_1	B_2	F_M	F_P
Heat exchanger	Fixed tubes	1.63	1.66	1	1
	Kettle	1.63	1.66	1	$F_{P,Kettle}$
Columns/vessel	/	2.25	1.82	1	1
Pumps	Centrifugal	1.89	1.35	1.5	1

Tab. 2.11: Bare module parameters

where the bare module factor is given by:

$$F_{BM} = B_1 + B_2 \cdot F_M \cdot F_P \quad (\text{B.4})$$

The F_M and F_P factors refers to the actual constructions materials and operating pressure while the B_i coefficients refers to the equipment typology (cf. Table 2.11).

The $F_{P,Kettle}$ value is given by:

$$\log_{10}(F_P) = 0.03881 - 0.11272 \cdot \log_{10}(P) + 0.08183 \cdot [\log_{10}(P)]^2 \quad (\text{B.5})$$

where P is the relative pressure in 10^5 Pascal.

For column trays bare module cost a slightly different correlation should be used:

$$C_{BM} = N \cdot C_P^0 \cdot F'_{BM} \cdot F_q \quad (\text{B.6})$$

where N is the real trays number, $F_{BM} = 1$ e F_q is given by the correlation:

$$\log_{10}(F_q) = 0.4771 + 0.08561 \cdot \log_{10}(N) - 0.3473 \cdot [\log_{10}(N)]^2 \quad \text{if } N < 20 \quad (\text{B.7})$$

$$F_q = 1 \quad \text{if } N \geq 20 \quad (\text{B.8})$$

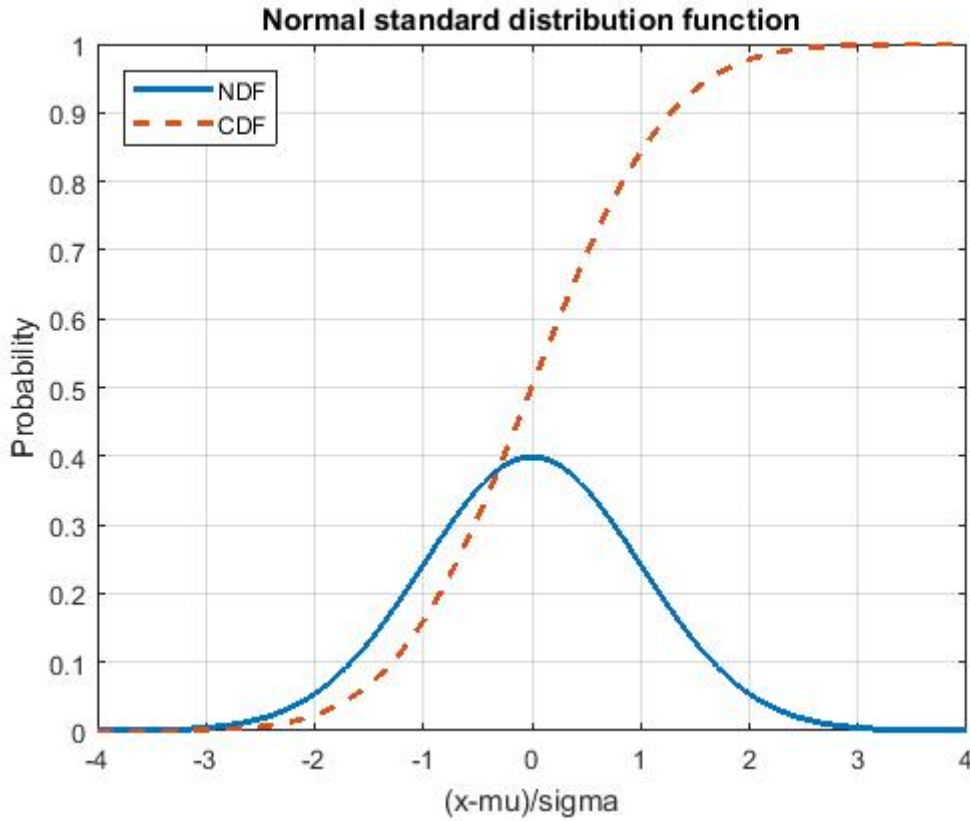


Fig. 2.27: 1D NDF and its CDF

C Probability distributions

C.1 Normal distribution function

As already mentioned, the condition of “general validity” is represented by the gaussian or normal probability distribution. It is symmetrical with respect to its mean and the 99.73% of cumulative probability falls in the range $[-3\sigma, +3\sigma]$.

The single variable Normal PDF (Figure 2.27) states as:

$$P(x) = \frac{1}{\sigma\sqrt{2\pi}} e^{-\frac{(x-\mu)^2}{2\sigma^2}} \quad (\text{C.1})$$

where μ is the mean and σ is the variance.

The bivariate Normal PDF (Figure 2.28), for a correlation between the variables $\rho = 0$, states as:

$$P(x) = \frac{1}{2\pi\sigma_1\sigma_2} e^{-\frac{y}{2}} \quad (\text{C.2})$$

where y is given by:

$$y = \frac{(x_1 - \mu_1)^2}{\sigma_1^2} + \frac{(x_2 - \mu_2)^2}{\sigma_2^2} \quad (\text{C.3})$$

Finally the most general n-variables normal PDF with can be defined as:

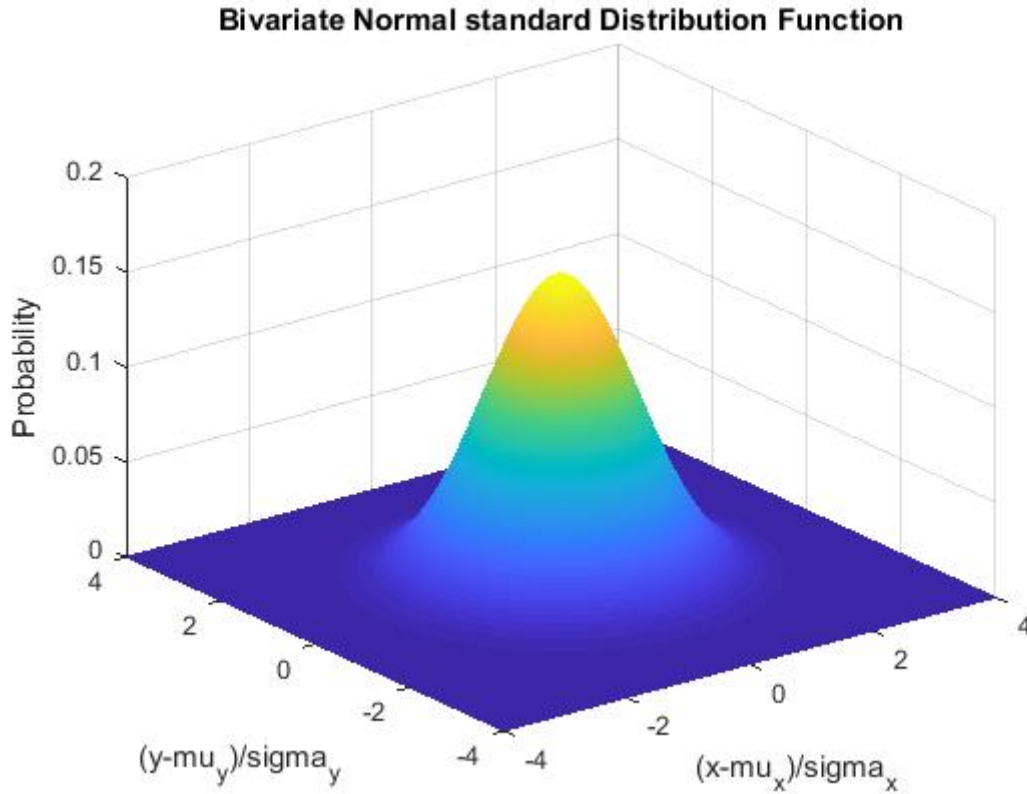


Fig. 2.28: 2D NDF

$$P(x) = \left(\frac{1}{2\pi}\right)^{n/2} \cdot |\Sigma|^{-\frac{1}{2}} \cdot e^{-\frac{1}{2} \cdot (x-\mu)' \Sigma^{-1} (x-\mu)} \quad (\text{C.4})$$

where Σ is the variance-covariance matrix, Σ^{-1} its inverse and $|\Sigma|$ its determinant.

Moreover we can standardize, i.e. reconstruct to a 0 mean value and variance equal to 1 (variance-covariance matrix equal to the identity matrix), the normal distribution by means of the independent variable substitution:

$$z = \frac{x - \mu}{\sigma} \quad (\text{C.5})$$

obtaining:

$$P(z) = \left(\frac{1}{2\pi}\right)^{n/2} \cdot |I|^{-\frac{1}{2}} \cdot e^{-\frac{1}{2} \cdot z' \cdot I \cdot z} \quad (\text{C.6})$$

for a general n variables standard normal probability distribution [19].

This transformation besides making the calculations easier allows to compare variables with different dimensions, e.g. temperature vs. flowrate vs. velocity etc.

The boundaries of the feasibility domain, if analytically available, have then to be rewritten as functions of the new variable z by inverting the equation C.5.

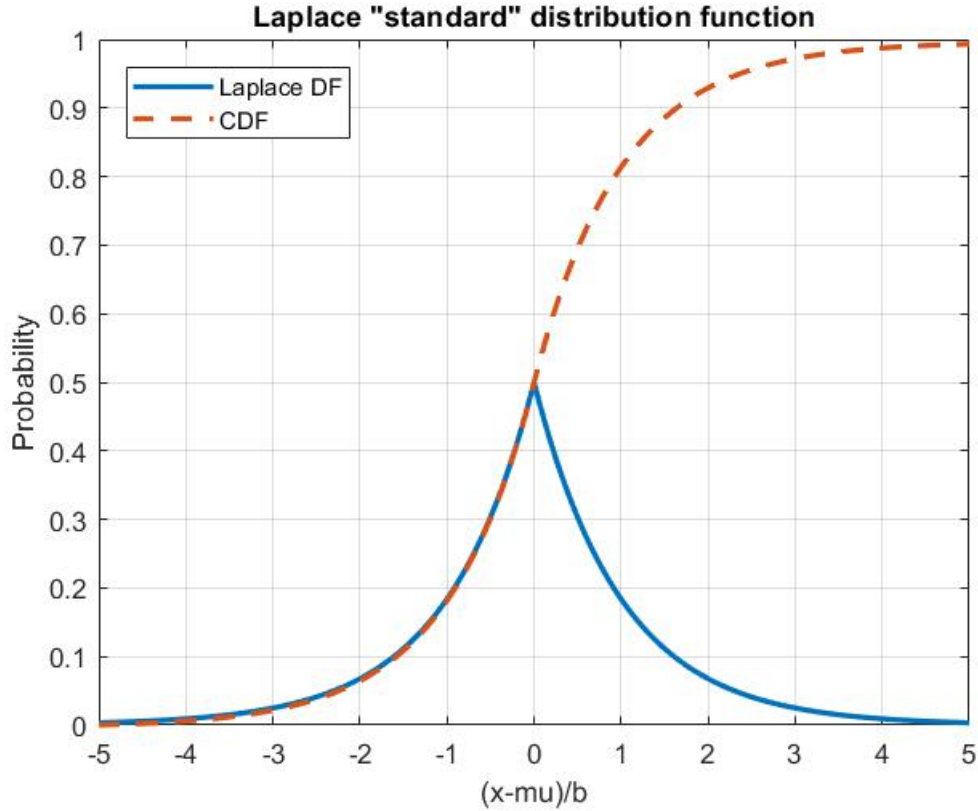


Fig. 2.29: 1D Laplace DF and its CDF

C.2 Laplace distribution function

The second distribution function used for the stochastic flexibility analysis is the so called Laplace PDF.

This distribution satisfies, in a sense, the same requirements needed by the system description, that is:

- the maximum probability is attained at the operating conditions;
- the probability value is not dependent on the deviation direction.

The analytical expression of the single variable Laplace PDF (Figure 2.29) states as:

$$P(x) = \frac{1}{2 \cdot b} e^{-\frac{|x-\mu|}{b}} \quad (\text{C.7})$$

where μ is the mean and b is the diversity local parameter.

Even in this case we can standardize the distribution, i.e. reconvert to a 0 mean value and diversity parameter equal to 1 by means of the independent variable substitution:

$$z = \frac{x - \mu}{\sigma} \quad (\text{C.8})$$

obtaining:

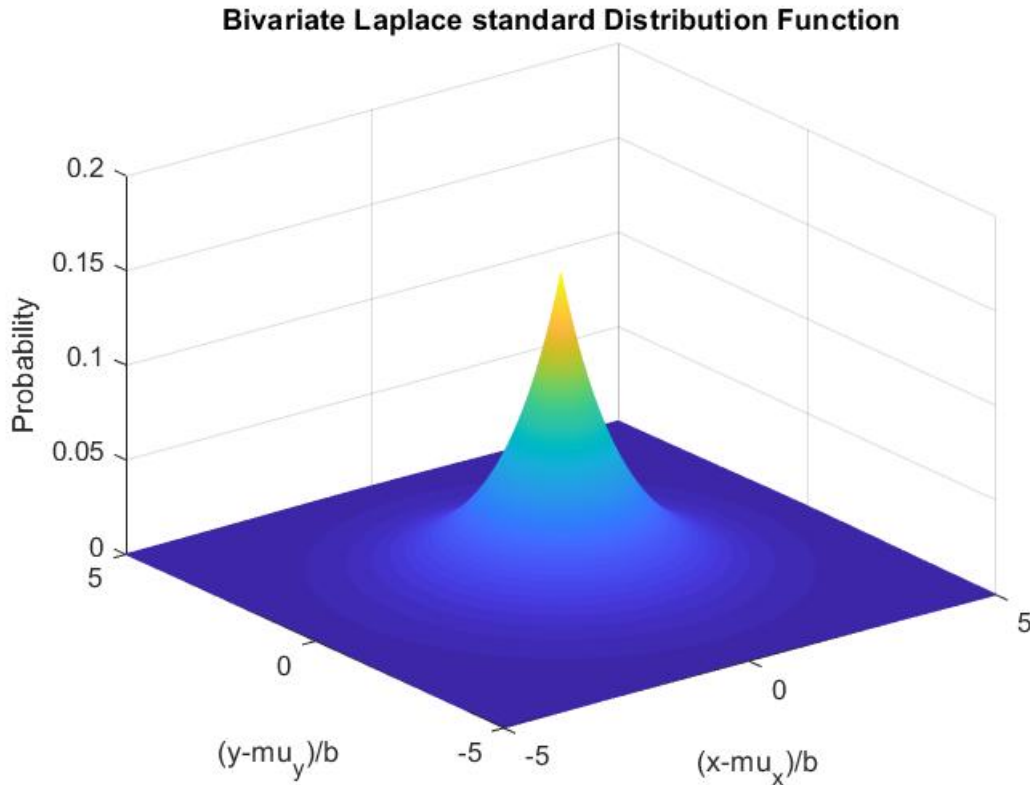


Fig. 2.30: 2D Laplace DF

$$P(z) = \frac{1}{2}e^{-|z|} \quad (\text{C.9})$$

Moreover, keeping in mind that:

$$|a| = \sqrt{a^2} \quad (\text{C.10})$$

the trivariate Laplace PDF (for the bivariate cf. Figure 2.30), for a correlation between the variables $\rho = 0$, states as:

$$P(x) = \frac{1}{8\pi}e^{-\sqrt{x_1^2+x_2^2+x_3^2}} \quad (\text{C.11})$$

The Laplace distribution function converges more slowly than the normal distribution, therefore we expect a lower flexibility increase by increasing the sizing, i.e. the costs.

References

- [1] P. M. Hoch and A. M. Eliceche, 'Flexibility Analysis Leads to a Sizing Strategy in Distillation Columns', *Computers & Chemical Engineering*, 20 (1996), S139–44 <[https://doi.org/10.1016/0098-1354\(96\)00034-8](https://doi.org/10.1016/0098-1354(96)00034-8)>.
- [2] R.E. Swaney and I.E. Grossmann, 'An Index for Operational Flexibility in Chemical Process Design. Part I: Formulation and Theory', *AIChE Journal*, 31 (1985), 621–30 <<https://doi.org/10.1002/aic.690310412>>.
- [3] Ak Saboo, M. Morari, and Dc Woodcock, 'Design of Resilient Processing Plants .8. a Resilience Index for Heat-Exchanger Networks', *Chemical Engineering Science*, 40.8 (1985), 1553–65 <[https://doi.org/10.1016/0009-2509\(85\)80097-X](https://doi.org/10.1016/0009-2509(85)80097-X)>.
- [4] Ignacio Grossmann and M. Morari, 'Operability, Resiliency, and Flexibility: Process Design Objectives for a Changing World', Department of Chemical Engineering, 1983 <<http://repository.cmu.edu/cheme/65>>.
- [5] Ignacio E. Grossmann, Christodoulos A. Floudas, 'Active constraint strategy for flexibility analysis in chemical processes', *Computers & Chemical Engineering*, 11, no. 6 (1 January 1987): 675–93. [https://doi.org/10.1016/0098-1354\(87\)87011-4](https://doi.org/10.1016/0098-1354(87)87011-4).
- [6] E. N. Pistikopoulos and T. A. Mazzuchi, 'A Novel Flexibility Analysis Approach for Processes with Stochastic Parameters', *Computers & Chemical Engineering*, 14.9 (1990), 991–1000 <[https://doi.org/10.1016/0098-1354\(90\)87055-T](https://doi.org/10.1016/0098-1354(90)87055-T)>.
- [7] Veniamin D. Dimitriadis and Efstratios N. Pistikopoulos, 'Flexibility Analysis of Dynamic Systems', *Industrial & Engineering Chemistry Research*, 34.12 (1995), 4451–62 <<https://doi.org/10.1021/ie00039a036>>.
- [8] Sau Man Lai and Chi Wai Hui, 'Measurement of Plant Flexibility', 2007.
- [9] Sau M. Lai and Chi-Wai Hui, 'Process Flexibility for Multivariable Systems', *Industrial & Engineering Chemistry Research*, 47.12 (2008), 4170–83 <<https://doi.org/10.1021/ie070183z>>.
- [10] Patricia M. Hoch, Ana M. Eliceche, and I.E. Grossmann, 'Evaluation of Design Flexibility in Distillation-Columns Using Rigorous Models', *Computers & Chemical Engineering*, 19 (1995), S669–74 <[https://doi.org/10.1016/0098-1354\(95\)00137-Q](https://doi.org/10.1016/0098-1354(95)00137-Q)>.
- [11] Christodoulos A. Floudas, Zeynep H. Gümüş, and Marianthi G. Ierapetritou, 'Global Optimization in Design under Uncertainty: Feasibility Test and

- Flexibility Index Problems', *Industrial & Engineering Chemistry Research*, 40.20 (2001), 4267–82 <<https://doi.org/10.1021/ie001014g>>.
- [12] R. E. Swaney and I. E. Grossmann, 'An Index for Operational Flexibility in Chemical Process Design. Part II: Computational Algorithms', *AIChE Journal*, 31.4 (1985), 631–41 <<https://doi.org/10.1002/aic.690310413>>.
- [13] Ruei-Shing Wu and Chuei-Tin Chang, 'Development of Mathematical Programs for Evaluating Dynamic and Temporal Flexibility Indices Based on KKT Conditions', *Journal of the Taiwan Institute of Chemical Engineers*, 73 (2017), 86–92 <<https://doi.org/10.1016/j.jtice.2016.09.009>>.
- [14] Weiqing Huang and others, 'Operation Feasibility Analysis of Chemical Batch Reaction Systems with Production Quality Consideration under Uncertainty', *Journal of Chemical Engineering of Japan*, 50.1 (2017), 45–52 <<https://doi.org/10.1252/jcej.16we119>>.
- [15] Kenneth M. Guthrie, 'Capital Cost Estimating', *Chemical Engineering*, 76.3 (1969), 114–42.
- [16] Kenneth M. Guthrie, *Process Plant Estimating, Evaluation, and Control* (Craftsman Book Company of America, 1974).
- [17] Gael D. Ulrich, *A Guide to Chemical Engineering Process Design and Economics* (Wiley, 1984).
- [18] Pablo F. Navarrete and William C. Cole, *Planning, Estimating, and Control of Chemical Construction Projects, Second Edition* (CRC Press, 2001).
- [19] Severini, T. A. (2011). *Elements of Distribution Theory* (1 edition). Cambridge: Cambridge University Press.

Part III. Thermodynamic Feasibility Assessment

Exploiting Residue Curve Maps to Assess Thermodynamic Feasibility Boundaries under Uncertain Operating Conditions

Alessandro Di Pretoro^{a,b}, Ludovic Montastruc^{a*}, Flavio Manenti^b, Xavier Joulia^a

^aLaboratoire de Génie Chimique, Université de Toulouse, CNRS/INP/UPS, Toulouse, France

^bPolitecnico di Milano, Dipartimento di Chimica, Materiali e Ingegneria Chimica «Giulio Natta», Piazza Leonardo da Vinci 32, 20133 Milano, Italy.

Abstract

The very first step of almost any separation process design is the thermodynamic feasibility analysis. In case of distillation, Residue Curve Maps (RCMs) represent an essential tool to assess whether the separation is feasible or not. However, the analysis is generally carried out by referring to nominal operating conditions and to product purities as specification. This means that, when process parameters are likely to undergo fluctuations, the prediction of the system response is not that obvious. An ABE/W (acetone-butanol-ethanol/water) mixture was then selected as a case study since it allows to discuss several non-ideal thermodynamic behaviors and because of the renewed interest in biorefinery and sustainable processes during recent years. Residue curve mapping was then exploited to determine the thermodynamic feasibility range for multi-component distillation processes as well as for distillation trains and process intensified solutions taking into account both product purity and product recovery specifications. The final product of this study is a thorough procedure to determine the flexibility boundaries of feed and products compositions as well as an immediate and intuitive graphical representation from a binary standard distillation column to a complex multicomponent dividing wall column application.

Highlights:

1. An a priori thermodynamic flexibility assessment could avoid a backward investigation on the system unfeasibility root causes when perturbations occur.
2. Biofuels purification is a challenging operation due to the high non-ideality of water-alcohols interactions and the seasonality of the feedstock.
3. Residue curve mapping has proved to be an effective methodology worth to be exploited even when uncertainty should be taken into account.

Keywords: Residue curve; thermodynamics; flexibility; distillation; ABE.

*Corresponding author, email address: ludovic.montastruc@ensiacet.fr

1 Introduction

Feasibility analysis is a key point and the very first step of any process design procedure independently on the process nature. It is usually carried out according to given operating conditions in order to proceed to the following design phases. After the solution to the initial problem has been preliminarily designed it is usually tested by varying design variables or operating parameters [1]. However, whether the process results to be unfeasible it could be very difficult to understand which is the constraining aspect that prevents the operation to achieve the desired specifications. The inability of a system to withstand operating conditions different from the ones according which it has been designed indeed can be either due to tight constraints, such as physical laws, or to loose constraints, such as available materials or design choices [2]. In the latter case, those limitations can be usually overcome by means of higher investments or at the cost of a lower profitability. On the contrary, in the former cases it doesn't exist any way to bypass the system failure and a different design solution should be employed. Moreover, in all those cases, an a priori thermodynamic flexibility assessment would have avoided the backward investigation on the unfeasibility root cause.

These considerations are obviously dependent on the uncertain variables deviation range as well as the deviation likelihood [1]. Petrochemical industry for instance is based on widely-studied and well-established processes and crude oil supplies are ruled by multi-year contracts involving oil blends whose properties are known and almost constant in time. However, the growing interest towards sustainable feedstocks during recent years implies considerable modifications in the process design approach. Biomasses nature indeed is ruled by the cycle of seasons and cannot ensure constant chemico-physical properties during the year [3, 4]; this causes the definition of "nominal operating conditions" to be of little significance and an a priori design under uncertainty to be extremely useful.

A relevant part of biobased processes indeed involves the use of a fermenter upstream the products separation section; the obtained fermentation broth is rich in water and alcohols in prevalent quantities that were not that present in petroleum feedstocks and that considerably complicate the thermodynamic behaviour due to the high non-ideality of their interactions. It wouldn't be then surprising if, during an operation, an external operating conditions perturbation or the malfunctioning of an upstream unit led the separation section conditions outside the feasibility boundaries with relevant implications on the delicate profitability of a fermentation process.

Among the most common operations in chemical plants, distillation is by far the most used and the one processing huge feedstock capacities. It involves relatively high energy costs and its separation effectiveness is of critical importance for the cost-effectiveness of the entire process.

For all these reasons this study deals with the thermodynamic flexibility assess-

ment of different typology of distillation processes involving compounds coming from an upstream microbial fermentation process as thoroughly described in the following chapters.

2 Methodology

Distillation feasibility is a widely spread and deeply-studied research domain since the very beginning of the 20th century. Several methodologies exist in order to assess whether a given mixture split is possible or not on the basis of components volatility. Some shortcut methods have been outlined as well for the preliminary design phase accounting for a constant relative volatility between the species and the heavy-light key components assumption. However, when thermodynamics gets complicated, equilibrium diagrams are the reference to be employed. A useful and well-established tool to assess the thermodynamic feasibility of a multicomponent mixture distillation process based on equilibrium diagrams is the residue curve mapping. Despite the robust theory behind them and their effective graphical representation allowing for an immediate understanding of the equilibrium phenomena, Residue Curve Maps (RCMs) are seldom used as the main tool to show the feasibility study results by process engineers.

Those curves were defined first at the beginning of the 20th century by Ostwald (1900)[5] and Schreinemakers (1901)[6] in Germany to describe ternary mixtures with the presence of azeotropic species. However, the country where they've seen the highest development after about fifty years is Russia; Gurkinov (1958)[7] indeed classified all the possible ternary diagrams and Zharov and Serafimov (1967, 1968a, 1968b, 1969, 1975)[8, 9, 10, 11, 12] completed his work for mixtures with a higher number of components. All those works remained untranslated from Russian for a long time.

The main research work concerning Residue Curves during recent years was performed by Petlyuk [13, 14] and it will be the mainly referenced author in this chapter. The residue curve represents the evolution of the mixture composition during the open evaporation process as shown in Figure 3.1.

From a numerical point of view, the mass balance on the i -th component can be reconducted, in correspondence of each infinitesimal amount of vaporized mixture $dL \rightarrow 0$, to the differential equation:

$$\frac{dx_i}{d\xi} = x_i - y_i \quad (2.1)$$

where $d\xi$ represents the infinitesimal dimensionless time span, i.e. the evaporation extent.

A residue curve is then given by the locus of points in the composition domain satisfying the ordinary differential equation corresponding to a certain moment of time and to a portion of evaporated liquid.

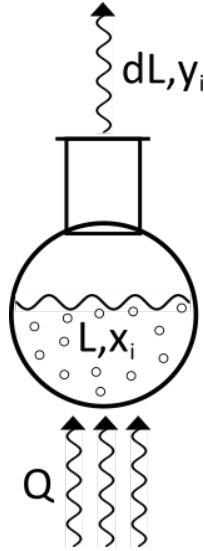


Fig. 3.1: Open evaporation process

Another physical interpretation that could result more appealing from a practical point of view concerns distillation columns. In particular, at total reflux, composition profiles of packed columns are described by residue curves whereas distillation lines coincides with the composition profiles of staged columns[15].

A close correspondence between RCMs and distillation trajectories at infinite reflux was also proved. Distillation trajectories represent the composition profile along the column equilibrium stages; at infinite reflux, as first discussed by Thormann (1928)[16], they're given by:

$$x_i^{(k+1)} = y_i^{(k)} = K_i(T^{(k)}, P^{(k)}, \bar{x}^{(k)}, \bar{y}^{(k)}) \cdot x_i^{(k)} \quad (2.2)$$

If we interpolate those broken lines with a continuous one, the so-called distillation c-lines can be obtained. Distillation lines and (equilibrium) tie-line curves are uniquely function of the Vapor-Liquid Equilibrium, independently from their analogies with the column composition profile. Thus, distillation lines are equivalent to residue curves as characteristics of the VLE in a thermodynamic sense although they do not coincide as discussed by Kiva et al. (2003)[17].

Residue curves indeed are oriented curves, they move from the unstable node that is the light component or azeotrope (the star in Figures 3.2a and 3.2b) to the stable node that is the heavy component or azeotrope (the square in Figures 3.2a and 3.2b) passing more or less close to an eventual saddle point representing the compound or species with an intermediate volatility (the circle in Figures 3.2a and 3.2b).

Whenever two or more distillation bundles are present, except for binary distillation, one or more particular residue curves called “separatrixes of saddle stationary points” delimiting them exist as well. Differently from the other RCs, the separatrixes begin or come to an end not in the node points but in the saddle

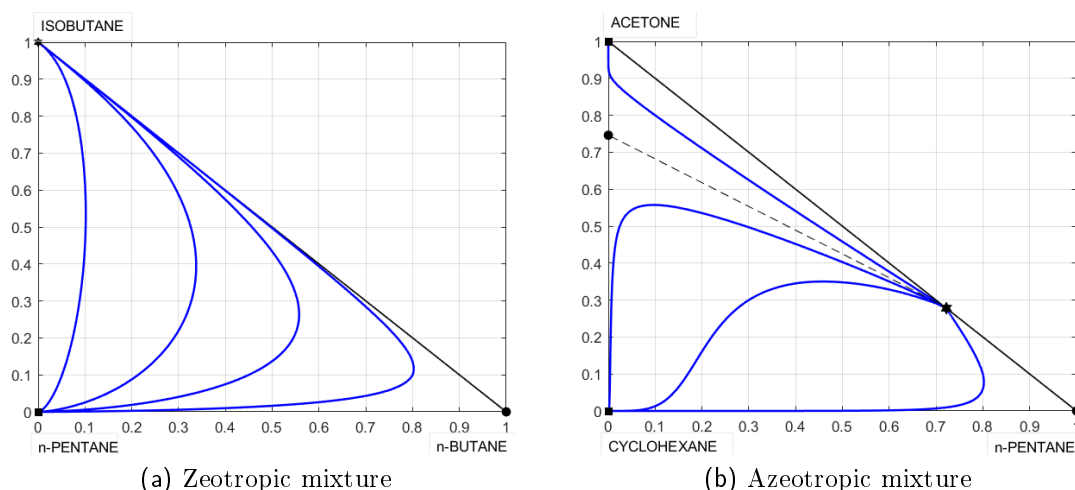


Fig. 3.2: RCMs examples (■ *stable*, ● *saddle*, ★ *unstable*)

points (cf Figure 3.2b). They separate two distillation regions, i.e. concentration bundles where all RCs have the same stable and unstable nodes in common. The main outcome related to the analysis of distillation regions is that separatrixes cannot be crossed, which means that we can't move between two points belonging to different distillation regions during a single distillation process.

In the light of the above, the important conclusion that can be drawn is that, in order to be part of the same distillation column, the characteristics points representing lateral feeds and products withdrawals should therefore have the same stable and unstable nodes, i.e. the RCs passing through them should belong to the same distillation region. This is a rule of general validity with the exception of a few particular cases when the VLE equilibrium behaviour exhibits a nonideality resulting in inflections of the total reflux trajectories. Those cases are not specifically treated in this study but a more accurate discussion can be found in Wahnschafft et al. (1992)[18] and Petlyuk (2004)[14].

Thus, the first goal of this study is to take advantage of the RCMs theory robustness in order to discuss distillation of complex multicomponent mixtures under uncertain operating conditions, i.e. the flexibility range of the operation. Flexibility will be evaluated according to the Resilience Index introduced by Saboo et al. (1985)[19] defined as the largest total disturbance load, independent of the direction of the disturbance, a system is able to withstand without becoming unfeasible.

An additional purpose of this study is then to provide graphic tools to ease the understanding of the multicomponent mixtures behaviour both for a single distillation column and for more complex distillation configurations using the product purity and its recovery ratio as specifications.

Calculations have been performed by coupling Matlab[®] for the numerical and graphical part with Simulis[®] Thermodynamics software providing the components

databank as well as the thermodynamic models and parameters.

3 Case study

It is widely agreed that sustainability can be identified as the worldwide central issue of the last (and the next) several years. According to the IEA Bioenergy Annual Report [20] biofuels will represent around 30% of energy consumption in transport by 2060. Their role is particularly important in sectors which are difficult to decarbonise, such as aviation, shipping and other long-haul transport. That's why several bioprocesses have seen a renewed interest in recent years both from a research and an industrial point of view.

For this reason the ABE/W (acetone-butanol-ethanol/water) mixture was selected as the case study analyzed in this paper. It comes from an upstream microbial fermentation process characterized by product inhibition[21] and the recovery of at least the most valuable products, n-butanol and acetone, is necessary for the profitability of the process. After a preliminary dewatering operation, usually liquid-liquid extraction or pervaporation[22, 23, 24], the remaining products can be separated by means of different distillation configurations. The fluctuation related to the feedstock nature requires a dedicated design procedure taking into account the inlet composition uncertainty and aiming to a flexible design choice.

An additional reason why this multicomponent mixture is particularly suitable for this flexibility assessment is that the complex and highly non-ideal thermodynamics allows to analyze interesting singular points such as homogeneous and heterogeneous azeotropes as well as to include liquid-liquid equilibrium in the distillation feasibility assessment and optimization discussion thanks to the aqueous-organic phase demixing.

From the most significant binary case studies to more complex multicomponent mixtures, both simple distillation and energy integrated configurations will be discussed by referring to these four compounds.

The process specifications accounted for in case of a single distillation column are:

- n-Butanol recovery ratio in the bottom: 0.9604;
- Bottom n-butanol mass fraction: 0.99.

In case of water-ethanol mixture the recovery specifications will be applied to water since, in order to obtain high purity ethanol with a single distillation column, the feed composition should be at least 95.63 % w/w pure (azeotropic composition) with a consequent poor flexibility interest.

More realistic specifications for the ethanol-water separation will be considered as listed here below:

- Water recovery ratio in the bottom: 0.95;

- Bottom water mass fraction: 0.95.

Furthermore, in case of a two distillation columns or Dividing Wall Column, the following constraints should be included in addition to the n-butanol ones:

- Acetone recovery ratio in the distillate: 0.985;
- Distillate acetone mass fraction: 0.995.

The single distillation column case studies will be then discussed first and the distillation trains as well as the DWC case studies will be presented at the end of the following chapters. All the distillation columns presented in this paper will refer to atmospheric operating pressure.

The most suitable thermodynamic model to describe the ABE/W mixture equilibrium behaviour is the Non-Random Two Liquids (NRTL)[25]. It results indeed to be the most accurate model able to describe water-alcohols as well as biofuels equilibria in general[24, 26, 27, 28].

4 The binary systems

Among the six possible binary systems of an ABE/W mixture, two in particular have been selected to conduct the flexibility limit analysis, namely the water-ethanol and water-butanol mixtures. The first reason of this choice was that it would be obviously meaningless to analyze mixtures with no saddles, e.g. acetone-ethanol, since it is always possible to perform a sharp separation by distillation with an infinite number of stages (that is the characteristic condition of RCMs). The second reason why it is worth discussing these two mixtures is that they allow us to show analogies and differences between homogeneous and heterogeneous azeotropes, i.e. whether the liquid phase can undergo demixing or not.

In a two component system the Residue Curve moves from the unstable to the stable node along a 1-D trajectory, i.e. the liquid phase composition curve. As distillation regions for N component mixtures are $N - 1$ dimensional spaces, in a binary system the distillation region is part of the x_1 domain.

The following chapter will then concern the well-known water-ethanol equilibrium under a flexibility perspective; after that a chapter related to the water-butanol binary system will be presented to show how introducing an additional operation, different from distillation, will affect the residue curve shape and the flexibility of the separation.

4.1 Homogeneous azeotrope

Among all binary mixtures showing a feasibility limit, water-ethanol is by far the most popular due to the several uses and to its ancient history. At atmospheric pressure, this mixture presents a minimum boiling point azeotrope at 78.2 °C

and at an ethanol composition of 95.63 % w/w corresponding to about 89.5 % mol/mol[29].

The y vs x and T vs xy equilibrium diagrams are reported in Figures 3.3a and 3.3b respectively. As it can be noticed, the residue curves, i.e. the composition of the residual liquid phase, in a binary plot are just represented by the diagonal of the y vs x diagram (since they correspond to the column profile at infinite reflux) or by the bubble curve in T vs xy . The azeotrope divides then the 1-D space into two distillation regions, $x_{eth} \in [0, 0.895]$ and $x_{eth} \in [0.895, 1]$ respectively. In the first distillation region the sharp split that can be obtained is pure water as bottom product and at the azeotropic composition as distillate product; in terms of Residue Curve vocabulary it can be stated that pure water is the stable node and the azeotrope is the unstable node in the first distillation region while, in the second distillation region, the azeotrope is still the unstable node but pure ethanol becomes the stable one.

Therefore, since 0.95 w/w water purity is desired, a first trivial conclusion can be immediately drawn: the feed ethanol molar fraction should be lower than the azeotropic one, i.e. the operating line will lie on the left side of the equilibrium diagram. The operating point corresponding to the bottom product is fixed according to the given specification $x_{eth}^w = 0.05$ ($x_{eth}^{mol} = 0.02$).

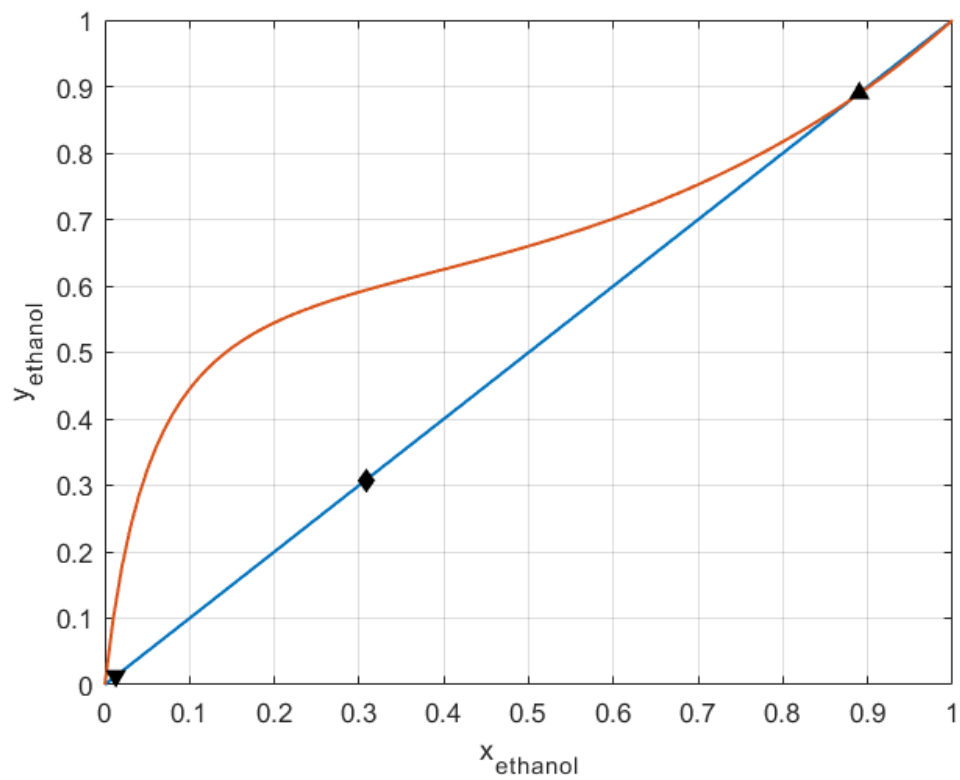
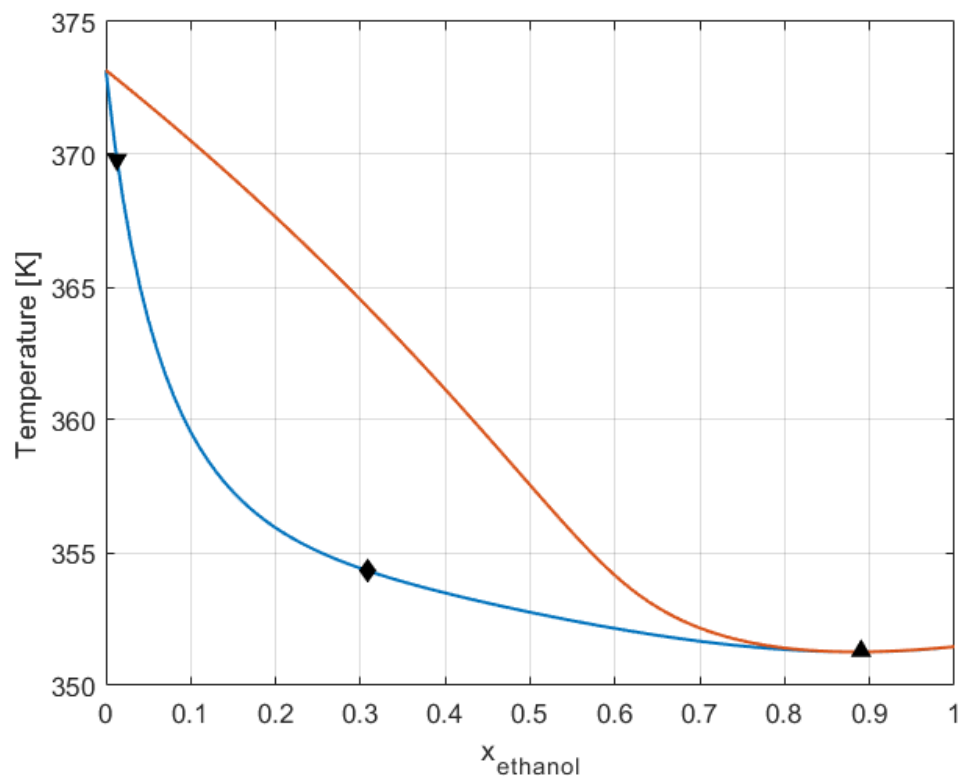
The other constraint related to the recovery ratio affects the feed split into the distillate and bottom streams; this coincides, from a geometrical point of view, to the application of the so-called lever rule:

$$\frac{\bar{z} - \bar{x}^B}{\bar{x}^D - \bar{z}} = \frac{D}{B} \quad (4.1)$$

Therefore, for any given feed composition, the bottom point location is fixed by means of the bottom composition specification and the distillate point can be located taking into account the mass balance.

With the exception of particular cases, the necessary and sufficient condition to state that a separation by distillation is possible is that feed, distillate and bottom composition points lie in the same distillation region, i.e. they all should have the same stable and unstable nodes (for further details about the theoretical background please refer to Petlyuk (2004)[14]). In case of binary distillation then they all should lie on the same side of the azeotrope.

By applying these rules to the ethanol-water case study under analysis it can be deduced that the maximum ethanol content in the feed stream is the one for which the distillate characteristic point lies on the distillation region boundary ($x_{eth}^D = x_{eth}^{azeo} = 0.895$). Thus, to satisfy the process specification (water recovery ratio in the bottom equal to 0.95) the maximum ethanol molar fraction in the feed is $z_{eth} = 0.308$. It means that, if the process operating conditions correspond to a lower value, there's a flexibility range $z_{eth} \in [0, 0.308]$ within which the feed ethanol content can fluctuate without compromising the desired separation feasibility with

(a) y vs x (b) T vs xy Fig. 3.3: Ethanol–Water equilibrium diagrams (\blacktriangledown *bottom*, \blacklozenge *feed*, \blacktriangle *distillate*)

a single distillation column. On the contrary, if feed composition perturbations above the limit value can be attained, the thermodynamic feasibility boundary is breached and there's no way to achieve the process specifications no matter the investment that we'd be willing to afford; in those cases the only solution is to design a different separation process.

In conclusion it is worth remarking that although this result is strictly related to the process specifications, the same methodology can be nevertheless applied to any distillation case study.

4.2 Heterogeneous azeotrope

Though at the first glance the water-butanol mixture could look similar to the water-ethanol one, it needs a considerably different procedure. Indeed the main difference can be immediately noticed by means of the equilibrium diagrams in Figures 3.4a and 3.4b. If making the assumption of simple distillation (no decanter), the operating points are represented by the thick empty markers (inverted triangle for the bottom, diamond for the feed and triangle for the distillate). Even for this case study, the heteroazeotrope $x_{wat}^{azeo} = 0.763$ [28] divides the 1-D space into two distillation regions, $x_{wat} \in [0, 0.763]$ and $x_{wat} \in [0.763, 1]$ respectively, and it is the unstable node for the region on the left hand side (pure n-butanol, heteroazeotrope) as well as for the region characterized by the heteroazeotrope-pure water split. Then, in order to obtain pure butanol with the desired recovery ratio, the feed stream should be located on the left of the heteroazeotrope.

The thermodynamic flexibility problem can then be solved analogously to the water-ethanol mixture (Figure 3.5 left); the bottom stream molar fraction is fixed according to the purity specification, the lever rule can be applied according to the recovery ratio and, being the maximum water content in the distillate $x_{wat}^D = x_{wat}^{azeo} = 0.763$, the maximum water content in the feed flowrate results to be $z_{wat} = 0.1434$.

However, in case of heterogeneous azeotrope, there's a well-established column configuration[30] aimed at increasing the operation effectiveness based on the use of a decanter instead of a conventional reflux drum (cf Figure 3.5 right). For the analysis we are trying to carry out, the addition of a decanter implies considerable modifications worth to be discussed before providing the corresponding results.

First of all, the distillation column with a decanter as reflux drum (as shown in Figure 3.5 right) has one degree of freedom less with respect to the standard configuration since the reflux flowrate is a direct consequence of the equilibrium demixing and cannot be managed by a dedicated control system to achieve a desired specification. Thus, the separation problem should be differently posed: for a given feed flowrate indeed it can be either imposed the butanol purity or the butanol recovery ratio. This means that one process specification must be loosened and transformed from equality into inequality constraint. It can then be

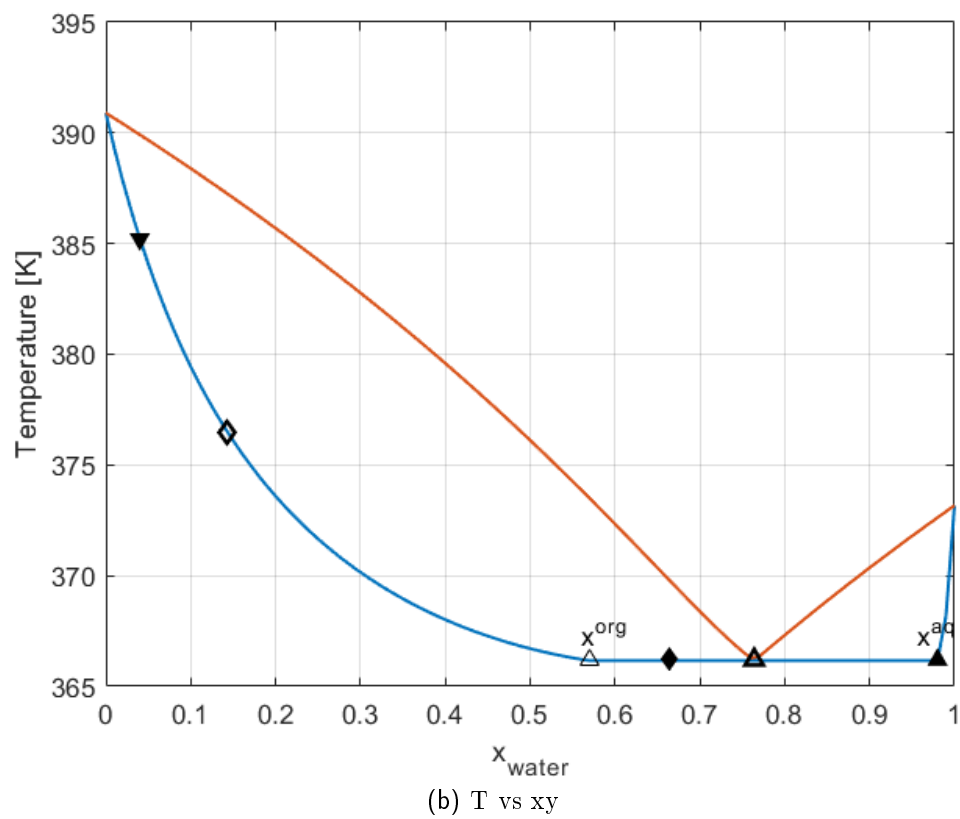
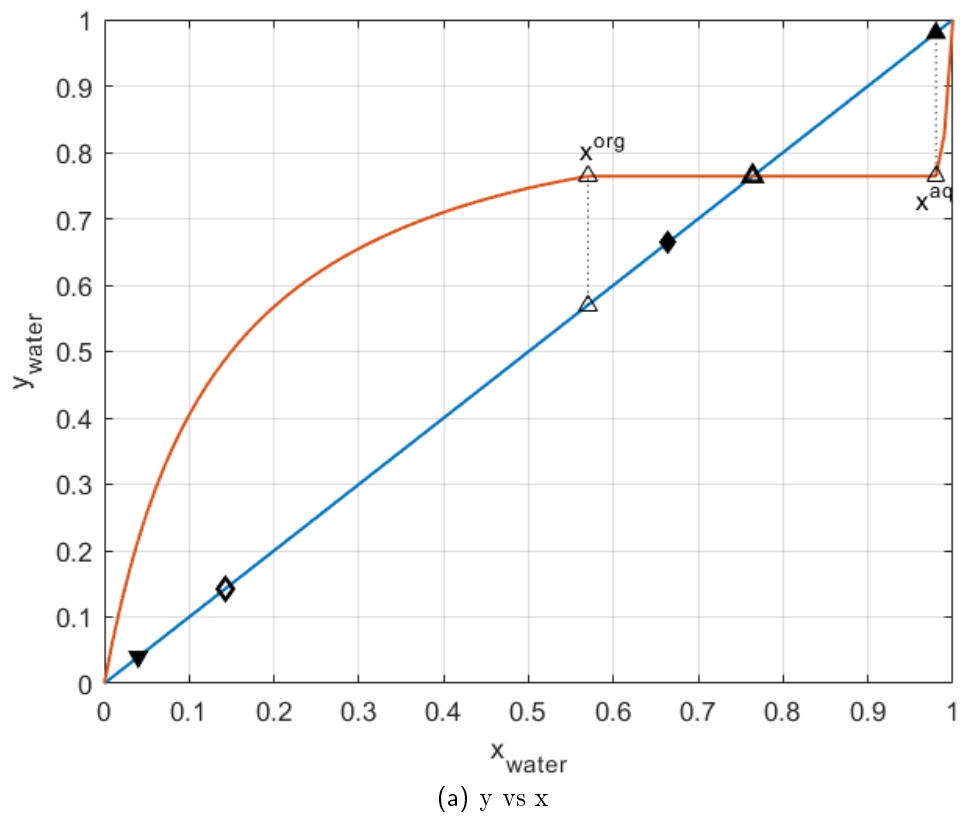


Fig. 3.4: n-Butanol–Water equilibrium diagrams (\blacktriangledown bottom, \blacklozenge feed, \blacktriangle distillate)

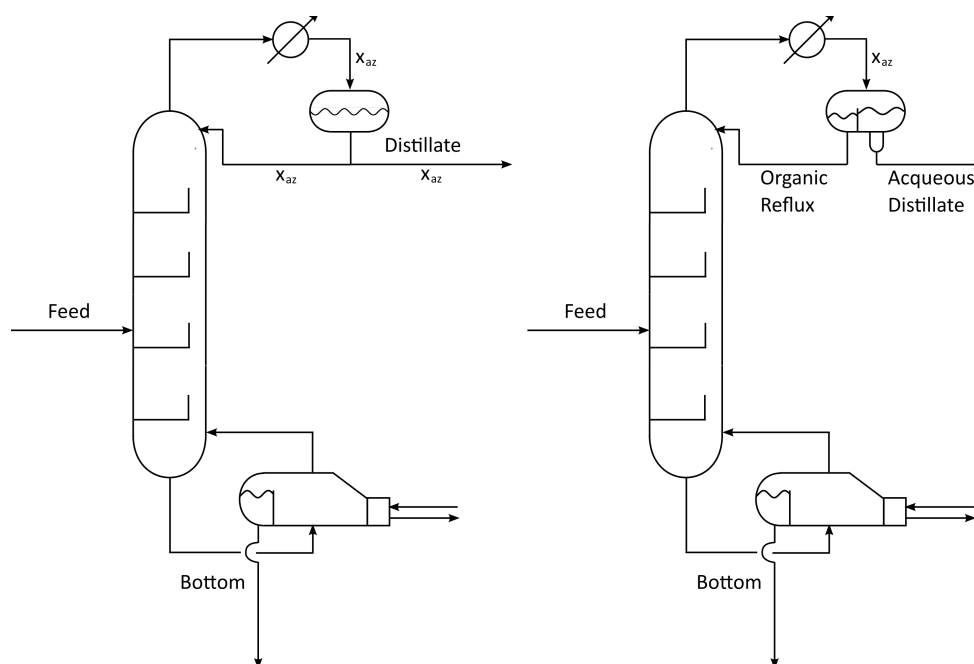


Fig. 3.5: Standard distillation column vs distillation column with decanter

stated that a 99 % w/w purity is required and a n-butanol recovery ratio equal at least to 0.9604.

The second main difference between the two configurations concerns the overcooling degree in the condenser. In the standard distillation column the reflux overcooling is unprofitable because it involves higher duty requirements both in the condenser and in the reboiler since a liquid phase further from the equilibrium conditions is recycled without affecting the distillate (and then the reflux) composition. On the contrary, when demixing occurs, the aqueous and organic phases compositions depend on temperature. The water content of the distillate stream can be then modified according to the overcooling degree enhancing the separation with a relatively poor cost increase since the condenser temperature allows the use of ambient water as cooling duty.

However, as evidenced by well-established experimental data[31, 32], the aqueous phase composition in the temperature range [0 °C, 91 °C] can only vary from 0.9727 to 0.9838 with a $x_{wat}^{aq} = 0.98$ value at the boiling point without considerably affecting the thermodynamics of the system. On the contrary, the water content in the organic reflux can significantly change; even though this parameter could improve the separation efficiency from an energetical point of view due to the fact that a lower amount of water circulates through the column, it doesn't modify the separation thermodynamic feasibility since the reflux stream does not take part in the overall mass balance. For all these reasons the thermodynamic feasibility analysis has been carried out without condenser overcooling.

The residue curve analysis results can be noticed in Figures 3.4a and 3.4b by referring to the full black markers (circle for the feed and diamonds for bottom and

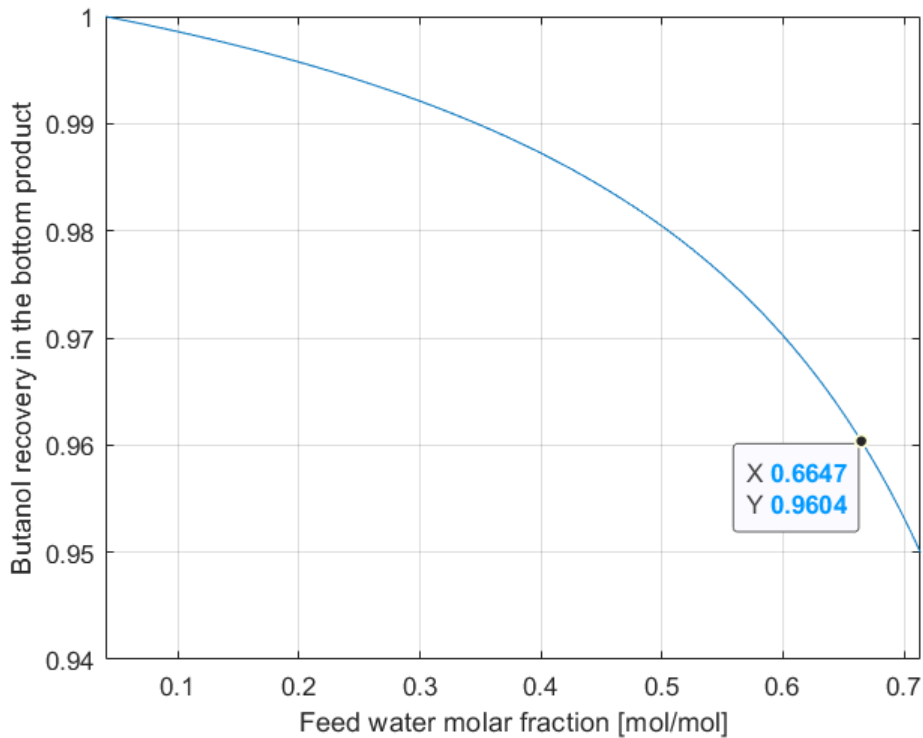


Fig. 3.6: Butanol recovery ratio in the bottom stream

distillate). The distillate water molar fraction shifted from $x_{wat}^D = x_{wat}^{azeo} = 0.763$ to $x_{wat}^D = x_{wat}^{aq} = 0.98$ with a relevant increase of the maximum water content allowed in the feed stream to $z_{wat}^{max} = 0.6647$.

Note that, if the feed composition is included in the range $[x_{wat}^{org}, 0.6647]$ it is worth feeding directly in the condenser in order to take advantage of the feed demixing and reduce the amount of water introduced in the column as discussed in Luyben (2008)[30].

The trend of the butanol recovery ratio in the bottom stream is represented in Figure 3.6 in the range $z_{wat} \in [x_{wat}^B, z_{wat}^{max}]$. It can be noticed that the butanol recovery specification is satisfied for any water content in the feed lower than the maximum value.

5 The multicomponent systems

Process feedstocks are usually composed by several different components even though sometimes only a few of them are worth to be recovered. Multicomponent mixtures equilibria can be visualized by means of multiphase diagram. The diagrams dimensionality is related to the number of compounds, namely N component mixtures require a $(N - 1)$ D diagram. For this reason, the thermodynamic flexibility assessment procedure will be graphically discussed here below up to 4 components, i.e. the limit of a 3D representation. These diagrams allow nevertheless the ABE/W mixture behaviour analysis. The procedure explained in the

following paragraphs is nonetheless of general validity independently on the number of mixture components. The analytical procedure in case of N higher than 4 is discussed in a dedicated chapter at the end of this section.

The mixture water content will still be used as uncertain variable since it has revealed to be the most critical parameter for the separation.

5.1 Ternary system

Since Butanol-Water and Ethanol-Water binary mixtures have been analyzed in the previous chapter, the ternary mixture Butanol-Ethanol-Water obtained combining them will be discussed first while Acetone will be added later as the fourth compound.

It's worth remarking that we're still dealing with a single distillation column whose specifications are related to the n-butanol recovery and purity as discussed in the "Case study" chapter.

Nominal operating conditions should be defined even though they have little importance with respect to the feasibility boundary composition. In order to do that, the limit composition of water-butanol mixture without decanter can be used and ethanol in the same amount as water can be added. Finally, by re-normalizing, the composition $\bar{z} = [z_{but}, z_{wat}, z_{eth}] = [0.75, 0.125, 0.125]$ is obtained. It is worth remarking that these values have been selected both to compare the water/butanol ratio that can be achieved in presence of a further component and to avoid that the new component addition drastically displace the operating point with respect to the distillation boundary in the composition space.

In ternary diagrams, residue curves can move from the unstable to the stable node in a bidimensional space. The mass balances are still represented by the lever rule.

RCMs related to nominal operating conditions are plotted in Figure 3.7a. The color notation is green for the feed, red for the distillate and blue for the bottom. The dark green slice shows the region where the liquid phase demixing occurs. In order to account for the eventual presence of two liquid phases, the option including liquid split calculation in Simulis[®] Thermodynamics has been ticked.

As it can be noticed, under nominal operating conditions, all the distillation column streams belong to the same distillation bundle where n-butanol is the stable node while the water-ethanol azeotrope is the unstable one. In order to be conservative, the temperature used to outline the immiscibility region is the boiling temperature of the unstable node since it corresponds the lowest value achieved along the residue curve.

Starting from this operating point, water can be added as usual in order to assess its maximum allowed molar fraction. The addition of water in a ternary diagram, keeping unchanged the quantity of the other compounds, consists of the operating point displacement towards the water vertex as shown by the black arrow

in Figure 3.7a. The distillate and the bottom product compositions can be then calculated based on the specifications and the equilibrium. Since the bottom product composition is fixed by the required butanol purity, by shifting the feed composition the distillate characteristic point location changes accordingly in order to satisfy the lever rule. The limit feasibility conditions are shown by the dotted lines in Figure 3.7a and correspond to the feed composition $\bar{z} = [0, 709, 0.173, 0.118]$. For a further water content increase indeed the distillate stream characteristic point crosses the distillation boundary and falls into the distillation region where the stable node is represented by water instead of n-butanol as shown in Figure 3.8c.

Beside the effective graphical visualization, there are a few remarks worth to be done from a quantitative point of view. The first observation refers to the water/butanol ratio at the feasibility limit; in the case of binary mixture without decantation this ratio is about 1:6.14 while, with the addition of ethanol, the separation feasibility is enhanced until a 1:4.1 ratio. This means, for this case study, that the maximum allowed amount of water is higher if a certain third compound is present.

The second remark states that the increase in this ratio quantitatively depends on the amount of the third species. In particular, from a graphical point of view, a higher ethanol addition reflects in a rotation towards the ethanol vertex $[0, 0]$ of the operating line.

Moreover, as it can be noticed from the plot, the residue curve related to the distillate stream enters the immiscibility region. In this case its calculation is based on the VLLE and accounts for the liquid phase demixing. The dotted line represents the boundary compositions in case the decanter is exploited to enhance the separation as previously discussed for the binary case study. The same remarks concerning the distillate overcooling keeps being valid for the ternary mixture as well due to the correlation between immiscibility region and operating temperature.

However, for this case study, the characteristic points are always far from this region, thus the separation is not concerned by heterogeneous phases in the column.

It is finally worth to highlight that all those results are strictly related to the system thermodynamics and do not take into account operating costs and controllability of the process that could affect the design choice.

5.2 Quaternary system

According to the procedure followed in the ternary case study, the previous boundary composition $\bar{z} = [0, 709, 0.173, 0.118]$ can be taken as initial value. Then an amount of acetone equal to the water molar fraction can be added and composition can be re-normalized to $\bar{z} = [0.604, 0.148, 0.100, 0.148]$.

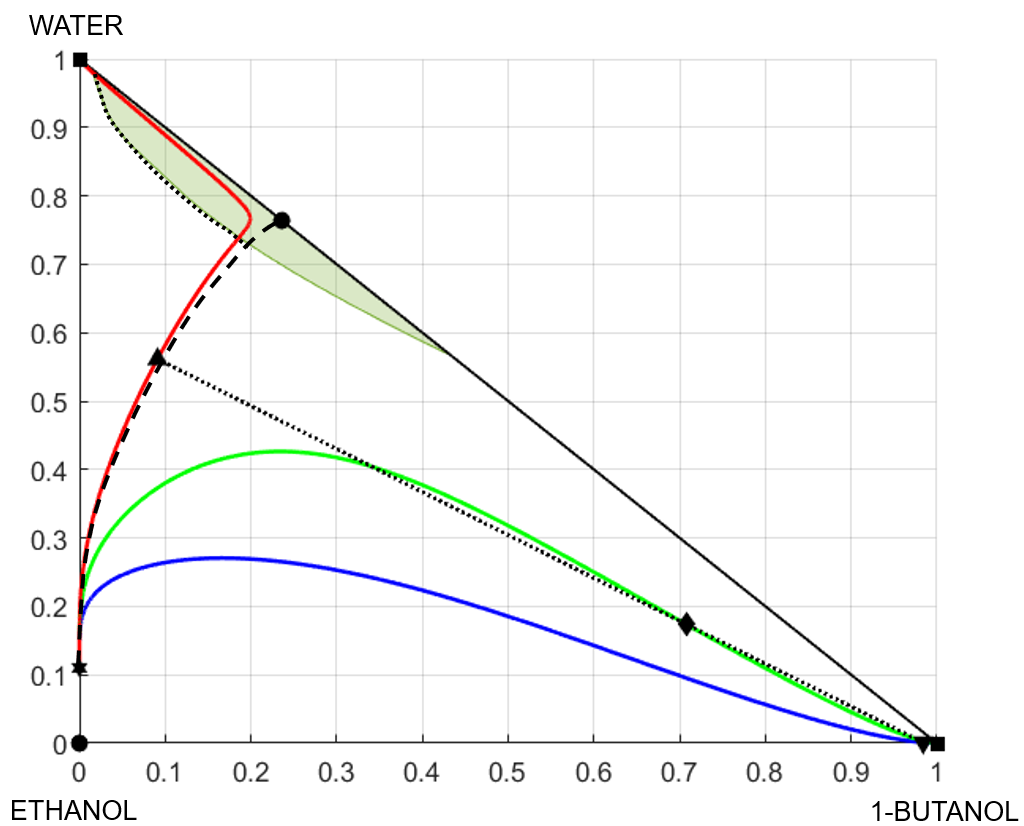
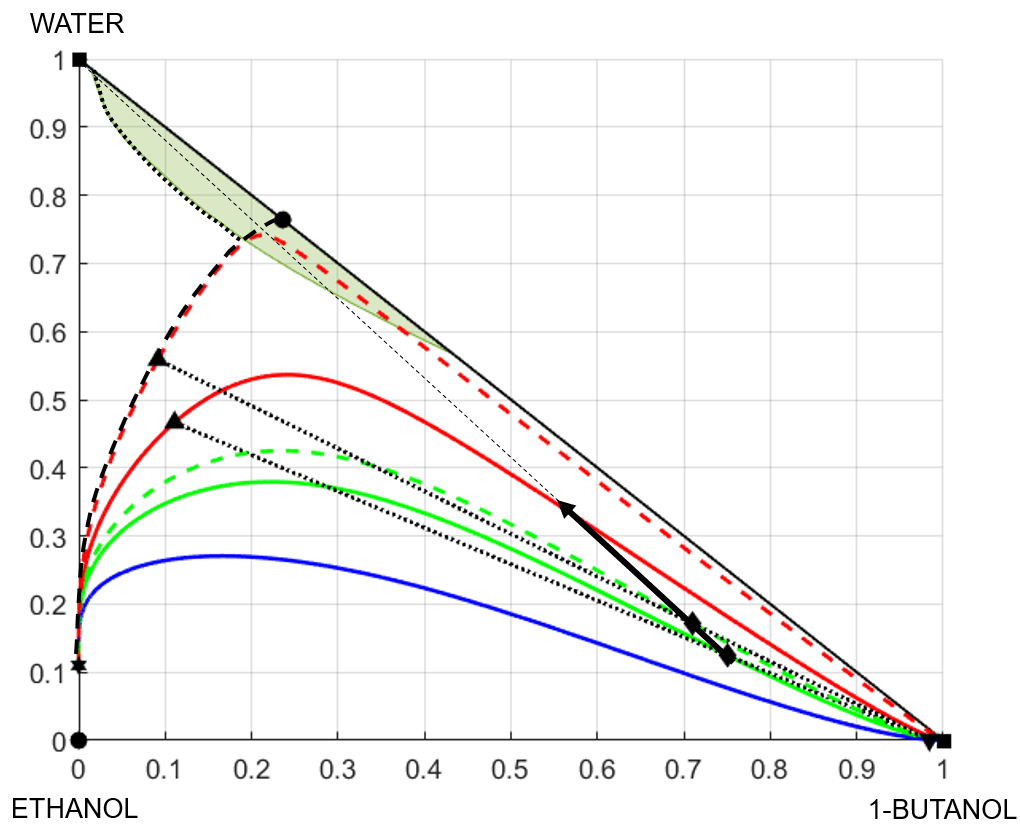


Fig. 3.7: Distillation RCM on ternary diagrams

The so obtained quaternary mixture can then be represented in a corresponding quaternary diagram. This diagram consists of a 3D pyramid whose vertices correspond to each pure component; the distillation region in a quaternary diagram is topologically defined by a 3D space and its boundary is a surface while the mass balance still lies on a line connecting the inlet/outlet characteristic points. Finally, since both the BWE and BWA mixtures show liquid phase demixing, the immiscibility region is a 3D space included between those two plans.

Residue curve mapping can be then performed under nominal operating conditions as shown in Figure 3.8a where pure ethanol corresponds to the origin of the axes $[0, 0, 0]$. All the three curves lie in the same distillation region and an additional water perturbation is possible with respect to the ternary case study. In a quaternary diagram the addition of a single species keeping unchanged the proportion between the other ones is carried out by shifting the operating point towards the corresponding vertex as usual. Thus a water increase in the distillation column feed is graphically represented by the black arrow in Figure 3.8a.

The extreme boundary condition is obtained for a feed composition equal to $\bar{z} = [0.594, 0.162, 0.099, 0.145]$ as shown in Figure 3.8b. For a further water content increase in the feed the residue curve passing through the distillate characteristic point (the red one in the Figure) overcomes the distillation boundary in analogy with the ternary case study and its stable nodes becomes pure water instead of pure butanol. Figure 3.8c shows the unfeasible conditions and the separatrix, that in this case is a surface, is represented by dashed contour lines.

In analogy with the previous case, it can be concluded that the addition of acetone has improved the separation by increasing the maximum allowed water/butanol ratio in the feed from 1:4.1 to 1:3.67.

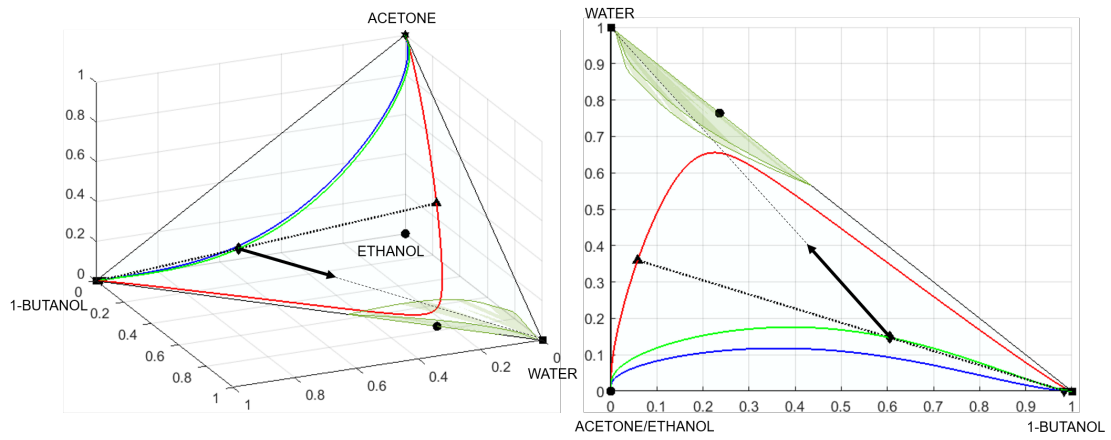
Even in this case the result quantitatively depends on the amount of the other species; the maximum allowed water content could indeed increase further for different values of acetone and ethanol content due to the convexity of the separatrix surface.

If the operating points lied in the pure water distillation region indeed the addition of acetone and/or ethanol would have reduced the operation flexibility due to inverse separatrix shape experienced from that side.

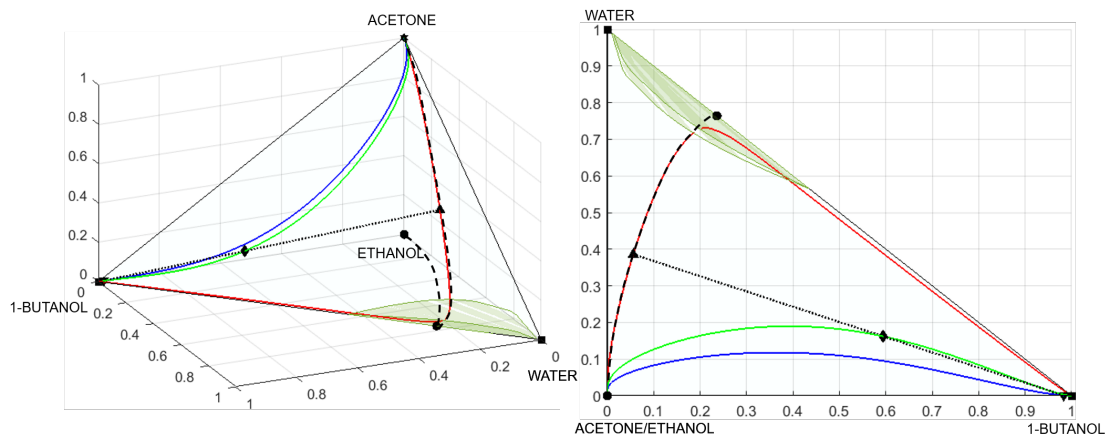
The same remarks about convexity applies to the ternary case as well as to mixtures with higher number of components even though they cannot be graphically represented in a physical space.

Even though calculations have been performed for a given value, the separatrix shape depends on thermodynamics only and the detailed study of the process feasibility boundaries allows to assess which could be the maximum allowed perturbation that could be withstood by the distillation system, i.e. its thermodynamic flexibility.

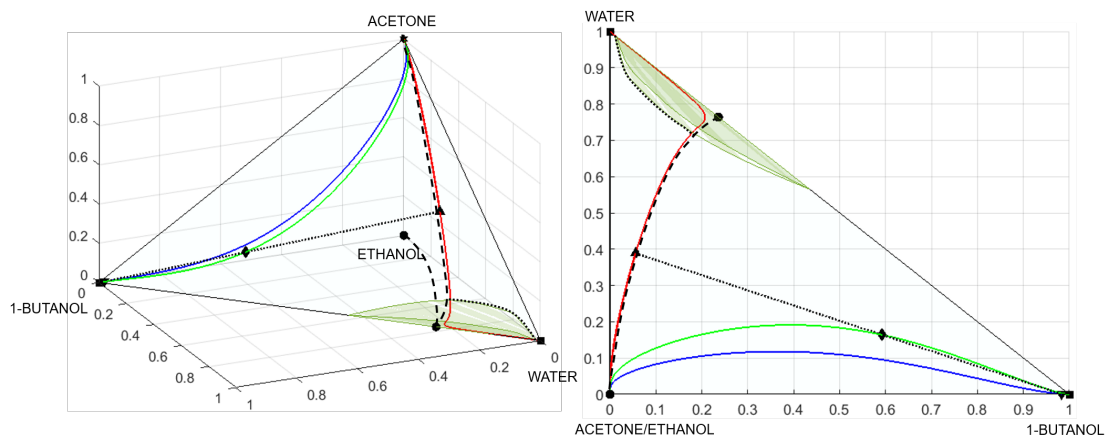
Moreover, it is worth remarking that this analysis refers to one purity and one recovery constraints on the same product (i.e. the separation yield), for different



(a) Nominal operating conditions



(b) Feasibility limit



(c) Unfeasible distillation

Fig. 3.8: Distillation RCM on quaternary diagrams lateral (left) and top (right) view

Stream	z_{But}	z_{Wat}	z_{Eth}	z_{Ace}	z_{Met}	Stable node	Unstable node
Feed	0.498	0.162	0.083	0.121	0.136	n-Butanol	Acetone-MeOH
Bottom	0.972	0.020	0.008	0	0	n-Butanol	Acetone-MeOH
Distillate	0.039	0.299	0.156	0.239	0.267	Water	Acetone-MeOH

Tab. 3.1: Analytical results for 5 components RCMs

specifications a dedicated study should be performed.

Finally it should be highlighted that this study doesn't account for economic or controllability aspects but it just establishes the physical distillation constraints that cannot be violated independently on the technological solution.

5.3 Systems with more than four components

All the examples presented so far are related to mixtures whose equilibrium diagrams can be visualized in a three dimensional (or lower) space.

When more than four components are present, the composition domain is a $(N - 1)$ D space and the graphical approach cannot be exploited for a more immediate physical understanding. However, from a computational point of view, the way residue curves can be outlined doesn't change. They are still one dimensional curves in the composition hyper-space whose coordinates can be obtained by the integration of the equation 2.1.

In order to have a practical example of the analytical approach for the feasibility boundaries estimation, let us consider the ABE/W mixture case study if some methanol is present as well in the fermentation broth. According to the usual procedure, given the boundary composition $\bar{z} = [0.594, 0.162, 0, 099, 0, 145]$, methanol can be added in the same amount as water and the final composition, after normalization, results to be $\bar{z} = [0.511, 0.139, 0, 086, 0, 125, 0.139]$.

Given the separation specifications and the mass balances, bottom and distillate streams compositions are then estimated and the residue curve passing through each one of the three characteristic points can be calculated as usual and stable and unstable nodes can be easily determined.

Under nominal operating condition the residue curves corresponding to the feed and the products have the same stationary points; thus, the separation still results to be feasible even after the addition of methanol. The feed water content can be then perturbed in order to assess the new boundary conditions.

The flexibility assessment results corresponding to the unfeasible condition are presented in Table 3.1. Although the presence of methanol implies one additional singular point in the composition space, i.e. the acetone-methanol azeotrope, it is able to further enhance the separation. As it can be noticed, the boundary composition for a water perturbation is $\bar{z} = [0.498, 0.162, 0, 083, 0, 121, 0.136]$, corresponding to a maximum molar water to butanol ratio in feed of about 1:3.25.

In general, in the feasible region, the unstable node shifts from “acetone” to “acetone-methanol azeotrope” while the stable one is still pure butanol. On the contrary, for higher water perturbations, the residue curve passing through the distillate characteristic point ends to the “pure water” node as already experienced in the previous chapters. In any case, the lack of a geometrical representation makes the understanding of the newly generated distillation bundles substantially more difficult.

The additional computational effort due to the presence of a fifth compound is comparable with those related to the previous scale up.

In conclusion, it is worth remarking that the procedure introduced here above may lead to a feasible domain underestimation when the VLE equilibrium behaviour exhibits a nonideality resulting in inflections of the total reflux trajectories as anticipated in the introduction. Those cases, that are not discussed in this research study, require an accurate separatrix hyper-surface estimation in order to check if it can be crossed or not in columns operating at total reflux.

6 Distillation trains and Dividing Wall Column

When more than two pure components should be recovered from multicomponent mixtures or if more than two specifications should be satisfied in order to have a profitable separation process, distillation columns can be combined in distillation trains. There exist several distillation train configurations named after the sequencing of the product purification. The most popular are the direct, indirect and midsplit configurations. The first two consist of several columns in series and the separation starts from the most volatile compound to the heaviest for the direct and the opposite for the indirect. The midsplit configuration is a parallel configuration where pure compounds are obtained downstream after previous partial splits.

An alternative solution to multicomponent mixtures separation is the Dividing Wall Column, i.e. a single distillation column whose central section is divided by one or more walls and with one or more side withdrawals. It represents the arrangement in a single distillation column shell of the Petlyuk column configuration[33]. This configuration is equivalent to the distillation train even though only two external duties are present. The reason why it has been studied in deep is that it is the only large-scale process intensification case where both CAPEX and OPEX as well as the required installation space can be drastically reduced[34, 35].

However, from a thermodynamic point of view, distillation trains and DWC can be considered equivalent configurations. The Petlyuk arrangement of the DWC, i.e. pre-fractionator and column, and the equivalent indirect configuration are shown in Figure 3.9 for an infinite number of equilibrium stages. The indirect configuration has been selected as a case study since Di Pretoro et al.[36, 37] already proved it to be particularly convenient for the n-butanol recovery in the

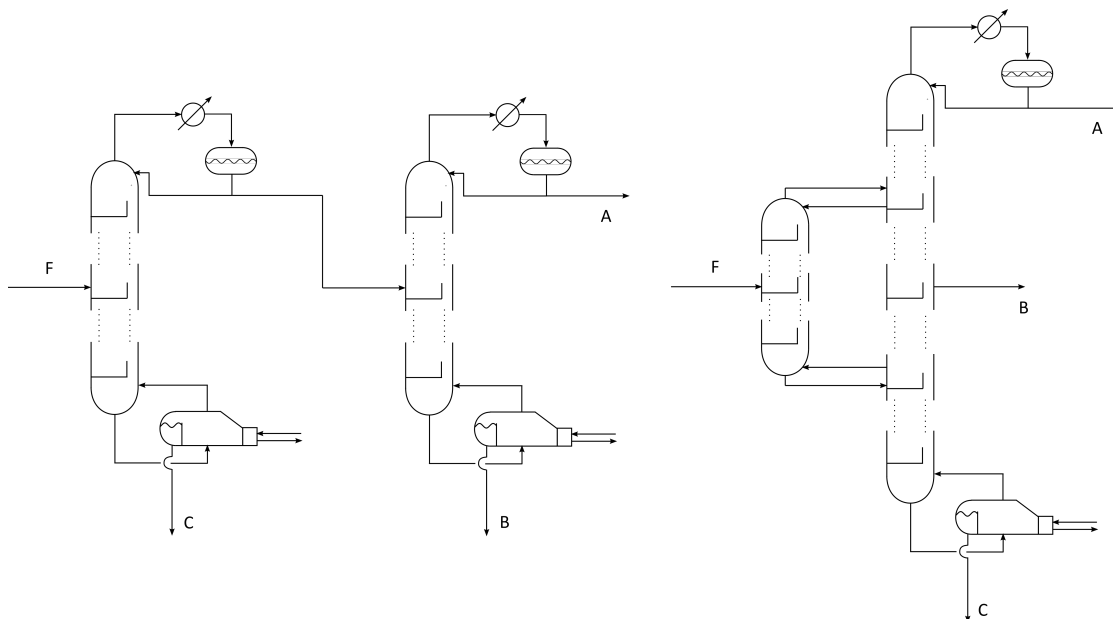


Fig. 3.9: Infinitely staged indirect distillation train (left) and DWC (right)

ABE separation. However, in this paper, the thermodynamic assessment has been extended including both the columns of the distillation train configuration. Furthermore, the following procedure can be scaled up to any number of columns, i.e. any number of walls and side streams in a DWC.

The residue curve interpretation doesn't considerably change. It still represents the column concentration profile for an infinite number of trays at infinite reflux ratio. The main consequence of this theoretical consideration is that the distillation feasibility condition still applies: in order to belong to the same distillation column profile, the residue curves passing through the characteristic point of every side stream should belong to the same distillation region, i.e. it should have the same stable and unstable nodes. Thus, the main change with respect to the single column case study is that all the streams entering or exiting the distillation train (or the DWC) should be included in the analysis.

As already anticipated in section 3, the additional specifications to be included will refer to the acetone purity and recovery ratio; this means that the side stream will contain the remaining components, i.e. mainly water and ethanol. While the specification related to a product purity directly provides its coordinate in the diagram, the recovery ratio constraint requires a reinterpretation.

Performing the overall mass balance on the entire system the following equation can be easily obtained:

$$F = D + S + B \quad (6.1)$$

that is:

$$1 = \frac{D}{F} + \frac{S}{F} + \frac{B}{F} \quad (6.2)$$

On the other hand the partial mass balance states as:

$$F \cdot \bar{z} = D \cdot \bar{x}_D + S \cdot \bar{x}_S + B \cdot \bar{x}_B \quad (6.3)$$

dividing everything by F the equation of a plane is achieved:

$$\bar{z} = \frac{D}{F} \cdot \bar{x}_D + \frac{S}{F} \cdot \bar{x}_S + \frac{B}{F} \cdot \bar{x}_B \quad (6.4)$$

This means that, for given product compositions (\bar{x}_D and \bar{x}_B) and recovery ratios (directly related to $\frac{D}{F}$ and $\frac{B}{F}$) the side stream molar fractions and flowrate can be assessed and the corresponding characteristic point lies on the same plane as the other three ones.

In conclusion, the mass balance in a quaternary diagram is translated into a coplanarity condition and the recovery ratios establish the relative position of the side stream characteristic point with respect to the distillate and the bottom ones.

Therefore a given inlet concentration $\bar{z} = [0.660, 0.120, 0.100, 0, 120]$ similar to the previous chapter ones is assumed. Residue curves under nominal operating conditions are calculated as usual for the four streams and plotted in Figure 3.10a. The orange curve refers to the side stream while the color notation for the other curves is unchanged. Water content, that is the most critical parameter, can be then perturbed as usual until feasibility limits are achieved for $\bar{z} = [0.641, 0.146, 0.097, 0, 116]$ as plotted in Figure 3.10b. For a further increase in the water molar fraction the residue curve related to the side stream crosses indeed the distillation boundary and doesn't attain the pure butanol vertex but the pure water one instead.

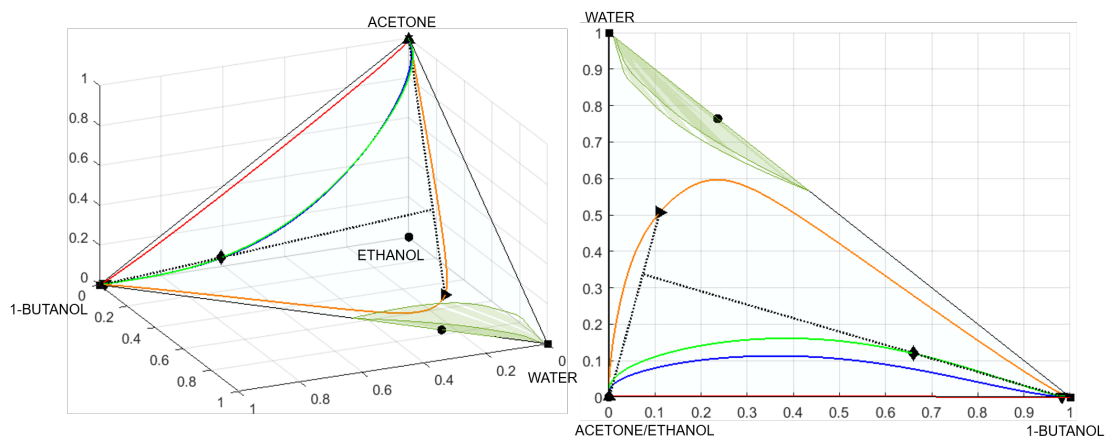
Even though the case study is different from the previous chapter one since a second compound, i.e. acetone, is recovered as well, the feasibility boundary values can be commented in analogy to the single distillation column.

First of all it is worth noticing that the separatrix surface is the same as the single column case study since it is a function of the system thermodynamics, i.e. of the components only.

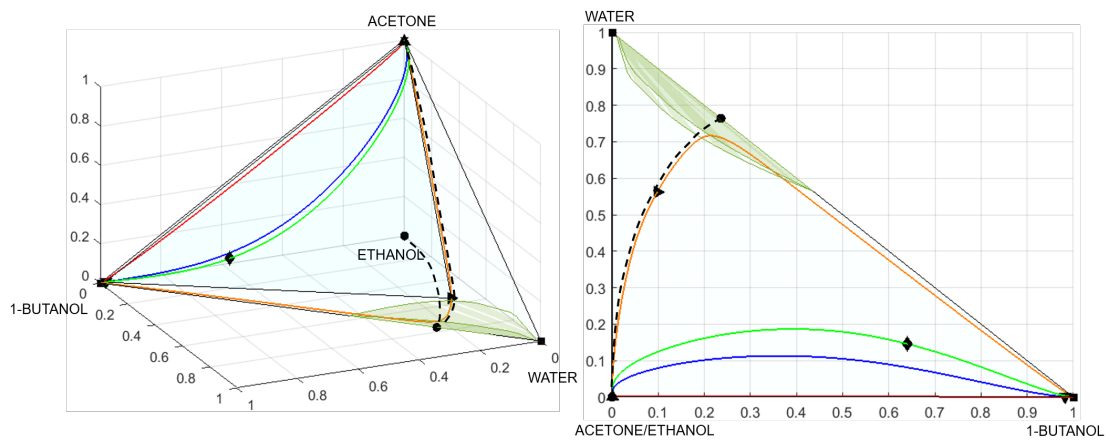
While for the single column the distillate stream is the one crossing the distillation boundary, in case of indirect distillation train and DWC the second column bottom stream and the side stream respectively are those who cause the process unfeasibility.

For this case study the limit water to butanol ratio is 1:4.4 resulting in a substantial decrease with respect to the previous cases where acetone was not purified. Due to the acetone recovery, a consistent amount of ethanol is indeed withdrawn in the distillate stream. This causes the side withdrawal to be richer in water both because acetone is not present anymore and because it carries with it part of the ethanol causing a faster shifting of the side stream operating point towards the pure water vertex.

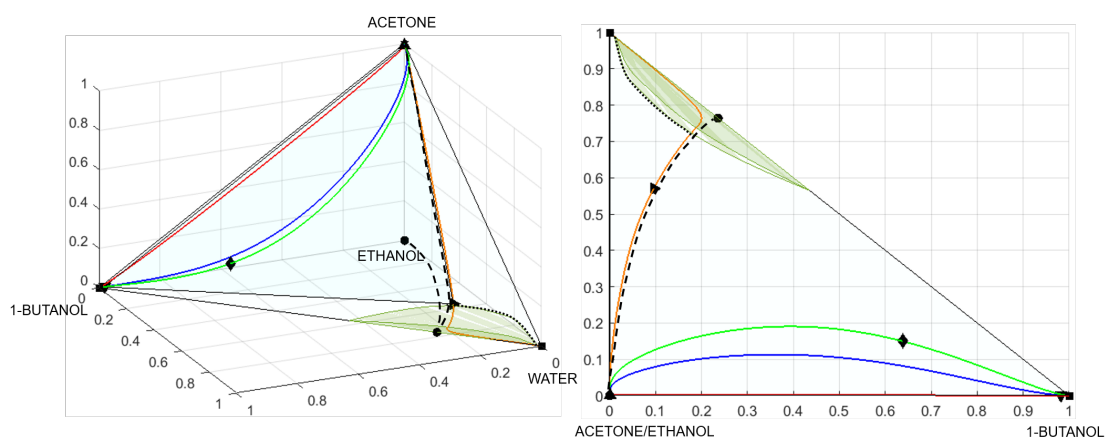
As anticipated this procedure has no upper limits concerning the number of



(a) Nominal operating conditions



(b) Feasibility limit



(c) Unfeasible distillation

Fig. 3.10: Distillation RCM for distillation train and DWC

species in the feed and the number of columns/walls but at least three components are required in order to have a useful employment of distillation trains or DWC.

7 Conclusions

Residue curve mapping has been deeply explored in this analysis. Three main outcomes can be identified from this study and are worth to be commented.

The first one is the definition of a thorough procedure to assess thermodynamic flexibility of distillation processes when the product recovery ratio is used as a separation specification. This parameter indeed can be directly correlated to the separation productivity that is the main income item in process design. Depending on the number of components, the recovery ratio fixes the relative position of the distillation column streams over the $N - 2$ dimensional space constrained by the mass balances.

The second useful tool described in this paper is the thermodynamic feasibility assessment and flexibility boundaries definition in case of distillation trains and integrated distillation systems such as the DWC as well as their graphical representation. Since at infinite reflux and number of equilibrium stages they are equivalent configurations there's no difference concerning the thermodynamic feasibility limits. However, when dealing with costs and control they are likely to show considerably different behaviours.

Finally, according to the shape of the N-dimensional separatrix boundary, RCM graphical representations allow to predict the effect of the presence of a further component in the feed stream from a flexibility point of view. The convexity/concavity of the separatrix would result respectively in a positive/negative impact on the separation effectiveness under uncertainty.

In conclusion this study provides a useful graphical and numerical tool to the decision maker in order to evaluate which are the potentialities and the limitations of the most common distillation processes applied to a given multicomponent mixture. Even though the presented results are case specific, the proposed procedure has a general validity and can be performed with any mixture and any of the most used flexibility indexes.

Residue curve mapping has proved indeed to be an effective methodology worth to be exploited even when uncertainty should be taken into account that is particularly the case with bio-based processes.

A List of acronyms and symbols

Symbol	Definition	Unit
<i>ABE/W</i>	Acetone-Butanol-Ethanol/Water	/
<i>B</i>	Bottom flowrate	<i>mol/s</i>
C_{ij}^n	Excess Gibbs energy coefficients	$J/(mol \cdot K^n)$
<i>CAPEX</i>	CAPital EXpenses	\$
<i>D</i>	Distillate flowrate	<i>mol/s</i>
<i>DWC</i>	Dividing Wall Column	/
<i>F</i>	Feed flowrate	<i>mol/s</i>
g_{ij}	NRTL excess Gibbs energy	J/mol
K_i	Equilibrium constant	1
<i>NRTL</i>	Non-Random Two Liquids	/
<i>OPEX</i>	OPerating EXpenses	$\$/y$
<i>P</i>	Pressure	<i>atm</i>
<i>R</i>	Gas constant	$J/(mol \cdot K)$
<i>RCMs</i>	Residue Curve Maps	/
<i>S</i>	Side stream flowrate	<i>mol/s</i>
<i>T</i>	Temperature	$^{\circ}C$
<i>VLLE</i>	Vapor-Liquid-Liquid Equilibrium	/
x_i^k	k-th stage liquid phase molar fraction of the i-th species	1
$x_i^{aq/org}$	Aqueous/organic phase molar fraction of the i-th species	1
\bar{x}	Liquid phase composition vector	1
y_i	Vapor phase molar fraction of the i-th species	1
\bar{y}	Vapor phase composition vector	1
z_i	Molar fraction of the i-th species in the feed	1
\bar{z}	Feed composition vector	1

Greek letters	Definition	Unit
α_{ij}	Non-randomness parameter	1
γ_i	Activity coefficient	1
ξ	Dimensionless time	1
τ_{ij}	NRTL dimensionless interaction parameter	1

B Thermodynamic model

As anticipated, according to a wide range of authors [24, 26, 27, 28], the most suitable activity model to describe the ABE/W mixture behaviour is the Non-Random Two Liquids (NRTL) [25]. It is able to describe both liquid and vapor phases non-idealities such as azeotropes and liquid immiscibility.

The activity coefficient for the species i in a mixture of n components is given by:

$$\ln(\gamma_i) = \frac{\sum_{j=1}^n x_j \cdot \tau_{ji} \cdot G_{ji}}{\sum_{k=1}^n x_k \cdot G_{ki}} + \sum_{j=1}^n \frac{x_j \cdot G_{ij}}{\sum_{k=1}^n x_k \cdot G_{kj}} \cdot \left(\tau_{ij} - \frac{\sum_{m=1}^n x_m \cdot \tau_{mj} \cdot G_{mj}}{\sum_{k=1}^n x_k \cdot G_{kj}} \right) \quad (\text{B.1})$$

where:

$$\ln(G_{ij}) = -\alpha_{ij} \cdot \tau_{ij} \quad (\text{B.2})$$

$$\alpha_{ij} = \alpha_{ij}^0 + \alpha_{ij}^1 \cdot T \quad (\text{B.3})$$

$$\tau_{ij} = \frac{\Delta g_{ij}}{R \cdot T} \quad (\text{B.4})$$

$$\Delta g_{ij} = g_{ij} - g_{jj} = C_{ij}^0 + C_{ij}^1 \cdot T \quad (\text{B.5})$$

where α_{ij} is called non-randomness parameter and τ_{ij} is called dimensionless interaction parameter.

Binary interaction parameters provided by process simulators are not compliant with each other and they're not always able to correctly predict the equilibrium compositions in proximity of the singularity points. Simulis[®] Thermodynamics database resulted the most reliable for water-alcohols interactions but some parameters for binary interaction coefficients among inorganic compounds are not available and needed to be integrated. After the binary coefficients adjustment the thermodynamic model results then able to meet the experimental data concerning azeotropes and liquid-liquid demixing provided in literature [29, 30, 31, 32, 38, 39].

References

- [1] Di Pretoro, A., Montastruc, L., Manenti, F., Joulia, X. Flexibility analysis of a distillation column: Indexes comparison and economic assessment. *Comput. Chem. Eng.* 2019, 124, 93–108. <https://doi.org/10.1016/j.compchemeng.2019.02.004>
- [2] Hoch, P.M., Eliceche, A.M., Grossmann, I.E. Evaluation of Design Flexibility in Distillation-Columns Using Rigorous Models. *Comput. Chem. Eng.* 1995, 19, S669–S674. [https://doi.org/10.1016/0098-1354\(95\)00137-Q](https://doi.org/10.1016/0098-1354(95)00137-Q)
- [3] Giuliano, A., Poletto, M., Barletta, D. Process optimization of a multi-product biorefinery: The effect of biomass seasonality. *Chem. Eng. Res. Des., Biorefinery Value Chain Creation* 2016, 107, 236–252. <https://doi.org/10.1016/j.cherd.2015.12.011>
- [4] Yue, D., You, F., Snyder, S.W. Biomass-to-bioenergy and biofuel supply chain optimization: Overview, key issues and challenges. *Comput. Chem. Eng.* 2014, 66, 36–56. <https://doi.org/10.1016/j.compchemeng.2013.11.016>
- [5] Ostwald, W. Dampfdrucke ternärer Gemische, *Abhandlungen der Mathematisch-Physischen Classe der Königl. Sachs. Gesellschaft der Wissenschaften* 1900, 25, 413–53 (Germ.).
- [6] Schreinemakers, F. A. H. Dampfdrucke ternärer Gemische. *J. Phys. Chem.* 1901, 36, 413–49 (Germ.).
- [7] Gurikov, Yu. V. Some Questions Concerning the Structure of Two-Phase Liquid–Vapor Equilibrium Diagrams of Ternary Homogeneous Solutions. *J. Phys. Chem.* 1958, 32, 1980–96 (Rus.).
- [8] Zharov, V. T. Free Evaporation of Homogeneous Multicomponent Solutions. *J. Phys. Chem.* 1967, 41, 1539–55 (Rus.).
- [9] Zharov, V. T. Free Evaporation of Homogeneous Multicomponent. Solutions. 2. Four Component Systems. *J. Phys. Chem.* 1968a, 42, 58–70 (Rus.).
- [10] Zharov, V. T. Free Evaporation of Homogeneous Multicomponent Solutions. 3. Behavior of Distillation Lines Near Singular Points. *J. Phys. Chem.* 1968b, 42, 195–211 (Rus.).
- [11] Serafimov, L. A. The Azeotropic Rule and the Classification of Multicomponent Mixtures. 4. N-Component Mixtures. *J. Phys. Chem.* 1969, 43, 981–3 (Rus.).
- [12] Zharov, V. T., Serafimov, L. A. *Physico-Chemical Foundations of Batch Open Distillation and Distillation*. Leningrad: Khimiya 1975, (Rus.).

- [13] Petlyuk, F.B., Danilov, R.Yu. Theory of Distillation Trajectory Bundles and its Application to the Optimal Design of Separation Units: Distillation Trajectory Bundles at Finite Reflux. *Chem. Eng. Res. Des., Distillation and Absorption* 2001, 79, 733–746.
- [14] Petlyuk, F.B. *Distillation Theory and its Application to Optimal Design of Separation Units*. Cambridge University Press 2004.
- [15] Laroche, L., Bekiaris, N., Andersen, H.W., Morari, M. Homogeneous azeotropic distillation: separability and flowsheet synthesis. *Ind. Eng. Chem. Res.* 1992, 31, 2190–2209. <https://doi.org/10.1021/ie00009a017>
- [16] Thormann, K. *Destillieren und Rektifizieren*. Leipzig: Verlag von Otto Spamer (Germ.), 1928.
- [17] Kiva, V.N., Hilmen, E.K., Skogestad, S. Azeotropic phase equilibrium diagrams: a survey. *Chem. Eng. Sci.* 2003, 58, 1903–1953. [https://doi.org/10.1016/S0009-2509\(03\)00018-6](https://doi.org/10.1016/S0009-2509(03)00018-6)
- [18] Wahnschafft, O.M., Koehler, J.W., Blass, E., Westerberg, A.W. The product composition regions of single-feed azeotropic distillation columns. *Ind. Eng. Chem. Res.* 1992, 31, 2345–2362. <https://doi.org/10.1021/ie00010a014>
- [19] Saboo, A., Morari, M., Woodcock, D. Design of Resilient Processing Plants .8. a Resilience Index for Heat-Exchanger Networks. *Chem. Eng. Sci.* 1985, 40, 1553–1565. [https://doi.org/10.1016/0009-2509\(85\)80097-X](https://doi.org/10.1016/0009-2509(85)80097-X)
- [20] IEA Bioenergy Annual Report 2018 retrieved at <https://www.ieabioenergy.com/wp-content/uploads/2019/04/IEA-Bioenergy-Annual-Report-2018.pdf>
- [21] García, V., Pääkkilä, J., Ojamo, H., Muurinen, E., Keiski, R.L. Challenges in biobutanol production: How to improve the efficiency? *Renew. Sustain. Energy Rev.* 2011, 15, 964–980. <https://doi.org/10.1016/j.rser.2010.11.008>
- [22] Ezeji, T.C., Qureshi, N., Blaschek, H.P. Bioproduction of butanol from biomass: from genes to bioreactors. *Current Opinion in Biotechnology, Energy biotechnology / Environmental biotechnology* 2007, 18, 220–227. <https://doi.org/10.1016/j.copbio.2007.04.0>
- [23] Xue, C., Zhao, J.-B., Chen, L.-J., Bai, F.-W., Yang, S.-T., Sun, J.-X. Integrated butanol recovery for an advanced biofuel: current state and prospects. *Appl. Microbiol. Biotechnol.* 2014, 98, 3463–3474. <https://doi.org/10.1007/s00253-014-5561->

- [24] Errico, M., Sanchez-Ramirez, E., Quiroz-Ramirez, J.J., Rong, B.-G., Segovia-Hernandez, J.G. Multiobjective Optimal Acetone–Butanol–Ethanol Separation Systems Using Liquid–Liquid Extraction-Assisted Divided Wall Columns. *Ind. Eng. Chem. Res.* 2017, 56, 11575–11583. <https://doi.org/10.1021/acs.iecr.7b03078>
- [25] Renon H., Prausnitz J. M. "Local Compositions in Thermodynamic Excess Functions for Liquid Mixtures", *AIChE J.* 1968, 14(1), S.135–144.
- [26] Kiss, A. A. Novel applications of dividing-wall column technology to biofuel production processes. *J. Chem. Technol. Biotechnol.* 2013, 88, 1387.
- [27] Okoli, C. O.; Adams, T. A., II Design of dividing wall columns for butanol recovery in a thermochemical biomass to butanol process. *Chem. Eng. Process* 2015, 95, 302.
- [28] Le, Q.-K., Halvorsen, I.J., Pajalic, O., Skogestad, S. Dividing wall columns for heterogeneous azeotropic distillation. *Chem. Eng. Res. Des., Distillation and Absorption* 2015, 99, 111–119. <https://doi.org/10.1016/j.cherd.2015.03.022>
- [29] Dortmund Data Bank, www.ddbst.de
- [30] Luyben, W.L. Control of the Heterogeneous Azeotropic n-Butanol/Water Distillation System. *Energy Fuels* 2008, 22, 4249–4258. <https://doi.org/10.1021/ef8004064>
- [31] Stockhardt, J.S., Hull, C.M. Vapor-Liquid Equilibria and Boiling-Point Composition Relations for Systems n-Butanol–Water and Isobutanol–Water_{1,2}. *Ind. Eng. Chem.* 1931, 23, 1438–1440. <https://doi.org/10.1021/ie50264a034>
- [32] Orr, V., Coates, J.. Versatile Vapor-Liquid Equilibrium Still. *Ind. Eng. Chem.* 1960, 52(1), 27–30. <https://doi.org/10.1021/ie50601a030>
- [33] Petlyuk F. B., 'Thermodynamically Optimal Method for Separating Multi-component Mixtures', *Int. Chem. Eng.* 1965, 5, 555–61.
- [34] K. Glinos and M.F. Malone, 'Optimality Regions for Complex Column Alternatives in Distillation Systems', *Chem. Eng. Res. Des.* 1988, 66, 3, 229–40.
- [35] Schultz, M.A., Stewart, D.G., Harris, J.M., Rosenblum, S.P., Shakur, M.S., O'Brien, D.E. Reduce costs with dividing-wall columns. *Chem. Eng. Prog.* 2002, 98, 64–71.
- [36] Di Pretoro, A., Montastruc, L., Manenti, F., Joulia, X. Flexibility Assessment of a Distillation Train: Nominal vs Perturbated Conditions Optimal Design, *Computer Aided Chemical Engineering, 29 European Symposium on Computer Aided Process Engineering* 2019, 46, pp. 667–672.

- [37] Di Pretoro, A., Montastruc, L., Manenti, F., Joulia, X. Flexibility assessment of a biorefinery distillation train: Optimal design under uncertain conditions. *Comput. Chem. Eng.* 2020, 138, 106831. <https://doi.org/10.1016/j.compchemeng.2020.106831>
- [38] Lee, M.-J., Tsai, L.-H., Hong, G.-B., Lin, H.-M., 2004. Multiphase equilibria for binary and ternary mixtures containing propionic acid, n-butanol, butyl propionate, and water. *Fluid Phase Equilibria* 216, 219–228. <https://doi.org/10.1016/j.fluid.2003.09.009>.
- [39] Kosuge, H., Iwakabe, K., 2005. Estimation of isobaric vapor–liquid–liquid equilibria for partially miscible mixture of ternary system. *Fluid Phase Equilibria* 233, 47–55. <https://doi.org/10.1016/j.fluid.2005.04.010>

Part IV. Optimal Design: Optimal Number of Equilibrium Stages

Optimal Design and Environmental Impact Assessment of Flexible Multistage Operations under Uncertain Conditions

Alessandro Di Pretoro^{a,b}, Xavier Joulia^a, Flavio Manenti^b, Ludovic Montastruc^{a*}

^aLaboratoire de Génie Chimique, Université de Toulouse, CNRS/INP/UPS, Toulouse, France

^bPolitecnico di Milano, Dipartimento di Chimica, Materiali e Ingegneria Chimica «Giulio Natta», Piazza Leonardo da Vinci 32, 20133 Milano, Italy.

Abstract

Operating expenses are increasingly the most expensive costs in chemical plants. They play a main role in all plants processing large amount of feedstock via well-established processes of the petrochemical industry. In staged operations the classical design procedure provides for the remaining degree of freedom fulfillment by means of an economic optimization. Operating and capital expenses are evaluated at each number of stages and the one corresponding to the minimum total annualized costs is selected. However, the design thus obtained is regarded to be “optimal” with respect to nominal operating conditions. This means that, for the designed equipment, external duties, and thus operating expenses, may considerably vary under the effect of external disturbances. The analysis outlined in this paper shows that appropriate higher investments, carefully assessed through a rigorous and quantitative procedure, could lead to a safer, more profitable and more flexible design accounting for external perturbations. Moreover, beside the economic assessment, a sustainability analysis has been carried out and coupled with the flexible procedure in order to show that different investment vs duty compromises could lead to more environmentally friendly design solutions as well.

Highlights:

1. Accounting for external perturbations could lead to a considerably different design choice in equilibrium staged operations design

2. The uncertainty characterization is of critical importance to have reliable cost estimations for flexible design

3. For a given economic assessment, sustainability plays a main role to shift the design choice towards higher investments and lower operating expenses

Keywords: OPEX; energy demand; flexibility; equilibrium-staged separations; optimal design; CO_2 emissions; GWP.

1 Introduction

Equilibrium-staged separations (especially distillation) are widespread operations present in the vast majority of chemical plants. In particular, they are a key step in all well-established processes aimed at the preliminary treatment of large capacity feedstocks, such as crude oil refining. They play a main role both on process and on utility sides consuming huge amount of energy in the form of heat and electricity. Common examples of these operations are crude oil topping, solvent regeneration in absorption or extraction processes, multi-stage non-adiabatic reactors, steam generation, drying operations as well as concentration processes such as crystallization or multiple-effect evaporation [1].

The conventional equipment design and sizing is usually performed by referring to nominal operating conditions and the remaining degrees of freedom are fulfilled by means of an economic optimization. In particular, for equilibrium-staged units, the optimal number of stages is found according to the Total Annualized Costs (TAC) function given both by CAPital and OPERating EXPenses (CAPEX and OPEX respectively). Investment costs usually show a linear increase by increasing the number of stages N since the unit size is proportionally enlarged while the external duty requirement has a hyperbolic decline with respect to N . The total annualized cost function then results in a curve with a global minimum corresponding to the optimal number of stages [2].

Once the unit is built according to the parameters previously obtained, the control system is aimed at:

- suppressing the influence of external disturbances;
- ensuring the stability of a chemical process;
- optimizing the performance of a chemical process [3].

So, basically, for a given equipment configuration, the control system manages the external duties according to the specifications to maintain, i.e. OPEX are the main cost item related to external disturbances suppression. In particular, the variation in external duties is much more appreciable in case of lower number of equilibrium stages. In brief, it can be stated that, in equilibrium-staged operations, operating expenses could be reduced at the cost of higher investments both for nominal or perturbed operating conditions.

Besides the economic point of view, there are more than one additional reason why it is not recommended to have considerable fluctuations in external duties. The most important one is safety: process valves are sized to optimally operate in a given range of their opening position. If they undergo fast and considerable oscillations between the “almost closed” and the “complete opening” positions, their risk of breakage is much higher which greatly reduces their lifetime and will

necessitate more maintenance. The same remarks apply to units overcharged by thermal duties.

Another inconvenience related to higher energy consumptions as a consequence of a non-robust design concerns the process sustainability. The energy consumption, in particular the electricity for compression and heat duties [4, 5, 6], is indeed the main item in the list of factors affecting the environmental impact of a process. Specifically, this impact depends both on the amount of energy consumed and on the sources employed for its production. Therefore, an appropriate system design is not only be profitable from an economic perspective, but it could also result to be more sustainable than the conventional process design solution associated with the nominal operating conditions.

For all these reasons, design under uncertainty has been one of the most relevant research field during recent years. In particular, several methodologies for process design optimization under uncertainty have been proposed in literature involving the use of genetic algorithm [7, 8], robust parameter design [9] or Bayesian model averaging [10].

However, in those studies uncertainty has not always the same meaning as it will be further detailed in the following section.

The part of this research field related to the design of processes able to withstand variable operating conditions can be referred to as flexible process design. Both deterministic [11, 12] and stochastic [13, 14] indicators aimed at quantifying the system flexibility have been proposed in literature during the last decades and several studies rely on them [15, 16, 17].

This article as well can be seen as a contribution to the latter research domain since we are intended to design process units under variable input parameters.

In particular, the purpose of this research is to present a procedure aimed at the assessment of the optimal number of stages in multistage operations accounting for process variables uncertainty. It can be seen as a dedicated application of the flexibility based design procedure to those cases where the uncertain parameters probability distribution function is known and the number of equilibrium stages should be optimized.

In order to provide a more complete introduction about this study concerning operating expenses and optimal design under uncertain operating conditions, a more detailed discussion about the way the uncertainty is treated is done in the dedicated following section.

Sections 4 and 5 present the application of the proposed procedure to two different case studies where the uncertain parameters affect the unit capacity and separation performance respectively.

Finally, an environmental assessment is performed both on the flexible and conventional design in order to compare them and to correlate the CO_2 emissions with the number of stages N .

2 The uncertainty characterization

Although the purpose of this study is to outline a thorough procedure of general validity, the results obtained are nevertheless qualitatively and quantitatively case specific. In particular, one of the aspects with the highest impact on the results is the probability distribution function (hereafter PDF) selected to describe the uncertain variables fluctuation likelihood.

Uncertainty indeed has been one of the key aspects related to design optimization methodologies during the past years. The different typology of uncertainty have been classified by Oberkampf and Helton (2001)[18] in three main categories:

- aleatory uncertainty (also referred to as stochastic uncertainty, irreducible uncertainty, inherent uncertainty or variability);
- epistemic uncertainty (also referred to as reducible uncertainty, subjective uncertainty, model form uncertainty or simply uncertainty);
- error.

This is the reference classification still used nowadays by the vast majority of authors dealing with uncertainty in different domains [19]. Aleatory uncertainty is defined as the inherent variation associated to the physical environment under consideration, while the epistemic uncertainty is defined as any lack of knowledge or information in any phase or activity of the modeling process. Error is defined as a recognizable deficiency in any phase or activity of modeling and simulation that is not due to lack of knowledge [18, 20, 21]. Epistemic uncertainty has been one of the most challenging topics during the past years and it can be concluded that its characterization is better carried out by means of fuzzy sets theory [22], Dempster-Shafer theory [23], possibility theory [24], and the theory of upper and lower previsions [25]. Several studies discussing computational methods for optimization accounting for this kind of uncertainty are available in literature for more details [26, 27, 28, 29].

On the other hand, aleatory uncertainty is particularly suitable for input data variability description and it is widely agreed that it can be characterized by using the probability theory, i.e. by means of probability distribution functions [18, 19, 30, 31]. This kind of design under stochastic uncertainty is typically referred to as flexibility based design as thoroughly discussed by several research works available in literature [12, 13, 14, 17, 32, 33, 34, 35].

Disturbance likelihood can be described both by discrete and continuous PDFs based on data collection and measurements related to the process or as the product of reasonable assumptions about the perturbation nature and magnitude. In this research work, the normal (Gaussian) and the Beta probability distributions, represented in Figures 4.1a and 4.1b with their cumulative functions, have been selected in order to describe two different process variables behaviours (for further

details about the mathematical formulation of the selected PDFs please refer to Severini (2011)[36]).

Indeed whenever no information is available, a general validity PDF should be employed and the normal distribution is the one usually describing this “general validity” condition. Moreover, uncertainty is often due not only to the uncertain variables fluctuation, but to the error related to its measurements. Once again the Gaussian PDF results to be the most suitable distribution to describe this phenomenon.

When shifting from the deterministic to the stochastic domain, the nominal operating conditions become the most probable operating conditions only. The symmetry of the normal PDF implies that negative deviations with respect to the nominal operating conditions are as probable as positive ones with the same magnitude. However, in chemical processes, this is not always the case since external perturbations often preferentially occur in one particular direction.

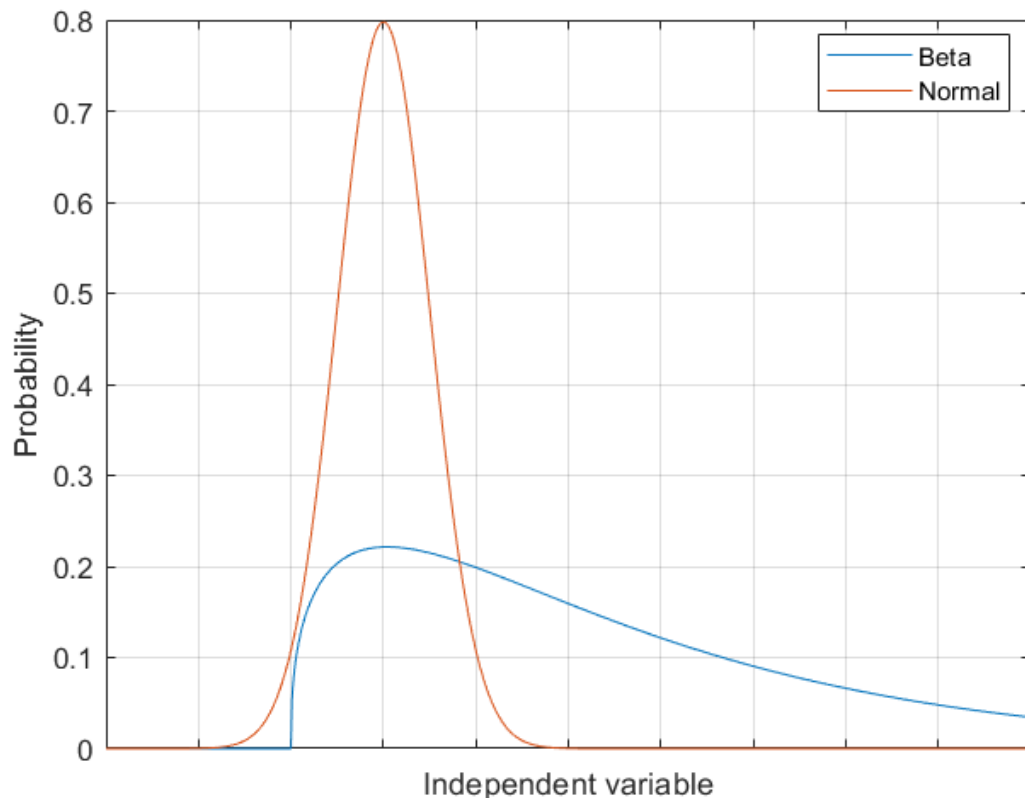
For this reason, the Beta PDF was included in the analysis. This particular PDF was considered a suitable choice to describe very common situations where the nominal value represents the most probable condition, but it actually underestimates the vast majority of the possible operating conditions. If the cumulative probability is considered, in correspondence with the operating point, i.e. the maximum likelihood, less than the 20 % of all possible operating conditions are actually included. From a process design point of view it means that, if the equipment sizing is performed with respect to nominal operating conditions, the obtained design is undersized for more than the 80 % of the plant operation.

In the light of these observations, it can be concluded that the normal PDF has been used in this analysis to describe the most common probability distribution taking into account the measurement errors as well, while the Beta has been included to describe all those processes whose input varies over a range with an asymmetrical behaviour.

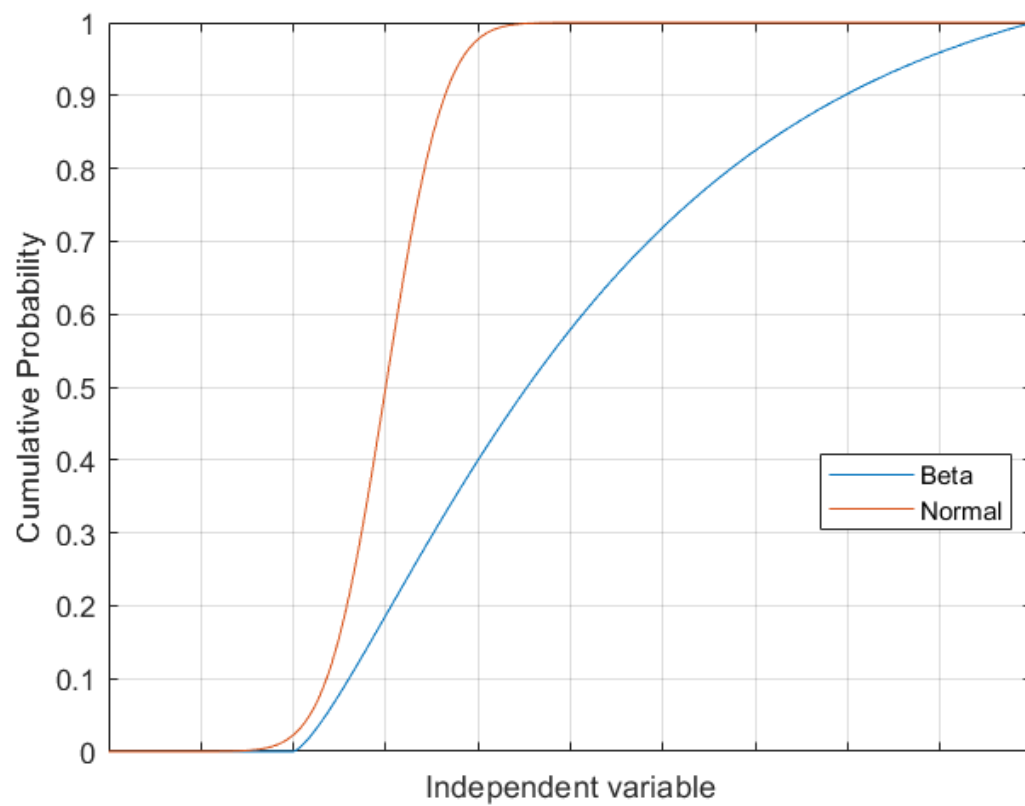
Beside determining the outcome properties, the choice of the PDF function affects the numerical aspects of the algorithm from a computational time point of view as well. Some properties of the PDF can be indeed useful to make simplifying hypotheses and to speed up the calculations, as well as to better outline the expected result even before computation is run.

Replacing one value with an entire function is indeed computationally cumbersome so it is worth to be done only when strictly required. Therefore, it is of major importance to have the sensitivity to preliminary assess whether the flexible design procedure would result in a considerably different design compared to the conventional one.

Let us consider for instance the case of a symmetric distribution function such as the Gaussian one and let us assume the equipment cost function to be linear with respect to the uncertain variable value or that it can be linearized over the considered uncertain domain. From an operational point of view, a linear function



(a) Probability Distribution Functions



(b) Cumulative Probability Distribution Functions

Fig. 4.1: Uncertainty characterization

can be considered an odd function with respect to any of its points; a convenient choice for the center of symmetry is the nominal operating conditions point $(\mu, f(\mu))$ since $x = \mu$ corresponds to the axis of symmetry of the normal PDF as well. This non-restrictive choice results in the property:

$$f(\mu + x) - f(\mu) = -(f(\mu - x) - f(\mu)) \quad (2.1)$$

The average weighted with respect to a weight function (e.g. likelihood distribution) of another general function is given by the integral of the product between the function itself and its weight over the integration domain and normalized with respect to the domain size. In this case then, the average of the cost function weighted with respect to the probability distribution over the range $[a, a]$ is calculated by definition as:

$$\bar{f} = \frac{1}{2 \cdot a} \cdot \int_a^a P(x) \cdot f(x) \cdot dx \quad (2.2)$$

The function $F(x) = P(x) \cdot f(x)$ is the product between an odd and a even function, i.e. an odd function. For this reason, its integral is equal to zero, which means $\bar{f} = 0 + f(\mu)$ considering that the axes were translated. The main outcome of this analysis is then that, if the uncertain variable probability distribution is symmetric and the cost function we want to average is linear or, in more general terms, is an odd function, the result obtained taking into account the deviation likelihood is the same obtained under nominal operating conditions whatever the variance. In brief, for these kinds of systems, it can be known “a priori” that a more detailed design procedure is not worth being used since it would only result in useless computational efforts.

However, for the case studies presented in the following sections, calculations with the Gaussian PDF will be nevertheless performed in order to validate this assumption even when the cost function is not exactly linear but close to it. A reliable perturbation range representing the x-axis of Figure 4.1a will be defined for each of them keeping the nominal operating conditions in correspondence with the highest probability (i.e. the mode).

3 Flexible design procedure

As already mentioned, the methodology proposed in this article to determine the optimal number of equilibrium stages in multistage unit operations under uncertain operating conditions is a stochastic method application to those cases where aleatory uncertainty can be described by a likelihood function.

The purpose of this section is to sum up the concepts previously presented and to couple them in the procedure that will be used for the selected case studies here below.

In order to characterize the uncertainty, two different probability distributions have been proposed as shown in Figure 1. However, the procedure can be applied to any function and is not restrained to those presented in the following case studies. These two trends have been selected in order to compare the impact of both symmetric and skewed disturbance likelihood on the final result.

The Beta and the normal PDF belong to the two-parameter distributions family, therefore two conditions should be fixed in order to uniquely defined them.

For this study, the first condition is that the nominal operating conditions corresponds to the maximum of the PDF curves, i.e. the operating condition most likely to occur. On the other hand, the two distribution have been selected so that they're variance is the same.

Given the uncertainty characterization, the operating conditions are then evaluated over the feasible part of the uncertain domain and the operating expenses are obtained by equation 2.2 as the previously discussed.

Thus, this procedure implies that a preliminary feasibility assessment is required. The multiple-effect evaporator case study presented in this paper do not show feasibility constraint over the uncertain domain since the selected uncertain parameter is the feed flowrate, i.e. the unit capacity, according to which the equipment has been already conservatively designed. The same remark applies to the distillation case study that presents an ideal mixture with no thermodynamic boundaries, otherwise a specific procedure should have been applied in order to determine the feasible composition space [37].

The TAC function is then calculated by accounting for both the CAPEX and the newly obtained OPEX trends. Thus, the optimal number of stages is finally assessed.

After the economic assessment, an environmental impact evaluation can be performed in order to check if the different optimal number of equilibrium stages with respect to the nominal operating conditions results in lower or higher emissions. In general, the flexible design requires more equilibrium stages than the conventional one corresponding to lower OPEX and then lower duty demand. In these cases, both economics and sustainability would benefit of the additional stages. On the contrary, the "a posteriori" environmental impact analysis wouldn't be sufficient and it should be included among the decision criteria related to N during the design phase.

The procedure described here above is applied in the following sections to two case case studies in order to show the substantially different outcome even for such simple operations.

4 Multiple-effect evaporator

The first case study refers to a cocurrent multiple-effect evaporator. It is a non-conventional unit operation made up of several flash units in series (cf Figure 4.2)

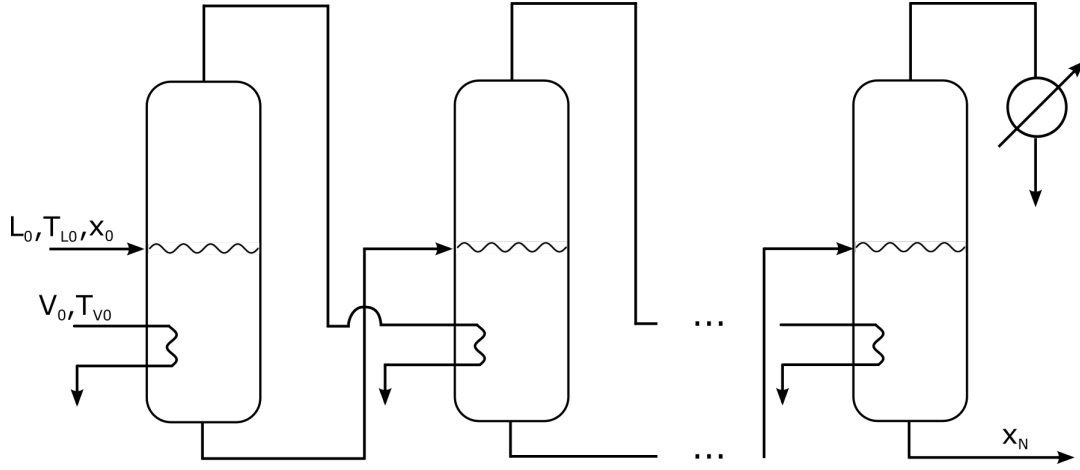


Fig. 4.2: Cocurrent multiple-effect evaporator

and it can be used either to concentrate a solution (sometimes up to crystallization) or to recover a valuable solvent from it. The main advantage of this unit, with respect to the corresponding single effect configuration, is that the outlet vapor of each effect can be used as external duty for the following one which enhances the separation. The cost of this operation improvement consists both of the need for an additional unit and also of the pressure drops required in order to reduce the solution boiling temperature below the previous vapor condensation one.

This basic operation was selected as a first example in order to show how, even for a simple and not very sensitive process, taking into account operating conditions fluctuations could lead to small but significant OPEX changes affecting the optimal design choice.

The cocurrent multiple-effect evaporator was modeled according to Di Pretoro et al. (2020)[38, 39]. For each effect the model equations state as follows:

- Overall mass balance:

$$L_{i-1} = L_i + V_i \quad (4.1)$$

where L and V are the vapor and liquid flowrates.

- Component mass balance:

$$L_{i-1} \cdot w_{i-1} = L_i \cdot w_i \quad (4.2)$$

where w is the solute mass fraction.

- Energy balance:

$$\begin{aligned} L_{i-1} \cdot c_P^L(w_{i-1}, T_{L,i-1}) \cdot T_{L,i-1} + V_{i-1} \cdot \Delta H_{ev}(T_{V,i-1}) = \\ = L_i \cdot c_P^L(w_i, T_{L,i}) \cdot T_{L,i} + V_i \cdot (c_P^{water} \cdot T_{L,i} + \Delta H_{ev}(T_{V,i})) \end{aligned} \quad (4.3)$$

where T_L and T_V are the vapor and liquid temperatures, c_P^L is the liquid

Property	Value	Unit
L_0	10000	kg/h
$T_{L,0}$	363.15	K
x_0	0.05	kg/kg
$T_{V,0}$	393.15	K
w_N	0.5	kg/kg

Tab. 4.1: Nominal Operating Conditions

specific heat and ΔH_{ev} is the evaporation enthalpy.

- Heat exchanger characteristic equation:

$$Q_i = V_{i-1} \cdot \Delta H_{ev}(T_{V,i-1}) = U_i \cdot A_i \cdot (T_{V,i-1} - T_{L,i}) \quad (4.4)$$

where Q is the heat duty, U is the heat transfer coefficient and A is the heat transfer surface area.

- Boiling point elevation:

$$\Delta T_{eb,i} = T_{L,i} - T_{V,i} = f(w_i) \quad (4.5)$$

For reasons related to economic convenience, all the units are equal to each other. As a consequence, every evaporator has the same heat transfer surface area that is large enough to manage the system perturbations.

Each evaporator thus has five degrees of freedom (L, V, w, T_L, T_V), each of which is satisfied by one of the five model equations. The specification x_N concerning the last effect fulfills the d.o.f related to the external steam duty V_0 .

Table 4.1 shows the feed stream properties as well as the external steam duty temperature and the outlet concentration specification for the case study under analysis in this paper.

4.1 Optimal Design under Nominal Operating Conditions

As already introduced here above, an increase in the number of consecutive evaporation stages, i.e. higher CAPEX, reflects in an OPEX decrease.

Since the product is always the same given amount of concentrated solution (for this case study $L_N = L_0 \cdot w_0/w_N = 1000 kg/h$), maximizing the net income corresponds to minimizing the total annualized costs (TAC). Capital expenses were calculated according to the Guthrie-Ulrich-Navarrete correlations [40, 41, 42, 43] and multiplied by the number of stages since, as already mentioned, all units are equal to each other. Operating expenses were calculated according to the actual price of steam per unit energy. The costs estimation formula for both CAPEX and OPEX are further detailed in Appendix B.

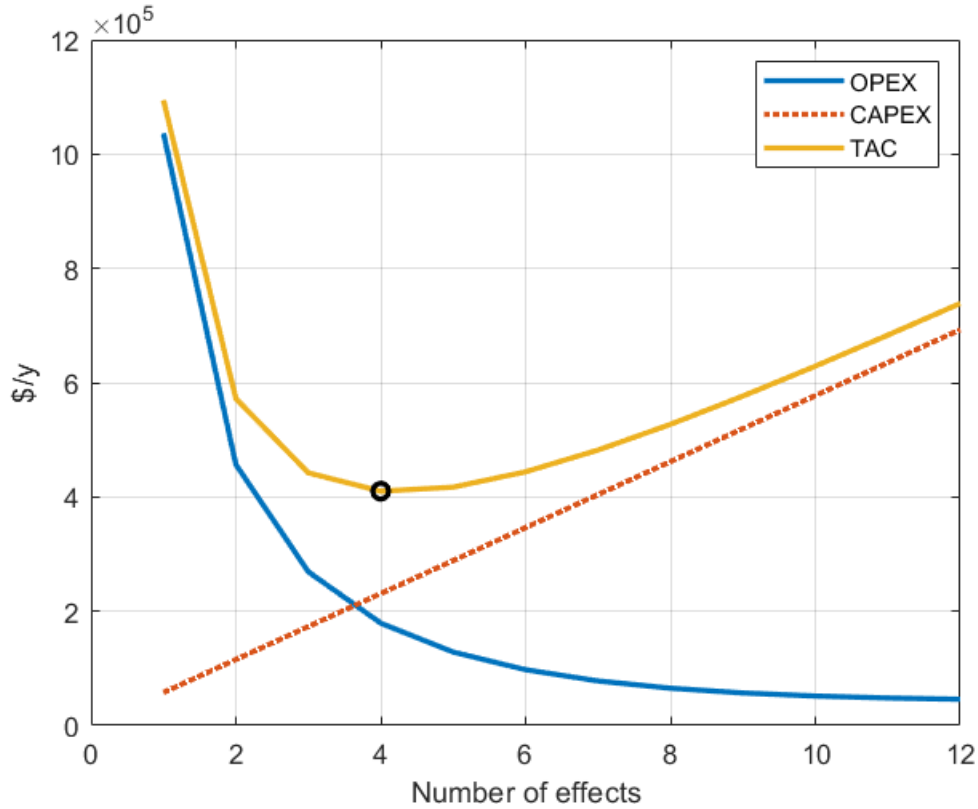


Fig. 4.3: Multiple effect TAC under nominal operating conditions

Finally, the TAC are defined as:

$$TAC = OPEX + \frac{CAPEX}{lifetime} \quad (4.6)$$

where a 12 years lifetime was used for this evaporator case study.

Figure 4.3 shows the trend of the two curves (in \$/year) as well as the total costs, obtained by the combination of the two, vs the number of effects. The OPEX trend, representing the external duty requirement, has a hyperbolic trend while the CAPEX has a linear increase with respect to the number of units employed. The optimal number of effects results then to be four and the corresponding total annualized cost is 410,056 \$/year.

4.2 Flexible Design

The very first step for a flexible design is the identification of the uncertain variables. For this first case study, the inlet flowrate was identified as the variable likely to undergo external disturbances. Given that the nominal operating conditions represent the operating point of maximum likelihood, according to the variance of the Gaussian and Beta probability distribution functions (PDF) described in section 2, the uncertain domain varies over the interval [9000, 16500] kg/h .

The multiple-effect evaporator model can then be solved both for a variable

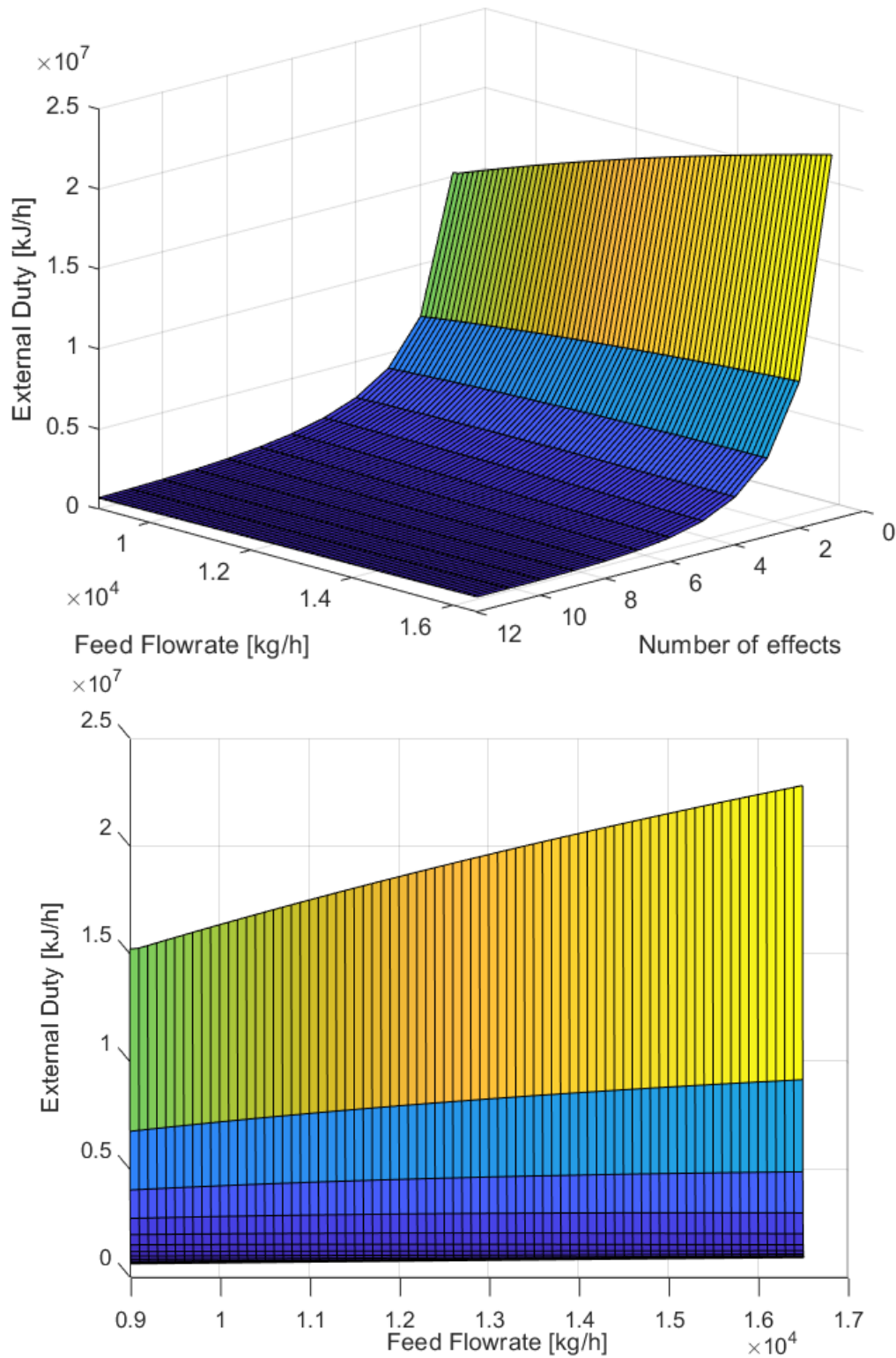


Fig. 4.4: External duty under uncertain operating conditions

number of stages and over the entire interval of uncertain operating conditions. Figure 4.4 (left) shows the external energy requirement for each number of effects at each value of the feed flowrate. This external duty represents the energy provided by the condensing steam utility in the first evaporation stage.

As expected, the steam needed to concentrate the solution up to the specification achievement is higher for a lower number of equilibrium stages and for a higher flowrate to be processed. Moreover, it can be noticed that the duty increase itself is higher for a lower number of effects (cf Figure 4.4-right). This means that the feed flowrate perturbation is distributed over the effects which becomes almost irrelevant for a number of effects higher than 10 for which we expect the flexible design to provide a result very similar to the classical one.

In light of the above, a relevant OPEX curve shift towards higher values can be expected which are higher as N is lower.

The operating costs were then averaged over the uncertain domain and a new OPEX trend was obtained reflecting the uncertainty contribution. As it can be noticed in Figure 4.4 (right), the external duty can be considered a linear function of the inlet feed flowrate ($R^2 = 0.9974$). The results obtained with the use of the normal distribution to describe the uncertain variable deviation give, as expected, the same values as the nominal case in Figure 4.3 independently from the selected variance due to the function properties already discussed in section 2.

On the other hand, Figure 4.5 represents the new TAC plot according to the deviation Beta PDF. The TAC trend is still calculated according to the equation 4.6 where CAPEX are still the same, since they depend on the equipment only, while OPEX are those obtained by the average weighted with respect to the uncertainty distribution according to the equation 2.2.

The results thus obtained reflect the expectations. In general, the total annualized costs are higher than the ones assessed by taking into account the nominal operating conditions. The minimum moves to the right due to the higher OPEX increase related to a low number of effects while the two curves asymptotically overlap each other for higher values of equilibrium stages.

The optimal design under uncertain operating conditions accounts for five evaporation stages with a TAC equal to 461,000 \$/year.

The outcome of the analysis carried out on this first case study may not look that impressive. However, given the simplicity of the selected process as well as its relatively low sensitivity with respect to the selected uncertain variable, this example shows how an a priori flexibility analysis can significantly affect the design choice and could allow for a more cost-saving decision.

In order to better show the uncertain operating conditions impact on the costs and the relevant bias usually neglected while performing a design optimization without considering external disturbances, a more sensitive process will be presented in the next section.

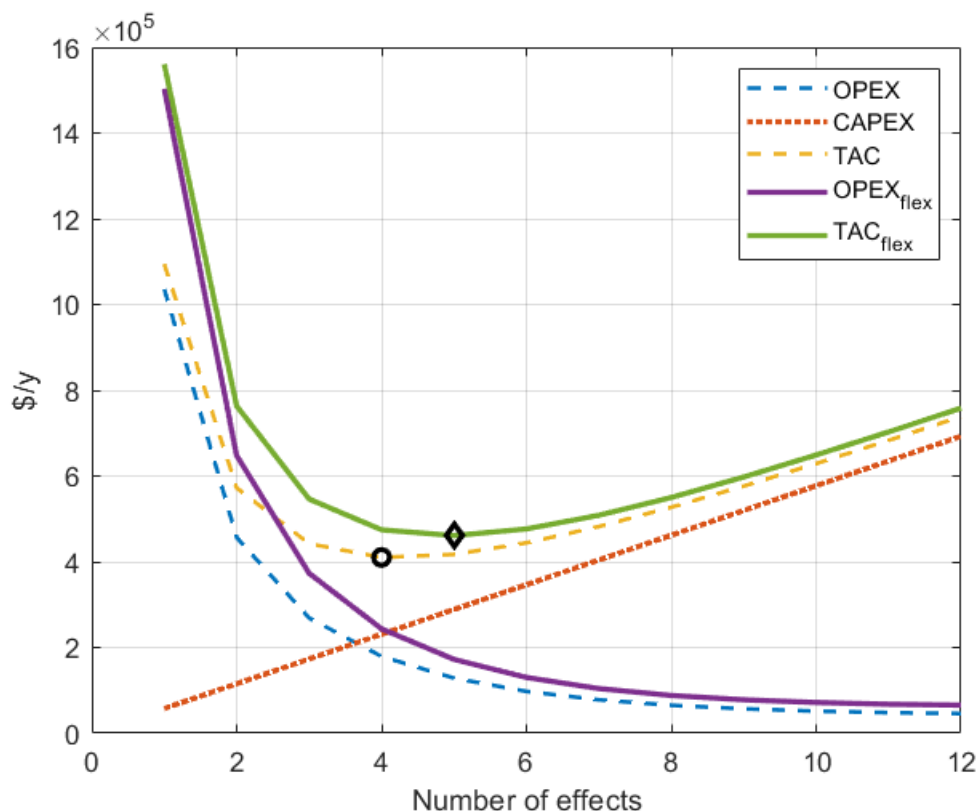


Fig. 4.5: Multiple effect TAC under uncertain operating conditions (Beta PDF)

5 Distillation column

The second case study refers to a standard binary distillation column unit. In Table 4.2 the feed properties under nominal operating conditions, the operating pressure as well as the distillate and bottom products specifications are listed. Despite the higher complexity of the process under analysis, a simple cyclohexanol/phenol mixture without thermodynamic singularities (such as azeotrope or unusual equilibrium curves) was selected for the separation in order to avoid results strictly related to the particular case study. Moreover, the selection of a common process is more suitable to show the methodology effectiveness even with respect to ordinary applications.

5.1 Optimal Design under Nominal Operating Conditions

The distillation column was simulated under nominal operating conditions by means of ProSim Plus[®] process simulator in order to assess the condenser and reboiler duties, the reflux ratio, and the maximum and minimum volumetric flowrates flowing along the unit. Given these data, the equipment sizing can be performed in order to evaluate the capital expenses for each number of theoretical trays.

Results are reported in Figure 4.6. As usual the operating costs show an

Property	Value	Unit
Feed		
F	38	$kmol/h$
T_{Feed}	397.15	K
z_{Phenol}	0.35	mol/mol
Specifications		
P_{top}	1.013	bar
$x_{Cyclohex}^D$	0.95	mol/mol
x_{Phenol}^B	0.80	mol/mol

Tab. 4.2: Feed properties and distillation nominal operating conditions

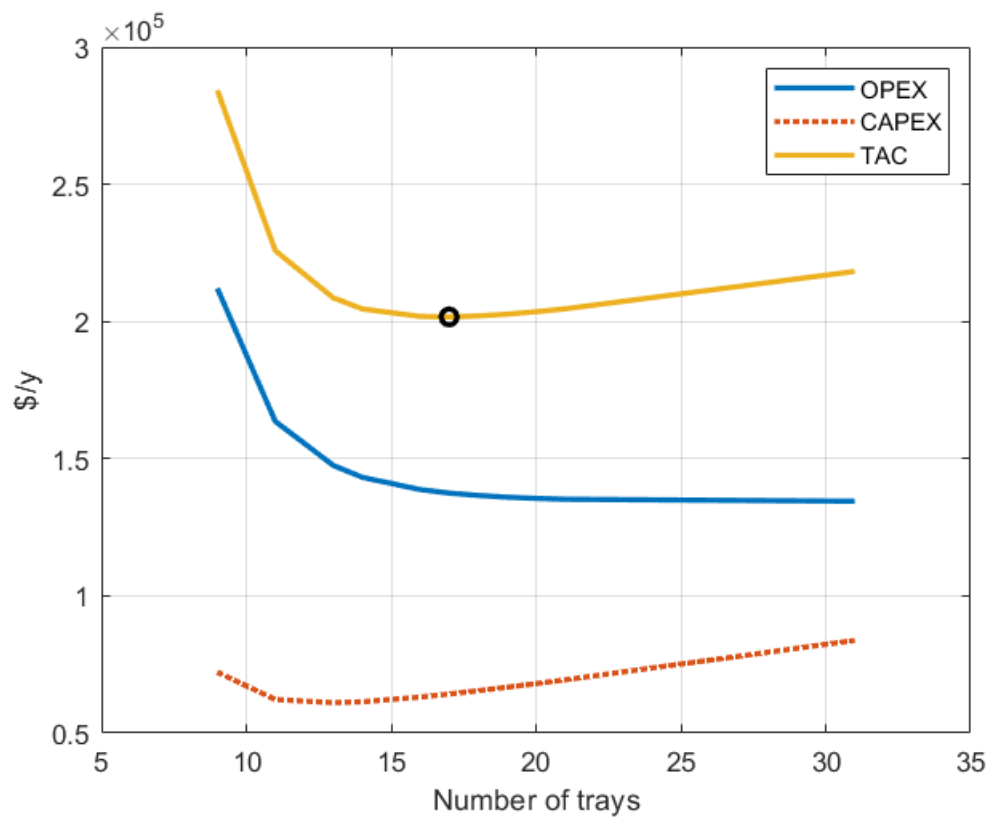


Fig. 4.6: Distillation TAC under nominal operating conditions

asymptotic trend with the increasing of the number of stages. The reflux ratio indeed approaches the R_{min} value as a higher number of stages is used. This lower reflux results in lower boilup and condenser duties, that explains the behaviour of the OPEX curve.

Capital costs have the standard linear trend as well, except for very low number of trays. This behaviour is due to the column diameter as well as reboiler and condenser heat transfer surface area oversizing related to the extremely high reflux ratio attained when getting close to the minimum number of stages ($N_{min} = 7$).

The total annualized costs function shows the typical trend with a minimum and the corresponding optimal number of theoretical equilibrium stages is 17 (reboiler included) with a TAC equal to 201,635 \$/y.

5.2 Flexible Design

Once the optimal design under nominal operating conditions is carried out, the uncertain variables have been identified as the inlet composition. The aim of this choice is to highlight the sensitivity of the process with respect to an intensive variable instead of the system capacity.

As usual, an initial sensitivity analysis was performed as represented in Figure 4.7(left). As expected, it reflects the typical higher energy demand for a lower number of equilibrium stages; an analogous trend can be detected for the condenser duty even though the cooling water contribution to operating expenses is one order of magnitude lower than the reboiler steam one.

Differently from the multiple effect evaporator case study, the heat duty trend with respect to the phenol molar fraction in the feed can be either increasing or decreasing in the considered interval according to the number of equilibrium stages.

This phenomenon can be more easily detected from a lateral perspective as shown in Figure 4.7(right). For a small number of stages, a higher duty is required if the feed phenol content is higher than the cyclohexanol one. However, for a large number of stages, a higher duty is required if the feed cyclohexanol content is higher than the phenol one. There exists as well an intermediate condition around 14 stages where the feed composition perturbation has a low impact on the duties. Once again, the OPEX can be averaged over the uncertain variable probability distribution function.

If the normal PDF is considered, almost the same result as the nominal design is obtained due to the symmetry of the distribution and the almost linear trend of the energy costs with respect to z_{Phenol} ($R^2 = 0.9912$).

On the other hand, the use of an asymmetric probability distribution such as the Beta PDF to describe the feed composition uncertainty results in a relevant impact. Figure 4.8 shows the new OPEX curve averaged with respect to the skewed distribution as well as the corresponding TAC function according to the

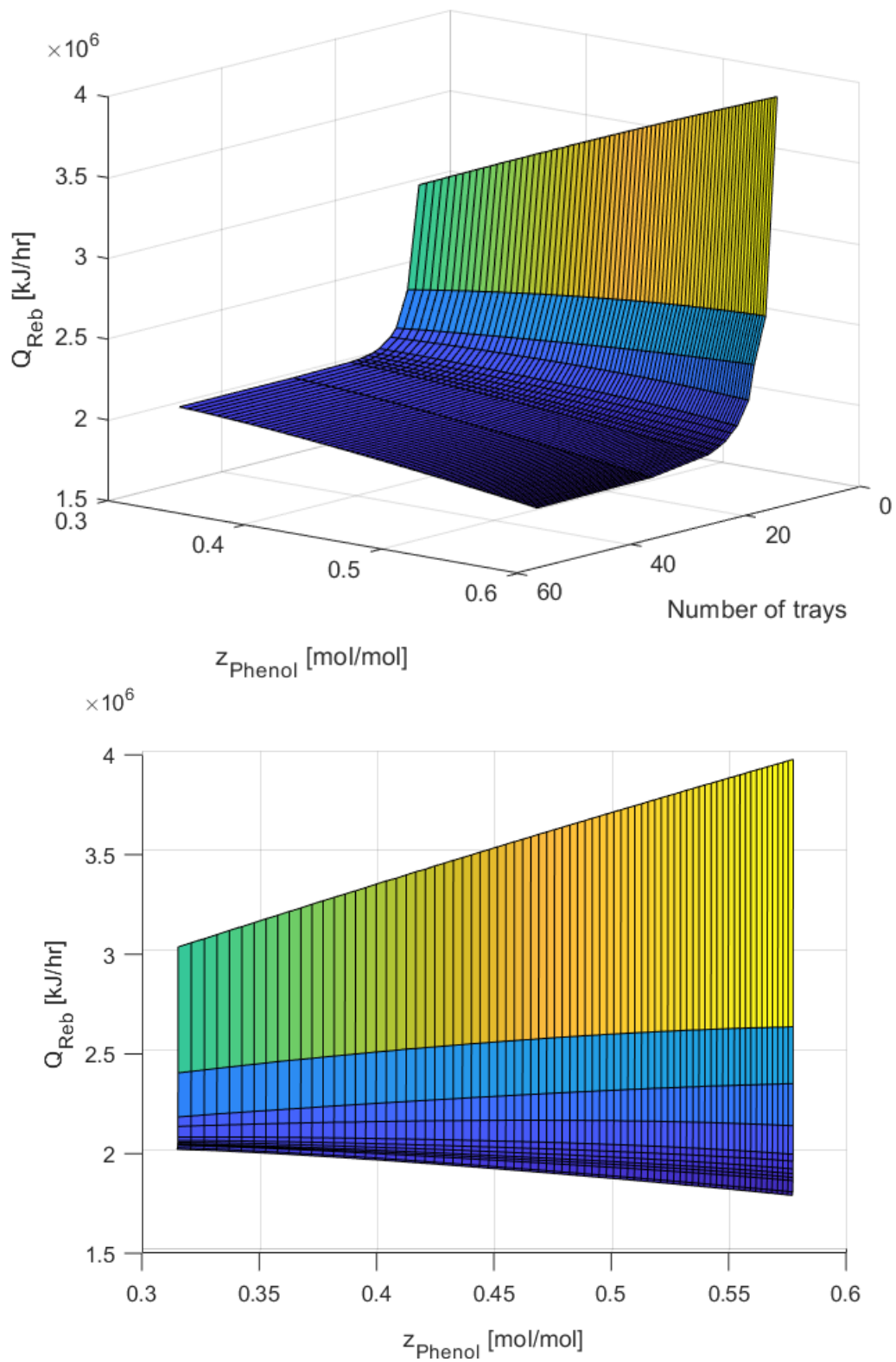


Fig. 4.7: Reboiler duty under uncertain operating conditions

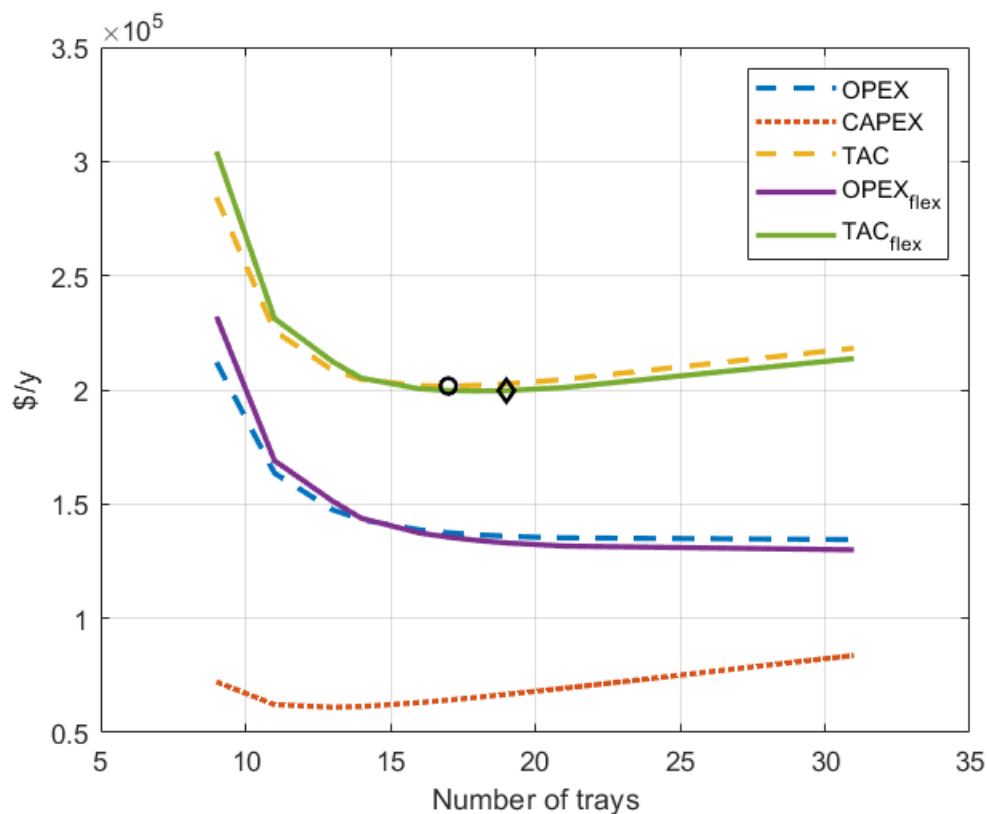


Fig. 4.8: Distillation TAC under uncertain operating conditions (Beta PDF)

procedure already explained in section 4.2.

The averaged costs for external duties under uncertain conditions are higher than those related to nominal operating conditions in case of low number of stages and lower for a high N value. This “rotation” of the OPEX curve causes the total costs point of minimum displacement to land at 19 equilibrium stages with a corresponding TAC value equal to 199,700 \$/y.

To conclude the results analysis of the distillation column case study, it can be observed that, differently from the multiple-effect case study where the OPEX function was stretched towards higher values for a low number of stages, in this case the OPEX curve rotates causing the new optimal TAC value to be even lower than the nominal one.

Moreover, the distillation process resulted to be particularly sensitive to the feed composition uncertainty. Indeed, 2 additional stages out of 17 is a non-negligible oversizing requirement; this result is even more appreciable if we take into account that the selected separation process involved an ideal mixture whose components can be easily separated.

Finally, in both cases the design based on flexible operating conditions resulted in a higher number of equilibrium stages able to mitigate duties additional costs if perturbations were to occur.

6 Environmental impact

Sustainability is by far the topic of major concern over the last years. The energy challenge is the key point of the environmentally friendly policies adopted by all of the most developed and industrialized countries worldwide.

For this purpose, Horizon 2020, i.e. the biggest EU Research and Innovation programme, was funded by the European Union over the 2014-2020 period [44].

On the other hand, the International Energy Agency defines renewables as the centre of the transition to a less carbon-intensive and more sustainable energy system [45]. However, since the transition from fossil fuels to renewables requires a considerable time span to establish itself, the short-term solution lies in more energy effective technologies.

In the light of these premises, it can be then stated that, while designing process equipment, the same costs in terms of CAPEX or OPEX have the same impact on the TAC from an economic point of view, but they substantially differ from each other when taking into account sustainability.

A lower number of equilibrium stages implies indeed a considerably higher energy demand in case of external perturbations even in the case that they resulted in a more profitable design. In particular, referring to the previous case studies, an overdesign would result both in a more profitable and more sustainable operation.

In order to quantify the environmental impact as a function of the energy demand of process units, the Global Warming Potential indicator was employed since it was proved to have the most adverse effect on the sustainability profile of the case study operations [46]. The CO_2 emissions were calculated according to the methodology followed by Gadalla et al. (2006)[47] as a direct function of the duty requirement.

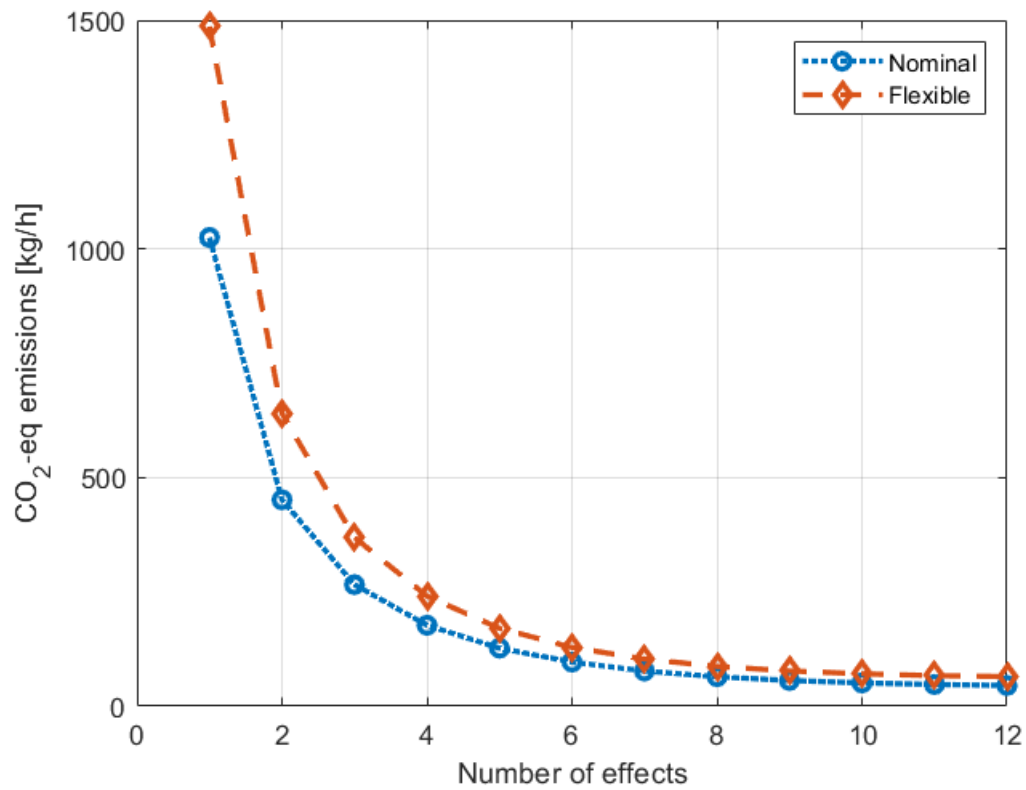
Even though CO_2 emissions are strictly correlated to the fuel employed to produce the required energy, this study carries out a comparison between different configurations of the same unit. Therefore, the study can be considered fuel independent. The results presented in this paper refer to natural gas.

For the same reason CO_2 emissions related to feedstock and products cancel out when computing the difference between two configurations.

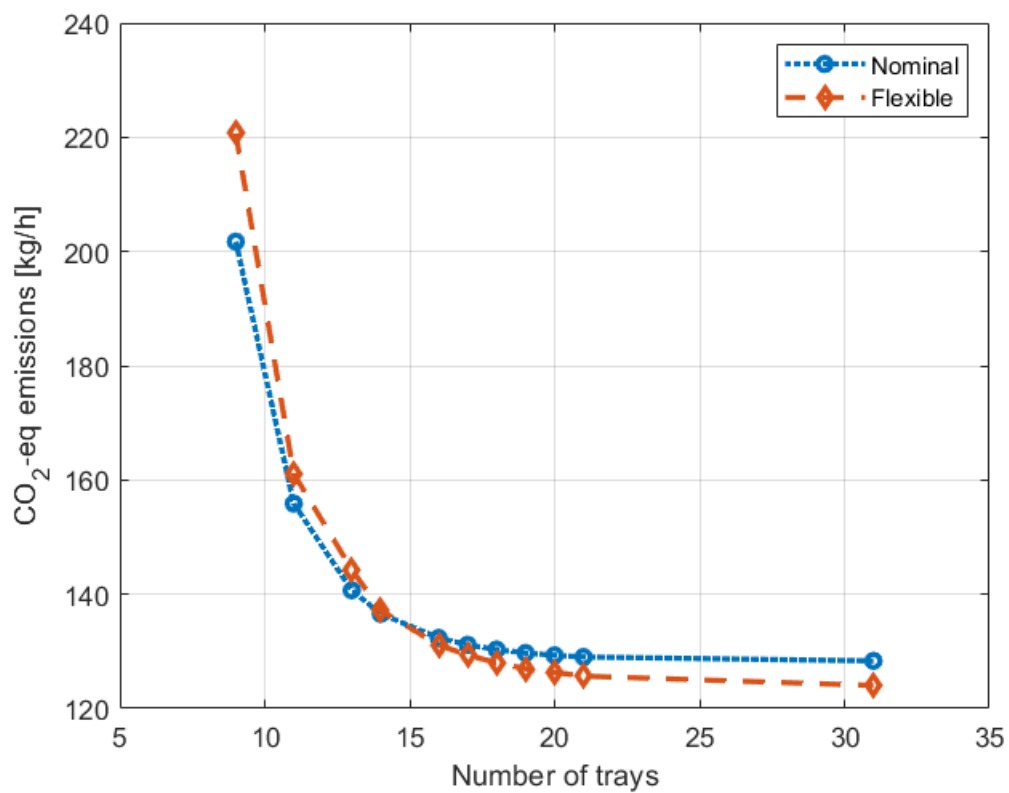
According to several authors [47, 48, 49, 50], taking into account the plant lifetime, the CO_2 emissions associated with the installation of additional units/stages are negligible with respect to the emissions related to the heat requirement. By analogy, although the CO_2 emissions due to pumping and cold duties have been thoroughly calculated by using a specific emissions factor of $51.1 \text{ kg}_{CO_2}/GJ$ as suggested by Waheed et al.[?], they resulted to be orders of magnitude lower with respect to the steam duty as already proved by several studies [6, 48, 49, 50].

For more details about the CO_2 emissions calculations please refer to Appendix C.

The average values of equivalent CO_2 emissions for the multiple-effect and for



(a) Multiple-effect evaporator



(b) Distillation column

Fig. 4.9: CO₂ average emissions

the distillation case studies are shown respectively in Figures 4.9a and 4.9b.

Both the plots reflect the OPEX function trend, that is the heat duty curve, as expected.

For a higher number of equilibrium stages, the energy demand is lower and thus the equivalent CO_2 emissions are lower, both under nominal and uncertain operating conditions, as well. These results validate the initial remark highlighting the fact that, for these particular case studies, a higher value of N implies both economic and environmental advantages with apparently no drawbacks.

However, in order to have a more reliable interpretation of these results, a further discussion is worth doing by using equivalent CO_2 emissions per functional unit as outlined by the ISO14040 [51] instead of the emissions per operating time. Regarding the functional unit, the two main possible choices are either a kg of treated stream or a kg of purified product. Since those units perform separation processes, it can be assumed that they are designed to treat feedstocks, and thus 1 kg of feed stream can be used as functional unit.

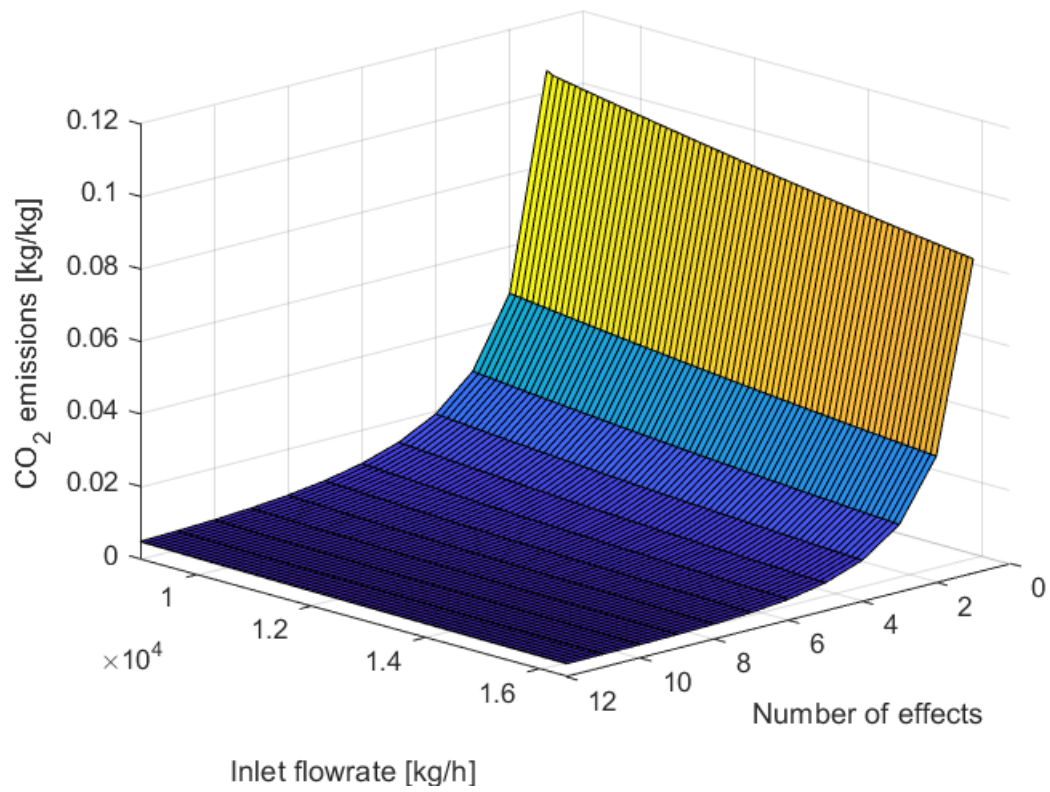
Moreover, for the multiple effect evaporator, both in case of solvent recovery and solution concentration, the product quantity is proportional to the feed flowrate due to the partial mass balance $L_N = L_0 \cdot w_0/w_N = 1000 \text{ kg/h}$. This means that the emissions per unit of feedstock differ by those per unit of product by a constant scale factor only.

On the other hand, a similar remark applies to the distillation column. Since both cyclohexanol and phenol are products which are to be purified, the feed mass flowrate is the same as the sum of the product streams flowrates. Therefore, 1 kg of feedstock corresponds to 1 kg of products. Since the design was performed for a given molar flowrate, the only difference taken into account will be the different molecular weight related to composition perturbations. However, given that the molecular weights of cyclohexanol (MW=100 g/mol) and phenol (MW=96 g/mol) are similar to each other, only a slight difference can be detected.

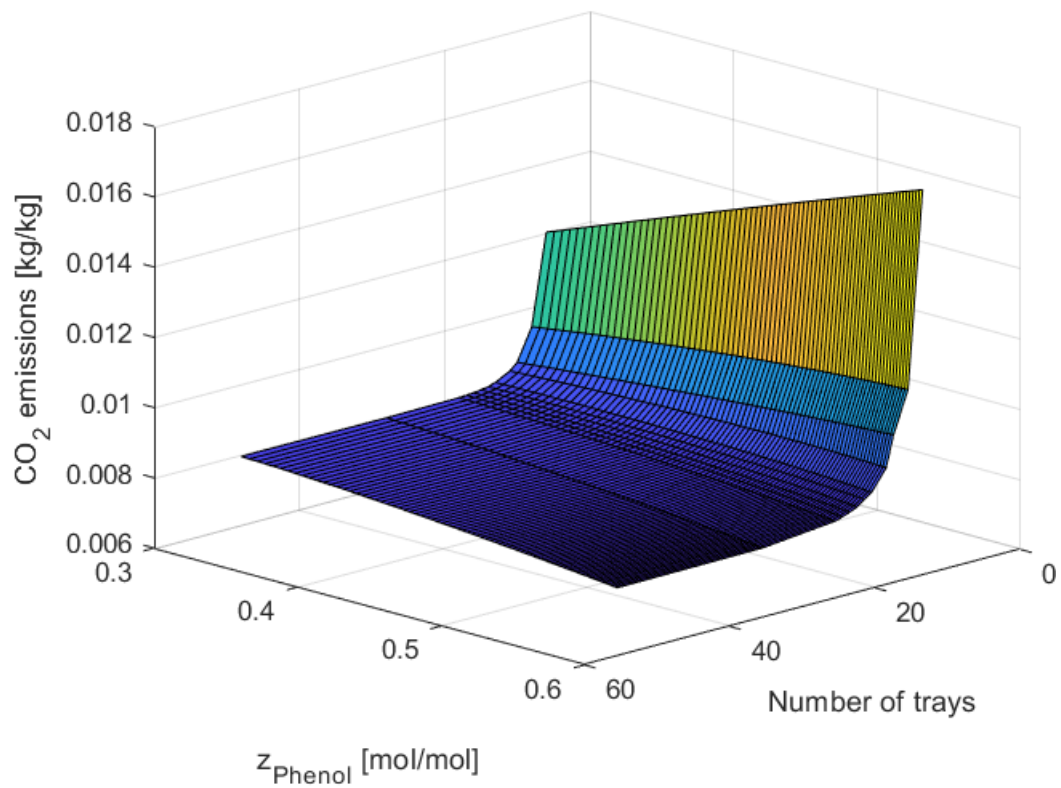
In Figures 4.10a and 4.10b the results with respect to 1 kg of treated feedstock are reported. First of all, it can be noticed that some differences in the emissions trends can be detected with respect to the uncertain variable value compared to the duties trend in Figures 4.4 and 4.7, respectively.

In fact, while the effect of a composition deviation shows an almost negligible scaling factor between the emissions per functional unit and the duty requirement, in the multiple effect evaporator case study the emissions per kg of feed decrease for a higher capacity of the system. This trend is related to the different approach between economic optimization based on the cash flow and the sustainability assessment based on the functional unit.

On the other hand, emissions are still decreasing with a hyperbolic behaviour when moving to higher number of equilibrium stages. This result validates once again the analogous trend of economic and environmental analysis towards higher investments.



(a) Multiple-effect evaporator



(b) Distillation column

Fig. 4.10: CO₂ emissions - sensitivity

However, even in the case of opposite trends with regard to environmental and economic indicators, a more detailed and complex multi-criteria decision making problem could be set in order to find an optimal compromise.

7 Conclusions

In this paper a thorough procedure to account for uncertainty in designing equilibrium staged operations has been proposed. A preliminary analysis about the uncertainty characterization was carried out since the flexibility assessment results always qualitatively and quantitatively reflect the deviation likelihood.

Hence, a flexible design procedure accounting for operating costs averaged over the uncertain domain was presented. First, a case study of a multiple effect evaporator was discussed for variable feed flowrate, i.e. unit capacity, followed by a distillation column example whose uncertain variable was the feed composition.

In both cases, for a symmetric deviation PDF, the optimal number of equilibrium stages stays unchanged due to the duties' linear trend with respect to the uncertain variables. On the contrary, when taking into account a skewed deviation PDF, the total costs optimum location shifts towards a higher number of equilibrium stages and the OPEX curve stretches and rotates for the first and second case studies respectively.

Even though the fact that a system oversizing leads to a more flexible design is rather intuitive, this paper shows that the addition of equilibrium stages should be thoroughly quantified since an approximative choice could lead to less profitable configurations as well as to additional costs that are not required in light of the considered perturbation likelihood.

A further purpose of this study was to quantify the inaccuracy made by the usual design procedure if disturbances are not taken into account. One additional effect out of 4 and 2 additional stages out of 17 for such simple processes substantially affects the decision making during the design phase. It is no exaggeration to say that non-ideal mixture processing as well as the sequencing of several operations in chemical plants could show an even more relevant difference between conventional and flexible design procedure results due to the highly nonlinear behaviour and to the input perturbations amplification respectively.

Finally, since this study is particularly focused on the energy demand of equilibrium staged operation, the economic assessment has been coupled with the sustainability. When dealing with more stages, indeed there is a double benefit, namely economic and environmental. In case the minimum of the total annualized costs shifts towards lower external duty consumption at the cost of higher investments, then the equivalent carbon dioxide emissions are lowered as a consequence. In the opposite case, an optimal compromise between the two can be found by means of one of the several multicriteria decision making procedures available in literature.

In conclusion, the procedure to assess the optimal number of equilibrium stages presented in this paper based on operating expenses under uncertain operating conditions resulted to be reliable and effective. However, beside the procedure itself, the main product of this analysis is the information required to understand whether its outcome is worth the higher computational effort and need for detailed information or not. While for a given process under certain external perturbations the additional work could provide the same result as the conventional procedure, for other processes or a different set of uncertain variables the flexible design accounting for uncertainty could be almost the unique way to have reliable estimations.

In any case, the decision maker experience is essential for the best application of this useful tool.

A List of acronyms and symbols

Symbol	Definition	Unit
A	Characteristic dimension	m^n
A	Heat transfer surface area	m^2
a	Limits of integration	-
$C\%$	Carbon content percentage	%
C_{BM}	Equipment bare module cost	\$
C_p^0	Purchase equipment cost in base conditions	\$
c_P	Specific heat at constant pressure	$kJ/(kg \cdot K)$
$CAPEX$	CAPital EXpenses	\$/y
C_{steam}	Steam cost	\$/y
F	Feed flowrate	$kmol/h$
F_{BM}	Bare module factor	-
F_M	Material factor	-
F_P	Pressure factor	-
F_q	Column trays factor	-
$f(x)$	Function	function
\bar{f}	Function average value	various
GWP	Global Warming Potential	$kg CO_2 - eq$
h_{steam}	Steam enthalpy	kJ/kg
ΔH_{ev}	Evaporation enthalpy	kJ/kg
I	Identity matrix	matrix
L	Liquid flowrate	kg/h
$M\&S$	Marshall & Swift cost index	-
N	Evaporator/Column equilibrium stages	-
N_{min}	Minimum number of equilibrium stages	-
NHV	Net Heating Value	kJ/kg
$OPEX$	OPerating EXpenses	\$/y
P	Pressure	bar
$P(x)$	Probability function	function
PDF	Probability distribution function	function

Symbol	Definition	Unit
Q	Heat duty	kJ/h
Q_{reb}	Reboiler heat duty	kJ/h
Q_{fuel}	Fuel heat duty	kJ/h
R	Reflux ratio	-
R^2	Coefficient of determination	-
R_{min}	Minimum reflux ratio	-
T_0	Standard temperature	K
T_F	Flame temperature	K
T_{Feed}	Feed stream temperature	K
T_L	Liquid stream temperature	K
T_S	Stack temperature	K
T_V	Vapor stream temperature	K
ΔT_{eb}	Boiling point elevation	K
TAC	Total Annualized Costs	$\$/y$
U	Heat transfer coefficient	$kJ/(m^2 \cdot h \cdot K)$
V	Vapor flowrate	kg/h
w_i	Solute mass fraction	kg/kg
x	Independent variable	various
x_i^B	i-th component fraction in the bottom	mol/mol
x_i^D	i-th component fraction in the distillate	mol/mol
z	Normalized independent variable	-
z_i	i-th component fraction in the feed	mol/mol

Greek letters	Definition	Unit
α	$CO_2 - to - C$ molar mass ratio	-
Γ	Gamma distribution function	function
θ	Gamma PDF scale parameter	-
κ	Gamma PDF shape parameter	-
λ_{steam}	Steam latent heat	kJ/kg
μ	Mean	-
σ	Variance	-

Equipment	Typology	K_1	K_2	K_3	A
Heat exchanger	Fixed tubes	4.3247	-0.3030	0.1634	Heat transfer area [m^2]
	Kettle	4.4646	-0.5277	0.3955	Heat transfer area [m^2]
Columns (vessel)	Packed/tray	3.4974	0.4485	0.1074	Volume [m^3]
Trays	Sieved	2.9949	0.4465	0.3961	Cross sectional area [m^2]

Tab. 4.3: Equipment cost in base conditions parameters

B Capital and operating expenses estimations

In order to evaluate the investment required to build up a process plant or for whatever economic analysis and comparison related to process equipment, the cost of every single unit needs to be estimated.

For this purpose the Guthrie-Ulrich-Navarrete correlations described in the following paragraphs have been employed [40, 41, 42, 43].

B.1 Purchase equipment cost in base conditions

The purchase equipment cost in base conditions is obtained by means of the following equation:

$$\log_{10}(C_P^0[\$]) = K_1 + K_2 \cdot \log_{10}(A) + K_3 \cdot [\log_{10}(A)]^2 \quad (\text{B.1})$$

where A is the unit characteristic dimension and the K_i coefficients are relative to the equipment typology (cf. Table 4.3).

The provided coefficients refer to a Marshall & Swift equipment cost index equal to 1110. In order to update the cost estimations, a M&S index equal to 1638.2 will be used in order to refer the calculations to the year 2018 by means of the correlation:

$$C_{P,2}^0 = \frac{M\&S_2}{M\&S_1} \cdot C_{P,1}^0 \quad (\text{B.2})$$

B.2 Bare module cost

The equipment bare module cost can be calculated according to the following correlation:

$$C_{BM} = C_P^0 \cdot F_{BM} \quad (\text{B.3})$$

Equipment	Typology	B_1	B_2	F_M	F_P
Heat exchanger	Fixed tubes	1.63	1.66	1	1
	Kettle	1.63	1.66	1	$F_{P,Kettle}$
Columns/vessel	/	2.25	1.82	1	1
Pumps	Centrifugal	1.89	1.35	1.5	1

Tab. 4.4: Bare module parameters

where the bare module factor is given by:

$$F_{BM} = B_1 + B_2 \cdot F_M \cdot F_P \quad (\text{B.4})$$

The F_M and F_P factors refers to the actual constructions materials and operating pressure while the B_i coefficients refers to the equipment typology (cf. Table 4.4).

The $F_{P,Kettle}$ value is given by:

$$\log_{10}(F_P) = 0.03881 - 0.11272 \cdot \log_{10}(P) + 0.08183 \cdot [\log_{10}(P)]^2 \quad (\text{B.5})$$

where P is the relative pressure in *bar*.

For column trays bare module cost a slightly different correlation should be used:

$$C_{BM} = N \cdot C_P^0 \cdot F'_{BM} \cdot F_q \quad (\text{B.6})$$

where N is the real trays number, $F_{BM} = 1$ e F_q is given by:

$$\begin{cases} \log_{10}(F_q) = 0.4771 + 0.08561 \cdot \log_{10}(N) - 0.3473 \cdot [\log_{10}(N)]^2 & \text{if } N < 20 \\ F_q = 1 & \text{if } N \geq 20 \end{cases} \quad (\text{B.7})$$

B.3 External heat duty cost

The annual energy costs related to the steam utility have been evaluated according to the following correlation:

$$C_{steam} [\$/y] = 7.78 \cdot 10^{-6} [\$/kJ] \cdot 8150 [h/y] \cdot V [kg/h] \cdot \Delta H_{ev} [kJ/kg]$$

The formula here above accounts for the steam price per unit energy, the amount of working hours per year, the steam flowrate and its latent heat.

C Global Warming Potential calculations

The indicator associated to the greenhouse effect impact category is the Global Warming Potential whose unit is $kg\ CO_2 - eq$ per unit. It has calculated, as suggested by Gadalla et al.[47], by means of the correlation:

$$CO_2 = \left(\frac{Q_{fuel}}{NHV} \right) \cdot \left(\frac{C\%}{100} \right) \cdot \alpha \quad (C.1)$$

where:

- CO_2 is the value of equivalent carbon dioxide emission in $[kg/h]$;
- NHV is the Net Heating Value and it is equal to $51,600\ kJ/kg$ for Natural Gas;
- $C\%$ is the carbon content in percentage and it is equal to 75.4 for Natural Gas;
- α is the CO_2 -to- C molar mass ratio and it is equal to 3.67 .

Finally the term Q_{fuel} identifying the combustion energy required to vaporize the desired amount of steam can be estimated as:

$$Q_{fuel} = \left(\frac{Q_{reb}}{\lambda_{steam}} \right) \cdot (h_{steam} - 419) \cdot \left(\frac{T_F - T_0}{T_F - T_S} \right) \quad (C.2)$$

where:

- Q_{reb} is the reboiler duty in kJ/h ;
- λ_{steam} is the steam latent heat in kJ/kg ;
- h_{steam} is the steam enthalpy in kJ/kg ;
- 419 is the water enthalpy at $100^\circ C$ in kJ/kg ;
- T_F is the flame temperature in K ;
- T_S is the stack temperature in K ;
- T_0 is the standard temperature in K .

On the other hand, the equivalent carbon dioxide emissions for pumping were estimated by multiplying the power needed by each pump and the amount of CO_2 per each GJ of electrical energy, i.e. $51.1\ kg_{CO_2}/GJ$ [6].

References

- [1] Green, D., Perry, R., Southard, M.Z., 2019. Perry's Chemical Engineers' Handbook, 9th Edition, 9 edizione. ed. McGraw-Hill Education, New York, NY.
- [2] Sinnott, R.K., Coulson, J.M., Richardson, J.F., 2005. Coulson & Richardson's chemical engineering. Vol. 6, Vol. 6,. Elsevier Butterworth-Heinemann, Oxford.
- [3] Stephanopoulos, G., 1983. Chemical Process Control: An Introduction to Theory and Practice, 1st edition. ed. Pearson College Div, Englewood Cliffs, N.J.
- [4] Gadalla, M., Olujić, Ž., de Rijke, A., Jansens, P.J., 2006. Reducing CO₂ emissions of internally heat-integrated distillation columns for separation of close boiling mixtures. *Energy, Double Special Issue: 2nd Dubrovnik Conference on Sustainable Development of Energy, Water and Environment Systems/PRES 03 and PRES 2004 Process Integration, Modelling and Optimisation for Energy Saving and Pollution Reduction* 31, 2409–2417. <https://doi.org/10.1016/j.energy.2005.10.029>
- [5] Oni, A. O., Waheed, M. A., 2015, Methodology for the Thermo-economic and Environmental Assessment of Crude Oil Distillation Units, *International Journal of Exergy*, Vol. 16, No. 4.
- [6] Waheed, M.A., Oni, A.O., Adejuyigbe, S.B., Adewumi, B.A., Fadare, D.A., 2014. Performance enhancement of vapor recompression heat pump. *Applied Energy* 114, 69–79. <https://doi.org/10.1016/j.apenergy.2013.09.024>
- [7] Quiroz-Ramírez, J.J., Sánchez-Ramírez, E., Hernández, S., Ramírez-Prado, J.H., Segovia-Hernández, J.G., 2017. Multiobjective Stochastic Optimization Approach Applied to a Hybrid Process Production–Separation in the Production of Biobutanol. *Ind. Eng. Chem. Res.* 56, 1823–1833.
- [8] Ibrahim, D., Jobson, M., Li, J., Guillén-Gosálbez, G., 2018. Optimization-based design of crude oil distillation units using surrogate column models and a support vector machine. *Chemical Engineering Research and Design* 134, 212–225. <https://doi.org/10.1016/j.cherd.2018.03.006>
- [9] Robinson, T.J., Brenneman, W.A., Myers, W.R., 2006. Process Optimization via Robust Parameter Design when Categorical Noise Factors are Present. *Quality and Reliability Engineering International* 22, 307–320. <https://doi.org/10.1002/qre.772>

- [10] Rajagopal, R., Castillo, E. del, 2005. Model-Robust Process Optimization Using Bayesian Model Averaging. *Technometrics* 47, 152–163. <https://doi.org/10.1198/004017005000000120>
- [11] Swaney, R.E., Grossmann, I.E., 1985. An index for operational flexibility in chemical process design. Part I: Formulation and theory. *AIChE J.* 31, 621–630. <https://doi.org/10.1002/aic.690310412>
- [12] Saboo, A.K., Morari, M., Woodcock, D., 1985. Design of Resilient Processing Plants .8. a Resilience Index for Heat-Exchanger Networks. *Chem. Eng. Sci.* 40, 1553–1565. [https://doi.org/10.1016/0009-2509\(85\)80097-X](https://doi.org/10.1016/0009-2509(85)80097-X)
- [13] Pistikopoulos, E.N., Mazzuchi, T.A., 1990. A Novel Flexibility Analysis Approach for Processes with Stochastic Parameters. *Comput. Chem. Eng.* 14, 991–1000. [https://doi.org/10.1016/0098-1354\(90\)87055-T](https://doi.org/10.1016/0098-1354(90)87055-T)
- [14] Lai, S.M., Hui, C.-W., 2008. Process Flexibility for Multivariable Systems. *Ind. Eng. Chem. Res.* 47, 4170–4183. <https://doi.org/10.1021/ie070183z>
- [15] Floudas, C.A., Gümüş, Z.H., Ierapetritou, M.G., 2001. Global Optimization in Design under Uncertainty: Feasibility Test and Flexibility Index Problems. *Ind. Eng. Chem. Res.* 40, 4267–4282. <https://doi.org/10.1021/ie001014g>
- [16] Huang, W., Yang, G., Qian, Y., Jiao, Z., Dang, H., Qiu, Y., Cheng, Z., Fan, H., 2017. Operation Feasibility Analysis of Chemical Batch Reaction Systems with Production Quality Consideration under Uncertainty. *J. Chem. Eng. Jpn.* 50, 45–52. <https://doi.org/10.1252/jcej.16we119>
- [17] Hoch, P.M., Eliceche, A.M., Grossmann, I.E., 1995. Evaluation of Design Flexibility in Distillation-Columns Using Rigorous Models. *Comput. Chem. Eng.* 19, S669–S674. [https://doi.org/10.1016/0098-1354\(95\)00137-Q](https://doi.org/10.1016/0098-1354(95)00137-Q)
- [18] Oberkampf, W., Helton, J., Sentz, K., 2012. Mathematical representation of uncertainty, in: 19th AIAA Applied Aerodynamics Conference. American Institute of Aeronautics and Astronautics. <https://doi.org/10.2514/6.2001-1645>
- [19] Agarwal, H., Renaud, J.E., Preston, E.L., Padmanabhan, D., 2004. Uncertainty quantification using evidence theory in multidisciplinary design optimization. *Reliability Engineering & System Safety, Alternative Representations of Epistemic Uncertainty* 85, 281–294. <https://doi.org/10.1016/j.res.2004.03.017>
- [20] Oberkampf, W.L., DeLand, S.M., Rutherford, B.M., Diegert, K.V., Alvin, K.F., 1999. New methodology for the estimation of total uncertainty in computational simulation. *Collection of Technical Papers -*

- AIAA/ASME/ASCE/AHS/ASC Structures, Structural Dynamics and Materials Conference 4, 3061–3083.
- [21] Oberkampf, W.L., Diegert, K.V., Alvin, K.F., Rutherford, B.M., 1998. Variability, uncertainty, and error in computational simulation. American Society of Mechanical Engineers, Heat Transfer Division, (Publication) HTD 357, 259–272.
- [22] Zimmermann, H., 2013. Fuzzy Set Theory - and Its Applications, 2nd ed. 1991. ed. Springer, Dordrecht.
- [23] Yager, R.R., Kacprzyk, J., Fedrizzi, M., 1994. Advances in the Dempster-Shafer theory of evidence. J. Wiley.
- [24] Dubois, D., Prade, H., 1988. Possibility Theory: An Approach to Computerized Processing of Uncertainty. Springer US. <https://doi.org/10.1007/978-1-4684-5287-7>
- [25] Walley, P., 1991. Statistical Reasoning with Imprecise Probabilities. Springer US.
- [26] Sahinidis, N.V., 2004. Optimization under uncertainty: state-of-the-art and opportunities. Computers & Chemical Engineering, FOCAPO 2003 Special issue 28, 971–983. <https://doi.org/10.1016/j.compchemeng.2003.09.017>
- [27] Janak, S.L., Lin, X., Floudas, C.A., 2007. A new robust optimization approach for scheduling under uncertainty: II. Uncertainty with known probability distribution. Computers & Chemical Engineering 31, 171–195. <https://doi.org/10.1016/j.compchemeng.2006.05.035>
- [28] Lin, X., Janak, S.L., Floudas, C.A., 2004. A new robust optimization approach for scheduling under uncertainty: I. Bounded uncertainty. Computers & Chemical Engineering, FOCAPO 2003 Special issue 28, 1069–1085. <https://doi.org/10.1016/j.compchemeng.2003.09.020>
- [29] Schuëller, G.I., Jensen, H.A., 2008. Computational methods in optimization considering uncertainties – An overview. Computer Methods in Applied Mechanics and Engineering, Computational Methods in Optimization Considering Uncertainties 198, 2–13. <https://doi.org/10.1016/j.cma.2008.05.004>
- [30] Ang, A.H.S., Tang, W.H., 1984. Probability Concepts in Engineering Planning and Design, Vol. 2: Decision, Risk, and Reliability, First Edition edition. ed. John Wiley & Sons Inc, New York.
- [31] Ang, A.H.S., Tang, W.H., 1975. Probability Concepts in Engineering Planning and Design, Basic Principles, Volume 1 edition. ed. Wiley, New York.

- [32] Hoch, P.M., Eliceche, A.M., 1996. Flexibility analysis leads to a sizing strategy in distillation columns. *Comput. Chem. Eng.* 20, S139–S144. [https://doi.org/10.1016/0098-1354\(96\)00034-8](https://doi.org/10.1016/0098-1354(96)00034-8)
- [33] Di Pretoro, A., Montastruc, L., Manenti, F., Joulia, X., 2019. Flexibility analysis of a distillation column: Indexes comparison and economic assessment. *Computers & Chemical Engineering* 124, 93–108. <https://doi.org/10.1016/j.compchemeng.2019.02.004>
- [34] Di Pretoro, A., Montastruc, L., Manenti, F., Joulia, X., 2019. Flexibility Assessment of a Distillation Train: Nominal vs Perturbated Conditions Optimal Design, *Computer Aided Chemical Engineering*, 29 European Symposium on Computer Aided Process Engineering, 46, pp. 667–672.
- [35] Di Pretoro, A., Montastruc, L., Manenti, F., Joulia, X., 2020. Flexibility assessment of a biorefinery distillation train: Optimal design under uncertain conditions. *Computers & Chemical Engineering* 138, 106831. <https://doi.org/10.1016/j.compchemeng.2020.106831>
- [36] Severini, T.A., 2011. *Elements of Distribution Theory*, 1 edition. ed. Cambridge University Press, Cambridge.
- [37] Di Pretoro, A., Montastruc, L., Manenti, F., Joulia, X., 2020. Exploiting Residue Curve Maps to Assess Thermodynamic Feasibility Boundaries under Uncertain Operating Conditions. *Ind. Eng. Chem. Res.* 59, 16004–16016. <https://doi.org/10.1021/acs.iecr.0c02383>
- [38] Di Pretoro, A., Manenti, F., 2020. Multiple-Effect Evaporation. *SpringerBriefs in Applied Sciences and Technology* 35–46. https://doi.org/10.1007/978-3-030-34572-3_4
- [39] Di Pretoro, A., Manenti, F., 2020. *Non-conventional Unit Operations: Solving Practical Issues*, PoliMI SpringerBriefs. Springer International Publishing. <https://doi.org/10.1007/978-3-030-34572-3>
- [40] Guthrie, K.M. , 1969. Capital cost estimating. *Chem. Eng.* 76 (3), 114–142 .
- [41] Guthrie, K.M. , 1974. *Process Plant Estimating, Evaluation, and Control*. Craftsman Book Company of America .
- [42] Ulrich G. D., 1984, ‘A Guide to Chemical Engineering Process Design and Economics’, Wiley.
- [43] Navarrete P. F. and Cole W. C., 2001, ‘Planning, Estimating, and Control of Chemical Construction Projects’, 2nd Edition, CRC Press.
- [44] Horizon 2020 programme retrieved at https://ec.europa.eu/programmes/horizon2020/sites/horizon2020/files/2020-07/2020-07-2020-programme_en.pdf

- [45] IEA Renewables 2019 report retrieved at <https://www.iea.org/reports/renewables-2019>
- [46] Hasheminasab, H., Gholipour, Y., Kharrazi, M., Streimikiene, D., 2018. A novel Metric of Sustainability for petroleum refinery projects. *Journal of Cleaner Production* 171, 1215–1224. <https://doi.org/10.1016/j.jclepro.2017.09.223>
- [47] Gadalla, M., Olujić, Ž., Jobson, M., Smith, R., 2006. Estimation and reduction of CO₂ emissions from crude oil distillation units. *Energy* 31, 2398–2408.
- [48] Yang, A., Sun, S., Eslamimanesh, A., Wei, S., Shen, W., 2019. Energy-saving investigation for diethyl carbonate synthesis through the reactive dividing wall column combining the vapor recompression heat pump or different pressure thermally coupled technique. *Energy* 172, 320–332. <https://doi.org/10.1016/j.energy.2019.01.126>
- [49] Yang, A., Jin, S., Shen, W., Cui, P., Chien, I.-L., Ren, J., 2019. Investigation of energy-saving azeotropic dividing wall column to achieve cleaner production via heat exchanger network and heat pump technique. *Journal of Cleaner Production* 234, 410–422. <https://doi.org/10.1016/j.jclepro.2019.06.224>
- [50] Tavan, Y., Shahhosseini, S., Hosseini, S.H., 2014. Design and simulation of ethane recovery process in an extractive dividing wall column. *Journal of Cleaner Production* 72, 222–229. <https://doi.org/10.1016/j.jclepro.2014.03.015>
- [51] ISO 14040:2006 Environmental management — Life cycle assessment — Principles and framework

Part V. Optimal Design: Sequence of Operations

Flexibility Assessment of a Biorefinery Distillation Train: Optimal Design under Uncertain Conditions

Alessandro Di Pretoro^{a,b}, Ludovic Montastruc^a, Flavio Manenti^b, Xavier Joulia^a

^aLaboratoire de Génie Chimique, Université de Toulouse, CNRS/INP/UPS, Toulouse, France

^bPolitecnico di Milano, Dipartimento di Chimica, Materiali e Ingegneria Chimica «Giulio Natta», Piazza Leonardo da Vinci 32, 20133 Milano, Italy.

Abstract

Multicomponent mixtures can be separated into their single components by means of different distillation system configurations. The typical distillation train design procedure consists of the assessment of the optimal columns configuration according to the economic and operational aspects. However, this optimal design is strictly related to the operating conditions, i.e. perturbations, when present, can seriously compromise the operation profitability. In these cases a flexibility analysis could be of critical importance to assess the operating conditions range of better performance for different system configurations. This is the typical case of biorefineries where the floating nature of the feedstock causes composition disturbances downstream the fermenter across the year's seasons. A brand new ABE/W mixture separation case study has been set up; this mixture derives from an upstream microbial conversion process and the successful recovery of at least biobutanol and acetone is crucial for the return on the investments. This paper then compares the possible distillation train configurations from a flexibility point of view. The analysis is focused in particular in highlighting the differences, if present, between the economic optimal solution and flexibility optimal configuration that could not be the same, causing this way a very profitable design to be much less performant under perturbed conditions. Furthermore, a detailed analysis correlating the complex thermodynamics to the operation under uncertain conditions is thoroughly discussed. The proposed design procedure allowed to highlight the differences between weak and strong flexibility constraints and resulted in a dedicated "additional costs vs. flexibility" trend useful to improve the decision making.

Highlights:

1. Distillation feasibility boundaries can be a priori determined by means of an accurate thermodynamic analysis via residue curve maps.
2. Since indexes assess different properties, in order to carry out a reliable flexibility assessment, the most suitable one should be identified according to the expected deviation

nature.

3. The higher flexibility of a process design is not sufficient to provide its final validation until its higher profitability is proved as well.

Keywords: flexibility, biorefinery, distillation, RCMs, trains.

1 Introduction

1.1 Conventional vs flexible design procedure

The typical methodology for chemical plants design is usually made up of several steps performed in series as listed in Figure 5.1. Given a preliminary feasibility assessment, the system configuration and equipment sizing is outlined according to the process specifications. If a certain number of degrees of freedom is still present, the optimal configuration or operating conditions are selected based on a total annualized costs optimization.

Process variables disturbances or uncertain operating conditions, if taken into account, are often discussed in a sensitivity analysis usually performed a posteriori. Whether the optimal design is not able enough to withstand external perturbations it can be modified at the cost of higher investments.

In case an equipment oversizing is not needed, the external duty response to process deviations is assessed during the control system design by means of a dynamic simulation leading (hopefully) to the final project validation.

One of the main problems related to this kind of procedure is that the sensitivity analysis is carried out on a design optimized with respect to other parameters than the system flexibility. This means that the model, or simulation, to which disturbances are applied is able to predict operating conditions and the corresponding costs variations of that specific predefined configuration. Moreover, when the process simulation is not able to converge, it could be very challenging to understand if the solution failure is due to the fact that the design optimized under nominal operating conditions is not able to accommodate the perturbed variables and more variables should have been included during the optimization phase, if the specifications cannot be physically achieved under the disturbed operating conditions or if the unconverged state is simply related to an algorithm convergence issue. For all those reasons, in recent years, the usual design procedure has been replaced by the flexible one as shown in Figure 5.2. Flexibility is defined as the ability of a process to accommodate a set of uncertain parameters (Hoch and Eliceche (1996)[1]) and it can be selected as one of the functions to optimize in the multi-objective optimal design.

Flexible design has become a non-negligible practice for all the systems likely to undergo perturbations or operating under uncertain conditions such as all processes based on biomass feedstocks whose nature floats across the seasons. During the last few years an extensive literature production was indeed published in order to deeply analyze the main features and applications of design under uncertainty. However, when discussing about flexibility, they usually refer to the optimal series of operations among a superstructure of alternatives or to the comparison of a discrete number of case studies with variable parameter values with a consequent MINLP to be solved.

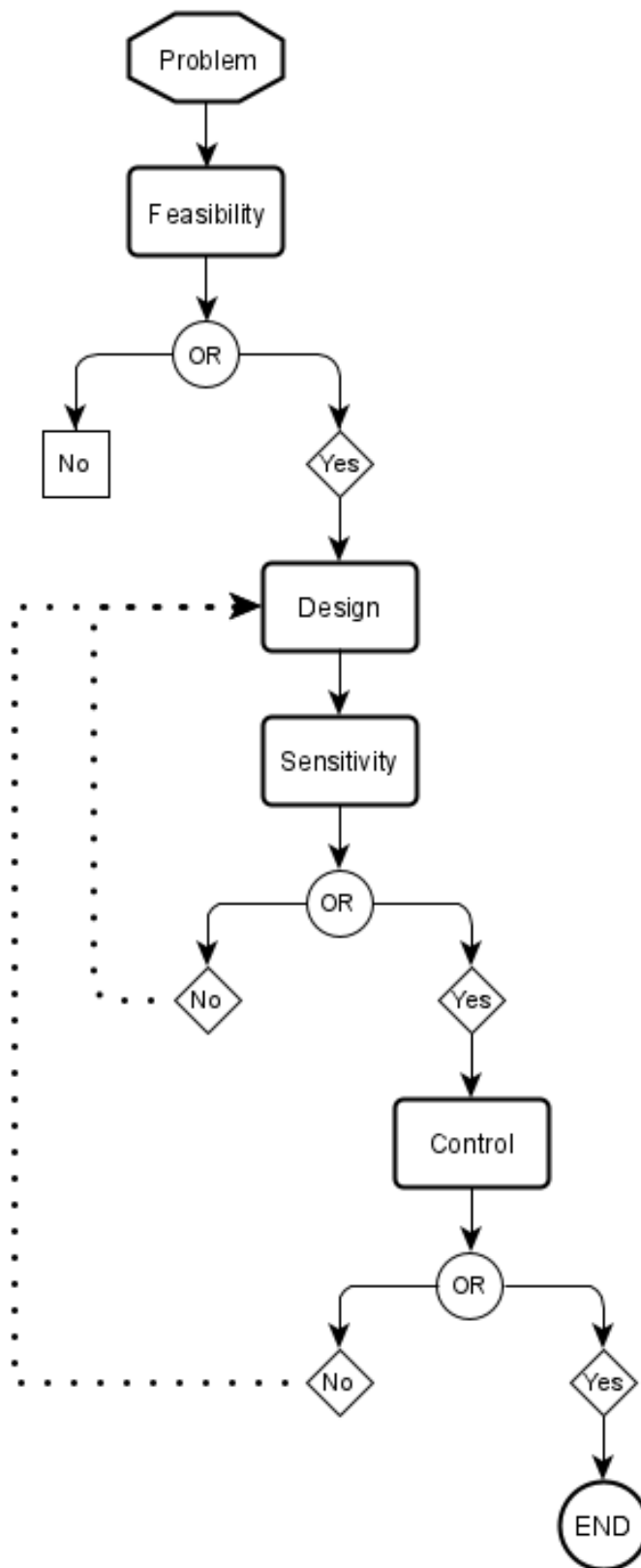


Fig. 5.1: Conventional design procedure

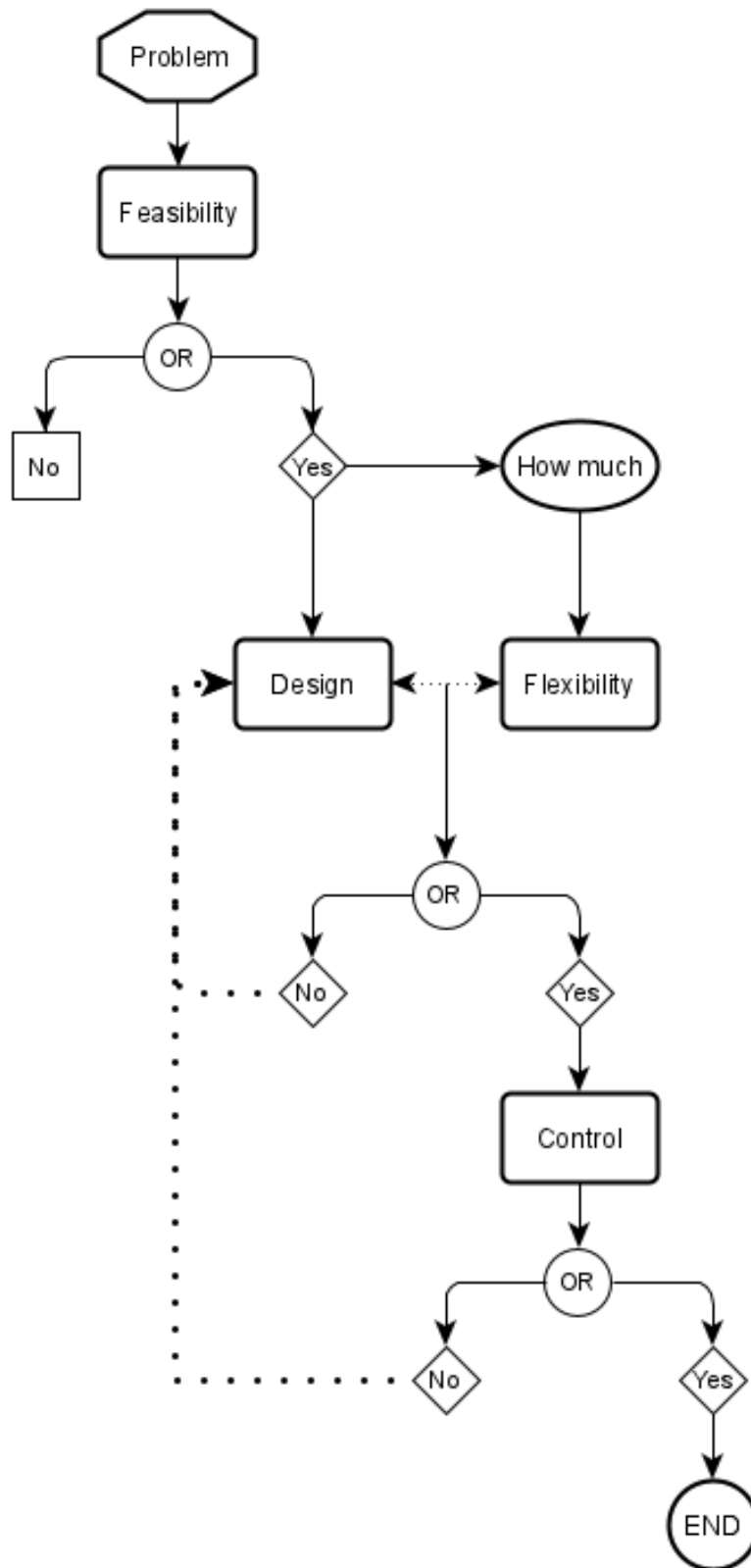


Fig. 5.2: Flexible design procedure

A different kind of flexibility analysis can be performed by using proper flexibility indexes, discussed in the corresponding section 2, over a continuous uncertain variables domain and correlate them to the corresponding optimal design and related costs.

An additional way to take advantage of a flexibility assessment can be the estimation of possible existing units reuse or adaptation in case of plant revamping or production changeover.

1.2 Multicomponent mixtures separation

Among refinery operations distillation has always been the leading process for mixtures separation into their single components. In fact it is based on a well-established technical know-how, it is suitable for high plant capacity and, for a given separation efficiency, it is relatively cheap with respect to more refined operations.

Distillation trains design is the most common practice for multicomponent mixtures separation. For instance the simplest configurations in case two components should be recovered are shown in Figure 5.3. They're namely defined as:

- A) Indirect configuration: sequential recovery from the heaviest to the lightest component;
- B) Direct configuration: sequential recovery from the lightest to the heaviest component;
- C) Midsplit configuration: a preliminary split between heaviest and lightest components is performed, then the separation is refined to achieve specification.

Each column (and its related equipment) is designed on the basis of the lowest total annualized costs and the cheapest train configuration is selected as the optimal one. The main limitation of this procedure is that the economic assessment and equipment design are strictly related to the nominal operating conditions, i.e. they don't take into account feedstock or operating conditions perturbations.

The direct consequence is that, whether a feed composition perturbation occurs, the system could not be able to achieve the separation specifications or at least a relevant operating costs increase can be detected causing the most profitable design not to be as profitable as expected.

In recent years integrated solutions for multicomponent mixtures separation have become the best practice. Modern multicomponent distillation design indeed employs Petlyuk/Keybal columns [2] or their arrangement in a single distillation column shell, also known as dividing wall column (DWC), as well as other various thermally integrated column arrangements[3, 4, 5, 6, 7].

However, although the theoretical background related to those units is wide and well-established, there's little evidence of their employment and, in particular, of the fact that they've completely replaced the traditional distillation systems. For this reason the flexibility analysis of classical distillation train and the corresponding economic assessment will be discussed in this paper with the aim of highlighting the main features and problems deriving from this procedure while the study of the design under uncertain conditions of more complex integrated distillation systems will be addressed in a dedicated paper.

In refinery's operation problems related to variables uncertainty are less appreciable since long-term contracts for crude oil supplying and blending processes ensure an almost constant and stable feedstock quality.

However, during last 15 years there has been an increasing interest for the production of chemicals and fuels from renewable resources because of growing concerns about global warming and climatic change, increasing crude oil price and existing legislations restricting the use of non-renewable energy sources. The direct consequence of this trend results in an even more increasing demand for bio-based fuels and raw materials, i.e. bio-refinery processes. Bio-processes are nevertheless highly subjected to composition perturbations downstream the fermenter across the year's seasons due to the floating nature of the feedstock. Being fermentation usually carried out as a batch process, in order to ensure the desired daily productivity, several fermenters working at the same time are required. On the other hand, even when continuous fermenters are used, their scale up and then the feed flowrate that can be processed has a limit. These conditions cause the fermentation process section to be very expensive, therefore a constantly good performance of the products recovery section is of critical importance for the profitability of the plant.

In the light of the above an a priori flexibility analysis of the different distillation train configurations is non-optional for this kind of separations in order to allow the decision maker to make a multi-criteria-based choice about the optimal design to be selected.

2 Flexibility operational definition and flexibility indexes

From a process engineering point of view flexibility is defined as the ability of a process to accommodate a set of uncertain parameters (Hoch and Eliceche (1996)[1]). As a direct consequence of this definition, flexibility can be seen as an accurate measure of feasibility.

In order to quantify this measurement an effective tool is required. For this purpose several flexibility indexes, both deterministic and stochastic, were proposed in literature. The first ones are the result of the works carried out by Swaney & Grossmann (1985a)[8] and Saboo et al. (1985)[9]. The Swaney and Grossmann flexibility index F_{SG} is defined as the maximum fraction of the expected

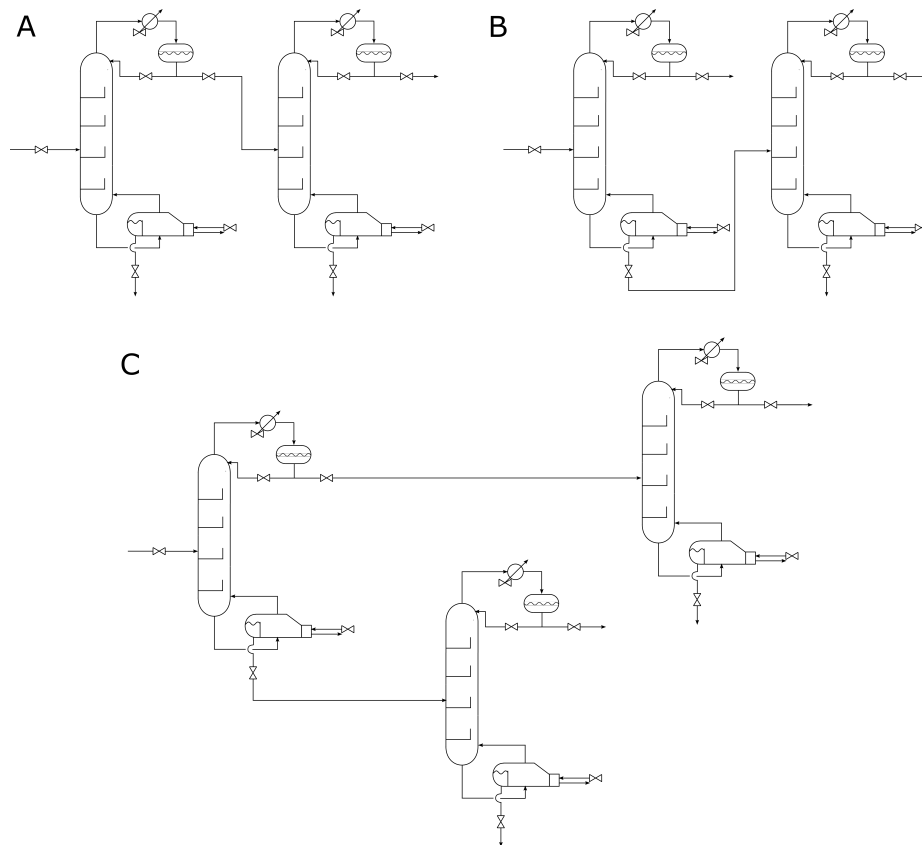


Fig. 5.3: Distillation train configurations for two components recovery

deviation of all the uncertain variables at once that can be accommodated by the system. On the other hand the resilience index RI by Saboo et al. is defined as the largest total disturbance load, independent of the direction of the disturbance, that a system is able to withstand without becoming unfeasible. Although they look similar they evaluate different properties of the same physical system; namely the former is much more conservative since, for a given flexibility index value, the perturbation to be withstood involves all the uncertain parameters at the same time. A graphical comparison between these two different indexes can be seen in Figure 5.4. From a geometrical point of view the F_{SG} index represents the distance between the nominal operating condition (the star) and the side of the maximum hyperrectangle that can be inscribed in the feasible space. On the other hand, given the maximum allowed parameter deviations independently of each other (green circles), the Resilience Index defines the distance between the operating conditions and the most constraining of them. Since these indexes assess different properties, in order to carry out a reliable flexibility assessment, the most suitable one should be identified. As it can be deduced from their definition, the compliance of the index is necessarily related to the expected deviation nature. In any case both of them assign to any deviation type and magnitude the same likelihood (that's why they can be defined as “deterministic”).

The need of estimating the perturbation likelihood was fulfilled by the intro-

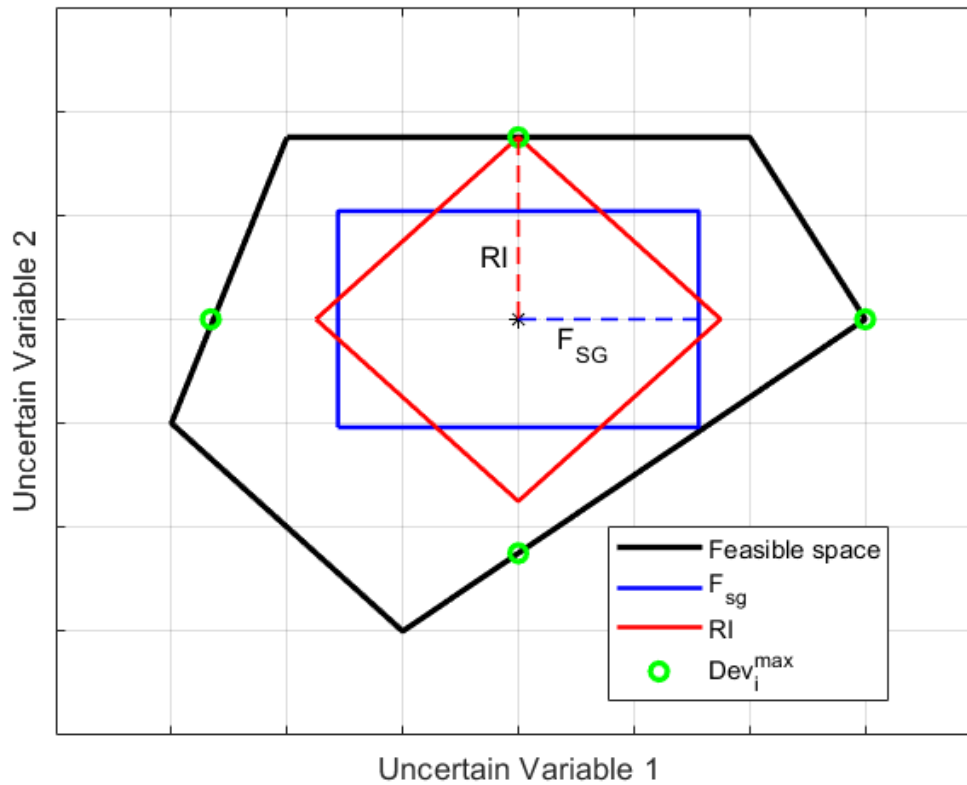


Fig. 5.4: Flexibility index (F_{SG}) vs Resilience Index (RI)[7]

duction of a stochastic flexibility index SF proposed by Pistikopoulos & Mazzuchi (1990)[10]. It is defined as the integral of the deviation probability density function over the feasible domain. The price to pay to use such a detailed index is the need to know the required probability function that is seldom available. In order to outline this probability function there are two main possible procedures:

- Data collection of the system disturbances and consequent fitting with the most compliant PDF form in order to obtain the corresponding parameters;
- A priori selection of a PDF according to the state of information (e.g. symmetric or skew PDF, normal distribution etc.) and parameters calculation according to reasonable hypothesis (e.g. maximum probability value under nominal operating conditions, variance selection in order to have almost the entire perturbation likelihood within the maximum deviation range etc)

In order to better understand the stochastic flexibility index a simple heat exchanger case study is shown in Figure 5.5. The feasibility constraint is represented by the heat transfer area of the available heat exchanger (red hyperbolic surface) according to the characteristic equation:

$$A = \frac{Q}{U \cdot \Delta T_{lm}} \quad (2.1)$$

As it can be noticed, a positive deviation of the cooling water temperature or

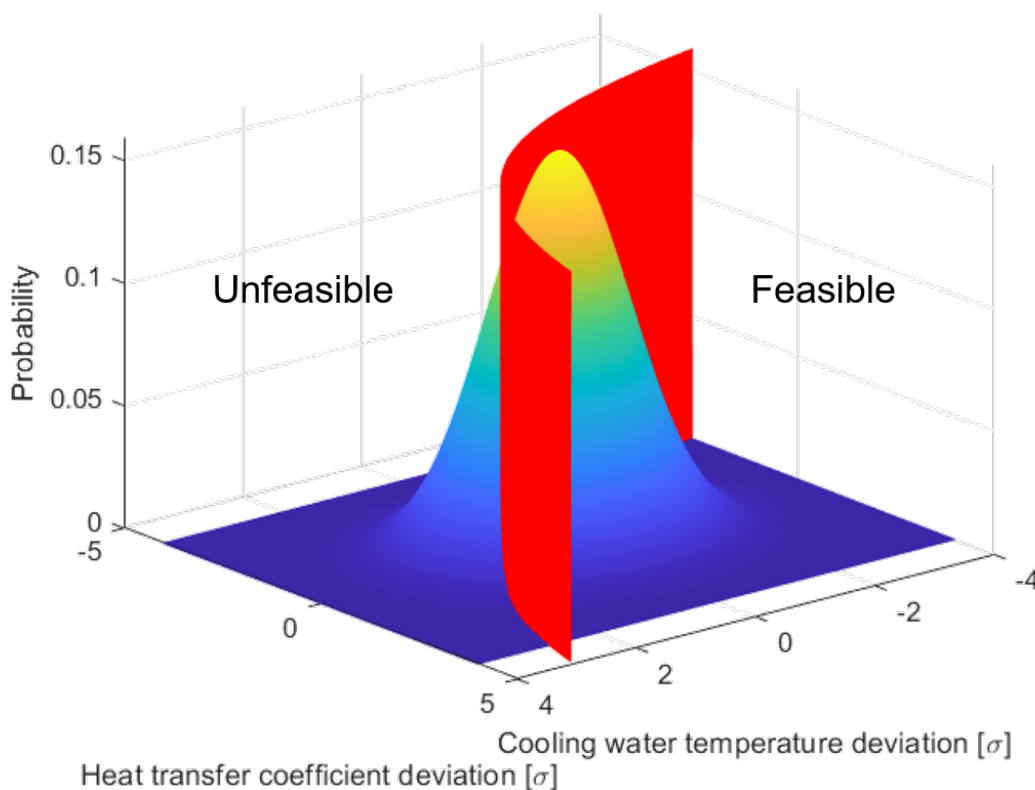


Fig. 5.5: Stochastic Flexibility (SF) assessment of a heat exchanger[7]

a negative deviation of the heat transfer coefficient make the cooling operation unfeasible. The stochastic flexibility index SF is then represented by the integral of the probability distribution function (colored Gaussian bell curve) over the right side of the uncertain space.

Finally a volumetric flexibility index F_V , whose properties can be associated to the stochastic one, was introduced by Lai and Hui (2007, 2008)[11, 12]. It is defined as the fraction of the expected deviation volume contained in the feasible domain. A more complete review about these indexes and a thorough procedure to integrate them in the distillation column design were provided by Di Pretoro et al. (2019)[13].

After the flexibility assessment an economic analysis needs to be performed in order to evaluate the additional costs related to a more flexible design. In case of deterministic indexes the distillation train design for which capital and operating costs should be estimated is univocally determined. On the contrary, if a stochastic index is employed, several design could lead to the same SF value. An economic optimization is thus required at each stochastic flexibility analysis step in order to find the cheapest system design providing the same SF value. This procedure corresponds to looking for the most flexible configuration for a given additional cost.

If cost minimization is not the most interesting or constraining condition a dif-

ferent constraint (e.g. controllability, energy consumption etc) should be provided in any case to fulfill the remaining degree of freedom of the flexibility problem. In the presented case study when the “x” stochastic flexibility design is discussed it will be referred to the cheapest design corresponding to the “x” SF value.

Capital and operating costs for the flexibility and economic based design coupling have been estimated using Guthrie (1969, 1975)[14, 15], Ulrich (1984)[16] and Navarrete (2001)[17] correlations. For further detail please refer to the dedicated section in the Appendix B.

3 The biorefinery case study

Several interesting flexibility analysis and design applications to distillation trains have been found in literature[18, 19, 20]. However, when talking about flexibility, they almost refer to the optimal operation sequencing or to the optimal system configuration with respect to a given number of different operating conditions. The main purpose of this paper instead is to assess the performances of several configurations under a continuous wide range of operating conditions. In order to do that, a new case study referring to the separation of an ABE/W (acetone, n-butanol, ethanol, water) mixture has been outlined. The history of ABE fermentation and its industrial applications during the 20th century are wide and complex. In 1912 Chaim Weizmann succeeded in isolating a bacterium strain (later named *Clostridium acetobutylicum*) which was capable of using starch as a substrate in the butanol production process with higher butanol and acetone product yields with respect to the previous ones. The fermentation process via *Clostridium acetobutylicum* replaced then the previous technology and, with some modifications, it is still the base for the industrial fermentation applications (Gabriel & Crawford, 1930)[21]. However, later studies highlighted that these microorganisms used in ABE fermentation still suffer from product inhibition, giving a low acetone and butanol final concentration. A complete review about this process and its future perspectives is provided by Garcia et al. (2011)[22].

Due to the high alcohols dilution in the fermentation broth a dewatering extraction column is present downstream the fermenter and before the distillation train. For the same reason the effectiveness of the separation process is a critical variable for the fraction and purity of recovered product.

Biorefinery operations are particularly suitable for flexibility assessment due to the feedstock composition fluctuations during the year as a consequence of the different biomasses to be treated. On the other hand feed perturbations can be also seen as the result of a lower effectiveness in the preliminary dewatering process. In fact, as discussed by Dalle Ave et al. (2018)[23], the outlet fermenter composition is strictly related to the selected extractant and to stable operating conditions. However this study will address the entire uncertain domain for water and n-butanol partial flowrates in order to provide a complete overview that could

Component\Property	Value	Unit
Acetone	12.030	<i>mol/s</i>
n-Butanol	61.328	<i>mol/s</i>
Ethanol	3.839	<i>mol/s</i>
Water	12.428	<i>mol/s</i>
Pressure	101.325	<i>kPa</i>
Temperature	361.26	<i>K</i>

Tab. 5.1: Feed composition and physical properties

be adapted to different extraction layouts.

Even though the ABE process is a well-established technology and it has been widely studied during the last years, it still results to be one of the most suitable examples for the addressed flexibility assessment due to its highly non-ideal thermodynamics. Due to the presence of homogeneous and heterogeneous azeotropes, liquid-liquid equilibrium and complex activity model, if the system flexibility were evaluated through a sensitivity analysis, it would be very difficult to understand whether the failure to achieve a physical results is due to the actual impossibility of the system to attain the desired specification or to the inability of the algorithm to converge. Further details about thermodynamic flexibility will be then discussed in the corresponding section 4.

The nominal feed composition and properties related to this case study are listed in Table 5.1. The successful recovery of at least biobutanol and acetone is considered crucial for the profitability of the operation. In order to accomplish this task, a minimum of two distillation columns are required and three configurations are possible as previously shown in Figure 5.3.

Midsplit configuration specifications are as follows:

- 1) Split column:
 - (a) Acetone recovery ratio in the distillate: 0.995;
 - (b) n-Butanol recovery ratio in the bottom: 0.98;
- 2) Acetone recovery column (top column):
 - (a) Acetone recovery ratio in the distillate: 0.995;
 - (b) Distillate acetone mass fraction: 0.995;
- 3) n-Butanol recovery column (bottom column):
 - (a) n-Butanol recovery ratio in the bottom: 0.98;
 - (b) Bottom n-butanol mass fraction: 0.99.

Specifications for direct and indirect configuration can be easily deduced from the midsplit ones.

The direct configuration resulted unfeasible under nominal operating conditions. The presence of acetone in the ABE/W mixture improves the separation performance, thus its preliminary removal moves the feed composition of the second column closer to the distillation region boundary (cf section 4) causing the desired butanol recovery at the designed purity to be impossible. Only indirect and midsplit configurations will be then discussed and compared.

As already mentioned, the complexity of the proposed case study, mainly caused by its highly non-ideal physical behaviour, results in the impossibility to obtain the desired split specifications independently on the operating conditions. This particular circumstances forces us to find a dedicated tool in order to preliminary assess the physical process limitations (strong flexibility constraints).

The selected methodology to perform the thermodynamic assessment will be then described in detail in the following ad-hoc chapter; in case of mixtures with no singular points, this analysis wouldn't be needed since all sharp splits would be possible with a sufficiently high number of equilibrium stages.

4 Thermodynamic flexibility analysis

4.1 RCMs overview

Thermodynamics of multicomponent mixtures is an ever-present research field in distillation theory. A widespread and well established tool to assess whether a mixture can be separated by distillation is the use of Residue Curve Maps (RCMs) on phase diagrams, usually ternary or quaternary. Despite their usefulness and the robustness of the theory behind them and although they are the more immediate and effective way to analyze the constraints of azeotropic multicomponent systems, RCMs have received relatively poor attention from engineers. These lines were introduced first by Ostwald (1900)[24] and Schreinemakers (1901)[25] to describe the thermodynamic behavior of three-component azeotropic mixtures but only after half a century Gurikov (1958)[26] developed the first classification of three-component residue curve diagrams. Later Zharov (1967, 1968a, 1968b)[27, 28, 29] and Serafimov (1969, 1975)[30, 31] generalized their application to the analysis and classification of four or higher multicomponent mixtures. However, most of these works were in Russian and were not available in the other countries. The application of residue curve bundles to reversible distillation and to finite reflux distillation column optimal design is due to Petlyuk (2004)[32] and the following discussion will mainly refer to its works.

A residue curve is defined as the locus of compositions satisfying the equation:

$$\frac{dx_i}{d\xi} = x_i - y_i \quad (4.1)$$

It represents both the change in a mixture composition during an open distillation process and the composition profile of an infinite column at infinite reflux. Each point of this line corresponds to a certain moment of time and to a portion of evaporated liquid as well as to an equilibrium tray of an infinite distillation column. RCMs are convenient for the description of phase equilibrium because they are continuous and noncrossing.

In order to clarify how to read a phase diagram when residue curve mapping is performed a few notation details by referring to Figure 5.6 will follow.

- Stable nodes (square): a stationary point at which all residue curves come to an end (the heavy compound (or pseudo-compound) of a distillation bundle);
- Unstable nodes (circle): a stationary point at which all residue curves start (the light compound (or pseudo-compound) of a distillation bundle);
- Saddles (triangle): a stationary point to which residue curves come close but neither start nor end;
- Separatrixes (black line): a boundary separating one bundle from another. In contrast to the other residue curves, the separatrixes begin or come to an end, not in the node points but in the saddle points. A characteristic feature of a separatrix is that in any vicinity of its every point, no matter how small it is, there are points belonging to two different bundles of residue curves;
- Immiscibility region (Green): the composition region where two liquid phases are present. The real compositions related to the aqueous and organic phase respectively are those at the extremal points of the corresponding tie line;
- Univolatility line (Red): they are lines where $\alpha_{ij} = \frac{K_i}{K_j} = 1$. Univolatility α -lines (α -surfaces and α -hypersurfaces) divide the concentration simplex into regions of order of components Reg_{ord}^{ijk} (in Reg_{ord}^{ijk} $K_i > K_j > K_k$).

Temperature increases moving from the unstable node to the stable one (the same direction of a residue curve). A residue curves bundle is defined as a subregion with its own stable and unstable points and it is separated by another bundle of the whole concentration space by means of a separatrix. In case of ideal mixtures the entire concentration space is filled with one RCMs bundle. From a topological point of view while residue curves keep being lines even for a four components system, the separatrix boundaries become surfaces (and hypersurfaces for higher dimension).

Separatrix lines are of critical importance to assess the distillation feasibility since they define at which side of the azeotropic composition the feed is located, i.e. the lightest and heaviest compounds that can be obtained by distillation for a given feed composition. That's why these subregions are also called distillation bundles and separatrixes are also called distillation boundaries. In general, if

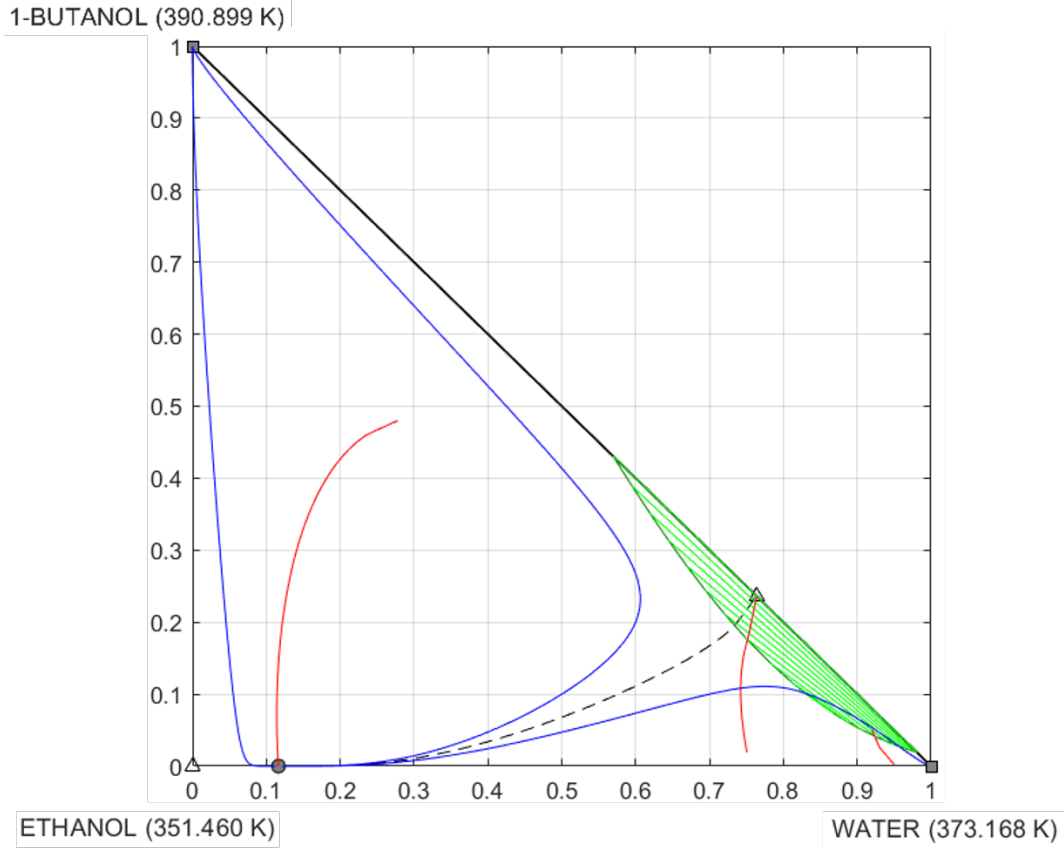


Fig. 5.6: RCMs on a ternary diagram

separatrixes have a relatively regular shape (i.e. not particularly skew) as for the vast majority of mixtures, it can be stated that separation by distillation is possible if feed, distillate and bottom composition points lie in the same distillation region (for further details about the theoretical background please refer to Petlyuk (2004)[32]).

4.2 Thermodynamic model

As suggested by Errico et al. (2017)[5], the selected thermodynamic model for the ABE/W mixture equilibrium description is the Non-Random Two Liquids (NRTL)[33]. Moreover, it results to be the most appropriate to describe water-alcohols as well as biofuels equilibria in general [3, 4, 6].

The activity coefficient for the species i in a mixture of n components is given by:

$$\ln(\gamma_i) = \frac{\sum_{j=1}^n x_j \cdot \tau_{ji} \cdot G_{ji}}{\sum_{k=1}^n x_k \cdot G_{ki}} + \sum_{j=1}^n \frac{x_j \cdot G_{ij}}{\sum_{k=1}^n x_k \cdot G_{kj}} \cdot \left(\tau_{ij} - \frac{\sum_{m=1}^n x_m \cdot \tau_{mj} \cdot G_{mj}}{\sum_{k=1}^n x_k \cdot G_{kj}} \right) \quad (4.2)$$

where:

$$\ln(G_{ij}) = -a_{ij} \cdot \tau_{ij} \quad (4.3)$$

$$a_{ij} = a_{ij}^0 + a_{ij}^1 \cdot T \quad (4.4)$$

$$\tau_{ij} = \frac{\Delta g_{ij}}{R \cdot T} \quad (4.5)$$

$$\Delta g_{ij} = g_{ij} - g_{jj} = C_{ij}^0 + C_{ij}^1 \cdot T \quad (4.6)$$

Not all the process simulators have provided standard binary interaction parameters able to correctly describe the azeotrope location and the liquid-liquid equilibrium. Only Simulis[®] Thermodynamics values resulted to be reliable for the azeotropes and the liquid-liquid equilibrium prediction, but unfortunately no coefficients for the organic binary mixtures (i.e. n-Butanol-Acetone, Acetone-Ethanol, n-Butanol-Ethanol) were present. In order to have a reliable thermodynamic model, a regression was then used to adjust the missing parameters with respect to experimental equilibrium data.

As it can be noticed in Figure 5.6, the NRTL activity model with the adjusted binary interaction parameters is able to correctly predict liquid-liquid demixing (green region) as well as heterogeneous (empty triangle on the Water-Butanol side) and homogeneous azeotropes (full circle on the Water-Ethanol side) at $x_{water} = 0.763$ and $x_{water} = 0.11$ respectively. These values corresponds to those obtained by Luyben (2008)[34] for what concerns the heteroazeotrope as well as to the values reported in the Dortmund Data Bank [35] for the homogeneous one. Moreover, the LLE described by the adjusted binary interaction parameters matches with the experimental data provided by Lee et al. (2004) [36] and agrees with the model prediction of Kosuge et al. (2005)[37].

4.3 Thermodynamic feasibility assessment

In the light of the above the thermodynamic feasibility assessment is straightforward. The mixture under analysis shows two azeotropes, namely the water-butanol heterogeneous azeotrope and the water-ethanol homogeneous one. Columns operating conditions and composition profiles are always far from the homogeneous azeotrope; moreover, even once butanol is removed, the presence of acetone mitigates the non-ideal behaviour of the remaining fractions. It can be then concluded that the critical operation in both midsplit and indirect configuration is the butanol separation even because the most likely perturbations downstream the fermenter are related to water and butanol relative content. Since RCMs refer to infinite columns at infinite reflux, the analysis of the sharp split AEW/B holds true for the midsplit configuration as well.

Given the feed composition and the butanol product purity the corresponding two points can be plotted in a quaternary phase diagram as shown in Figure 5.7a (violet diamonds). Since recovery ratio is fixed the lever rule resulting from mass

balances can be applied in order to obtain the third point related to the distillate composition. The RCMs passing through these points were then calculated and plotted as well. It can be noticed that all these RCMs have the same stable and unstable nodes, that means separation by simple distillation is possible under nominal operating conditions.

In order to assess the thermodynamic feasibility boundaries the uncertain variables need to be perturbed. The most constraining variable is the water content in the feed stream, in particular we expect the distillation to be more critical, i.e. the butanol recovery at the desired purity to be more difficult, for a higher water fraction. The increase in water partial flowrate keeping unchanged the amount of the other components in the mixture can be represented on phase diagrams by moving the feed characteristic point along the line connecting the actual feed point and the pure water vertex (cf black arrow in Figure 5.7a). For an increase in the water content up to 8 % the RCMs corresponding to distillate, feed and bottom still lie in the same distillation bundle as shown in Figure 5.7b. When a 9 % deviation is applied, on the contrary, the stable node of the residue curve related to the distillate stream moves from pure butanol to pure water, i.e. it crosses a separatrix (cf Figure 5.7c). The separatrix crossing results in the impossibility of obtaining such a distillate from the given feed by means of a distillation.

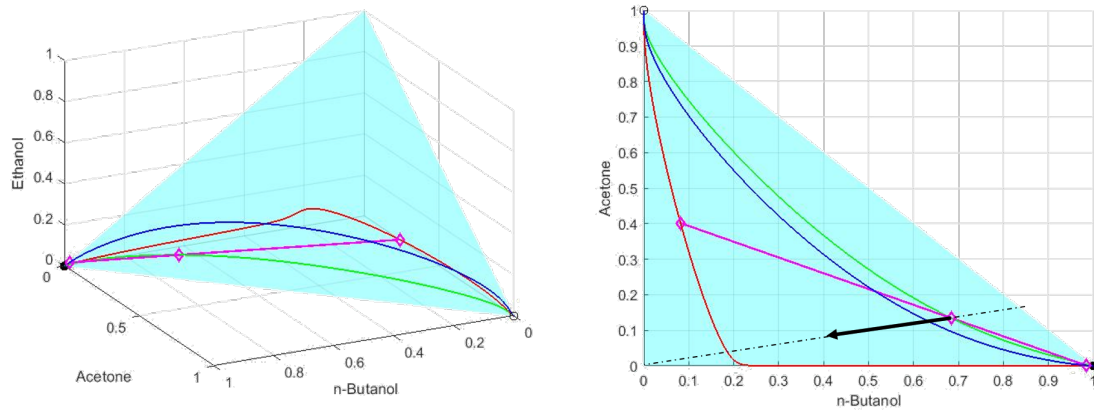
The same analysis was carried out with respect to each of the four components. As expected, the water molar fraction resulted to be the most constraining variable from a flexibility point of view. It can be then stated that the system thermodynamic flexibility limit is about 8 %. This value represents the chemico-physical constraint to this operation whatever the affordable investment to design the distillation train is. If a higher flexibility is required the only possible solution is to select a different separation process for such a mixture.

The same procedure was performed for the F_{SG} index, i.e. by simultaneously varying both butanol and water partial flowrates, and a value about 5 % was found.

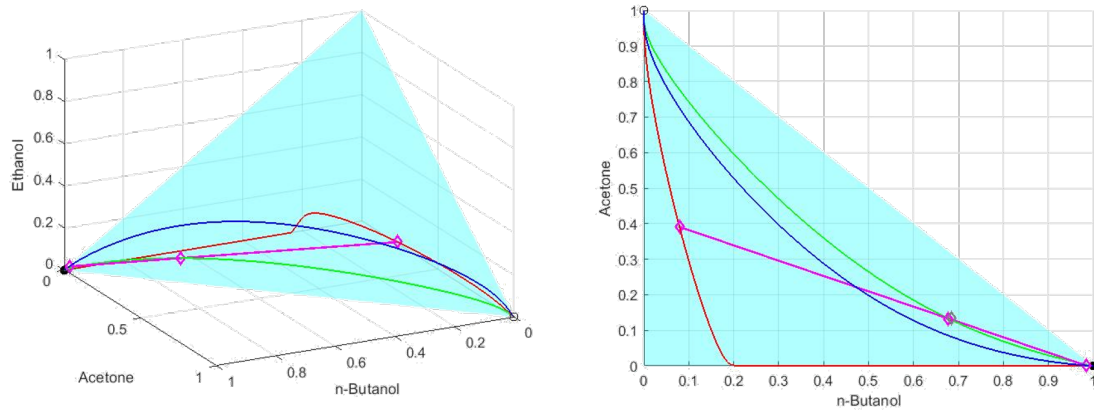
Residue curve maps analysis was carried out by interfacing Matlab[®], used to solve the ODE system 4.1 and to plot the corresponding graphs, to the software Simulis[®] Thermodynamics aimed to provide the equilibrium data related to the NRTL model previously described.

5 Economic assessment and optimal design under uncertain conditions

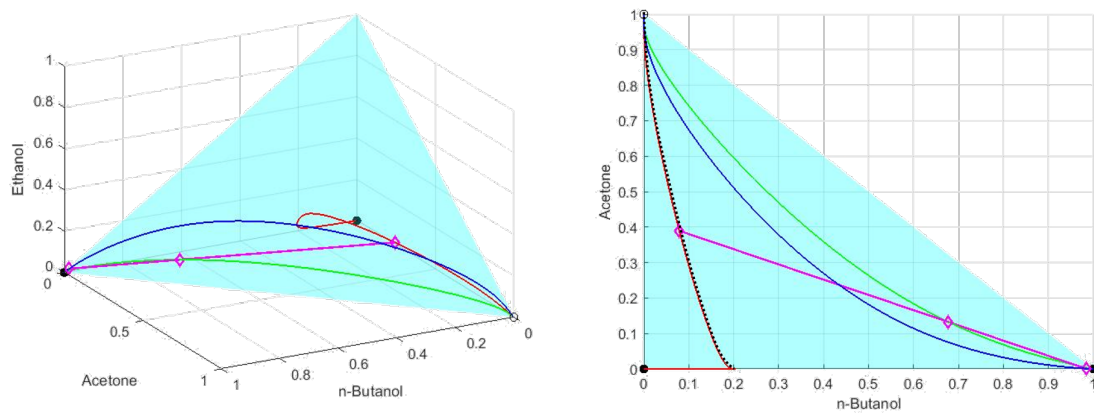
As already mentioned, the ordinary design procedure has been conducted as usual: CAPital and OPERating EXPenses have been evaluated for each column of the two configurations at different numbers of stages with the optimal feed location under nominal operating conditions. Considering a life span of 10 years, for each column the number of stages corresponding to the minimum annualized cost, given by the



(a) Nominal operating conditions



(b) Perturbed conditions (8%)



(c) Unfeasible distillation

Fig. 5.7: Feasibility boundaries assessment via residue curve maps

		Indirect	Midsplit
1st Column	N (feed)	16 (10)	35 (9)
	Cost (\$/y)	580 016	455 493
2nd Column	N (feed)	50 (46)	50 (47)
	Cost (\$/y)	353 493	352 224
3rd Column	N (feed)	/	16 (8)
	Cost (\$/y)	/	276 365
Total cost		933 509	1 084 082

Tab. 5.2: Distillation train optimal design

expression

$$TAC = OPEX + \frac{CAPEX}{lifetime} \quad (5.1)$$

was then identified and the overall annualized cost of each configuration was calculated.

All simulations required for the columns design were carried out by means of ProSim Plus[®] process simulator. An equilibrium based distillation model with no simplifying assumptions was employed. Among the several available distillation column models, the three-phase distillation column model accounting for liquid phase demixing was selected. Optimal number of stages, feed tray and relative TAC for each column of each configuration are listed in Table 5.2. With a total cost of 933,509 \$/y vs 1,084,082 \$/y the indirect configuration results to be the most convenient with respect to the midsplit one under nominal operating conditions. The addition of a preliminary column indeed does not substantially affect the acetone column utilities consumption.

In order to validate this design configuration under uncertain conditions the flexibility analysis should be then performed. The most critical parameters, as already discussed in section 4, are water and butanol feed content, that's why their partial flowrates were selected as uncertain parameters for the analysis. The flexibility assessment results via process simulation confirmed the preliminary thermodynamic evaluation providing a F_{SG} value about 5% (4% for the midsplit) and a RI value about 8% (7% for the midsplit) for both configurations as shown in Figure 5.8. With a proper deviation range discretization, several simulations were run over the whole uncertain domain by using as process variables initial guess the previously converged values in the closest point; the green squares refer to simulations that revealed themselves as feasible and operable, while blue squares correspond to operating conditions that didn't allow the specifications achievement. In particular midsplit configuration resulted slightly less flexible due to the difficulty to recover enough acetone without the preliminary butanol removal. The stochastic index SF corresponding values are respectively 77.86% for the indirect

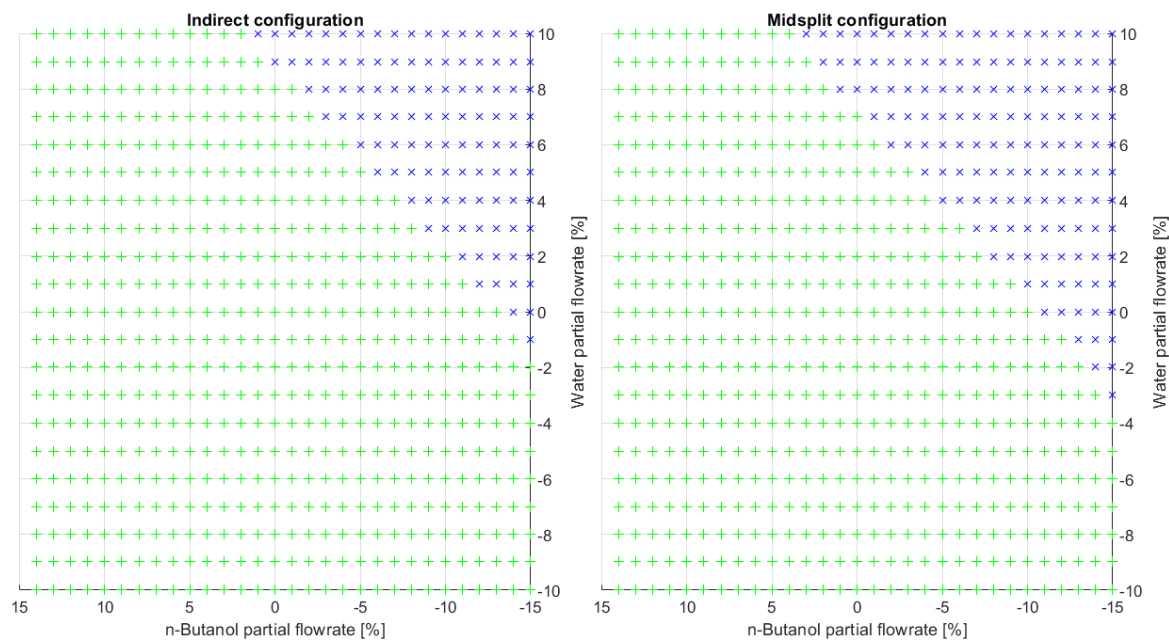


Fig. 5.8: Indirect vs midsplit feasibility (Green: feasible, Blue: unfeasible)

configuration and 75.85% for the midsplit configuration in case of a perturbation normal PDF with a 10% variance (i.e. more than 99% disturbance likelihood within the 30% disturbance range). This PDF parameters were selected taking into account the higher butanol concentration boundary in the fermentation broth due to product inhibition [22] and in a way that water perturbations, related to the dewatering process inefficiency, affected the analysis result with a comparable magnitude. The F_V volumetric flexibility index analysis was not carried out since it can be reconducted to a particular case of the stochastic flexibility assuming a step PDF for the uncertain variables as shown by Di Pretoro et al. (2019)[13].

Given these results the indirect configuration results slightly more flexible than the midsplit one. However, the higher flexibility of a process design is not sufficient to provide its final validation under uncertain conditions until its higher profitability is proved as well.

Flexibility analysis was then coupled to the economic assessment according to the procedure suggested by Di Pretoro et al. (2019)[13]. The costs corresponding to every perturbed operating conditions were calculated and correlated to the different flexibility values by means of the corresponding indexes. Even in this case the cost of an additional preliminary column was not compensated by a lower utility consumption and the indirect design still results the more convenient. Total annualized costs vs. partial flowrates perturbations have been plotted for the indirect configuration in Figure 5.9. An analogous trend with higher values was obtained for the midsplit configuration. Costs result to be higher whether a bigger oversizing is necessary, i.e. positive deviation for both water and butanol flowrates, and under operating conditions close to the feasibility boundary. Figure 5.10 shows for instance the trend of the first column reboiler heat transfer surface

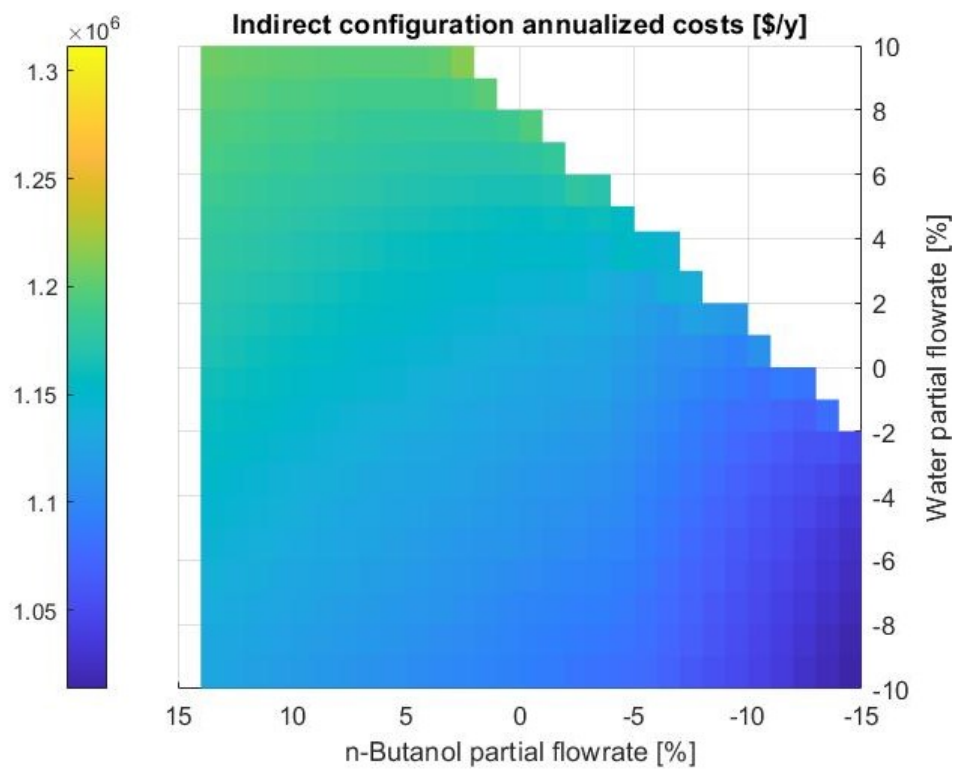


Fig. 5.9: Total annualized costs vs. partial flowrates perturbations

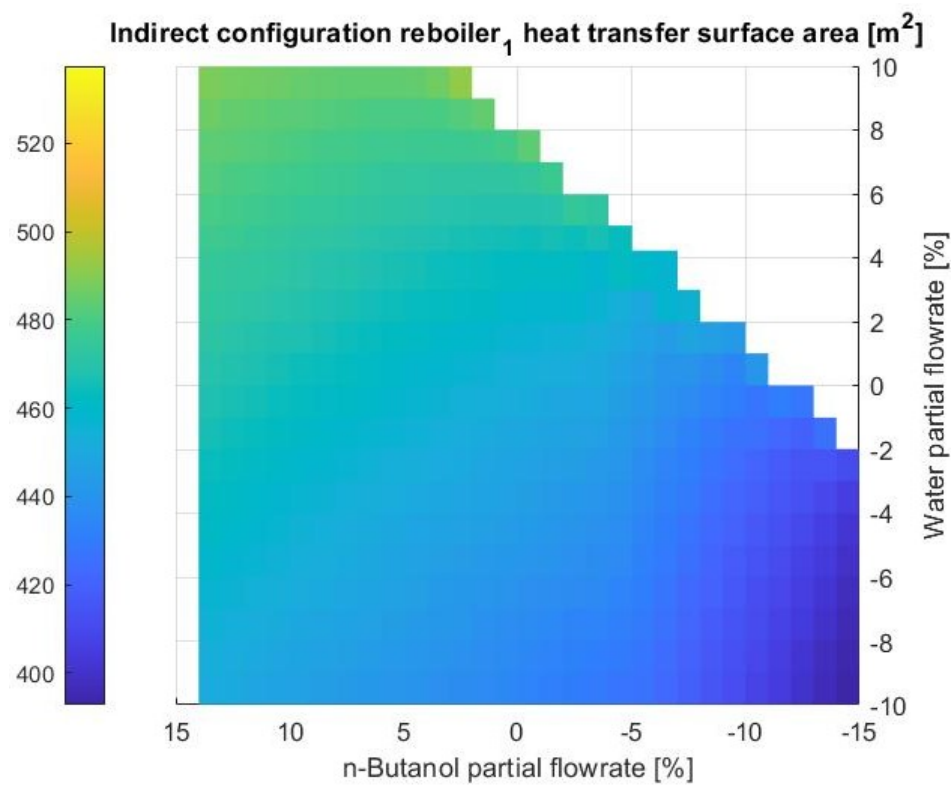


Fig. 5.10: First column reboiler heat transfer surface

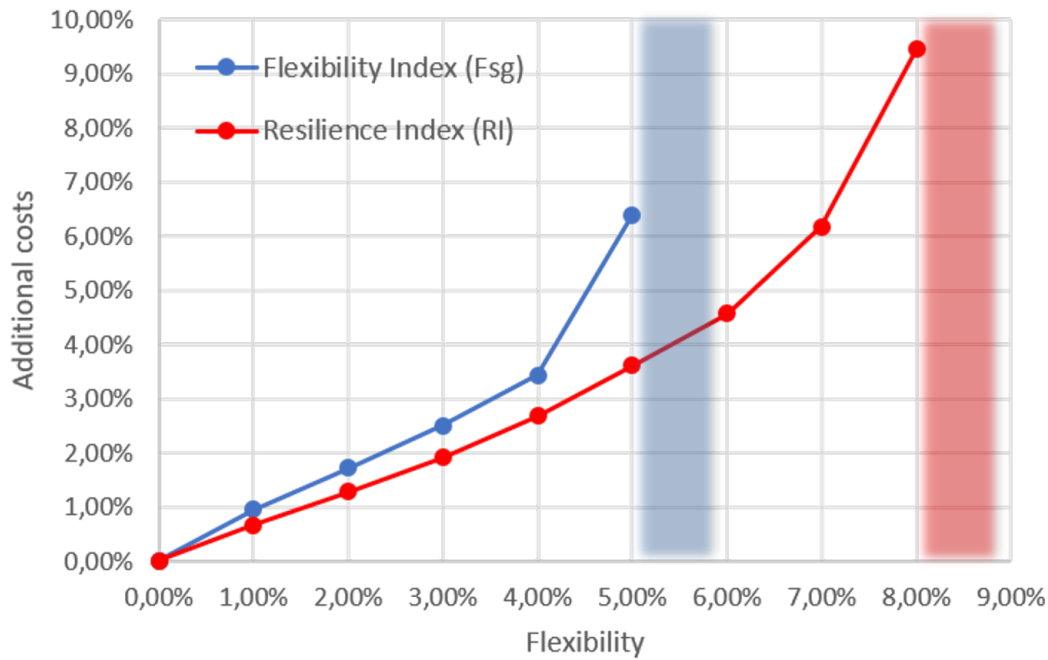


Fig. 5.11: Deterministic indexes economic comparison

area, that is one of the most sensitive parameters, varying over a range going from 393 to 538 m^2 , i.e. more than 35% deviation with respect to the nominal operating conditions value.

The plot resuming the indirect configuration additional cost vs. flexibility for the deterministic indexes is then reported in Figure 5.11. The shaded regions represent the flexibility limit that can't be overcome despite the affordability of a higher expense. As expected by their definition the F_{SG} index results more conservative than the RI one since it involves the simultaneous deviation of all the uncertain variables at once. Moreover in both cases it can be noticed that after 4% flexibility (7% for RI) much higher additional investments are required for a corresponding flexibility increase of 1% only.

The stochastic flexibility SF index trend is plotted in Figure 5.12. Differently from deterministic indexes, stochastic flexibility has non-null value even at nominal operating conditions since the designed system is already able to withstand part of the negative perturbations. Another characteristic feature of this index is the asymptotical trend when SF approaches the feasibility boundary value. This behaviour is independent on the selected PDF and its interpretation is that an always increasing investment should be afforded if the lowest risk of underperformance has to be attained.

The conclusions that the engineer or the decision maker in general can derive from these results are different and mainly depend on his needs and his resources. In general, except if really needed, it is not profitable to design a system in the region after the cost vs. flexibility line slope increase or close to the asymptote in case SF is used. Moreover, if a stochastic analysis is performed, an optimal

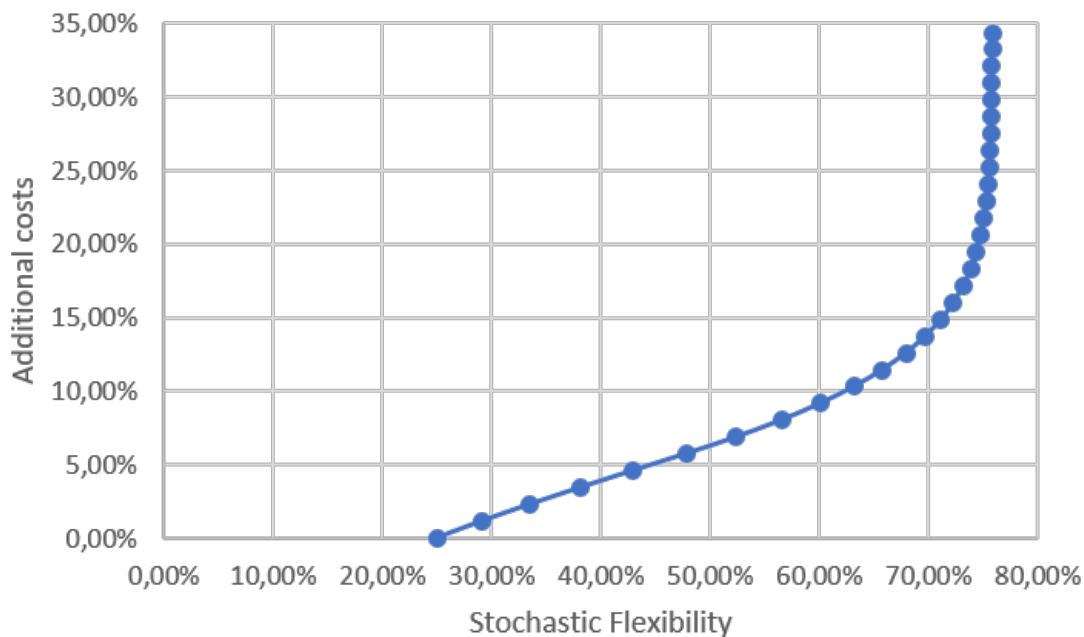


Fig. 5.12: Additional costs vs. stochastic flexibility

design region can be calculated as shown in Di Pretoro et al. (2019)[13].

An alternative solution in case of plant capacity variation across the year could be the design of more than one unit in parallel and shut down/start up scheduling optimization for some of them according to the feed to be processed. In general this option is rather expensive but in specific cases it can meet other system needs (e.g. safety, maintenance operations etc) and thus become more convenient.

6 Conclusions

The aim of this paper is to define a thorough procedure to design a distillation train under uncertain conditions. This procedure is based on an economic and flexibility multi-criteria design optimization and analysis of the possible train configurations. A biorefinery products separation section was selected as case study due to the characteristic fluctuations related to fermentation processes; in particular the object of this analysis was the ABE process since among the biomass based processes it is one of those with the most promising future perspectives according to the goals of the fossil fuel replacement politics.

An a priori thermodynamic feasibility assessment was carried out via residue curve maps to evaluate the maximum attainable flexibility from a physical point of view and its results were confirmed by process simulation. Then the standard design procedure was carried out to detect the best configuration under nominal operating conditions. It was then followed by a flexibility assessment coupled to an economic analysis to validate the result. Both deterministic and stochastic indexes have been used in order to make a comparison and provide a complete

overview according to several possible perturbation natures.

The final product of this procedure is an additional costs vs. flexibility plot allowing the decision maker to make the most possible informed choice.

The indirect configuration, that was the cheapest one under nominal operating conditions, resulted to be also slightly more flexible than the midsplit configuration. The economic gap due to the additional column is not compensated by a lower external duty demand and it is conserved under uncertain conditions as well. Although this design solution provides a maximum flexibility of $F_{SG} = 5\%$ ($RI = 8\%$ and $SF = 77.86\%$) it can be stated that beyond $F_{SG} = 4\%$ ($RI = 7\%$ and $SF = 67\%$) it is less worth investing since the additional costs line becomes steeper.

Beside the numerical results, the outcome of general validity is that, in thermodynamically constrained system, the feasibility and flexibility boundaries cannot go over a certain value by investing more. An a priori flexibility analysis and economic assessment could then be crucial for making the best design choice and to know the system limitation if perturbations are likely to occur.

Finally it is worth remarking that, even if the provided results are case specific, the proposed procedure can be considered valid for any analogous case study.

A List of acronyms and symbols

Symbol	Definition	Unit
A	Characteristic dimension	m^n
ABE/W	Acetone-Butanol-Ethanol/Water	Acronym
a_{ij}	NRTL non-randomness parameters	1
$CAPEX$	CApital EXpenses	\$
C_{ij}^n	Excess Gibbs energy coefficients	$J/(mol \cdot K^n)$
C_{BM}	Equipment bare module cost	\$
C_p^0	Purchase equipment cost in base conditions	\$
F_{BM}	Bare module factor	1
F_M	Material factor	1
F_P	Pressure factor	1
F_q	Column trays factor	1
F_{SG}	Swaney & Grossmann flexibility index	1
F_V	Lai & Hui flexibility index	1
g_{ij}	NRTL excess Gibbs energy	J/mol
K_i	Vapor-liquid distribution ratio	1
LLE	Liquid-Liquid Equilibrium	Acronym
$MINLP$	Mixed Integer Non-Linear Programming	Acronym
$M\&S$	Marshall & Swift cost index	1
NDF	Normal distribution function	Function
$NRTL$	Non-Random Two Liquids	Acronym
ODE	Ordinary Differential Equation	Acronym
$OPEX$	OPerating EXpenses	$\$/y$
P	Pressure	bar
PDF	Probability distribution function	Function
Q	Exchanged heat duty	W
R	Gas constant	$J/(mol \cdot K)$
RCM	Residue Curve Map	Function
Reg_{ord}^{ijk}	Region of order of components	\
RI	Resilience index	1

SF	Stochastic flexibility index	1
U	Heat transfer coefficient	$W/(m^2 \cdot K)$
T	Temperature	K
TAC	Total Annualized Cost	$\$/y$
ΔT_{lm}	Logarithmic mean temperature difference	K
x_i	Liquid molar fraction	1
y_i	Vapor molar fraction	1

Greek letters	Definition	Unit
α_{ij}	Relative volatility	1
ξ	RCMs integration variable	s
τ_{ij}	NRTL dimensionless interaction parameter	1

Equipment	Typology	K_1	K_2	K_3	A
Heat exchanger	Fixed tubes	4.3247	-0.3030	0.1634	Heat transfer area [m^2]
	Kettle	4.4646	-0.5277	0.3955	Heat transfer area [m^2]
Columns (vessel)	Packed/tray	3.4974	0.4485	0.1074	Volume [m^3]
Trays	Sieved	2.9949	0.4465	0.3961	Cross sectional area [m^2]

Tab. 5.3: Equipment cost in base conditions parameters

B Capital costs estimations

In order to evaluate the investment cost required for the whole system or make any kind of economic consideration and comparison, the cost of every single unit needs to be estimated.

For this purpose the Guthrie-Ulrich-Navarrete correlations described in the next paragraphs will be used [14, 15, 16, 17].

B.1 Purchase equipment cost in base conditions

The purchase equipment cost in base conditions is obtained by means of the following equation:

$$\log_{10}(C_P^0[\$]) = K_1 + K_2 \cdot \log_{10}(A) + K_3 \cdot [\log_{10}(A)]^2 \quad (\text{B.1})$$

where A is the characteristic dimension and the K_i coefficients are relative to the equipment typology (cf. Table 5.3).

The provided coefficients refer to the year 2001 and to a M&S index equal to 1110. In order to update the costs estimation to the year 2016 calculations will refer to a M&S index equal to 1245.2 by means of the correlation:

$$C_{P,2}^0 = \frac{M\&S_2}{M\&S_1} \cdot C_{P,1}^0 \quad (\text{B.2})$$

B.2 Bare module cost

The equipment bare module cost can be calculated according to the following correlation:

$$C_{BM} = C_P^0 \cdot F_{BM} \quad (\text{B.3})$$

Equipment	Typology	B_1	B_2	F_M	F_P
Heat exchanger	Fixed tubes	1.63	1.66	1	1
	Kettle	1.63	1.66	1	$F_{P,Kettle}$
Columns/vessel	/	2.25	1.82	1	1
Pumps	Centrifugal	1.89	1.35	1.5	1

Tab. 5.4: Bare module parameters

where the bare module factor is given by:

$$F_{BM} = B_1 + B_2 \cdot F_M \cdot F_P \quad (\text{B.4})$$

The F_M and F_P factors refers to the actual constructions materials and operating pressure while the B_i coefficients refers to the equipment typology (cf. Table 5.4).

The $F_{P,Kettle}$ value is given by:

$$\log_{10}(F_P) = 0.03881 - 0.11272 \cdot \log_{10}(P) + 0.08183 \cdot [\log_{10}(P)]^2 \quad (\text{B.5})$$

where P is the relative pressure in *bar*.

For column trays bare module cost a slightly different correlation should be used:

$$C_{BM} = N \cdot C_P^0 \cdot F'_{BM} \cdot F_q \quad (\text{B.6})$$

where N is the real trays number, $F_{BM} = 1$ e F_q is given by the correlation:

$$\log_{10}(F_q) = 0.4771 + 0.08561 \cdot \log_{10}(N) - 0.3473 \cdot [\log_{10}(N)]^2 \quad \text{if } N < 20 \quad (\text{B.7})$$

$$F_q = 1 \quad \text{if } N \geq 20 \quad (\text{B.8})$$

References

- [1] Hoch, P.M., Eliceche, A.M., 1996. Flexibility analysis leads to a sizing strategy in distillation columns. *Comput. Chem. Eng.* 20, S139–S144. [https://doi.org/10.1016/0098-1354\(96\)00034-8](https://doi.org/10.1016/0098-1354(96)00034-8)
- [2] Petlyuk F. B., ‘Thermodynamically Optimal Method for Separating Multi-component Mixtures’, *Int. Chem. Eng.* 5 (1965): 555–61.
- [3] Kiss, A. A. Novel applications of dividing-wall column technology to biofuel production processes. *J. Chem. Technol. Biotechnol.* 2013, 88, 1387.
- [4] Okoli, C. O.; Adams, T. A., II Design of dividing wall columns for butanol recovery in a thermochemical biomass to butanol process. *Chem. Eng. Process.* 2015, 95, 302.
- [5] Errico, M., Sanchez-Ramirez, E., Quiroz-Ramirez, J.J., Rong, B.-G., Segovia-Hernandez, J.G., 2017. Multiobjective Optimal Acetone–Butanol–Ethanol Separation Systems Using Liquid–Liquid Extraction-Assisted Divided Wall Columns. *Ind. Eng. Chem. Res.* 56, 11575–11583. <https://doi.org/10.1021/acs.iecr.7b03078>
- [6] Le, Q.-K., Halvorsen, I.J., Pajalic, O., Skogestad, S., 2015. Dividing wall columns for heterogeneous azeotropic distillation. *Chem. Eng. Res. Des., Distillation and Absorption* 99, 111–119. <https://doi.org/10.1016/j.cherd.2015.03.022>
- [7] Ramapriya, G.M., Tawarmalani, M., Agrawal, R., 2018. A systematic method to synthesize all dividing wall columns for n-component separation: Part II. *AIChE J.* 64, 660–672. <https://doi.org/10.1002/aic.15963>
- [8] Swaney, R.E., Grossmann, I.E., 1985. An index for operational flexibility in chemical process design. Part I: Formulation and theory. *AIChE J.* 31, 621–630. <https://doi.org/10.1002/aic.690310412>
- [9] Saboo, A.K., Morari, M., Woodcock, D., 1985. Design of Resilient Processing Plants .8. a Resilience Index for Heat-Exchanger Networks. *Chem. Eng. Sci.* 40, 1553–1565. [https://doi.org/10.1016/0009-2509\(85\)80097-X](https://doi.org/10.1016/0009-2509(85)80097-X)
- [10] Pistikopoulos, E.N., Mazzuchi, T.A., 1990. A Novel Flexibility Analysis Approach for Processes with Stochastic Parameters. *Comput. Chem. Eng.* 14, 991–1000. [https://doi.org/10.1016/0098-1354\(90\)87055-T](https://doi.org/10.1016/0098-1354(90)87055-T)
- [11] Lai, S.M., Hui, C.-W., 2008. Process Flexibility for Multivariable Systems. *Ind. Eng. Chem. Res.* 47, 4170–4183. <https://doi.org/10.1021/ie070183z>
- [12] Lai, S.M., Hui, C.W., 2007. Measurement of Plant Flexibility.

- [13] Di Pretoro, A., Montastruc, L., Manenti, F., Joulia, X., 2019. Flexibility analysis of a distillation column: Indexes comparison and economic assessment. *Comput. Chem. Eng.* 124, 93–108. <https://doi.org/10.1016/j.compchemeng.2019.02.004>
- [14] Guthrie, K.M. , 1969. Capital cost estimating. *Chem. Eng.* 76 (3), 114–142 .
- [15] Guthrie, K.M. , 1974. *Process Plant Estimating, Evaluation, and Control*. Craftsman Book Company of America .
- [16] G. D. Ulrich, 1984, ‘A Guide to Chemical Engineering Process Design and Economics’, Wiley.
- [17] P. F. Navarrete and W. C. Cole, 2001, ‘Planning, Estimating, and Control of Chemical Construction Projects’, 2nd Edition, CRC Press.
- [18] Adams II, T.A., Thatho, T., Le Feuvre, M.C., Swartz, C.L.E., 2018. The Optimal Design of a Distillation System for the Flexible Polygeneration of Dimethyl Ether and Methanol Under Uncertainty. *Front. Energy Res.* 6. <https://doi.org/10.3389/fenrg.2018.00041>
- [19] Benz, S.J., Cerda, J., 1992. Optimal synthesis of flexible heat-integrated distillation trains. *Comput. Chem. Eng., An International Journal of Computer Applications in Chemical Engineering* 16, 753–776. [https://doi.org/10.1016/0098-1354\(92\)80059-I](https://doi.org/10.1016/0098-1354(92)80059-I)
- [20] Caballero, J.A., Grossmann, I.E., 2001. Generalized Disjunctive Programming Model for the Optimal Synthesis of Thermally Linked Distillation Columns. *Ind. Eng. Chem. Res.* 40, 2260–2274. <https://doi.org/10.1021/ie000761a>
- [21] Gabriel, C. L., Crawford, F. M., 1930. Development of the butyl-acetonic fermentation industry. *Ind Eng Chem*, 22,1163–5.
- [22] García, V., Pääkilä, J., Ojamo, H., Muurinen, E., Keiski, R.L., 2011. Challenges in biobutanol production: How to improve the efficiency? *Renew. Sustain. Energy Rev.* 15, 964–980. <https://doi.org/10.1016/j.rser.2010.11.008>
- [23] Dalle Ave, G., Adams, T.A., 2018. Techno-economic comparison of Acetone-Butanol-Ethanol fermentation using various extractants. *Energy Convers. Manag.* 156, 288–300. <https://doi.org/10.1016/j.enconman.2017.11.020>
- [24] Ostwald, W. (1900). Dampfdrucke ternärer Gemische, *Abhandlungen der Mathematisch-Physischen Classe der Königl. Sachs. Gesellsch. der Wissenschaften*, 25, 413–53 (Germ.).

- [25] Schreinemakers, F. A. H., 1901. Dampfdrucke ternärer Gemische. *J. Phys. Chem.*, 36, 413–49 (Germ.).
- [26] Gurikov, Yu. V., 1958. Some Questions Concerning the Structure of Two-Phase Liquid–Vapor Equilibrium Diagrams of Ternary Homogeneous Solutions. *J. Phys. Chem.*, 32, 1980–96 (Rus.).
- [27] Zharov, V. T., 1967. Free Evaporation of Homogeneous Multicomponent Solutions. *J. Phys. Chem.*, 41, 1539–55 (Rus.).
- [28] Zharov, V. T., 1968a. Free Evaporation of Homogeneous Multicomponent Solutions. 2. Four-Component Systems. *J. Phys. Chem.*, 42, 58–70 (Rus.).
- [29] Zharov, V. T., 1968b. Free Evaporation of Homogeneous Multicomponent Solutions. 3. Behavior of Distillation Lines Near Singular Points. *J. Phys. Chem.*, 42, 195–211 (Rus.).
- [30] Zharov, V. T., & Serafimov, L. A., 1975. *Physico-Chemical Foundations of Batch Open Distillation and Distillation*. Leningrad: Khimiya (Rus.).
- [31] Serafimov, L. A., 1969. The Azeotropic Rule and the Classification of Multicomponent Mixtures. 4. N-Component Mixtures. *J. Phys. Chem.*, 43, 981–3 (Rus.).
- [32] Petlyuk, F.B., 2004. *Distillation Theory and its Application to Optimal Design of Separation Units*. Cambridge University Press.
- [33] Renon H., Prausnitz J. M., 1968. "Local Compositions in Thermodynamic Excess Functions for Liquid Mixtures", *AIChE J.*, 14(1), S.135–144.
- [34] Luyben, W.L., 2008. Control of the Heterogeneous Azeotropic n-Butanol/Water Distillation System. *Energy Fuels* 22, 4249–4258. <https://doi.org/10.1021/ef8004064>
- [35] Dortmund Data Bank, www.ddbst.de
- [36] Lee, M.-J., Tsai, L.-H., Hong, G.-B., Lin, H.-M., 2004. Multiphase equilibria for binary and ternary mixtures containing propionic acid, n-butanol, butyl propionate, and water. *Fluid Phase Equilibria* 216, 219–228. <https://doi.org/10.1016/j.fluid.2003.09.009>.
- [37] Kosuge, H., Iwakabe, K., 2005. Estimation of isobaric vapor–liquid–liquid equilibria for partially miscible mixture of ternary system. *Fluid Phase Equilibria* 233, 47–55. <https://doi.org/10.1016/j.fluid.2005.04.010>

Part VI. Process intensification

A Feasible Paths Based Approach for Dividing Wall Column Design Procedure

Alessandro Di Pretoro^{a,b}, Flavia Ciranna^a, Xavier Joulia^b,
Ludovic Montastruc^b, Flavio Manenti^{a*}

^aPolitecnico di Milano, Dipartimento di Chimica, Materiali e Ingegneria Chimica «Giulio Natta», Piazza Leonardo da Vinci 32, 20133 Milano, Italy

^bLaboratoire de Génie Chimique, Université de Toulouse, CNRS/INP/UPS, Toulouse, France

Abstract

Process integration has become the best practice over the last years in separation units design. In particular, distillation trains can be reduced in a single column shell by means of internal separating wall under the name of Dividing Wall Column. This configuration allows on average for a 30% total costs reduction and is more and more popular for multicomponent mixtures purification.

However, the DWC design optimization results much more complex than the one related to a series of standard distillation columns due to the higher number of column sections and side cuts. Moreover, in case of process simulation assisted design, the model convergence is very sensitive with respect to the initial guess, resulting in discontinuities in the sequence of optimization steps.

In this paper an innovative design procedure based on feasible paths is presented for an ABEW mixture separation case study. Starting from a converged design based on shortcut methods, the number of trays can be increased and or removed from the proper column section selected with the help of composition profiles analysis.

This procedure results to be particularly effective for non-ideal mixtures separations, such as the ABEW one, likely to undergo simulation convergence failures. This design algorithm provides an optimized solution really close to the optimal one in a relatively short time and without the need to solve the related MINLP problem.

Highlights:

1. A feasible-path based procedure allows to bypass the simulation failures due to the non-ideal thermodynamics or complex optimization algorithms.
2. The proposed procedure use a shortcut design provided by ProSimPlus[®] process simulator to start the design algorithm avoiding MINLP problem solution or other computationally demanding procedures.
3. Although “non-optimal”, the DWC design obtained via the feasible-paths based procedure fulfills the economic and an environmental expectations with respect to the equivalent distillation train.

Keywords: DWC, feasible paths, optimal design, process integration, biomass.

1 Introduction: DWC design state of the art

Multicomponent mixtures separation processes, whose main exponent is represented by distillation, has always been the leading research field in process engineering during the last century. In particular, during the second half of the 20th century, the need for more energy and cost effective solution moved the research focus from optimal distillation column sequencing to intensified process units design discussed first in the work of Petlyuk (1965)[1].

Beside the simple arrangement of standard distillation columns in series, more complex designs exist such as columns with side draws, side strippers, side rectifiers or prefractionators both with (pseudo-Petlyuk) or without (Petlyuk) its own reboiler and condenser [1, 2]. In particular, the Dividing Wall Column (hereafter DWC) represents the arrangement in a single column shell of the Petlyuk column configuration [3].

Among all those non-standard configurations the DWC was studied in deep since it is the only large-scale process intensification case where both capital and operating costs as well as the required installation space can be drastically reduced [4].

The first DWC theoretical analysis is described in detail always by Petlyuk and reported in his comprehensive work published in 2004[5]. He concludes that the work of this column can be extended to the separation of a different number of components, following these rules:

- In each column section, the key components are the components with extreme volatilities, which can be the lightest or the heaviest. For this reason, a column needs $n \cdot (n - 1)$ sections for the separation of n component, differently from the conventional scheme in which $2 \cdot (n - 1)$ sections are needed.
- Independent on the number of components, only one reboiler and one condenser are enough.
- All the n products can be obtained with high purity.

The DWC unit has a complex structure resulting in a complex design procedure. A first detailed mathematical model and optimization procedure were proposed in 1999 by Dunnebie and Pantelides [6].

However, to perform an optimal DWC design, an adequate model and computer-based simulations are necessary and the latter in particular is not provided by commercial process simulators. For this reason, various alternative DWC decomposed configurations have been proposed in the past years [7].

In general, the very first steps in the DWC column design are the same as a standard column, namely the selection of the column configuration, operating pressure and thermodynamic model. Then a choice between short-cut and detailed models should be made followed by the number of stages/reflux ratio optimization,

the equipment sizing and finally the control system design. During this procedure, to ensure the convergence of the simulation, the design parameters require good initial guesses and some guidance [8].

The following heuristics are proposed by Becker, Godorr, and Kreis [9] in this regard:

- Design a conventional two-column system as a base case, for example, an indirect sequence;
- The DWC total number of stages is set equal to the 80% of the total number of stages required for the indirect configuration: $N_{DWC} = 0.8 \cdot (N_1 + N_2)$;
- The dividing wall is placed in the middle third of the column (33-66%): $Wall = 0.33 \cdot D_{column}$;
- Reboiler and condenser duty is evaluate as the 70% of the overall distillation train duty requirement: $Q_{DWC} = 0.7 \cdot (Q_1 + Q_2)$;
- Use equalized vapor and liquid splits ($r_v = r_l = 0.5$) as initial values.

Finally it is worth remarking that these empirical correlations are only reliable for a first approach.

On the other hand, the rigorous study of the DWC design is more complex and computationally demanding. It depends on the modeling approach and the selected configuration. The first DWC design approach was published by Triantafyllou and Smith [10] based on the Fenske-Underwood-Gilliland-Kirkbride (FUGK) method aimed respectively at the definition of:

- Fenske: minimum number of equilibrium stage;
- Underwood: minimum reflux;
- Gilliland: number of stages corresponding to the chosen operating reflux ratio;
- Kirkbride: feed stage for a given separation.

The FUGK model is nevertheless based on two assumptions: constant relative volatility and constant molar flows.

Another similar short-cut methodology was proposed in 2002 by Muralikrishna et al. [11] and proposes a visual tool to compare the possible configurations in the same plot. This tool can be also employed for the unit optimization by means of simple calculations and it is suitable even for more than three component, such as the ABE/W mixture analyzed in this article case study, as already confirmed by Mueller and Kenig (2002)[12].

In 2001 Amminudin and Smith [13] found out that the Kirkbride equation to find the thermal coupling location brings inaccuracies when switching to the rigorous design. Therefore they proposed an alternative semi-rigorous methodology based on the operation leaf definition already applied to azeotropic distillation sections [14].

More recently, Sotudeh and Shaharaki (2008)[15], proposed a new method neglecting the minimum number of trays calculated by means of the Fenske correlation and exploiting the Underwood equation only.

On the other hand Rangaiah et al. (2009)[16] suggest the use of equilibrium based column simulation (AspenTech HYSYS[®]) to design the DWC unit given the tray efficiency or the HETP value in case of a packed column.

Further developments in the DWC design are related to the need to overcome DWC simulation discontinuities over the operating conditions domain. Gomez-Castro et al. [17, 18] and Vasquez and Castillo (2009)[19] for instance used the application of a genetic algorithm to optimize the DWC design. Genetic algorithms were still used in combination with an optimization method based on radial basis function neural network (RBFNN) by Ge et al. [20].

In 2010 a constrained stochastic multiobjective technique for the optimization of an extractive DWC was employed by Bravo et al. [21].

In 2011 Dejianovic et al. [22] proved that multiple-partition-wall DWC could be a possible optimal solution for industrial applications by means of a four-product aromatic mixture separation case study.

Moreover, not a few authors employed the response surface methodology (RSM) to optimize the DWC design. Among them Sangal et al. (2012)[23] used Box–Behnken design (BBD) under RSM to optimize the DWC structural and operational parameters. Safe et al. (2013)[24] deepened a Reactive Divided Wall Batch distillation column using both RSM and differential evolution to achieve high purity of ethyl acetate.

Further studies about Reactive Divided Wall Column (RDWC) were presented by Wang et al. (2014)[25], who also deepened the Azeotropic DWC (ADWC) unit, and Qian et al. in 2015[26] who investigated a particle swarm optimization (PSO) algorithm for optimal design of RDWC.

Hoffmann et al. in 2016[27] embedded the process simulation into an optimization problem to find feasible design parameters using suitable nonlinear optimization algorithms. Zitzewitz and Fieg in the same year [28] presents an innovative methodology for the model-based process design with superimposed multiobjective optimization.

Jia et al. in 2017[29] studied the optimal design for a three-product DWC using support vector machine (SVM).

In 2017[30] Seihoub et al. improved the short-cut procedure in order to relax some complications related to the design efficiency. The novel method indeed reduces the bothersome and tedious iterations encountered in composition matching

of interlinking stages in rigorous simulation. Furthermore, it provides much more accuracy with respect to the average composition of the interconnecting streams between pre-fractionator and main column than the competing methodologies.

Two consecutive works of Staak et al. (2014)[31] and Lorenz et al. (2018)[32] studied the design of DWC with two-columns and four-columns models starting from a short-cut model and resolving the problem of the initialization of the interlinking streams.

The problem of stream initialization was handled by Nyguen et al. (2016)[33] as well who analyzed the rigorous simulation of a DWC in the ProSimPlus[®] software. The investigated procedure allows for a quick parameters estimation and can provide good initialization values for a rigorous simulation.

A design strategy, whose fundamentals are taken into account in this article as well, was proposed by Pan et al. (2018) [34] who optimized the DWC optimal design minimizing the TAC through the variation of the number of trays in the different sections of the column.

The Petlyuk column control was discussed first by Lestak & Smith in 1993 [35] followed by Wolff and Skogestad in 1995 [36]. Recently a new optimal design and control for an extractive divided wall column with vapor recompression was proposed by Lyuben in 2019 [37].

Li in 2016 [38] presents the rigorous design of the RDWC for MeAc Hydrolysis. In the same year Wang et al. [39] presented a study on a reactive DWC for the separation of azeotropic mixture of acetonitrile/N-propanol. The steady-state design of the two processes was optimized by minimizing the total annual cost (TAC) via a sequential iterative optimization procedure on the diameters of the two columns and reflux ratio of the main one.

Still in 2016 Uwitonze et al. [40] presented a new design methodology for a fully thermally coupled distillation column (simulated as pre-fractionator and main column). This new procedure resulted particularly effective to determine operating conditions and the distillation column structure and was finally validated via rigorous simulations on Aspen HYSYS[®].

Further developments were presented during the last year by Yang et al. who published an innovative study based on an RDWC for the production of TAME in 2017 [41] and presented in 2018 a further DWC optimization strategy using a sensibility analysis and global optimization based on a proposed CPOM model [42].

A recent research work about DWC optimal design by Waltermann et al. (2019)[43] suggests to solve the optimization problem as a series of relaxed (SR) MILNP problems in which each equilibrium stage is based on the rigorous MESH equations. Part of the procedure presented in this paper has been inspired by those authors and will be further discussed in the following chapters.

The very last available work about DWC optimal design was published in 2020 by Li et al. [44] and presents a high efficiency industrial-scale DWC accounting

for the heat transfer across the wall.

The purpose of this DWC related literature walkthrough is to highlight the complexities during its design phase and the corresponding solution alternatives. All those results represented indeed the starting point of our research and part of the design strategies proposed so far have been employed in this research as well.

Further details about the DWC simulation layout is discussed in section 3 after the case study introduction.

2 The ABE mixture case study

Over the last years, biofuels have seen renewed attention both because of the increasing price of fossil fuels and because of the need to reduce CO_2 emissions. The International Energy Agency annual report [45] estimates them to satisfy around 30% of energy consumption demand in transport by 2060. Their role is particularly important in sectors which are difficult to decarbonise, such as aviation, shipping and other long-haul transport.

In particular bio-butanol is a possible substitute of bio-ethanol thanks to its higher energy density, lower volatility, and lower hygroscopicity. Bio-butanol can be produced from different cellulosic biomasses and can be used as well for further processing of advanced biofuels such as butyl levulinate [46]. It is already employed both as fuel additive and as pure fuel instead of standard gasoline because, differently from ethanol, it can be directly and efficiently used in gasoline engines. Furthermore, it can be also shipped and distributed through existing pipelines and filling stations [47].

However, the major limit for an industrial-scale production of bio-butanol is the high separation cost due to the presence of other fermentation products (especially water) and to its low final concentration in the ABE fermentation broth [48]. Therefore both process and cost efficient methods for separation of the ABE mixture from the broth (mainly water) and subsequent separation of the ABE mixture products themselves are required in order to scale it up at an industrial scale. That's why the employment of a DWC column is particularly suitable for this kind of application as already discussed by several authors [49, 50].

Moreover, the non-ideal thermodynamic behaviour of this mixtures meets the need of an optimization algorithm able to overcome the eventual process simulation convergence failures at the design phase.

The ABE/W separation example proposed by Di Pretoro et al. (2020)[51], for which the indirect configuration design already exists, was selected for this study. It refers to the product stream downstream a preliminary dewatering section whose properties and separation specifications are listed in Tables 6.1 and 6.2 respectively and the corresponding distillation train and DWC layouts are shown in Figure 6.1.

The selected activity model is the Non-Random Two Liquids model [52] since

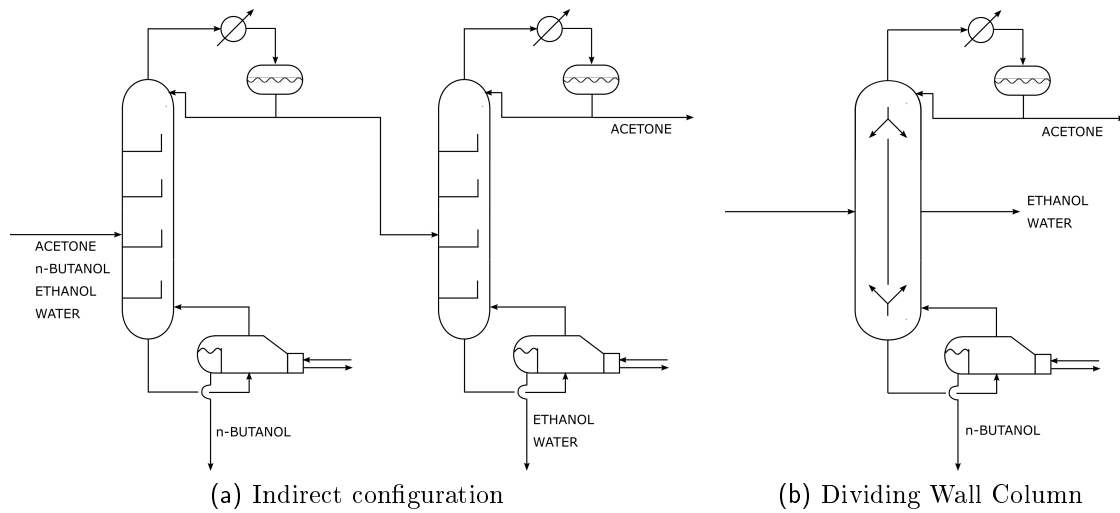


Fig. 6.1: Distillation train vs DWC

Component\Property	Value	Unit
Acetone	12.030	<i>mol/s</i>
n-Butanol	61.328	<i>mol/s</i>
Ethanol	3.839	<i>mol/s</i>
Water	12.428	<i>mol/s</i>
Pressure	101.325	<i>kPa</i>
Temperature	361.26	<i>K</i>

Tab. 6.1: Feed properties

Specification	Stream	Value	Unit
Acetone purity	Distillate	0.995	<i>kg/kg</i>
Acetone recovery	Distillate	0.985	<i>kg/kg</i>
n-Butanol purity	Bottom	0.99	<i>kg/kg</i>
n-Butanol recovery	Bottom	0.9604	<i>kg/kg</i>

Tab. 6.2: Process specifications

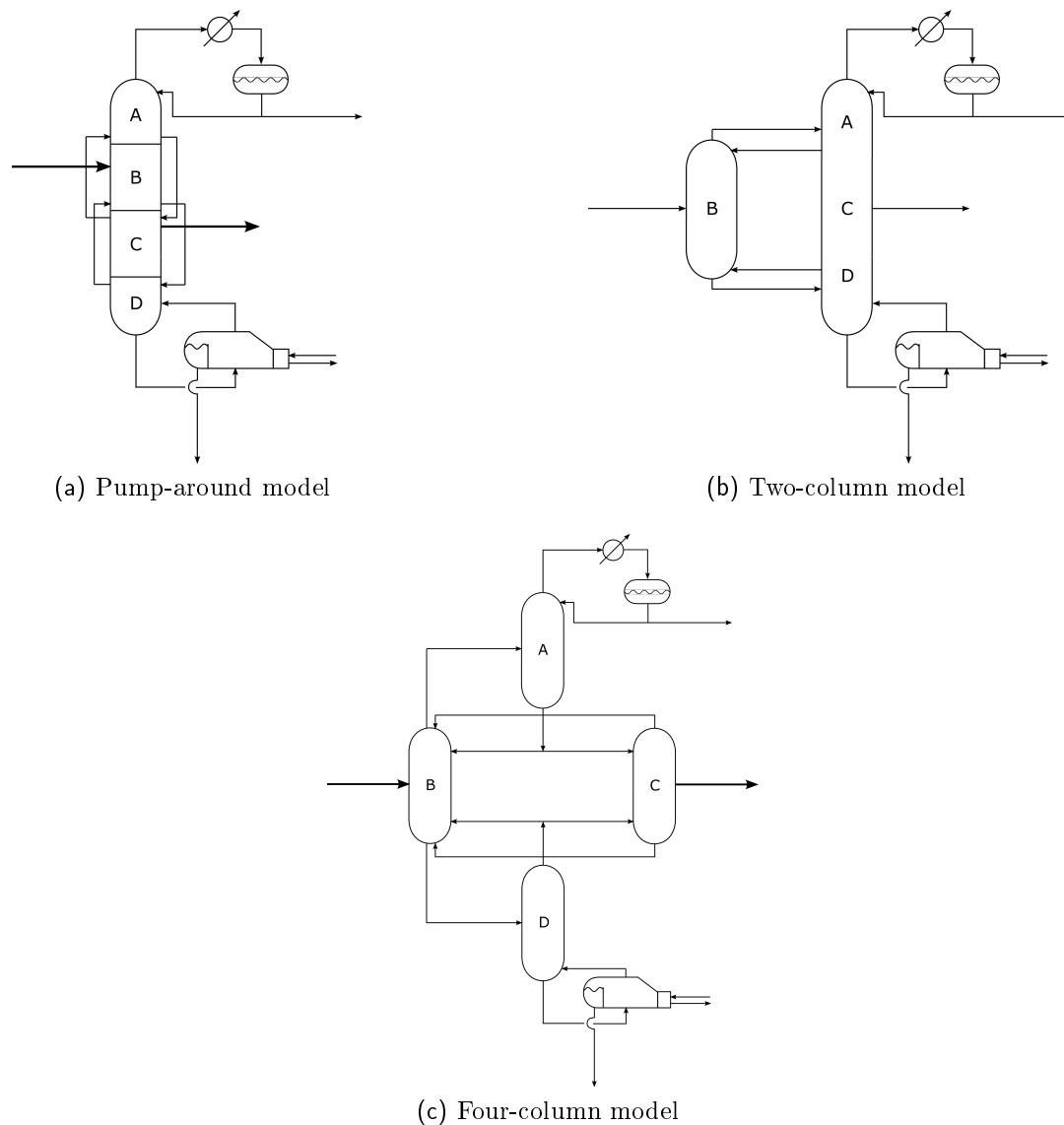


Fig. 6.2: DWC equivalent configurations

it is able to correctly describe the mixture VLE and LLE as already discussed by several authors [49, 50, 51, 52, 53, 54, 55]. For further details about NRTL model and binary interactions parameters please refer to Appendix B.

The separation feasible space for the ABE/W mixture with these process specifications is already discussed by Di Pretoro et al.(2020)[53]. Thus, the feed composition was already selected in order to avoid simulation failures due to thermodynamic feasibility related limitations.

Further details about the DWC unit are presented in the following section.

3 DWC equivalent layouts

Available process simulators do not include dedicated modules to model the DWC unit. However, alternative and equivalent configurations can be built by mod-

ifying and combining one or more distillation columns with multiple feeds and intermediate withdrawals.

Different DWC equivalent layouts with different features can then be found in literature. The most common alternatives are shown in Figure 6.2. The pump-around model (cf Figure 6.2a) is based on the vertical connection of the four column sections by means of side streams similarly to a distillation column with pump-arounds. It is easier to initialize and computationally simple but it can also lead to convergence issues since, in practice, it has four internal recycles. The four-column model (cf Figure 6.2c) results to better cope with parameters modification but the presence of so many interlinking streams cause the initialization much more difficult and its convergence is slow [56]. Thus, after several attempts, the Petlyuk column configuration (cf Figure 6.2b) resulted to be the most suitable for the case study under analysis. Just two streams should be initialized and the two columns are sequentially and iteratively solved until convergence. In any case the procedure presented in this publication can be employed independently on the selected model.

As discussed in the previous chapter, on the one hand 4 specifications are present but, on the other hand, the DWC has 5 degrees of freedom, namely the three main column outlet streams, vapor and liquid splits [35]. The vapor split control is highly impractical [3] and it is usually considered as design variable. The cost of this operability compromise is a significant energy loss in case of external disturbances that would be much lower with a variable vapor split [57]. In this study the possibility to control the vapor split will be taken into account when removing or adding equilibrium stages to compensate the reflux ratio variation and minimize the energy consumption.

The simulations were performed both with ProSimPlus[®] process simulator, that provides the DWC shortcut module as well as interlinking streams initialization, and with SimCentral[®] process simulator by AVEVA to modify the column design.

4 DWC design algorithm

The main goal of this study is to propose an alternative “quasi-optimal” design procedure for the DWC design able to simplify the required calculations by means of a feasible path based algorithm.

Among the cited literature several authors propose effective but computationally demanding procedures requiring the solution of a complex MINLP problem based on a superstructure [6, 43], the use of stochastic optimization methodologies [49] or genetic algorithms [18, 19, 20].

Moreover, while iterating, in case of highly non-ideal thermodynamics in particular, some simulations required to assess the process design and the Total Annualized Cost (TAC) could not converge. In case of non-converged iterations no

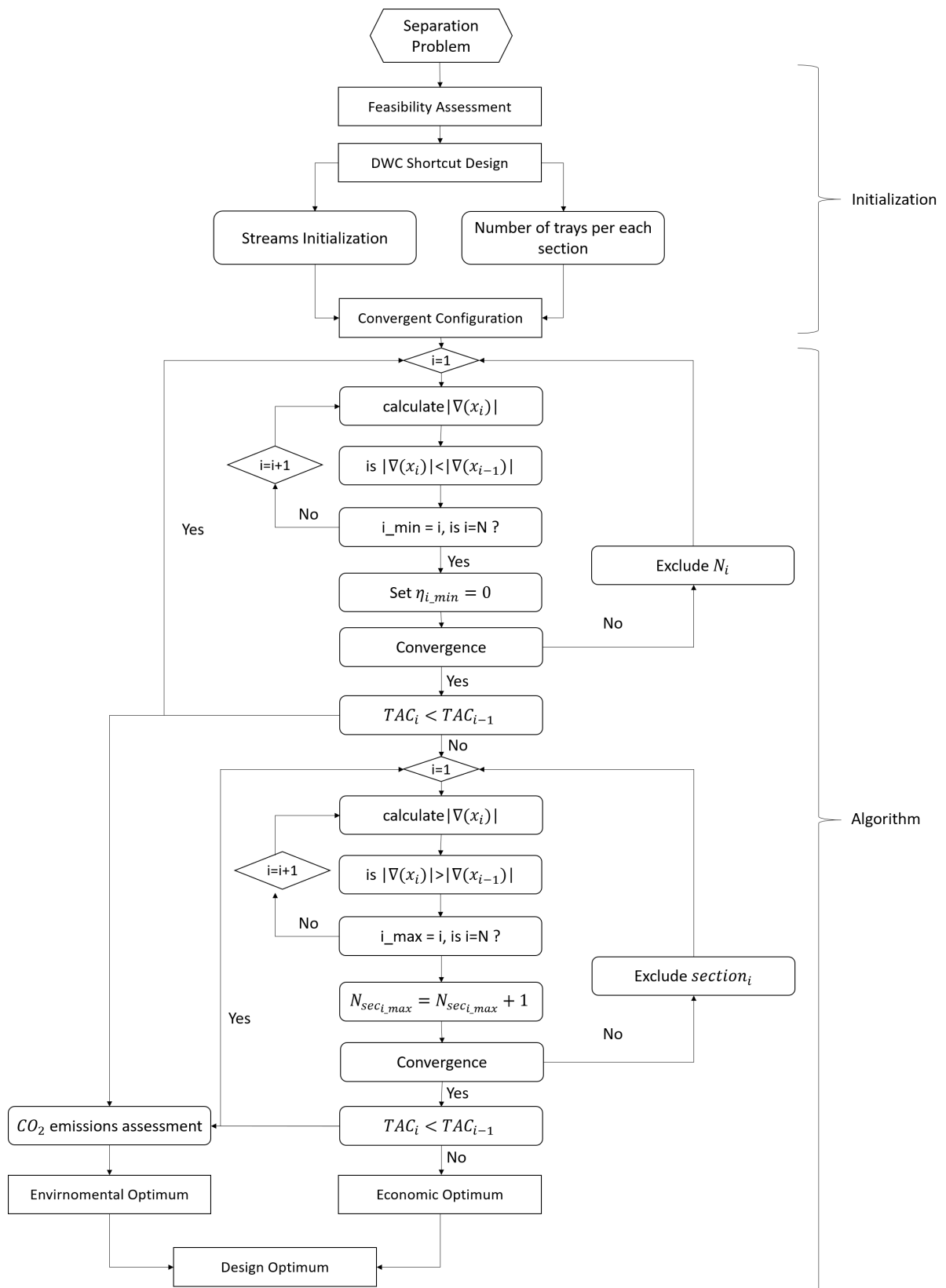


Fig. 6.3: DWC design algorithm

information can be obtained about the failure reason.

The main idea behind the algorithm presented in this paper is to maximize and take advantage of the converged steps in order to approach the DWC optimal configuration with a path made of all feasible design alternatives.

The design procedure is shown in Figure 6.3. The first part of the algorithm aims at finding a feasible DWC configuration to start the design procedure.

The feasibility assessment is mainly based on thermodynamic eventual boundaries related to the mixture singularities as discussed by Di Pretoro et al. (2020)[53] for the ABE/W mixture. The most important step during this phase is the design of a converging DWC layout even though non-optimal. This step is performed by means of the DWC shortcut module provided by ProSimPlus[®] process simulator whose model equations are described in detail by Nguyen et al. (2016)[33]. The module output refers to the two-column model (cf Figure 6.2b) and, beside the number of trays for each column section, it provides reliable estimation for the initialization streams composition and flowrates (i.e. vapor and liquid splits).

After that, the obtained configuration is simulated with SimCentral[®] process simulator as previously mentioned. In particular, it can be observed that the provided design is usually oversized since the purpose of the DWC shortcut module is the convergence and not the optimality.

Starting from this configuration the first loop can be implemented. The equilibrium stage corresponding to the smallest concentration gradient $|\nabla x_i|$ is detected and its efficiency is set to zero. Note that the stage is not removed in order to avoid the solver restart while the simulator takes advantage of the relaxed profile adaptation to the new efficiency value enhancing the simulation convergence. If the simulation doesn't converge then the tray efficiency is restored and the following tray with the lowest concentration gradient undergoes the same procedure. If the simulation converges the TAC is calculated according to the correlations provided by Guthrie [58, 59], Ulrich [60] and Navarrete & Cole [61] both for OPEX and CAPEX estimation described in detail in Appendix C. The resulting value is then compared to the one related to the previous design configuration and the procedure is repeated until the minimum is found.

Before moving forward, it is worth highlighting that the reasons behind the missing convergence are not further investigated in this study since it is not the purpose of the research. However, in case of no convergence issues, the algorithm do not require any modifications in order to be exploited for the DWC design providing a result that is equally valid.

Beside the economic assessment, the process environmental impact is estimated as well. The Global Warming Potential indicator was used since it was proved to have the most adverse effect on the sustainability profile of distillation operations [62]. The CO_2 emissions were then calculated according to the methodology used by Gadalla et al. (2006)[63] mainly accounting for the reboiler heat duty since it provides the most important contribution to the GWP as discussed by several

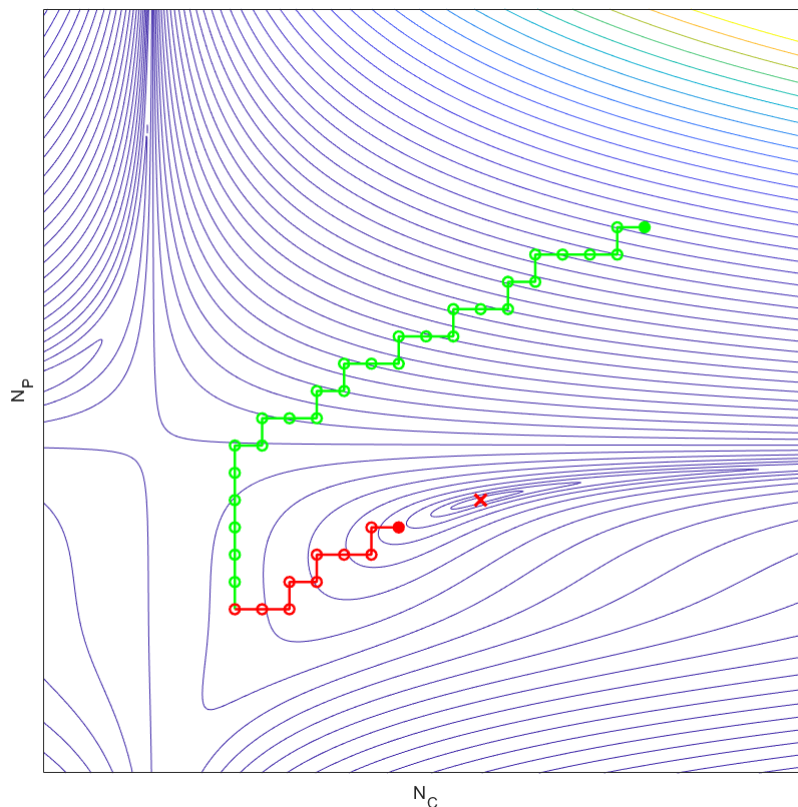


Fig. 6.4: TAC minimum search domain and algorithm path

authors (cf Appendix D for details about correlations). Those data will be used in the very last step of the design procedure in order to assess the best compromise between economic and sustainability optima.

Once no lower TAC can be obtained by reducing the number of stages, the backward algorithm is performed by increasing N in the section where the trays with the most important concentration variation is present in order to check if a column configuration with a higher number of stages could be more convenient. In particular, if any tray whose efficiency was previously set equal to zero is present in this section, its value is now restored to 1 instead of adding additional trays in order to ease the solver convergence.

The fact that a $N + 1$ configuration was already taken into account doesn't imply that it was the best design solution related to that number of equilibrium stages. The previous stage indeed was removed from the flattest concentration profile section while the additional stage is now added in the section with the most relevant concentration variation.

This loop is analogous to the previous one and, once the minimum TAC condition is met, the result thus obtained is analyzed from a sustainability point of view. If the corresponding environmental impact doesn't exceed the emissions constraints then it is confirmed as the final design. Otherwise the cheapest design respecting the environmental limitations is adopted.

From a mathematical point of view this feasible paths based methodology is

worth a better discussion. The analysis of feasible paths follows a well-established procedure and is widely used in computer science and software programming to optimize the execution time and detect the possible reasons of code failure [67, 68]. By definition a control flow path through a procedure is feasible if there is an assignment to input values, (i.e. global variables and parameters) which drives execution down the path [67] that in our case is represented by the simulation convergence.

In order to have a visualization tool to better describe the algorithm behaviour, we can refer to a generic sample plot as the one represented in Figure 6.4.

Since the DWC has six different sections a 6D domain should be used to thoroughly represent the minimum search space. However, in order to ease the algorithm understanding, the six different sections have been condensed into pre-fractionator N_P and main column N_C total number of equilibrium stages that have been used as independent variables for this example to allow a geometrical visualization.

Moreover, it should be observed that the DWC column has 5 degrees of freedom and for this problem 4 equality constraints should be satisfied and the vapor split R_V can be either considered as a fixed design variable or it can be managed in order to minimize the energy consumption as discussed by several authors [36, 57] and as performed in this study. Therefore, for a given design, the system variables are univocally determined.

The initial point given by the shortcut design configuration is represented by the green dot at the top right. The first part of the algorithm (green path) moves towards a lower total number of equilibrium stages, i.e. bottom-left, decreasing the TAC at each step according to the converged configurations.

Once the TAC cannot be further reduced by decreasing the number of stages or no simulation converges with a smaller column, the second part of the algorithm starts moving backwards (i.e. top-right) in order to reduce the Total Annualized Costs by increasing the number of stages. As we can notice, for the same total number of stages the forward and backward paths can both cross each other or not according to the section where the stages are removed or added.

When no further TAC reduction can be obtained by the second part of the algorithm or no convergence can be found, the algorithm stops and the red circle in Figure 6.4 represents the solution obtained.

The goal of this algorithm is then to move towards the descent direction, even if not the steepest one, with a fixed length step passing through all feasible simulations.

On the one hand, the algorithm thus defined cannot ensure that the final point actually corresponds to the optimum we are looking for since, among the algorithm stopping criteria, simulation convergence plays the main role and it is strictly affected by the reliability of the initial point.

On the other hand, it can be nevertheless checked if the obtained solutions

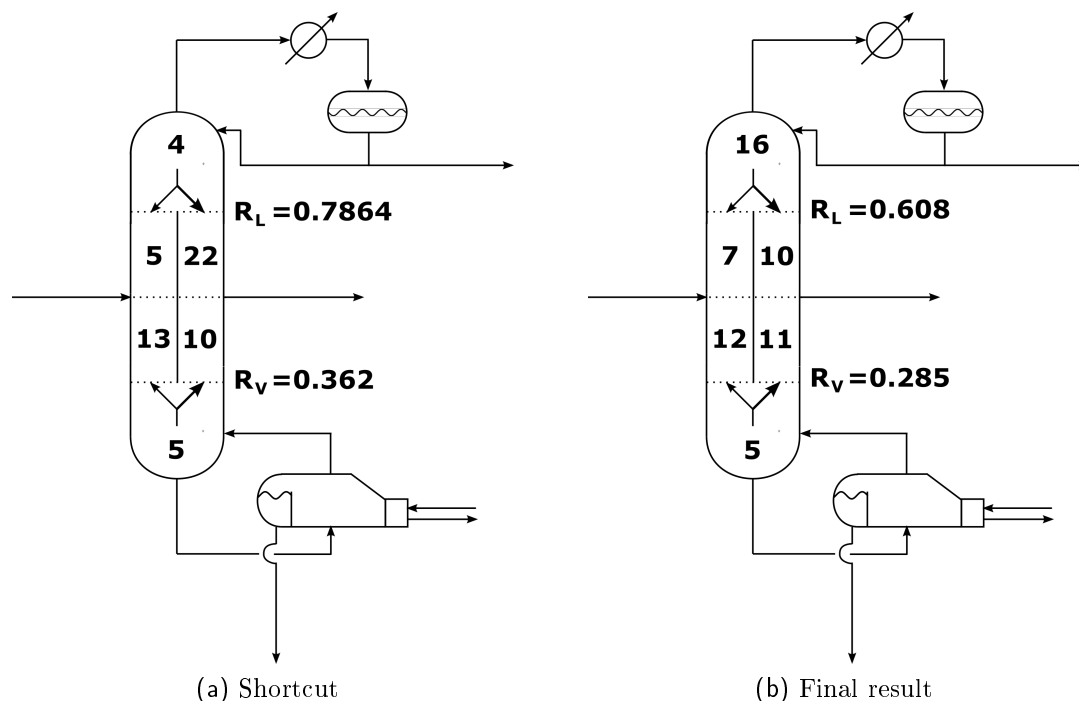


Fig. 6.5: ABE case study configurations

satisfies a given set of requirements such as a (substantially) higher profitability and lower environmental impact of the Dividing Wall Column with respect to the equivalent distillation train configuration.

The outcome of the algorithm application to the selected case studies is presented and commented in the following chapter.

5 Results

The design procedure described in the previous chapter has been applied to the ABE case study. The initial configuration provided by the shortcut module in ProSimPlus[®] process simulator is shown in Figure 6.5a. It accounts for an overall number of stages equal to 41 with the right side of the wall considerably bigger than the left one.

The final configuration has 42 stages as shown in Figure 6.5b. Twelve trays from the top-right side of the wall have been moved to the top section of the column resulting in a more balanced number of trays in the central section that eases the unit construction as well. The left side of the wall results in negligible modifications while the bottom section remains completely unchanged.

The first part of the algorithm led to a minimized configuration of 30 number of stages (4; 5:10 ; 12:11 ; 5) below which no convergence has been obtained. Then the number of trays has been increased backward until the final solution is obtained. The TAC trend as a function of the number of stages is plotted in Figure 6.6 in the proximity of the solution. In particular, the red descending

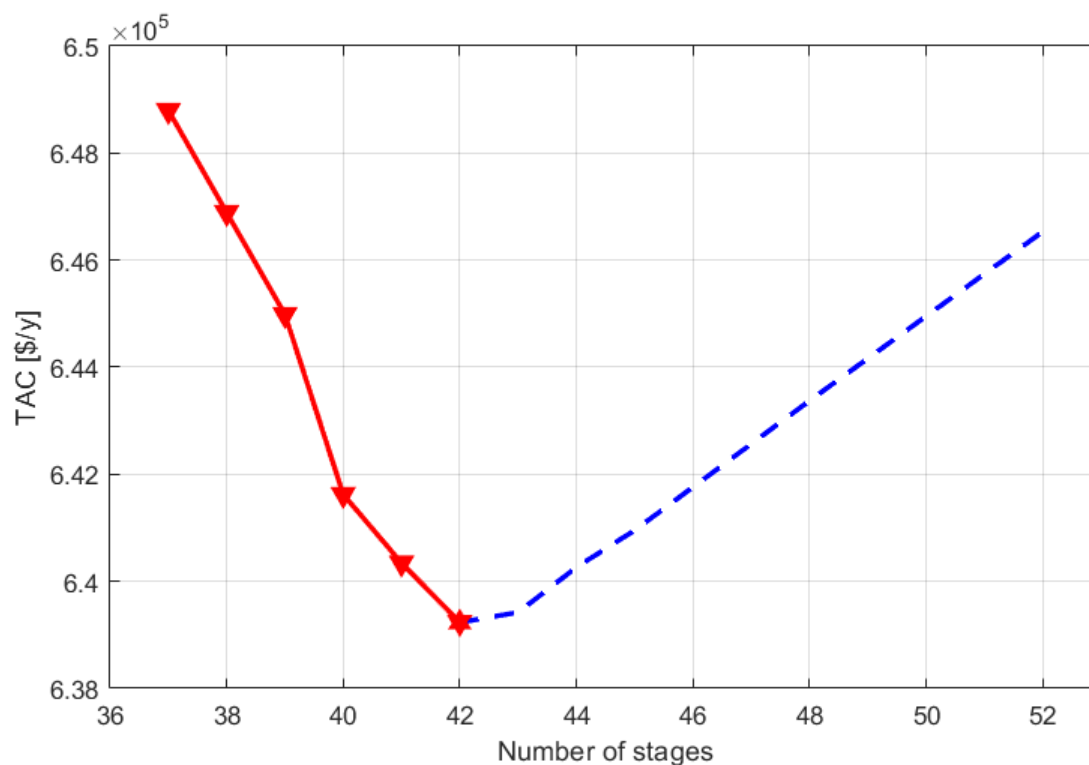


Fig. 6.6: TAC vs Number of stages

trend represents the last part of the design algorithm backward path until the final solution (red star) while the blue dashed line corresponds to the eventual iterations in case further equilibrium stages were added to the DWC section with the most relevant concentration gradient.

As it can be noticed, the TAC value over the considered range varies in a span of 10,000 \$/year. However, a minimum can be detected in correspondence of the configuration previously described.

Furthermore, the indirect distillation train has been compared to the obtained DWC unit. Figure 6.7a shows that both configurations are energy demanding and that external duties represent the most consistent contribution to the total costs. While investment costs are only slightly lower, the operating expenses difference between the two configurations is appreciable and an overall 29.8% saving (that corresponds to about 950 kW) can be obtained thanks to the process integration in line with other research studies [3, 64, 65, 66].

Analogous remarks can be made from an environmental point of view as plotted in Figure 6.7b. The two main impact items are the pump electricity and the reboiler heat duty. However the first one contributes to about the 5% only with respect to the overall CO_2 emissions while the heat duty represents the main source for both configurations. Even in this case the emissions can be reduced by 32.9% taking advantage of the lower total external duty required by the dividing wall column with respect to the distillation train.

An additional aspect not to be neglected is the required installation space

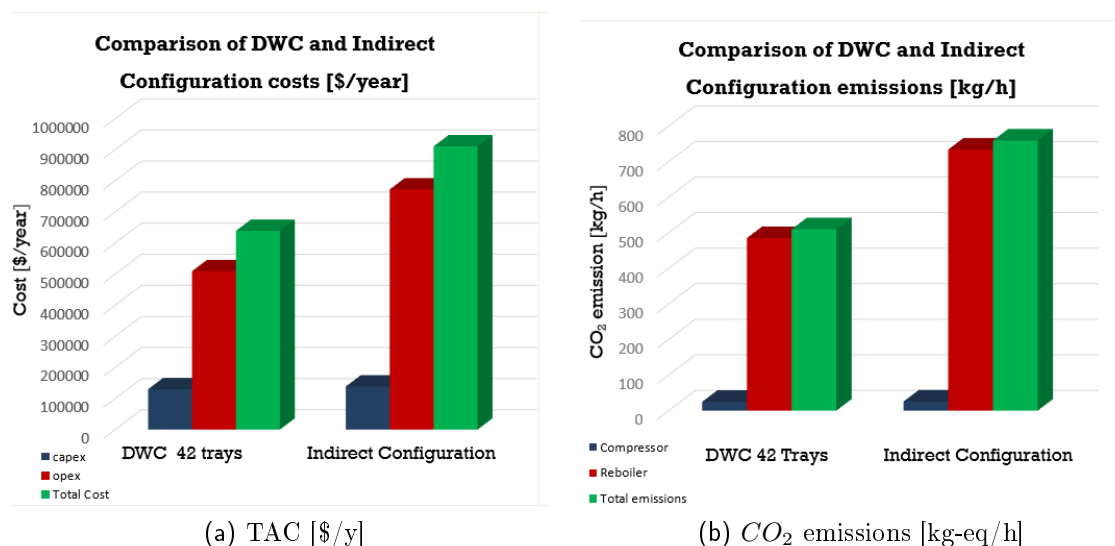


Fig. 6.7: Indirect configuration vs DWC

reduction as well as the lower instrumentation needed with respect to two columns (or three in case of mid-split configuration).

In conclusion, although the DWC design obtained via the proposed feasible-path based procedure cannot be rigorously defined “optimal”, it fulfills the expected savings both in terms of costs and environmental impact with respect to the optimal series of distillation column aimed at the same separation process.

6 Conclusions

The goal of this study is to outline a DWC design algorithm alternative to the rigorous but more computationally demanding ones proposed in literature based on MINLP, genetic algorithm or stochastic optimization.

The algorithm has the goal to elude failures related to non-converging simulations due to the complexity of the unit and, sometimes, of the mixture thermodynamics. With a sequence of feasible design solutions it approaches the “good configurations” region and finds a suitable solution for the separation problem.

The algorithm initial point as well as the interlinking streams initialization are provided by shortcut correlations implemented in a commercial package whose main goal is to outline a converging configuration not too far from the optimal one.

The decision criteria to add or remove equilibrium stages are based on the concentration profile analysis.

In order to validate the proposed methodology an ABE mixture separation case study has been set up and the results discussed and commented. The final design configuration differs mainly from the shortcut one in the top section of the column. A similar total number of trays is found but differently distributed. In particular a comparable size for the left and right sides of the wall was obtained.

The outcome obtained without a rigorous optimization nevertheless satisfies the expected features of a DWC configuration with respect to the equivalent distillation train in terms of costs and emissions validating the proposed procedure. Moreover, it has required a relatively small number of iterations and a short computational time.

Finally it is important to highlight the main limitations of such a design strategy:

- The final solution and the amount of iterations required to achieve it are strictly related to the starting design, i.e. to the reliability of the shortcut methodologies used for the separation problem under analysis.
- Since the algorithm doesn't account for the entire set of possible configurations, there are several combination of stages per section that will never be considered. The consequence is that the final design is highly influenced by the followed path.

The solution provided by the algorithm can be used then both as the design choice or, whether the optimal solution for the DWC design problem is strictly required, as a first design estimation providing higher accuracy than the shortcut correlations with a only slightly higher computational efforts.

As already discussed, the algorithm might stop not only because no lower TAC can be obtained but also because all the simulations related to the possible design alternatives fail. In case the process requirements (higher profitability, sustainability etc.) were not met, further research works could target an algorithm reinitialization strategy in order to make the entire "optimization" procedure more robust and enhance the quality of its final result.

A List of acronyms and symbols

Symbol	Definition	Unit
A	Characteristic dimension	m^2
A	Heat transfer surface area	m^2
ABE/W	Acetone-Butanol-Ethanol/Water	1
$ADWC$	Azeotropic Divided Wall Column	1
BBD	Box-Behnken design	1
$C\%$	Carbon content percentage	%
C_{ij}^n	Excess Gibbs energy coefficients	$J/(mol \cdot K^n)$
C_{BM}	Equipment bare module cost	\$
C_p^0	Purchase equipment cost in base conditions	\$
$CAPEX$	CAPital EXpenses	\$/y
$CPOM$	Complete the Optimization Method	1
D_{column}	Diameter of the column	m
DWC	Divided Wall Column	1
F_{BM}	Bare module factor	1
F_M	Material factor	1
F_P	Pressure factor	1
F_q	Column trays factor	1
$FUGK$	Fenske-Underwood-Gilliland-Kirkbride	1
g_{ij}	NRTL excess Gibbs energy	J/mol
GWP	Global Warming Potential	$kgCO_2 - eq$
h_{steam}	Steam enthalpy	kJ/kg
$HETP$	Height equivalent of theoretical plate	1
LLE	Liquid-Liquid equilibrium	1
$M\&S$	Marshall & Swift cost index	1
$MILNP$	Mixed Integer Non Linear Programming	1
N	Column equilibrium stages	1
N_C	Number of the main column stages	1
N_{DWC}	Number of divided wall column stages	1
N_{min}	Minimum number of equilibrium stages	1

N_P	Number of the prefractionator stages	1
NHV	Net Heating Value	kJ/kg
$NRTL$	Non-Random Two Liquid model	1
$OPEX$	OPERating EXPenses	$\$/y$
P	Pressure	bar
PSO	Particle Swarm Optimization	1
Q	Heat duty	kJ/h
Q_{DWC}	Heat duty of the divided wall column	kJ/h
Q_{reb}	Reboiler heat duty	kJ/h
Q_{fuel}	Fuel heat duty	kJ/h
R_L	Liquid split ratio	1
R_V	Vapor split ratio	1
R	Ideal gas constant	$J/K/mol$
$RBFNN$	Radial Basis Function Neural Network	1
$RDWC$	Reactive divided wall column	1
RSM	Response Surface Methodology	1
SR	Series of Relaxed	1
SVM	Support Vector Machine	1
T	Temperature	K
TAC	Total Annualized Cost	1
$TAME$	Tert-Amyl Methyl Ether	1
VLE	Vapor-Liquid equilibrium	1
x_i	Liquid phase composition	1

Greek letters	Definition	Unit
α	$CO_2 - to - C$ molar mass ratio	1
α_{ij}	Non-randomness parameter	1
γ_i	Activity coefficient	1
η_i	Efficiency	1
λ_{steam}	Steam latent heat	kJ/kg
τ_{ij}	NRTL dimensionless interaction parameter	1

Component 1	Component 1	C_{ij}^0	C_{ji}^0	C_{ij}^1	C_{ji}^1	$\alpha_{ij}^0 = \alpha_{ji}^0$
Water	Acetone	1197.410	631.046	/	/	0.5343
Water	Ethanol	1616.810	-635.560	2.018	0.991	0.1448
Water	1-Butanol	2622.650	420.557	/	/	0.4269
Acetone	Ethanol	36.2965	434.823	/	/	0.2987
Acetone	1-Butanol	-578.135	876.239	/	/	0.2963
Ethanol	1-Butanol	-717.723	1005.13	/	/	0.2952

Tab. 6.4: NRTL Binary interaction parameters

B Thermodynamic model

As already anticipated, several authors [49, 50, 51, 52, 53, 54, 55] state that the Non-Random Two Liquids (NRTL) [52] is the most suitable activity model to describe the ABE/W mixture behaviour. It is able to describe both liquid and vapor phases non-idealities such as azeotropes and liquid immiscibility.

The activity coefficient for the species i in a mixture of n components is given by:

$$\ln(\gamma_i) = \frac{\sum_{j=1}^n x_j \cdot \tau_{ji} \cdot G_{ji}}{\sum_{k=1}^n x_k \cdot G_{ki}} + \sum_{j=1}^n \frac{x_j \cdot G_{ij}}{\sum_{k=1}^n x_k \cdot G_{kj}} \cdot \left(\tau_{ij} - \frac{\sum_{m=1}^n x_m \cdot \tau_{mj} \cdot G_{mj}}{\sum_{k=1}^n x_k \cdot G_{kj}} \right) \quad (\text{B.1})$$

where:

$$\ln(G_{ij}) = -\alpha_{ij} \cdot \tau_{ij} \quad (\text{B.2})$$

$$\alpha_{ij} = \alpha_{ij}^0 + \alpha_{ij}^1 \cdot T \quad (\text{B.3})$$

$$\tau_{ij} = \frac{\Delta g_{ij}}{R \cdot T} \quad (\text{B.4})$$

$$\Delta g_{ij} = g_{ij} - g_{jj} = C_{ij}^0 + C_{ij}^1 \cdot T \quad (\text{B.5})$$

where α_{ij} is called non-randomness parameter and τ_{ij} is called dimensionless interaction parameter.

Binary interaction parameters provided by process simulators are not compliant with each other and they're not always able to correctly predict the equilibrium compositions in proximity of the singularity points. Simulis[®] Thermodynamics database resulted the most reliable for water-alcohols interactions but some parameters for binary interaction coefficients among inorganic compounds are not available and needed to be adjusted in order to meet the experimental data. The binary interaction coefficients values used in this research study, for a Δg expressed in kcal/kmol, are listed in Table 6.4.

Equipment	Typology	K_1	K_2	K_3	A
Heat exchanger	Fixed tubes	4.3247	-0.3030	0.1634	Heat transfer area [m^2]
	Kettle	4.4646	-0.5277	0.3955	Heat transfer area [m^2]
Columns (vessel)	Packed/tray	3.4974	0.4485	0.1074	Volume [m^3]
Trays	Sieved	2.9949	0.4465	0.3961	Cross sectional area [m^2]

Tab. 6.5: Equipment cost in base conditions parameters

C Capital costs estimations

In order to evaluate the investment required to build up a process plant or for whatever economic analysis and comparison related to process equipment, the cost of every single unit needs to be estimated.

For this purpose the Guthrie-Ulrich-Navarrete correlations described in the following paragraphs have been employed [58, 59, 60, 61].

C.1 Purchase equipment cost in base conditions

The purchase equipment cost in base conditions is obtained by means of the following equation:

$$\log_{10}(C_P^0[\$]) = K_1 + K_2 \cdot \log_{10}(A) + K_3 \cdot [\log_{10}(A)]^2 \quad (\text{C.1})$$

where A is the unit characteristic dimension and the K_i coefficients are relative to the equipment typology (cf. Table 6.5).

The provided coefficients refer to a Marshall & Swift equipment cost index equal to 1110. In order to update the cost estimations, a M&S index equal to 1638.2 will be used in order to refer the calculations to the year 2018 by means of the correlation:

$$C_{P,2}^0 = \frac{M\&S_2}{M\&S_1} \cdot C_{P,1}^0 \quad (\text{C.2})$$

C.2 Bare module cost

The equipment bare module cost can be calculated according to the following correlation:

$$C_{BM} = C_P^0 \cdot F_{BM} \quad (\text{C.3})$$

Equipment	Typology	B_1	B_2	F_M	F_P
Heat exchanger	Fixed tubes	1.63	1.66	1	1
	Kettle	1.63	1.66	1	$F_{P,Kettle}$
Columns/vessel	/	2.25	1.82	1	1
Pumps	Centrifugal	1.89	1.35	1.5	1

Tab. 6.6: Bare module parameters

where the bare module factor is given by:

$$F_{BM} = B_1 + B_2 \cdot F_M \cdot F_P \quad (C.4)$$

The F_M and F_P factors refers to the actual constructions materials and operating pressure while the B_i coefficients refers to the equipment typology (cf. Table 6.6).

The $F_{P,Kettle}$ value is given by:

$$\log_{10}(F_P) = 0.03881 - 0.11272 \cdot \log_{10}(P) + 0.08183 \cdot [\log_{10}(P)]^2 \quad (C.5)$$

where P is the relative pressure in *bar*.

For column trays bare module cost a slightly different correlation should be used:

$$C_{BM} = N \cdot C_P^0 \cdot F'_{BM} \cdot F_q \quad (C.6)$$

where N is the real trays number, $F_{BM} = 1$ e F_q is given by:

$$\begin{cases} \log_{10}(F_q) = 0.4771 + 0.08561 \cdot \log_{10}(N) - 0.3473 \cdot [\log_{10}(N)]^2 & \text{if } N < 20 \\ F_q = 1 & \text{if } N \geq 20 \end{cases} \quad (C.7)$$

D Global Warming Potential calculations

The indicator associated to the greenhouse effect impact category is the Global Warming Potential whose unit is $kg\ CO_2 - eq$ per unit.

$$CO_2 = \left(\frac{Q_{fuel}}{NHV} \right) \cdot \left(\frac{C\%}{100} \right) \cdot \alpha \quad (D.1)$$

where:

- CO_2 is the value of equivalent carbon dioxide emission in $[kg/h]$;
- NHV is the Net Heating Value and it is equal to $51,600\ kJ/kg$ for Natural Gas;
- $C\%$ is the carbon content in percentage and it is equal to 75.4 for Natural Gas;
- α is the CO_2 -to- C molar mass ratio and it is equal to 3.67 .

Finally the term Q_{fuel} identifying the combustion energy required to vaporize the desired amount of steam can be estimated as:

$$Q_{fuel} = \left(\frac{Q_{reb}}{\lambda_{steam}} \right) \cdot (h_{steam} - 419) \cdot \left(\frac{T_F - T_0}{T_F - T_S} \right) \quad (D.2)$$

where:

- Q_{reb} is the reboiler duty in kJ/h ;
- λ_{steam} is the steam latent heat in kJ/kg ;
- h_{steam} is the steam enthalpy in kJ/kg ;
- 419 is the water enthalpy at $100^\circ C$ in kJ/kg ;
- T_F is the flame temperature in K ;
- T_S is the stack temperature in K ;
- T_0 is the standard temperature in K .

On the other hand, the equivalent carbon dioxide emissions for pumping were estimated by multiplying the power needed by each pump and the amount of CO_2 per each GJ of electrical energy [63].

References

- [1] Petlyuk, F.B., 1965. Thermodynamically Optimal Method for Separating Multicomponent Mixtures. *Int. Chem. Eng.* 5, 555–561
- [2] Glinos, K., Malone, M.F., 1988. Optimality regions for complex column alternatives in distillation systems. *Chemical Engineering Research and Design* 66, 229–240
- [3] Kiss, A.A., 2013. *Advanced Distillation Technologies: Design, Control and Applications*, 1 edition. ed. Wiley, Chichester, West Sussex, United Kingdom
- [4] Schultz, M.A., Stewart, D.G., Harris, J.M., Rosenblum, S.P., Shakur, M.S., O'Brien, D.E., 2002. Reduce costs with dividing-wall columns. *Chemical Engineering Progress* 98, 64–71
- [5] Petlyuk, F.B., 2004. *Distillation Theory and its Application to Optimal Design of Separation Units*. Cambridge University Press
- [6] Dünnebier, G., Pantelides, C.C., 1999. Optimal Design of Thermally Coupled Distillation Columns. *Ind. Eng. Chem. Res.* 38, 162–176. <https://doi.org/10.1021/ie9802919>
- [7] Yildirim, Ö.S., Kiss, A.A., Kenig, E.Y., 2011. Dividing wall columns in chemical process industry: A review on current activities. <https://doi.org/10.1016/j.seppur.2011.05.009>
- [8] Dejanovic, I., Matijašević, L., Olujić, Ž., 2010. Dividing wall column—A breakthrough towards sustainable distilling. <https://doi.org/10.1016/j.cep.2010.04.001>
- [9] Becker, H., Godorr, S., Kreis, H., Vaughan, J., 2001. Partitioned Distillation Columns -- Why, When & How. *Chemical Engineering* 108, 68–68
- [10] Triantafyllou, C., Smith, R., 1992. The design and optimisation of fully thermally coupled distillation columns: Process design. *Chem. eng. res. des* 70, 118–132
- [11] Muralikrishna, V., Madhavan, K.P., Shah, S.S., 2002. Development of dividing wall distillation column design space for a specified separation. <https://doi.org/10.1205/026387602753501870>
- [12] Mueller, I., Kenig, E.Y., 2007. Reactive Distillation in a Dividing Wall Column: Rate-Based Modeling and Simulation. *Ind. Eng. Chem. Res.* 46, 3709–3719. <https://doi.org/10.1021/ie0610344>

- [13] Amminudin, K.A., Smith, R., 2001. Design and Optimization of Fully Thermally Coupled Distillation Columns: Part 2: Application of Dividing Wall Columns in Retrofit. *Chemical Engineering Research and Design, Distillation and Absorption* 79, 716–724. <https://doi.org/10.1205/026387601753192037>
- [14] Castillo, F.J.L., Thong, D.Y.-C., Towler, G.P., 1998. Homogeneous Azeotropic Distillation. 1. Design Procedure for Single-Feed Columns at Nontotal Reflux. *Ind. Eng. Chem. Res.* 37, 987–997. <https://doi.org/10.1021/ie970480b>
- [15] Sotudeh, N., Shahraki, B.H., 2008. Extension of a Method for the Design of Divided Wall Columns. *Chemical Engineering & Technology* 31, 83–86. <https://doi.org/10.1002/ceat.200700378>
- [16] Rangaiah, G.P., Ooi, E.L., Premkumar, R., 2009. A Simplified Procedure for Quick Design of Dividing-Wall Columns for Industrial Applications. <https://doi.org/10.2202/1934-2659.1265>
- [17] Gómez-Castro, F.I., Segovia-Hernández, J.G., Hernández, S., Gutiérrez-Antonio, C., Briones-Ramírez, A., 2008. Dividing Wall Distillation Columns: Optimization and Control Properties. *Chemical Engineering & Technology* 31, 1246–1260. <https://doi.org/10.1002/ceat.200800116>
- [18] Gómez-Castro, F.I., Rodríguez-Ángeles, M.A., Segovia-Hernández, J.G., Gutiérrez-Antonio, C., Briones-Ramírez, A., 2011. Optimal Designs of Multiple Dividing Wall Columns. *Chemical Engineering & Technology* 34, 2051–2058. <https://doi.org/10.1002/ceat.201100176>
- [19] Vazquez-Castillo, J.A., Venegas-Sánchez, J.A., Segovia-Hernández, J.G., Hernández-Escoto, H., Hernández, S., Gutiérrez-Antonio, C., Briones-Ramírez, A., 2009. Design and optimization, using genetic algorithms, of intensified distillation systems for a class of quaternary mixtures. *Computers & Chemical Engineering* 33, 1841–1850. <https://doi.org/10.1016/j.compchemeng.2009.04.011>
- [20] Ge, X., Yuan, X., Ao, C., Yu, K.-K., 2014. Simulation based approach to optimal design of dividing wall column using random search method. *Computers & Chemical Engineering* 68, 38–46. <https://doi.org/10.1016/j.compchemeng.2014.05.001>
- [21] Bravo-Bravo, C., Segovia-Hernández, J.G., Gutiérrez-Antonio, C., Durán, A.L., Bonilla-Petriciolet, A., Briones-Ramírez, A., 2010. Extractive Dividing Wall Column: Design and Optimization. *Ind. Eng. Chem. Res.* 49, 3672–3688. <https://doi.org/10.1021/ie9006936>

- [22] Dejanović, I., Matijašević, Lj., Halvorsen, I.J., Skogestad, S., Jansen, H., Kaibel, B., Olujić, Ž., 2011. Designing four-product dividing wall columns for separation of a multicomponent aromatics mixture. *Chemical Engineering Research and Design, Special Issue on Distillation & Absorption* 89, 1155–1167. <https://doi.org/10.1016/j.cherd.2011.01.016>
- [23] Sangal, V.K., Kumar, V., Mishra, I.M., 2012. Optimization of structural and operational variables for the energy efficiency of a divided wall distillation column. *Computers & Chemical Engineering* 40, 33–40. <https://doi.org/10.1016/j.compchemeng.2012.01.015>
- [24] Safe, M., Khazraee, S.M., Setoodeh, P., Jahanmiri, A.H., 2013. Model reduction and optimization of a reactive dividing wall batch distillation column inspired by response surface methodology and differential evolution. *Mathematical and Computer Modelling of Dynamical Systems* 19, 29–50. <https://doi.org/10.1080/13873954.2012.691521>
- [25] Wang, S.-J., Chen, W.-Y., Chang, W.-T., Hu, C.-C., Cheng, S.-H., 2014. Optimal design of mixed acid esterification and isopropanol dehydration systems via incorporation of dividing-wall columns. *Chemical Engineering and Processing: Process Intensification* 85, 108–124. <https://doi.org/10.1016/j.cep.2014.08.011>
- [26] Qian, X., Jia, S., Luo, Y., Yuan, X., Yu, K.-T., 2015. Selective hydrogenation and separation of C3 stream by thermally coupled reactive distillation. *Chemical Engineering Research and Design, Distillation and Absorption* 99, 176–184. <https://doi.org/10.1016/j.cherd.2015.03.029>
- [27] Hoffmann, A., Bortz, M., Burger, J., Hasse, H., Küfer, K.-H., 2016. A new scheme for process simulation by optimization: distillation as an example, in: Kravanja, Z., Bogataj, M. (Eds.), *Computer Aided Chemical Engineering*, 26 European Symposium on Computer Aided Process Engineering. Elsevier, pp. 205–210. <https://doi.org/10.1016/B978-0-444-63428-3.50039-4>
- [28] Zitzewitz, P., Fieg, G., 2017. Multi-objective optimization superimposed model-based process design of an enzymatic hydrolysis process. *AIChE Journal* 63, 1974–1988. <https://doi.org/10.1002/aic.15609>
- [29] Jia, S., Qian, X., Yuan, X., 2017. Optimal design for dividing wall column using support vector machine and particle swarm optimization. *Chemical Engineering Research and Design* 125, 422–432. <https://doi.org/10.1016/j.cherd.2017.07.028>
- [30] Seihib, F.-Z., Benyounes, H., Shen, W., Gerbaud, V., 2017. An Improved Shortcut Design Method of Divided Wall Columns Exemplified by

- a Liquefied Petroleum Gas Process. *Ind. Eng. Chem. Res.* 56, 9710–9720. <https://doi.org/10.1021/acs.iecr.7b02125>
- [31] Staak, D., Grützner, T., Schwegler, B., Roederer, D., 2014. Dividing wall column for industrial multi purpose use. *Chemical Engineering and Processing: Process Intensification* 75, 48–57. <https://doi.org/10.1016/j.cep.2013.10.007>
- [32] Lorenz, H.-M., Staak, D., Grutzner, T., Repke, J.-U., 2018. Divided Wall Columns: Usefulness and Challenges. 1 69, 229–234. <https://doi.org/10.3303/CET1869039>
- [33] Nguyen, T.D., Rouzineau, D., Meyer, M., Meyer, X., 2016. Design and simulation of divided wall column: Experimental validation and sensitivity analysis. *Chemical Engineering and Processing: Process Intensification* 104, 94–111. <https://doi.org/10.1016/j.cep.2016.02.012>
- [34] Pan, H., Wu, X., Qiu, J., He, G., Ling, H., 2019. Pressure compensated temperature control of Kaibel divided-Wall column. *Chemical Engineering Science* 203, 321–332. <https://doi.org/10.1016/j.ces.2019.03.061>
- [35] Lestak, F., Smith, R., 1993. The control of a dividing wall column. *Chem. Eng. Res. Des.* 71, 307.
- [36] Wolff, E.A., Skogestad, S., 1995. Operation of Integrated Three-Product (Petlyuk) Distillation Columns. *Ind. Eng. Chem. Res.* 34, 2094–2103. <https://doi.org/10.1021/ie00045a018>
- [37] Luyben, W.L., 2019. Improved control structure for extractive divided-wall column with vapor recompression. *Chemical Engineering Research and Design* 149, 220–225. <https://doi.org/10.1016/j.cherd.2019.07.010>
- [38] Lumin Li, L.S., Lumin Li, L.S., 2016. Reactive dividing wall column for hydrolysis of methyl acetate: Design and control. *Chinese Journal of Chemical Engineering* 24, 1360–1368. <https://doi.org/10.1016/j.cjche.2016.05.023>
- [39] Wang, X., Xie, L., Tian, P., Tian, G., 2016. Design and control of extractive dividing wall column and pressure-swing distillation for separating azeotropic mixture of acetonitrile/N-propanol. *Chemical Engineering and Processing: Process Intensification* 110, 172–187. <https://doi.org/10.1016/j.cep.2016.10.009>
- [40] Uwitonze, H., Suk Hwang, K., Lee, I., 2016. A new design method and operation of fully thermally coupled distillation column. *Chemical Engineering and Processing: Process Intensification* 102, 47–58. <https://doi.org/10.1016/j.cep.2015.12.010>

- [41] Yang, A., Lv, L., Shen, W., Dong, L., Li, J., Xiao, X., 2017. Optimal Design and Effective Control of the tert-Amyl Methyl Ether Production Process Using an Integrated Reactive Dividing Wall and Pressure Swing Columns. *Ind. Eng. Chem. Res.* 56, 14565–14581. <https://doi.org/10.1021/acs.iecr.7b03459>
- [42] Yang, A., Wei, R., Sun, S., Wei, S., Shen, W., Chien, I.-L., 2018. Energy-Saving Optimal Design and Effective Control of Heat Integration-Extractive Dividing Wall Column for Separating Heterogeneous Mixture Methanol/Toluene/Water with Multiazeotropes. *Ind. Eng. Chem. Res.* 57, 8036–8056. <https://doi.org/10.1021/acs.iecr.8b00668>
- [43] Waltermann, T., Sibbing, S., Skiborowski, M., 2019. Optimization-based design of dividing wall columns with extended and multiple dividing walls for three- and four-product separations. *Chemical Engineering and Processing - Process Intensification* 146, 107688. <https://doi.org/10.1016/j.cep.2019.107688>
- [44] Li, C., Zhang, Q., Xie, J., Fang, J., Li, H., 2020. Design, optimization, and industrial-scale experimental study of a high-efficiency dividing wall column. *Separation and Purification Technology* 247, 116891. <https://doi.org/10.1016/j.seppur.2020.116891>
- [45] IEA Bioenergy Annual Report 2018 retrieved at <https://www.ieabioenergy.com/wp-content/uploads/2019/04/IEA-Bioenergy-Annual-Report-2018.pdf>
- [46] Kraemer, K., Harwardt, A., Bronneberg, R., Marquardt, W., 2011. Separation of butanol from acetone–butanol–ethanol fermentation by a hybrid extraction–distillation process. *Computers & Chemical Engineering, Selected Papers from ESCAPE-20 (European Symposium of Computer Aided Process Engineering - 20)*, 6-9 June 2010, Ischia, Italy 35, 949–963. <https://doi.org/10.1016/j.compchemeng.2011.01.028>
- [47] Yang, S.-T., El-Ensashy, H., Thongchul, N. (Eds.), 2013. *Bioprocessing Technologies in Biorefinery for Sustainable Production of Fuels, Chemicals, and Polymers*, 1 edition. ed. Wiley-AIChE, Hoboken, New Jersey.
- [48] Garcia, V., Pääkkilä, J., Ojamo, H., Muurinen, E., Keiski, R., 2011. Challenges in biobutanol production: How to improve the efficiency ?; *Renewable and Sustainable Energy Reviews*, 15, 964-980.
- [49] Errico, M., Sanchez-Ramirez, E., Quiroz-Ramírez, J.J., Rong, B.-G., Segovia-Hernandez, J.G., 2017. Multiobjective Optimal Acetone–Butanol–Ethanol Separation Systems Using Liquid–Liquid Extraction-Assisted Divided Wall Columns. *Ind. Eng. Chem. Res.* 56, 11575–11583. <https://doi.org/10.1021/acs.iecr.7b03078>

- [50] Patraşcu, I., Bildea, C.S., Kiss, A.A., 2017. Eco-efficient butanol separation in the ABE fermentation process. *Separation and Purification Technology* 177, 49–61. <https://doi.org/10.1016/j.seppur.2016.12.008>
- [51] Di Pretoro, A., Montastruc, L., Manenti, F., Joulia, X., 2020. Flexibility assessment of a biorefinery distillation train: Optimal design under uncertain conditions. *Computers & Chemical Engineering* 138, 106831. <https://doi.org/10.1016/j.compchemeng.2020.106831>
- [52] Renon H., Prausnitz J. M., 1968. "Local Compositions in Thermodynamic Excess Functions for Liquid Mixtures", *AIChE J.*, 14(1), S.135–144.
- [53] Di Pretoro, A., Montastruc, L., Manenti, F., Joulia, X., 2020. Exploiting Residue Curve Maps to Assess Thermodynamic Feasibility Boundaries under Uncertain Operating Conditions. *Ind. Eng. Chem. Res.* 59, 16004–16016. <https://doi.org/10.1021/acs.iecr.0c02383>
- [54] Kiss, A. A. Novel applications of dividing-wall column technology to biofuel production processes. *J. Chem. Technol. Biotechnol.* 2013, 88, 1387.
- [55] Okoli, C. O.; Adams, T. A., II Design of dividing wall columns for butanol recovery in a thermochemical biomass to butanol process. *Chem. Eng. Process.* 2015, 95, 302.
- [56] Dimian, A.C., Bildea, C.S., Kiss, A.A., 2014. *Integrated Design and Simulation of Chemical Processes*, 2 edition. ed. Elsevier Science, Amsterdam Boston Heidelberg.
- [57] Dwivedi, D., Strandberg, J.P., Halvorsen, I.J., Preisig, H.A., Skogestad, S., 2012. Active Vapor Split Control for Dividing-Wall Columns. *Ind. Eng. Chem. Res.* 51, 15176–15183. <https://doi.org/10.1021/ie3014346>
- [58] Guthrie, K.M. , 1969. Capital cost estimating. *Chem. Eng.* 76 (3), 114–142 .
- [59] Guthrie, K.M. , 1974. *Process Plant Estimating, Evaluation, and Control*. Craftsman Book Company of America .
- [60] G. D. Ulrich, 1984, 'A Guide to Chemical Engineering Process Design and Economics', Wiley.
- [61] P. F. Navarrete and W. C. Cole, 2001, 'Planning, Estimating, and Control of Chemical Construction Projects', 2nd Edition, CRC Press.
- [62] Hasheminasab, H., Gholipour, Y., Kharrazi, M., Streimikiene, D., 2018. A novel Metric of Sustainability for petroleum refinery projects. *Journal of Cleaner Production* 171, 1215–1224. <https://doi.org/10.1016/j.jclepro.2017.09.223>

- [63] Gadalla, M., Olujić, Ž., Jobson, M., Smith, R., 2006. Estimation and reduction of CO₂ emissions from crude oil distillation units. *Energy* 31, 2398–2408.
- [64] Yang, A., Sun, S., Eslamimanesh, A., Wei, S., Shen, W., 2019. Energy-saving investigation for diethyl carbonate synthesis through the reactive dividing wall column combining the vapor recompression heat pump or different pressure thermally coupled technique. *Energy* 172, 320–332. <https://doi.org/10.1016/j.energy.2019.01.126>
- [65] Yang, A., Jin, S., Shen, W., Cui, P., Chien, I.-L., Ren, J., 2019. Investigation of energy-saving azeotropic dividing wall column to achieve cleaner production via heat exchanger network and heat pump technique. *Journal of Cleaner Production* 234, 410–422. <https://doi.org/10.1016/j.jclepro.2019.06.224>
- [66] Tavan, Y., Shahhosseini, S., Hosseini, S.H., 2014. Design and simulation of ethane recovery process in an extractive dividing wall column. *Journal of Cleaner Production* 72, 222–229. <https://doi.org/10.1016/j.jclepro.2014.03.015>
- [67] Goldberg, A., Wang, T.-C., Zimmerman, D., 1994. Applications of feasible path analysis to program testing, in: *ISSTA '94*. <https://doi.org/10.1145/186258.186523>
- [68] Ding, S., Tan, H.B.K., 2013. Detection of Infeasible Paths: Approaches and Challenges, in: Maciaszek, L.A., Filipe, J. (Eds.), *Evaluation of Novel Approaches to Software Engineering, Communications in Computer and Information Science*. Springer, Berlin, Heidelberg, pp. 64–78. https://doi.org/10.1007/978-3-642-45422-6_5

Part VII. Process intensification under Uncertainty

Flexibility and Environmental Assessment of Process-intensifying Design Solutions: a DWC Case Study

Alessandro Di Pretoro^{a,b}, Matteo Fedeli^a, Xavier Joulia^b, Ludovic Montastruc^b, Flavio Manenti^{a*}

^aPolitecnico di Milano, Dipartimento di Chimica, Materiali e Ingegneria Chimica «Giulio Natta», Piazza Leonardo da Vinci 32, 20133 Milano, Italy

^bLaboratoire de Génie Chimique, Université de Toulouse, CNRS/INP/UPS, Toulouse, France

Abstract

In recent years both energy and process integration have become the most spread practices to optimize chemical processes both from economic and environmental perspectives. Their outcome is often quite effective but the design of the integrated configuration and the classical one are usually compared by referring to nominal operating conditions only. Being flexibility another key topic in the process system engineering domain, it would be interesting to assess the effect of process integration under uncertain operating conditions. The goal of this paper indeed is to compare different design solutions for the same integrated unit as well as the performance under uncertain conditions of the classical design option by means of an ABE separation mixture case study. An indirect distillation train and different configurations of Dividing Wall Column have been designed and compared in order to assess the environmental and economic advantages of the one with respect to the other for different flexibility ranges. The proposed methodology allows to select the most suitable configuration for the required performance and to have a more conscious expectation about investment costs when flexibility is taken into account.

Highlights:

1. Process intensifying solutions results to be more profitable and sustainable but their design is usually optimized with respect to nominal operating conditions only.
2. In case of bio-processes accounting for external deviations is of critical importance due to the feedstock nature fluctuations over the seasons.
3. An a priori flexibility assessment during the design phase allows to identify the best design configuration corresponding to different flexibility requirements.

Keywords: DWC, flexibility, GWP, optimal design, process integration, ABE.

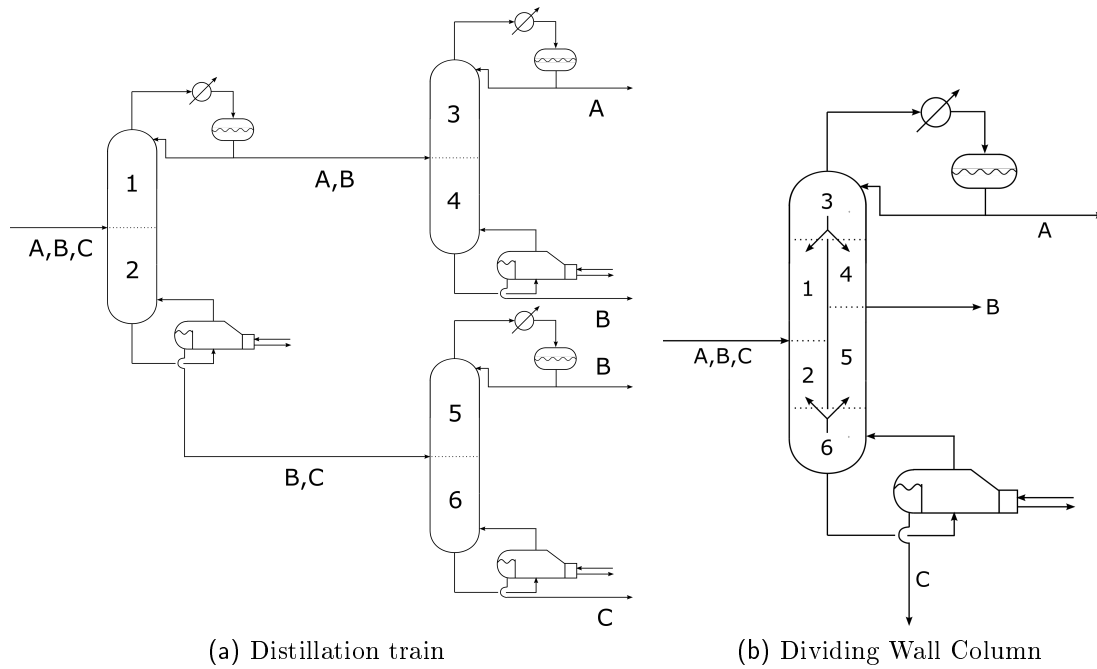


Fig. 7.1: Conventional vs intensified distillation

1 Introduction

During the last decades, process intensification has become the best practice in chemical engineering due to the need of more effective and profitable operations and equipment as well as to the concerns related to the CO_2 emissions associated to energy demanding processes [1].

Process intensification is defined by Stankiewicz & Moulijn (2000)[2] as the analysis of two main areas:

- process-intensifying equipment, such as novel reactors, and intensive mixing, heat-transfer and mass-transfer devices;
- process-intensifying methods, such as new or hybrid separations, integration of reaction and separation, heat exchange, or phase transition (in so-called multifunctional reactors), techniques using alternative energy sources (light, ultrasound, etc.), and new process-control methods (like intentional unsteady-state operation).

Obviously, these areas are the two sides of the same coin since new methodologies may involve innovative types of equipment to be designed and vice versa, while already developed novel units make often use of new, unconventional processing methods.

Among the separation processes in process industry the distillation is by far the most common and the most energy demanding as well. Several design alternatives have been proposed in literature in order to make the standard distillation column more effective. The most common one is the heat pump assisted distilla-

tion (HPAD) column taking advantage of a vapor recompression cycle in order to save about one third of the energy demand [3, 4].

The conventional distillation trains for multicomponent mixtures purification have been replaced by the most compact and effective Dividing Wall Column (hereafter DWC) as shown in Figure 7.1 where the numbers correspond to the equivalent sections. In recent years this intensified distillation unit has been considered the best practice in case of multicomponent separation since, among all those non-standard configurations, it is the only large-scale process intensification case where both capital and operating costs as well as the required installation space can be drastically reduced [5].

The first idea of intensified distillation column configuration was first introduced by Petlyuk in 1965 [6] as the connection between a prefractionator and a standard column with condenser and reboiler. In particular, the Dividing Wall Column represents the Petluk column configuration arrangement in a single column shell [7].

The analysis of the process characteristics corresponding to an intensified solution that performs better than the classical sequences of standard column has been widely discussed [8, 9] and resulted in a set of well-established conditions collected and analyzed by Petlyuk in its work [10]. Moreover, several procedures for the DWC design have been proposed in literature during the last decades both with shortcut methods [11, 12, 13] and detailed optimization algorithms [14, 15, 16, 17].

All those research studies confirm the higher profitability and sustainability of the DWC alternative with respect to the classical distillation train. However, all those analyses are strictly related to nominal operating conditions, i.e. they do not account for external disturbances. If those design solutions can be suitable for refinery related applications, in case of bio-processes neglecting the intrinsic variable nature of the feedstock during the year seasons could result to be rather restrictive.

In the light of these remarks flexibility, another current topics of major concern in process system engineering, should be included in the optimal design procedure. Flexibility is defined as the ability of a process to accommodate a set of uncertain parameters [18]. Several flexibility indexes both deterministic [19, 20] and stochastic [21, 22] have been proposed in literature by several authors. Their detailed comparison on a distillation column case study can be found in a publication by Di Pretoro et al. (2019)[23].

In particular, in this paper, the two most common deterministic flexibility indexes will be used, namely the Swaney and Grossmann F_{SG} flexibility index [19] and the Resilience Index RI proposed by Saboo and Morari (1985)[20] since no estimations about deviation likelihood to evaluate the stochastic flexibility are available.

They are defined respectively as the maximum fraction of the expected deviation of all the uncertain variables at once that can be accommodated by the

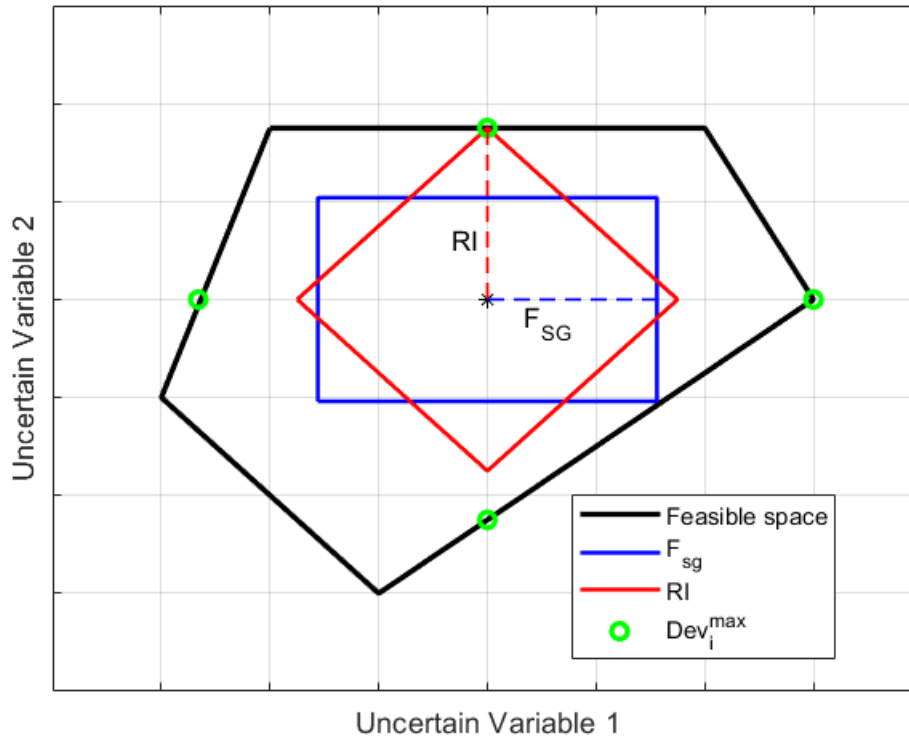


Fig. 7.2: Flexibility index (F_{SG}) vs Resilience Index (RI)[23]

system and the largest total disturbance load, independent of the direction of the disturbance, that a system is able to withstand without becoming unfeasible. For a more immediate comprehension their geometrical representation is shown in Figure 7.2.

In particular, flexibility can be coupled with the economic assessment as already proposed in previous studies [23, 24] in order to have a rigorous assessment of the additional investment costs related to a more flexible unit and to verify the actual higher profitability of a process intensifying configuration with respect to the standard distillation train.

Due to the actual concern about environmental impact, the same procedure can be applied by coupling flexibility analysis and CO_2 emissions quantification in order to have a more reliable assessment about the real sustainability gap between DWC and the conventional column sequence under uncertain operating conditions.

In addition to the comparison between the two different process configurations, the flexibility based design can be applied to define the optimal number of stages N for the Dividing Wall Column as well. For this reason, beside the optimal DWC layout under nominal operating conditions, the system behaviour under uncertainty will be assessed for separation units with a lower and a higher N as well both from an economic and an environmental perspective. In fact, for a give Total Annualized Cost, the different expenses distribution between OPEX and CAPEX could result in a different equivalent CO_2 emissions. In particular, higher investments could allow a lower external duties demand in case process variables

Component\Property	Value	Unit
Acetone	12.030	<i>mol/s</i>
n-Butanol *	61.328	<i>mol/s</i>
Ethanol	3.839	<i>mol/s</i>
Water *	12.428	<i>mol/s</i>
Pressure	101.325	<i>kPa</i>
Temperature	361.26	<i>K</i>

Tab. 7.1: Feed properties

perturbations should be compensated with a corresponding utility management.

The final goal of this research is then the comparison between equivalent conventional and intensified solutions by combining flexibility, economic and environmental analyses in a more complete design procedure. This new tool will allow the decision maker to have a more conscious overview of the design alternatives within a range of operating conditions and not only the nominal one.

2 The ABE mixture case study

The case study presented in this paper for the process intensification flexibility analysis is an ABE/W (Acetone-Butanol-Ethanol/Water) mixture separation process whose design under nominal operating conditions was already provided by Di Pretoro et al. (2020)[24] for the conventional distillation train configuration.

The two main reasons why this example has been selected are namely its limitations related to the complex thermodynamic behaviour of the mixture to be processed and the renewed interest in bioprocesses from a sustainability perspective and biofuels in particular as recently discussed in the International Energy Agency yearly report [25].

As reported by several studies concerning different bacterial strains, the ABE/W fermentation suffers from product inhibition [26], that means there is a n-butanol threshold beyond which the bacteria are poisoned by the same fermentation product. For this reason the fermentation broth is rich in water that should be preliminary removed according to one of the processes proposed in literature such as pervaporation [27], liquid-liquid extraction [28] etc.. Due to its high latent heat indeed such a huge amount of water would be very expensive to be treated during the pure components purification phase, in particular if the product purification is carried out by an energy demanding process such as distillation.

On the one hand then there's the need to describe the oscillations in the butanol yield downstream the fermentation process related to the feedstock seasonality and to the selected bacterial strain; on the other hand the description of the dewatering section performances and its eventual malfunctioning should be accounted for.

Therefore, in the light of these premises, the water and n-butanol content in the feed streams were selected as uncertain variables for this separation process case study. Moreover, the amount of water and butanol in the mixture are critical parameters from a thermodynamic perspective because of the feasibility constraints related to the butanol-water heteroazeotrope.

The feed properties are listed in Table 7.1. As already discussed by Di Pretoro et al. (2020)[29], at least n-butanol and acetone should be recovered for the profitability of the process. Therefore the process specifications are as follows:

- Acetone:
 - 1) Recovery ratio in the distillate: 0.985;
 - 2) Mass fraction in the distillate: 0.995;

- n-Butanol:
 - 1) Recovery ratio in the bottom product: 0.9604;
 - 2) Mass fraction in the bottom product: 0.990;

In practice the DWC side stream has the same purpose of the second column bottom product in the indirect distillation train, i.e. the removal of a water-ethanol rich stream that could be optionally sent to a further purification process after a more accurate quantification of the additional ethanol recovery profitability.

The thermodynamic flexibility analysis of the same distillation process was already carried out by Di Pretoro et al. (2020)[30]. The physical feasibility boundaries indeed do not depend on the affordable investment but just on the mixture properties and process specifications. This preliminary analysis of the thermodynamically feasible domain has then the purpose to outline the maximum flexibility values that can be achieved when neglecting “lower” constraints such as profitability, controllability and safety.

The thermodynamic model used for process simulation is the Non-Random Two Liquids described in detail in Appendix B. It is able indeed to correctly predict VLE and LLE and, in particular, homogeneous and heterogeneous azeotropes as already discussed by several authors [7, 24, 28, 30, 31, 32].

Due to the low amount of ethanol and to the lack of interest in its purifications, the water-ethanol azeotrope does not affect the process feasibility. On the contrary, even though the operating conditions are always far from liquid-liquid equilibrium region, the water-butanol azeotrope is a saddle point and defines a distillation boundary according to the Residue Curve Mapping [30]. In case of high water content in the feed then the minimum amount of n-butanol lost in the water rich stream because of water-butanol interactions becomes considerable and endangers the butanol recovery specification.

Further details about the DWC column design and its process simulation under uncertain operating conditions are commented in the following section.

3 DWC design

In the last years the Dividing Wall Column optimal design procedure has been a topic of major concern in the Process System Engineering domain. The main complication with respect to the equivalent sequence of standard distillation columns is related to the higher number of degrees of freedom to be fulfilled at the same time for all the column sections due to the impossibility to optimize them in series as for the distillation train.

However, this effort worthiness has been largely proved in literature since the DWC allows on average the 30% savings both from an economic and an equivalent CO_2 emissions point of view and implies a considerable installation space reduction as well as a lower amount of instrumentation needed with respect to two (or three) columns.

Several design procedures were proposed in literature including a wide range of computational tool for the design optimization such as the rigorous solution of the MINLP problem by using a superstructure [14, 17], the employment of genetic algorithms [28] and stochastic optimization strategies [33, 34, 35]. Among them, some research work for the ABE mixture can be found as well under nominal operating conditions [28, 31, 32].

As already discussed, the DWC design under nominal operating conditions used in this flexibility assessment is the one obtained by Di Pretoro et al. (2020)[29] with a feasible paths based procedure. Starting from a column layout and streams initialization provided by the DWC shortcut module in ProSimPlus[®] process simulator [36], equilibrium stages are added and removed in each column section based on a concentration profile analysis until the lowest Total Annualized Cost for a converging simulation is obtained.

In particular, the study of this paper accounts for three different DWC configurations: the 42 stages configuration whose TAC was found to be the lowest one, a second column with a lower number of stages (37) and a third column with a higher number of equilibrium stages (52). The fact that the 42 stages column resulted the optimal configuration under nominal operating conditions indeed doesn't imply that it is still the most profitable solution when taking into account the feed perturbations as well. According to the relationship between investment and operating costs a higher number of stages indeed could mitigate the required duty response to the external perturbations as discussed in Di Pretoro et al. (2020)[37].

On the other hand, the design of the distillation train for the same separation process was already performed and optimized with respect to nominal operating conditions by Di Pretoro et al. (2020)[24] and its flexibility assessment with different flexibility indexes is already carried out in the same paper. The indirect configuration resulted to be the most profitable and flexible due to the removal of bio-butanol first that is the most abundant component in the feed downstream the preliminary dewatering process.

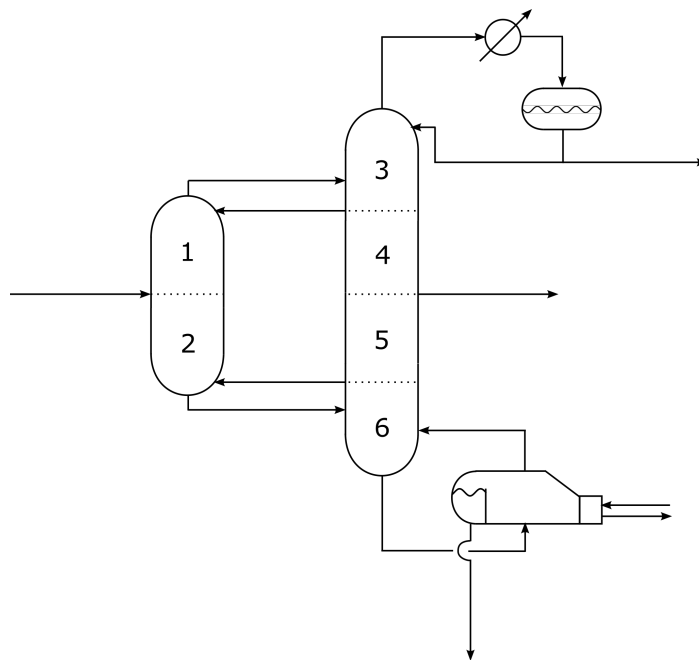


Fig. 7.3: Two-column model (Petlyuk)

The main inconvenient for the DWC process simulation is the absence of dedicated modules in commercial process simulators. The DWC can be nevertheless simulated thanks to thermodynamic equivalent configurations [38] made up of more simple columns connected to each other. There are three most common alternative layouts for a DWC that are namely the pump-around model, the two-column model also referred to as the Petlyuk column configuration and the four-column model.

In this study, the Petlyuk configuration show in Figure 7.3 will be employed since it results the best compromise between number of units and interlinking streams to be initialized for the simulation convergence. Moreover, it is the configuration for which the shortcut design provides all the required data without the need of equivalent conversions and the same layout used to perform the design under nominal operating conditions.

The interlinking streams reflect as well the two degrees of freedom related to the liquid and vapor splits that are manipulated in the flexibility analysis in order to meet the process specifications when operating conditions change. The streams initialization is valid for the first iteration, after that the sensitivity analysis tool is used to carry out the flexibility assessment and the first guess value of each step is based on the results achieved in the previous iteration.

ProSimPlus[®] process simulator was used for the shortcut design and interlinking streams initialization while the process simulation for the equipment design and for the flexibility assessment was carried out by means of AVEVA SimCentral[®] process simulator.

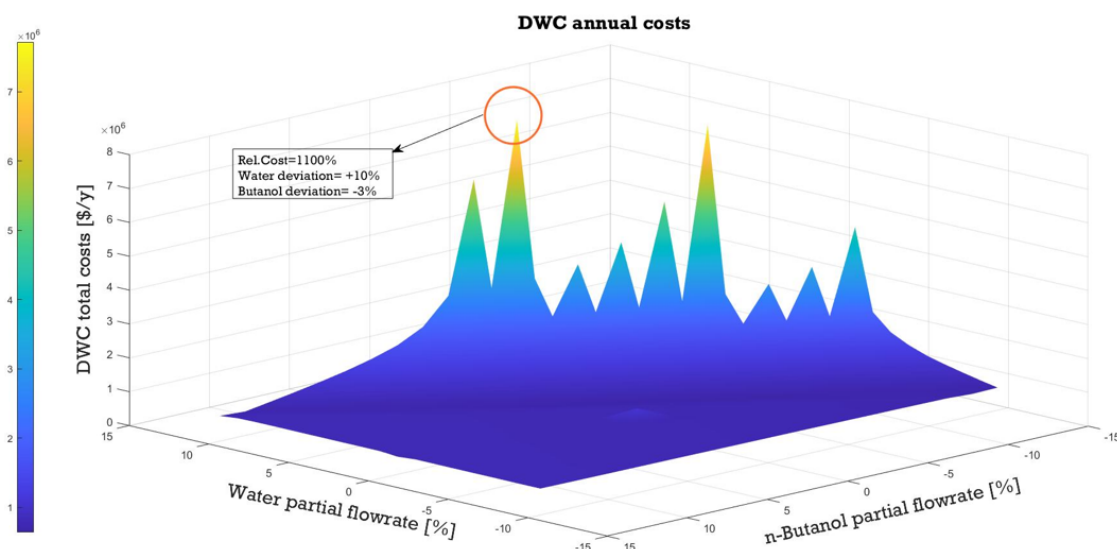


Fig. 7.4: DWC total costs vs uncertain domain

4 Results

The results of both the flexibility and the environmental assessments are reported and discussed in the corresponding section of this chapter. Both of them will be accounted for in order to make the final design choice.

4.1 Flexibility assessment

The flexibility assessment was successfully carried out for the different DWC configurations. The same thermodynamic limitations highlighted by Di Pretoro et al. (2020)[30] have been found with process simulations both for the Swaney and Grossmann flexibility index F_{SG} and for the Resilience Index RI . In particular, the feasibility boundary has the same quasi-linear trend for a constant water/butanol flowrate ratio equal about to 0.225 [24].

Figure 7.4 shows the Total Annualized Costs sensitivity of the configuration optimized under nominal operating conditions (i.e. 42 stages) with respect to both water and butanol flowrate deviations. To be more precise the reported costs have been normalized with respect to the nominal operating conditions one and calculated according to the Guthrie-Ulrich-Navarrete correlations [39, 40, 41, 42] described in detail in the corresponding Appendix C.

The most important outcome of the sensitivity analysis worth to be discussed is the direction of higher costs increase. This is mainly related to the higher reflux ratio required to compensate the feed composition perturbation and differently to what occurs for ideal separation processes it doesn't take place in the direction of the higher capacity, i.e. positive deviation both for water and butanol flowrates, but it can be detected when the operating conditions approach the thermodynamic feasibility boundary.

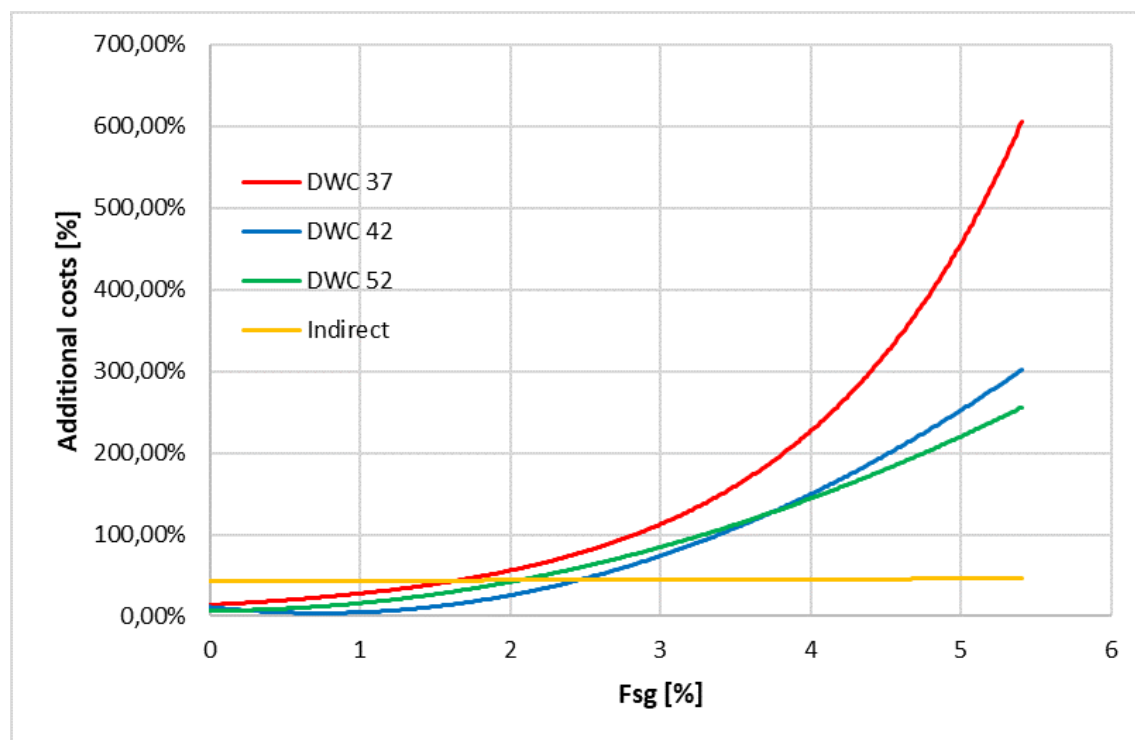


Fig. 7.5: Additional costs vs Flexibility (F_{SG})

When the feed butanol content decreases and the water flowrate increases the separation indeed becomes more challenging due to the difficulty to satisfy the process specifications related to the butanol recovery and purity. The manipulated variable mainly affected by this disturbance is the reflux ratio. Its increase results not only in a more considerable reboiler heat and condenser cooling duties but also in higher investment costs due to a larger column diameter, needed to avoid flooding when larger flowrates are circulating in the column, as well as a more relevant heat transfer surface areas both in the reboiler and in the condenser in order to ensure an effective heat transfer.

The TAC increase from the nominal operating point towards the feasibility boundary has an exponential trend resulting in a more and more expensive unit as the water/butanol ratio becomes higher achieving twelve times the nominal costs in the proximity of the unfeasible region. In order to switch from a sensitivity analysis to a flexibility assessment perspective the corresponding indexes should be used to measure the required design for a given flexibility value (or viceversa). This procedure was discussed in detail by Di Pretoro et al. (2019)[23] and allows to plot an “additional costs vs. flexibility” curve based on the required equipment oversizing able to give an immediate overview on the actual investment costs under perturbed conditions.

Figure 7.5 shows the additional costs required for a given Swaney and Grossmann flexibility index F_{SG} for the three DWC configurations normalized with respect to the optimal one under nominal operating conditions, i.e. 42 stages (blue).

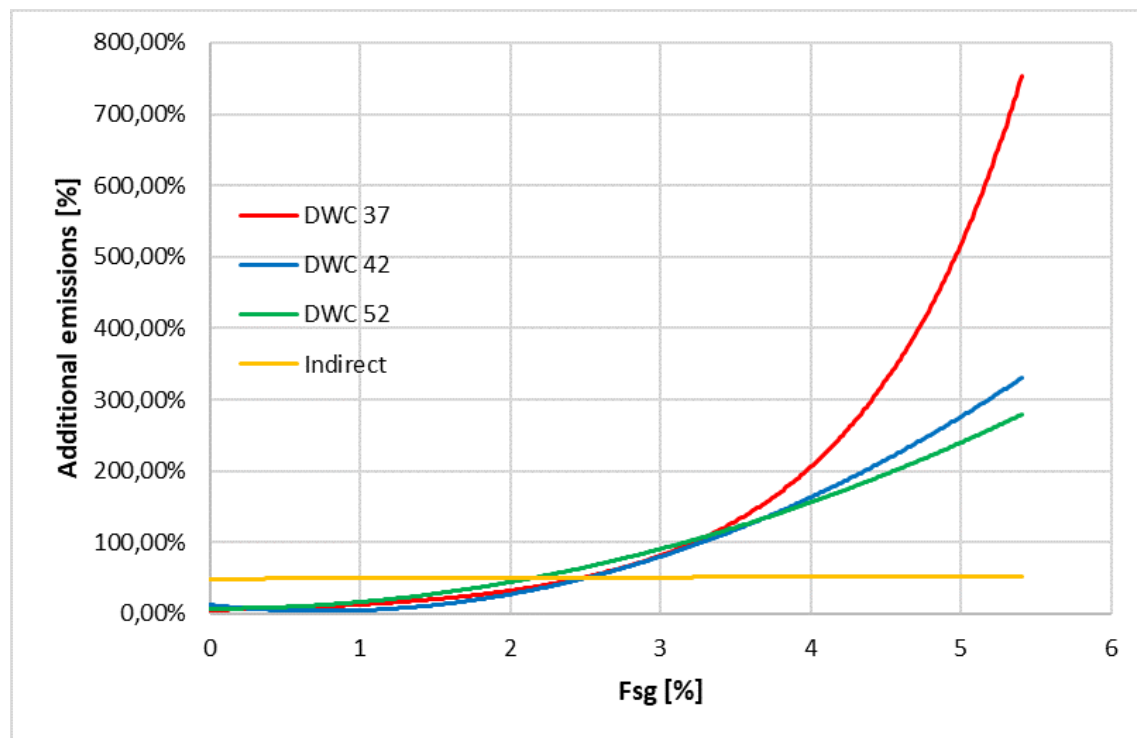


Fig. 7.6: Additional costs vs Flexibility (RI)

First of all it can be noticed that all the curves follow an almost linear trend until for low flexibility values while they progressively increase when approaching the thermodynamic flexibility boundary where the slope becomes much steeper. In particular, this sudden increase in the unit additional costs is observed first in the configuration with a lower number of equilibrium stages while it occurs later for oversized distillation column.

On the one hand the 37 stages DWC results (red) always less profitable than the 42 stages one and the presence of external disturbances could only emphasize this gap. On the other hand, even though under nominal operating conditions the 42 stages DWC results more profitable than the 52 stages one (green), there exists a given flexibility value after which the two curves cross each other and the presence of additional stages is able to mitigate the external perturbations and reduce the reflux ratio required to withstand them.

Thus, the optimal design configuration when accounting for uncertain operating conditions cannot be uniquely defined but it strictly depends on the expected deviation range and on its likelihood.

In the same Figure 7.5 the comparison between the conventional indirect configuration train (yellow) and the process intensifying solutions can be carried out. As it can be noticed the DWC allows saving about 30 % of the total annual costs with respect to the series of columns under nominal operating conditions. However, the additional costs required to achieve a desired flexibility index value increase much more slowly with respect to the dividing wall column causing the two configurations to have the same TAC at about $F_{SG} = 2.5\%$. This behaviour

is due to the fact that, in case of columns sequencing, only the column aimed at the butanol recovery design and the corresponding utilities should be managed in order to compensate the external disturbances. That results in minor changes on the equipment sizing while, in case of process intensification, the entire unit and both the external utilities are affected by the reflux ratio increase and need to be oversized.

Figure 7.6 shows the similar trends for the Resilience Index RI as well. As expected, the resilience index resulted less conservative than the F_{SG} since it assesses the deviation of one uncertain parameter at a time; thus, the curve profiles result more relaxed and the flexibility limit lies at about $RI = 11\%$.

However, since the RI is a deterministic index as well, the changes in the curve slope are analogous to the F_{SG} index ones. A higher profitability of the indirect configuration with respect to the DWC one is obtained for $RI \leq 4.5\%$ and after $RI = 9\%$ the operation with the intensified configuration becomes practically unfeasible.

The most important outcome of this flexibility analysis is then that the higher profitability of process integration design solutions should be properly verified not only under nominal but also under perturbed operating conditions. In particular, if external disturbances are likely to occur, a preliminary flexibility assessment is of critical importance to understand which actually is the optimal design configuration between the conventional distillation train and the DWC and quantify their actual costs and benefits that were not properly estimated when accounting for operating conditions only.

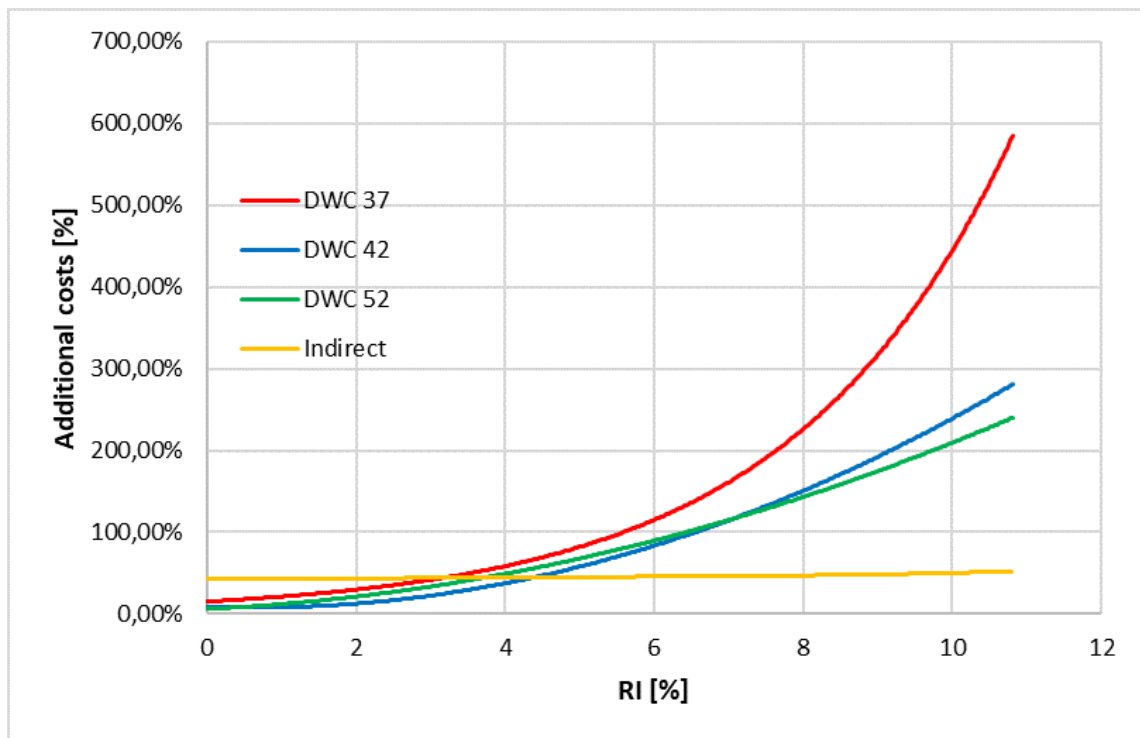
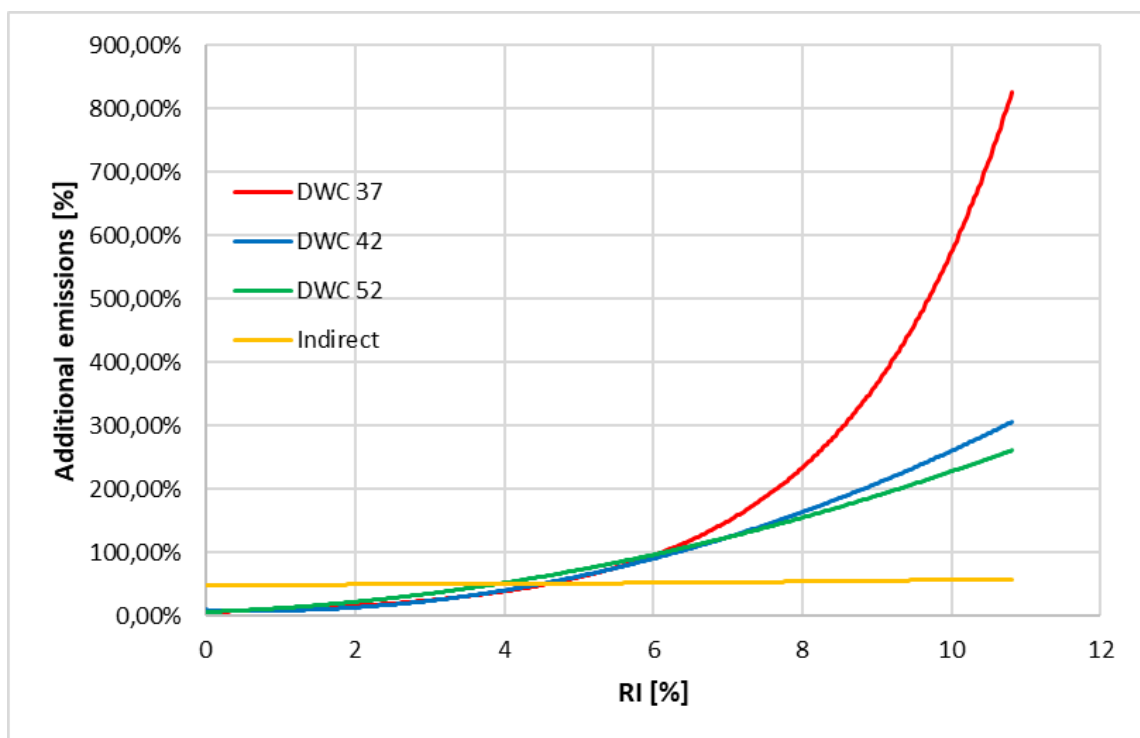
The same remarks related to the optimal design configuration apply as well when selecting the optimal number of equilibrium stages. In particular, a higher number of stages could not be the optimal solution under nominal operating conditions but could considerably help to mitigate the reflux ratio increase in case of high magnitude perturbations.

The observations related to the economic aspects are extended to the sustainability one accounting for the process GWP in the following section.

4.2 Environmental Assessment

The Global Warming Potential under perturbed operating conditions has been assessed for the indirect distillation train configuration as well as for the three Dividing Wall Column design layouts. Further details about the employed correlations can be found in Appendix D.

As discussed by several authors [43, 44, 45, 46], over the entire plant life, the CO_2 emissions related to the equipment can be neglected with respect to those considerably higher related to the energy consumption. In particular, for distillation columns, the reboiler heat duty plays the main role from a GWP perspective followed by the emissions related to the electricity consumption required for pump-

Fig. 7.7: GWP vs F_{SG} Fig. 7.8: GWP vs RI

ing.

If we look at the corresponding Figures 7.7 & 7.8 indeed they reflect the trend of OPERating Expenses and the additional costs in general. The DWC with respect to the indirect distillation train shows about 30 % lower emissions under nominal operating conditions. However, as for the economic assessment, higher reflux ratio and then external duties are required in case of external perturbations to be accommodated. In the DWC configuration, since only two duties can be managed, the energy demand for the process integrated solution increases much faster than for the distillation train where the majority of the perturbation is mitigated in the first column that purifies the most abundant component (i.e. butanol).

In Figure 7.7, the three curves for a DWC with 37, 42 and 52 equilibrium stages respectively are compared according to the F_{SG} Swaney & Grossman flexibility index. Under nominal operating conditions and until $F_{SG} = 3.6\%$ the configuration with 42 stages results to be the one with the lower emissions. In particular, the difference between the 37 and 42 stages curves start from a negligible value under nominal operating conditions and becomes higher and higher as flexibility increases since the lower number of stages implies a faster increase in the reflux ratio with respect to the other configurations. The same behaviour can be detected for the 42 stages configuration as well; when flexibility approaches $F_{SG} = 3.6\%$ indeed the 52 stages DWC is still able to mitigate the perturbation, and thus the reflux ratio, while the 42 stages column goes closer to the exponential growth of the reflux ratio as for the economic assessment.

On the other hand, as for the economic assessment, there is a breakeven point between the DWC and the indirect distillation train emissions at about $F_{SG} = 2.4\%$ that makes the intensified configuration less sustainable than the conventional one. This gap becomes particularly significant for a flexibility higher than $F_{SG} = 4\%$ where the DWC becomes extremely unsustainable from a GWP perspective.

Analogous remarks apply to the Resilience Index as well. In particular, for a resilience index RI value of about 4% the additional emissions curve of the DWC overcomes the indirect configuration one whose slope is considerably lower. Moreover, after the 9.2% flexibility, where the additional equivalent CO_2 emissions are already two times higher, the slope of the DWC trend, drastically increases making the operation practically impossible to afford from an environmental point of view.

If we compare the three DWC configurations, the Resilience Index value after which the higher number of equilibrium stages brings benefits from a sustainability perspective shifts to about 7 % due to the less conservative nature of this index with respect to the F_{SG} one.

It can then be stated that the environmental assessment provided the decision maker a useful tool to evaluate the process design solution with the lower GWP according to each flexibility range. In particular, the distillation train has worse

performances with respect to process integrated design choices such as DWC but its features result more stable even when operating conditions are likely to undergo external perturbations.

In the range of DWC different layouts, the best number of stages from a sustainability perspective depends on the expected perturbation magnitude. To be more precise, columns with a higher number of stages are able, as expected, to mitigate the system response thanks to the capacity of better distributing the disturbance along the column trays.

5 Conclusions

The main goal of this paper is to analyze and discuss the criticalities associated to process integration when operating conditions uncertainty should be accounted for. For this purpose, an ABE/W mixture separation process whose design under nominal operating conditions was already available both for the indirect distillation train and Dividing Wall Column configurations has been employed.

Under nominal operating conditions indeed the DWC investment costs result about the 30% lower with respect to the distillation train and an analogous trend can be found for the equivalent CO_2 emissions. However, when external disturbances are included the integrated design solution requires a more considerable oversizing than the conventional configuration due to the lower number of duties and reflux streams that can be independently managed.

This behaviour causes the DWC column to progressively lose its higher profitability with respect to the series of standard distillation columns until it becomes even more expensive than the equivalent distillation train and, after a limit flexibility value, practically unaffordable.

The optimal number of stages for the integrated solution was discussed as well. On the one hand, for low flexibility values, the optimal design configuration still remains the most profitable one. On the other hand, whether the perturbation intensity to be withstood becomes considerably higher, a higher derivative is obtained for the additional costs vs. flexibility curve. In those cases, increasing the number of equilibrium stages with respect to the nominal value would be of critical importance for the column in order to mitigate the external disturbances without the need of an excessive reflux ratio and then external duty requirement resulting in bigger equipment as well.

From the environmental point of view a similar trend can be outlined. Under nominal operating conditions the DWC unit allows to reduce the CO_2 emissions by 33 %. The GWP resulted mainly affected by the reboiler heat duty and the electricity for pumping (5%) and for this reason reflects the operating costs related to a higher reflux ratio when deviations occur. Even in this case there exists a flexibility value after which process integration is not a more sustainable solution anymore.

The same remarks about the DWC number of stages apply from the sustainability perspective as well. While for low flexibility values there are no considerable advantages in the addition of equilibrium stages from an environmental perspective, for substantially higher deviation magnitude indeed more equilibrium stages can ensure a lower energy requirement and thus lower CO_2 emissions reinforcing the results already obtained during the economic assessment.

It can be then concluded that the analysis revealed not only that the optimal configuration (indirect vs. DWC) under nominal operating conditions could underperform in case of external perturbations but also that, for a given configuration, the number of stages allowing for a profitable operation could vary according to the expected deviation magnitude.

In conclusion, this study makes us aware that, even though process integration is considered the best practice, it is important to know its limitations and a preliminary flexibility assessment is strictly required when operating conditions are likely to undergo external disturbances in order to be sure about the “optimality” of the employed design solution for each deviation range.

A List of acronyms and symbols

Symbol	Definition	Unit
A	Characteristic dimension	m^2
A	Heat transfer surface area	m^2
ABE/W	Acetone-Butanol-Ethanol/Water	1
$C\%$	Carbon content percentage	%
C_{ij}^n	Excess Gibbs energy coefficients	$J/(mol \cdot K^n)$
C_{BM}	Equipment bare module cost	\$
C_p^0	Purchase equipment cost in base conditions	\$
$CAPEX$	CAPital EXpenses	$\$/y$
DWC	Divided Wall Column	1
F_{BM}	Bare module factor	1
F_M	Material factor	1
F_P	Pressure factor	1
F_q	Column trays factor	1
F_{SG}	Swaney and Grossman Index	1
g_{ij}	NRTL excess Gibbs energy	J/mol
GWP	Global Warming Potential	$kgCO_2 - eq$
h_{steam}	Steam enthalpy	kJ/kg
$HPAD$	Heat pump assisted distillation	1
LLE	Liquid-Liquid equilibrium	1
$M\&S$	Marshall & Swift cost index	1
$MILNP$	Mixed Integer Non Linear Programming	1
N	Number of equilibrium stages	1
NHV	Net Heating Value	kJ/kg
$NRTL$	Non-Random Two Liquid model	1
$OPEX$	OPERating EXpenses	$\$/y$
P	Pressure	bar
Q	Heat duty	kJ/h
Q_{reb}	Reboiler heat duty	kJ/h
Q_{fuel}	Fuel heat duty	kJ/h

R	Ideal gas constant	$J/K/mol$
RI	Resilience Index	1
T	Temperature	K
TAC	Total Annualized Cost	1
VLE	Vapor-Liquid equilibrium	1

Greek letters	Definition	Unit
α	$CO_2 - to - C$ molar mass ratio	1
α_{ij}	Non-randomness parameter	1
γ_i	Activity coefficient	1
λ_{steam}	Steam latent heat	kJ/kg
τ_{ij}	NRTL dimensionless interaction parameter	1

B Thermodynamic model

As already anticipated, several authors [7, 24, 28, 30, 31, 32] state that the Non-Random Two Liquids (NRTL) [47] is the most suitable activity model to describe the ABE/W mixture behaviour. It is able to describe both liquid and vapor phases non-idealities such as azeotropes and liquid immiscibility.

The activity coefficient for the species i in a mixture of n components is given by:

$$\ln(\gamma_i) = \frac{\sum_{j=1}^n x_j \cdot \tau_{ji} \cdot G_{ji}}{\sum_{k=1}^n x_k \cdot G_{ki}} + \sum_{j=1}^n \frac{x_j \cdot G_{ij}}{\sum_{k=1}^n x_k \cdot G_{kj}} \cdot \left(\tau_{ij} - \frac{\sum_{m=1}^n x_m \cdot \tau_{mj} \cdot G_{mj}}{\sum_{k=1}^n x_k \cdot G_{kj}} \right) \quad (\text{B.1})$$

where:

$$\ln(G_{ij}) = -\alpha_{ij} \cdot \tau_{ij} \quad (\text{B.2})$$

$$\alpha_{ij} = \alpha_{ij}^0 + \alpha_{ij}^1 \cdot T \quad (\text{B.3})$$

$$\tau_{ij} = \frac{\Delta g_{ij}}{R \cdot T} \quad (\text{B.4})$$

$$\Delta g_{ij} = g_{ij} - g_{jj} = C_{ij}^0 + C_{ij}^1 \cdot T \quad (\text{B.5})$$

where α_{ij} is called non-randomness parameter and τ_{ij} is called dimensionless interaction parameter.

Binary interaction parameters provided by process simulators are not compliant with each other and they're not always able to correctly predict the equilibrium compositions in proximity of the singularity points. Simulis[®] Thermodynamics database resulted the most reliable for water-alcohols interactions but some parameters for binary interaction coefficients among inorganic compounds are not available and needed to be adjusted in order to meet the experimental data.

Equipment	Typology	K_1	K_2	K_3	A
Heat exchanger	Fixed tubes	4.3247	-0.3030	0.1634	Heat transfer area [m^2]
	Kettle	4.4646	-0.5277	0.3955	Heat transfer area [m^2]
Columns (vessel)	Packed/tray	3.4974	0.4485	0.1074	Volume [m^3]
Trays	Sieved	2.9949	0.4465	0.3961	Cross sectional area [m^2]

Tab. 7.3: Equipment cost in base conditions parameters

C Capital costs estimations

In order to evaluate the investment required to build up a process plant or for whatever economic analysis and comparison related to process equipment, the cost of every single unit needs to be estimated.

For this purpose the Guthrie-Ulrich-Navarrete correlations described in the following paragraphs have been employed [39, 40, 41, 42].

C.1 Purchase equipment cost in base conditions

The purchase equipment cost in base conditions is obtained by means of the following equation:

$$\log_{10}(C_P^0[\$]) = K_1 + K_2 \cdot \log_{10}(A) + K_3 \cdot [\log_{10}(A)]^2 \quad (\text{C.1})$$

where A is the unit characteristic dimension and the K_i coefficients are relative to the equipment typology (cf. Table 7.3).

The provided coefficients refer to a Marshall & Swift equipment cost index equal to 1110. In order to update the cost estimations, a M&S index equal to 1638.2 will be used in order to refer the calculations to the year 2018 by means of the correlation:

$$C_{P,2}^0 = \frac{M\&S_2}{M\&S_1} \cdot C_{P,1}^0 \quad (\text{C.2})$$

C.2 Bare module cost

The equipment bare module cost can be calculated according to the following correlation:

$$C_{BM} = C_P^0 \cdot F_{BM} \quad (\text{C.3})$$

Equipment	Typology	B_1	B_2	F_M	F_P
Heat exchanger	Fixed tubes	1.63	1.66	1	1
	Kettle	1.63	1.66	1	$F_{P,Kettle}$
Columns/vessel	/	2.25	1.82	1	1
Pumps	Centrifugal	1.89	1.35	1.5	1

Tab. 7.4: Bare module parameters

where the bare module factor is given by:

$$F_{BM} = B_1 + B_2 \cdot F_M \cdot F_P \quad (\text{C.4})$$

The F_M and F_P factors refers to the actual constructions materials and operating pressure while the B_i coefficients refers to the equipment typology (cf. Table 7.4).

The $F_{P,Kettle}$ value is given by:

$$\log_{10}(F_P) = 0.03881 - 0.11272 \cdot \log_{10}(P) + 0.08183 \cdot [\log_{10}(P)]^2 \quad (\text{C.5})$$

where P is the relative pressure in *bar*.

For column trays bare module cost a slightly different correlation should be used:

$$C_{BM} = N \cdot C_P^0 \cdot F'_{BM} \cdot F_q \quad (\text{C.6})$$

where N is the real trays number, $F_{BM} = 1$ e F_q is given by:

$$\begin{cases} \log_{10}(F_q) = 0.4771 + 0.08561 \cdot \log_{10}(N) - 0.3473 \cdot [\log_{10}(N)]^2 & \text{if } N < 20 \\ F_q = 1 & \text{if } N \geq 20 \end{cases} \quad (\text{C.7})$$

D Global Warming Potential calculations

The indicator associated to the greenhouse effect impact category is the Global Warming Potential whose unit is $kg\ CO_2 - eq$ per unit.

$$CO_2 = \left(\frac{Q_{fuel}}{NHV} \right) \cdot \left(\frac{C\%}{100} \right) \cdot \alpha \quad (D.1)$$

where:

- CO_2 is the value of equivalent carbon dioxide emission in $[kg/h]$;
- NHV is the Net Heating Value and it is equal to $51,600\ kJ/kg$ for Natural Gas;
- $C\%$ is the carbon content in percentage and it is equal to 75.4 for Natural Gas;
- α is the CO_2 -to- C molar mass ratio and it is equal to 3.67 .

Finally the term Q_{fuel} identifying the combustion energy required to vaporize the desired amount of steam can be estimated as:

$$Q_{fuel} = \left(\frac{Q_{reb}}{\lambda_{steam}} \right) \cdot (h_{steam} - 419) \cdot \left(\frac{T_F - T_0}{T_F - T_S} \right) \quad (D.2)$$

where:

- Q_{reb} is the reboiler duty in kJ/h ;
- λ_{steam} is the steam latent heat in kJ/kg ;
- h_{steam} is the steam enthalpy in kJ/kg ;
- 419 is the water enthalpy at $100^\circ C$ in kJ/kg ;
- T_F is the flame temperature in K ;
- T_S is the stack temperature in K ;
- T_0 is the standard temperature in K .

On the other hand, the equivalent carbon dioxide emissions for pumping were estimated by multiplying the power needed by each pump and the amount of CO_2 per each GJ of electrical energy [43].

References

- [1] Reay, D., Ramshaw, C., Harvey, A., 2011. *Process Intensification: Engineering for Efficiency, Sustainability and Flexibility*. Butterworth-Heinemann
- [2] Stankiewicz, A.I. and Moulijn, J.A. (2000) *Process Intensification: Transforming Chemical Engineering*. *Chemical Engineering Progress*, 96, 22-34.
- [3] Díez, E., Langston, P., Ovejero, G., Romero, M.D., 2009. Economic feasibility of heat pumps in distillation to reduce energy use. *Applied Thermal Engineering* 29, 1216–1223. <https://doi.org/10.1016/j.applthermaleng.2008.06.013>
- [4] Jana, A.K., 2014. Advances in heat pump assisted distillation column: A review. *Energy Conversion and Management* 77, 287–297. <https://doi.org/10.1016/j.enconman.2013.09.055>
- [5] Schultz, M.A., Stewart, D.G., Harris, J.M., Rosenblum, S.P., Shakur, M.S., O'Brien, D.E., 2002. Reduce costs with dividing-wall columns. *Chemical Engineering Progress* 98, 64–71
- [6] Petlyuk, F.B., 1965. Thermodynamically Optimal Method for Separating Multicomponent Mixtures. *Int. Chem. Eng.* 5, 555–561
- [7] Kiss, A.A., 2013. *Advanced Distillation Technologies: Design, Control and Applications*, 1 edition. ed. Wiley, Chichester, West Sussex, United Kingdom
- [8] Glinos, K., Malone, M.F., 1988. Optimality regions for complex column alternatives in distillation systems. *Chemical Engineering Research and Design* 66, 229–240
- [9] Becker, H., Godorr, S., Kreis, H., Vaughan, J., 2001. Partitioned Distillation Columns -- Why, When & How. *Chemical Engineering* 108, 68–68
- [10] Petlyuk, F.B., 2004. *Distillation Theory and its Application to Optimal Design of Separation Units*. Cambridge University Press
- [11] Triantafyllou, C., Smith, R., 1992. The design and optimisation of fully thermally coupled distillation columns: Process design. *Chem. eng. res. des* 70, 118–132
- [12] Muralikrishna, V., Madhavan, K.P., Shah, S.S., 2002. Development of dividing wall distillation column design space for a specified separation. <https://doi.org/10.1205/026387602753501870>
- [13] Seihoub, F.-Z., Benyounes, H., Shen, W., Gerbaud, V., 2017. An Improved Shortcut Design Method of Divided Wall Columns Exemplified by a Liquefied Petroleum Gas Process. *Ind. Eng. Chem. Res.* 56, 9710–9720. <https://doi.org/10.1021/acs.iecr.7b02125>

- [14] Dünnebier, G., Pantelides, C.C., 1999. Optimal Design of Thermally Coupled Distillation Columns. *Ind. Eng. Chem. Res.* 38, 162–176. <https://doi.org/10.1021/ie9802919>
- [15] Amminudin, K.A., Smith, R., 2001. Design and Optimization of Fully Thermally Coupled Distillation Columns: Part 2: Application of Dividing Wall Columns in Retrofit. *Chemical Engineering Research and Design, Distillation and Absorption* 79, 716–724. <https://doi.org/10.1205/026387601753192037>
- [16] Hoffmann, A., Bortz, M., Burger, J., Hasse, H., Küfer, K.-H., 2016. A new scheme for process simulation by optimization: distillation as an example, in: Kravanja, Z., Bogataj, M. (Eds.), *Computer Aided Chemical Engineering, 26 European Symposium on Computer Aided Process Engineering*. Elsevier, pp. 205–210. <https://doi.org/10.1016/B978-0-444-63428-3.50039-4>
- [17] Waltermann, T., Sibbing, S., Skiborowski, M., 2019. Optimization-based design of dividing wall columns with extended and multiple dividing walls for three- and four-product separations. *Chemical Engineering and Processing - Process Intensification* 146, 107688. <https://doi.org/10.1016/j.cep.2019.107688>
- [18] Hoch, P.M., Eliceche, A.M., 1996. Flexibility analysis leads to a sizing strategy in distillation columns. *Comput. Chem. Eng.* 20, S139–S144. [https://doi.org/10.1016/0098-1354\(96\)00034-8](https://doi.org/10.1016/0098-1354(96)00034-8)
- [19] Swaney, R.E., Grossmann, I.E., 1985. An index for operational flexibility in chemical process design. Part I: Formulation and theory. *AIChE J.* 31, 621–630. <https://doi.org/10.1002/aic.690310412>
- [20] Saboo, A.K., Morari, M., Woodcock, D., 1985. Design of Resilient Processing Plants .8. a Resilience Index for Heat-Exchanger Networks. *Chem. Eng. Sci.* 40, 1553–1565. [https://doi.org/10.1016/0009-2509\(85\)80097-X](https://doi.org/10.1016/0009-2509(85)80097-X)
- [21] Pistikopoulos, E.N., Mazzuchi, T.A., 1990. A Novel Flexibility Analysis Approach for Processes with Stochastic Parameters. *Comput. Chem. Eng.* 14, 991–1000. [https://doi.org/10.1016/0098-1354\(90\)87055-T](https://doi.org/10.1016/0098-1354(90)87055-T)
- [22] Lai, S.M., Hui, C.-W., 2008. Process Flexibility for Multivariable Systems. *Ind. Eng. Chem. Res.* 47, 4170–4183. <https://doi.org/10.1021/ie070183z>
- [23] Di Pretoro, A., Montastruc, L., Manenti, F., Joulia, X., 2019. Flexibility analysis of a distillation column: Indexes comparison and economic assessment. *Comput. Chem. Eng.* 124, 93–108. <https://doi.org/10.1016/j.compchemeng.2019.02.004>

- [24] Di Pretoro, A., Montastruc, L., Manenti, F., Joulia, X., 2020. Flexibility assessment of a biorefinery distillation train: Optimal design under uncertain conditions. *Computers & Chemical Engineering* 138, 106831. <https://doi.org/10.1016/j.compchemeng.2020.106831>
- [25] IEA Bioenergy Annual Report 2018 retrieved at <https://www.ieabioenergy.com/wp-content/uploads/2019/04/IEA-Bioenergy-Annual-Report-2018.pdf>
- [26] García, V., Päckilä, J., Ojamo, H., Muurinen, E., Keiski, R.L., 2011. Challenges in biobutanol production: How to improve the efficiency? *Renew. Sustain. Energy Rev.* 15, 964–980. <https://doi.org/10.1016/j.rser.2010.11.008>
- [27] Xue, C., Zhao, J.-B., Chen, L.-J., Bai, F.-W., Yang, S.-T., Sun, J.-X., 2014. Integrated butanol recovery for an advanced biofuel: current state and prospects. *Appl Microbiol Biotechnol* 98, 3463–3474. <https://doi.org/10.1007/s00253-014-5561-6>
- [28] Errico, M., Sanchez-Ramirez, E., Quiroz-Ramirez, J.J., Rong, B.-G., Segovia-Hernandez, J.G., 2017. Multiobjective Optimal Acetone–Butanol–Ethanol Separation Systems Using Liquid–Liquid Extraction-Assisted Divided Wall Columns. *Ind. Eng. Chem. Res.* 56, 11575–11583. <https://doi.org/10.1021/acs.iecr.7b03078>
- [29] Di Pretoro, A., Ciranna, F., Fedeli, M., Joulia, X., Montastruc, L., Manenti, F., 2020. A Feasible Paths Based Approach for an Optimal Dividing Wall Column Design Procedure. SUBMITTED
- [30] Di Pretoro, A., Montastruc, L., Manenti, F., Joulia, X., 2020. Exploiting Residue Curve Maps to Assess Thermodynamic Feasibility Boundaries under Uncertain Operating Conditions. *Ind. Eng. Chem. Res.* 59, 16004–16016. <https://doi.org/10.1021/acs.iecr.0c02383>
- [31] Patraşcu, I., Bîldea, C.S., Kiss, A.A., 2017. Eco-efficient butanol separation in the ABE fermentation process. *Separation and Purification Technology* 177, 49–61. <https://doi.org/10.1016/j.seppur.2016.12.008>
- [32] Okoli, C. O.; Adams, T. A., II Design of dividing wall columns for butanol recovery in a thermochemical biomass to butanol process. *Chem. Eng. Process.* 2015, 95, 302.
- [33] Gómez-Castro, F.I., Rodríguez-Ángeles, M.A., Segovia-Hernández, J.G., Gutiérrez-Antonio, C., Briones-Ramírez, A., 2011. Optimal Designs of Multiple Dividing Wall Columns. *Chemical Engineering & Technology* 34, 2051–2058. <https://doi.org/10.1002/ceat.201100176>

- [34] Vazquez–Castillo, J.A., Venegas–Sánchez, J.A., Segovia–Hernández, J.G., Hernández–Escoto, H., Hernández, S., Gutiérrez–Antonio, C., Briones–Ramírez, A., 2009. Design and optimization, using genetic algorithms, of intensified distillation systems for a class of quaternary mixtures. *Computers & Chemical Engineering* 33, 1841–1850. <https://doi.org/10.1016/j.compchemeng.2009.04.011>
- [35] Ge, X., Yuan, X., Ao, C., Yu, K.-K., 2014. Simulation based approach to optimal design of dividing wall column using random search method. *Computers & Chemical Engineering* 68, 38–46. <https://doi.org/10.1016/j.compchemeng.2014.05.001>
- [36] Nguyen, T.D., Rouzineau, D., Meyer, M., Meyer, X., 2016. Design and simulation of divided wall column: Experimental validation and sensitivity analysis. *Chemical Engineering and Processing: Process Intensification* 104, 94–111. <https://doi.org/10.1016/j.cep.2016.02.012>
- [37] Di Pretoro, A., Montastruc, L., Manenti, F., Joulia, X., 2020. Optimal Design and Environmental Impact Assessment of Flexible Multistage Operations under Uncertain Conditions. *Ind. Eng. Chem. Res.*, ACCEPTED.
- [38] Ramapriya, G.M., Tawarmalani, M., Agrawal, R., 2014. Thermal coupling links to liquid-only transfer streams: A path for new dividing wall columns. *AIChE Journal* 60, 2949–2961. <https://doi.org/10.1002/aic.14468>
- [39] Guthrie, K.M. , 1969. Capital cost estimating. *Chem. Eng.* 76 (3), 114–142 .
- [40] Guthrie, K.M. , 1974. *Process Plant Estimating, Evaluation, and Control*. Craftsman Book Company of America .
- [41] G. D. Ulrich, 1984, ‘A Guide to Chemical Engineering Process Design and Economics’, Wiley.
- [42] P. F. Navarrete and W. C. Cole, 2001, ‘Planning, Estimating, and Control of Chemical Construction Projects’, 2nd Edition, CRC Press.
- [43] Gadalla, M., Olujić, Ž., Jobson, M., Smith, R., 2006. Estimation and reduction of CO₂ emissions from crude oil distillation units. *Energy* 31, 2398–2408.
- [44] Yang, A., Sun, S., Eslamimanesh, A., Wei, S., Shen, W., 2019. Energy-saving investigation for diethyl carbonate synthesis through the reactive dividing wall column combining the vapor recompression heat pump or different pressure thermally coupled technique. *Energy* 172, 320–332. <https://doi.org/10.1016/j.energy.2019.01.126>

- [45] Yang, A., Jin, S., Shen, W., Cui, P., Chien, I.-L., Ren, J., 2019. Investigation of energy-saving azeotropic dividing wall column to achieve cleaner production via heat exchanger network and heat pump technique. *Journal of Cleaner Production* 234, 410–422. <https://doi.org/10.1016/j.jclepro.2019.06.224>
- [46] Tavan, Y., Shahhosseini, S., Hosseini, S.H., 2014. Design and simulation of ethane recovery process in an extractive dividing wall column. *Journal of Cleaner Production* 72, 222–229. <https://doi.org/10.1016/j.jclepro.2014.03.015>
- [47] Renon H., Prausnitz J. M., 1968. "Local Compositions in Thermodynamic Excess Functions for Liquid Mixtures", *AIChE J.*, 14(1), S.135–144.

Part VIII. Switchability

Accounting for Dynamics in Flexible Process Design: a Switchability Index

Alessandro Di Pretoro^{a,b}, Ludovic Montastruc^b, Xavier Joulia^b, Flavio Manenti^a

^aPolitecnico di Milano, Dipartimento di Chimica, Materiali e Ingegneria Chimica «Giulio Natta», Piazza Leonardo da Vinci 32, 20133 Milano, Italy

^bLaboratoire de Génie Chimique, Université de Toulouse, CNRS/INP/UPS, Toulouse, France.

Abstract

Flexible operations design is one of the key challenges of process engineering over the last years. However, even when uncertainty during the design phase is taken into account, the vast majority of research works refer to steady state conditions only, neglecting the system behaviour during the transition from the nominal state to the perturbed one. The final design validation indeed can be obtained only accounting for process dynamics, i.e. for the process control configuration.

This research work then carries out the dynamic flexibility assessment both for simple and more complex systems, such as a CSTR and a distillation column case studies. The deep insight into the dynamics of operating conditions that change in time allows the definition of a new switchability index able to describe the relationship between dynamic and steady state performances from a flexibility point of view.

This additional indicator provided to the decision maker resulted to be a quick and effective tool to carry out a more conscious design choice. Beside allowing a more reliable equipment sizing, it enables the comparison between different control strategies as well as different tuning methodologies and the identification of the optimal ones related to different flexibility ranges.

Furthermore, this innovative indicator results suitable to be exploited in a future perspective for the optimization of startup and shutdown procedures.

Highlights:

1. Uncertain operating conditions can compromise the control loop performances even in case optimized tuning parameters.
2. When accounting for dynamic flexibility, the optimality of the designed control structures can considerably differ with respect to the results obtained with the conventional procedure.
3. The defined switchability index and the related graphical representations have proved to be quick and effective tools to compare different design configurations and to assess the impact of dynamics from a flexibility point of view.

Keywords: dynamics; flexibility; process control; MPC; switchability index.

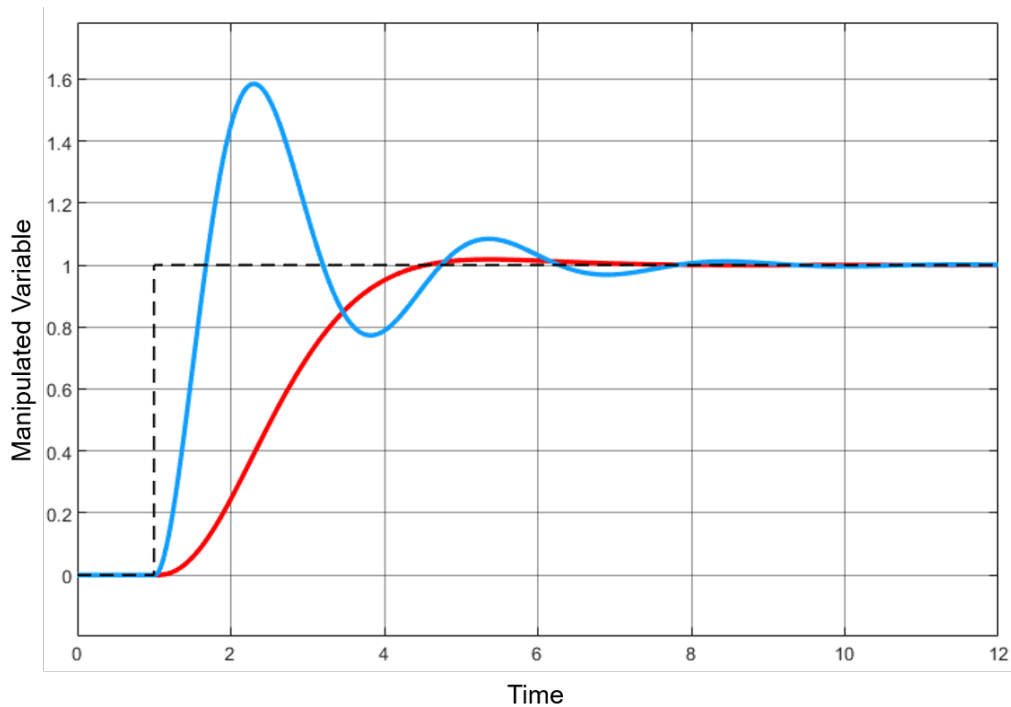


Fig. 8.1: Relevant vs negligible overshoot in process control

1 Introduction

Design under uncertainty is a topic of major concern during the last decades in process engineering. Specifically, the research field related to aleatory uncertainty and better identified as flexibility analysis and flexible design is of particular interest.

Modern processes indeed are more and more asked to accommodate the fast-changing market demand and the seasonality of bio-resources in a sustainability perspective. Several flexibility related research works are available in literature not only for chemical process design[1, 2, 3, 4, 5]. Even though flexibility is sometimes confused with sensitivity, it is properly defined by Hoch et al. (1996)[6] as the capability of a system to accommodate a set of uncertain parameters and it generally results in a system oversizing (or better sizing) with respect to the nominal operating conditions.

A more flexible system then implies higher capital expenses to avoid excessive energy duty demand in order to compensate the external disturbances occurrence to keep the final product compliant with the desired specification. In case of multistage operation for instance a higher number of stages with respect to nominal operating conditions can be preferred to lower the energy consumption as discussed by Di Pretoro et al. (2020)[7]. For complex systems, made of several units combined together, a flexibility assessment could help to identify the most constraining parameters under perturbed operating conditions and to better distribute the investments.

However, even when flexibility assessment and unit sizing are merged in the same phase of the process design procedure, there is the risk that the resulting equipment is still undersized with respect to the desired flexibility value or that, for already designed units, flexibility is overestimated. This is due to the fact that a substantial part of process simulations and flexibility analyses usually refers to steady state conditions only. When shifting from steady state to dynamic process validation it is not unusual to perform a rough oversizing and to involve non-optimized startup/shutdown procedures. In any case, a flexibility assessment based on the process dynamic behaviour can be rarely found in literature and even less frequently in the industrial practice.

The bias in the unit design associated to a neglected transient state can be better explained by means of the example shown in Figure 8.1. When switching from nominal operating condition to perturbed ones, in order to achieve the process specifications, manipulated variable settles to a new steady state value. This transition is optimized with respect to different performance indicators (maximum overshoot, decay ratio, ISE, IAE, ITAE etc) and in general the purpose is to minimize the out-of-spec operating time[8, 9, 10, 11].

Let us assume the two red and blue behaviours with similar settling time in Figure 8.1 to be the maximum vapor volumetric flowrate along a distillation column. In case of standard design procedure, the minimum column diameter related to the flooding constraint is estimated by using the vapor flowrate value at nominal operating conditions $t = 0$. In case of steady state flexible design, the vapor flowrate value at $t = 10$ is used instead. However, while switching from the condition $t = 0$ to $t = 10$, the vapor flowrate can also assume higher values than the perturbed condition ones causing the new operating conditions to be unattainable despite the steady state result.

In case of negligible transition, i.e. red trend, the flexibility overestimation is not really relevant, especially if considering that column diameters are already designed accounting for the 80 % of the flooding condition. On the contrary, in case of appreciable oscillations, a substantially bigger unit is required for the same flexibility value and, inversely, a considerably lower flexibility can be observed for a given design.

The dynamic behaviour described is necessarily related to the adopted control configuration. Classical control strategies such as PID controllers are still the most employed in the industrial practice. However, even when optimized according to the most common and established tuning methodologies, they might exhibit a relatively appreciable overshoot. A more effective control loop design and the best practice in industrial applications is the Model Predictive Control also defined as optimal control. It shows relatively little overshoot and thus it could be a better reference when dealing with dynamic flexibility assessment[12].

The ability of a system to switch between two different states is referred to as “switchability”. This property has already been studied in the available literature

in terms of dynamic response to market demand variation (servo problem)[13] and control performances under uncertainty (regulation problem)[14]. Several studies are available as well concerning the mathematical formulation of the switchability problem[15, 16].

On the contrary, only few old studies[17, 18, 19, 20] are available about flexible equipment design accounting for dynamics resilience as defined by Morari [21] and “switchability assessment”.

In Process Systems Engineering, the switchability-based design domain indeed has been merged with the more general topic defined as “unification of process design and control”[22]. The analysis carried out in this paper indeed can be seen as a contribution to the development of effective tools aiming at the integrated process design and optimization. This concept was conceived first by Sargent in 1967[23] and it is still one of the most relevant ones in this sector.

The field of simultaneous control and process design was mainly pioneered by Perkins and Wong[24], who further refined the previous definition of “functional controllability”[25] and showed some practical applications, as well as by Narraway and Perkins[26, 27], who proposed the “back-off approach” to provide a rigorous procedure to determine the best compromise among the possible controlled and manipulated variable pairs. In 1994 Walsh and Perkins[28] presented an integrated PI control scheme and process design study that was later generalized in a systematic formulation by Narraway and Perkins[27, 29] to couple economic assessment and control design.

In recent years the simultaneous design and control approach has been investigated and extended to the Model Predictive Control[30] and the better performances from an economic point of view with respect to the PI control strategies have been further proved on several process units[31, 32].

In the light of the presented advances in process design and control, this research work aims then to define a thorough procedure and reliable indicators to accurately assess both dynamic flexibility and switchability of chemical processes by using practical case studies. A more detailed analysis about these properties quantification is then carried out in the following chapter by means of dedicated flexibility indexes.

After that, a first case study is analyzed to compare the classical PID and the MPC control strategies. In particular, the PID controller has been tuned according to two different methodologies in order to assess the impact of the tuning parameters from a flexibility point of view. The results thus obtained are compared both graphically and numerically by means of the proposed switchability index.

In addition, a further case study concerning a distillation unit with the two most common control configurations is discussed in order to couple economic and switchability assessment as well as to compare the effect of the control structure from a dynamic flexibility perspective.

Conclusive remarks about advantages and deficiencies of the new index are finally discussed.

2 Index definition

Several flexibility indexes, both deterministic[33, 34] and stochastic[35], as well as several flexibility based applications can be found in literature. However, the vast majority of them refers to steady state flexibility, i.e. no transient state is accounted for.

The only dynamic flexibility index available in literature was proposed by Dimitriadis and Pistikopoulos in 1995[36]. Indeed, they proposed to extend the uncertain variables finite domain to a semi-infinite domain with the addition of the time variable $t \in [0, \infty]$. It was proposed as the dynamic extension of the steady state Swaney and Grossmann F_{SG} flexibility index[33] but it can be easily adapted to any available index with little modification in the procedure.

From a numerical point of view the solution complexity and the calculation efforts increase as well since both the dynamic feasibility and flexibility problems are formulated as two-stage, semi-infinite, dynamic optimization problems with an infinite number of decision variables.

In particular, the mathematical formulation of the Swaney and Grossmann flexibility index (F_{SG})[33] problem states as:

$$F_{SG} = \max \delta \quad (2.1)$$

$$s.t. \max_{\theta \in T(\delta)} \min_z \max_{j \in J} f_j(d, z, \theta) \leq 0 \quad (2.2)$$

where:

- θ^N are the nominal values of the uncertain parameters;
- $\Delta\theta^+$, $\Delta\theta^-$ are the expected deviations for each parameter;
- d are design variables associated to the equipment;
- z are the control variables.

The F_{SG} index then represents the maximum fraction of the expected deviation δ that can be accommodated by the system. Moreover, for constraints jointly quasi-convex in z and $1D$ quasi-convex in θ , the problem can be decomposed into a two level optimization problem as:

$$F_{SG} = \min_k \delta^k \quad (2.3)$$

$$\delta^k = \max_z \delta \quad (2.4)$$

$$f_j(d, z, \theta^k) \leq 0 \quad j \in J \quad (2.5)$$

$$\theta^k = \theta^N + \delta \cdot \Delta\theta^k \quad (2.6)$$

and the solution lies at a vertex of the hyperrectangle.

On the other hand, the dynamic flexibility problem treats the uncertain and control parameters as a function of time. Therefore the dynamic flexibility index problem[36] becomes:

$$DF(d) = \max \delta \quad (2.7)$$

$$s.t. \max_{\theta(t) \in T(\delta, t)} \min_{z(t) \in Z(t)} \max_{j \in J, t \in [0, H]} f_j(d, x(t), z(t), \theta(t), t) \leq 0 \quad (2.8)$$

$$x(0) = x^0 \quad (2.9)$$

$$\delta \geq 0 \quad (2.10)$$

$$\Theta(\delta, t) = \{\theta(t) | \theta^N(t) - \delta \cdot \Delta\theta^-(t) \leq \theta(t) \leq \theta^N(t) + \delta \cdot \Delta\theta^+(t)\} \quad (2.11)$$

$$Z(t) = \{z(t) | z^L(t) \leq z(t) \leq z^U(t)\} \quad (2.12)$$

Qualitatively, the dynamic flexibility index, DF, represents the largest scaled deviation of the uncertain parameter profile that the design can tolerate while remaining feasible within the horizon considered.

Thus, the main limitations overcome by a dynamic index is that steady state flexibility quantifies the feasibility of a system under a precise perturbed operating conditions without accounting from the path required to switch from the nominal operating conditions to the new ones. This trajectory indeed could cross the feasibility boundaries causing the perturbed operating conditions, expected as feasible, to be impossible to achieve. In the most convenient case the perturbed steady state conditions are the most constraining one. Let us consider for instance the feasible domain at different times as shown in Figure 8.2. The uncertain variables are defined as θ_i and θ^N represents the nominal operating conditions. At the time $t_{ss,old}$ the system switches from its steady state condition (black) to a new one (blue), whose system constraints are described by the blue boundaries, achieved at $t_{ss,new}$. During the transition, at a generic time t_d , the system passes through the operating conditions represented by the red boundaries.

For a better understanding, the three F_{SG} hyperrectangles are represented Figure 8.2. Even though the uncertain conditions represented by the black rectangle can be accommodated at $t_{ss,old}$, some of them cannot be withstood at $t_{ss,new}$. On the other hand, although the blue rectangle uncertain domain can be accommodated both at $t_{ss,old}$ and $t_{ss,new}$, some of its operating points become infeasible at t_d .

In reference to the process dynamics example presented in Figure 8.2, the geometric representation of the steady state F_{SG} index, according to the mathematical formulation previously described, is given by the blue rectangle. In case the same optimization problem is solved over the semi-infinite time domain, the

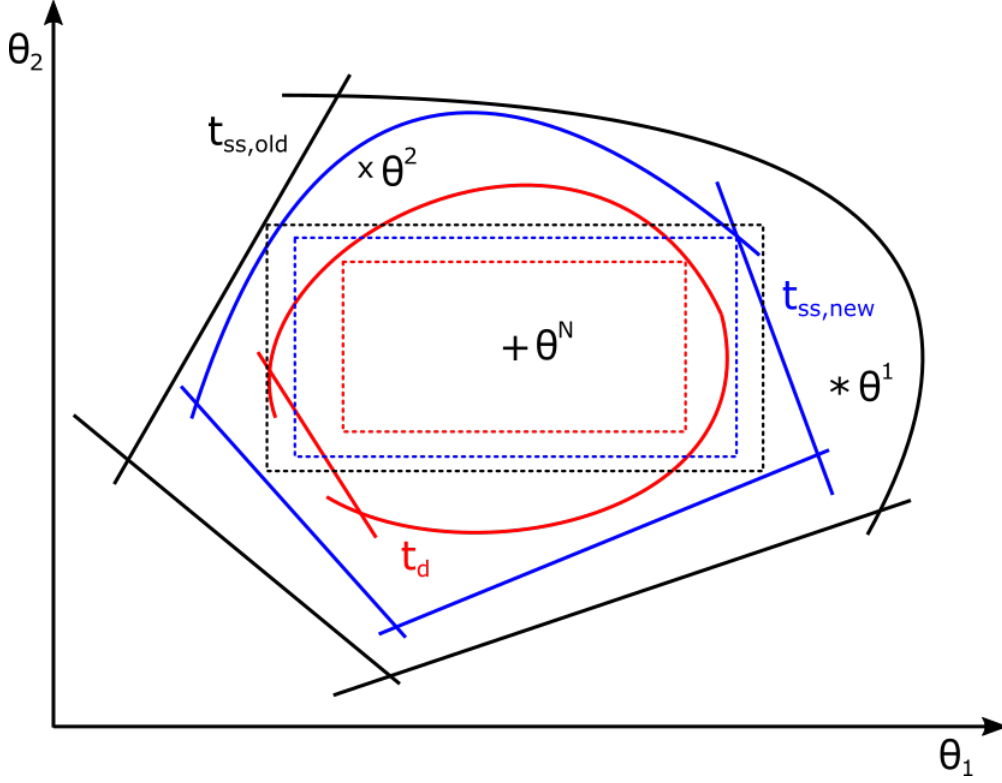


Fig. 8.2: Feasible domain dynamic behaviour

red rectangle should be considered as the image of the DF index instead.

More importantly, the dynamic flexibility analysis makes us aware of the impossibility to achieve either the operating condition θ^1 or θ^2 starting from the nominal operating conditions θ^N while the steady state results would have classified all these three points as feasible.

Inversely, for a given design, the steady state flexibility assessment overestimates the corresponding index value.

Thus, in order to evaluate the impact of dynamics from a flexibility point of view, a new so-called “switchability index” SI can be defined as the ratio between indexes of the same type corresponding to dynamic and steady state behaviour respectively:

$$SI = \frac{DF}{F} \quad (2.13)$$

Since the same flexibility index accounting for dynamics cannot be higher than the corresponding steady state one as already discussed, being both of them positive values, the switchability index SI defined here above can vary over a $[0, 1]$ range. In particular, the boundary conditions can be interpreted respectively as:

- $SI = 0$ means that the system behaviour causes the violation of the feasible domain boundaries during the perturbed transient state. Thus, there is no way to switch towards the new perturbed condition with the actual system design.

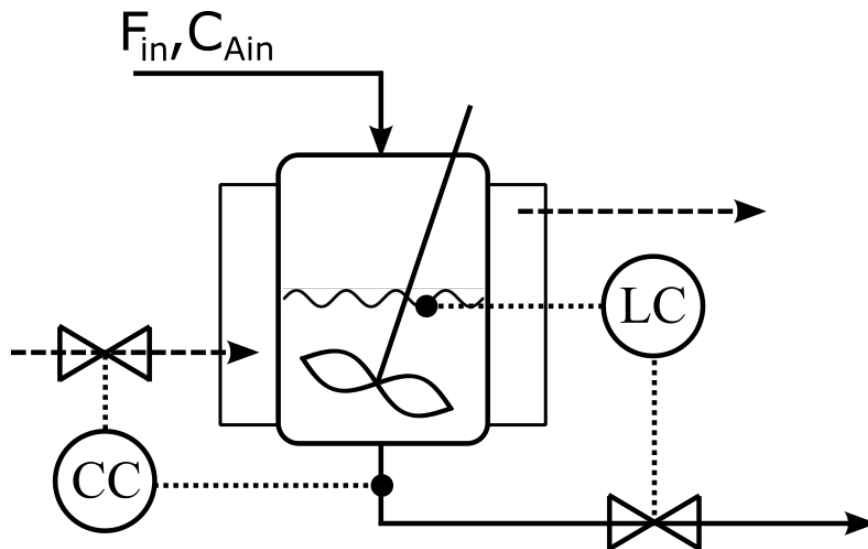


Fig. 8.3: Non-isothermal CSTR reactor layout

- $SI = 1$ means that $DF = F$, therefore no limitations due to dynamics have been detected on this system design.

Analogous remarks apply to those conditions close to the boundaries. However, from the index value itself little information can be derived.

The switchability index value, being defined on the basis of the dynamic one, is indeed a function of the employed control configuration. The most optimistic case to refer to is the design of an optimal control strategy. However, even in case of MPC configuration, we have access to several possible objective functions to minimize rather than the simple offset.

From this perspective, it is worth remarking indeed that the main use of those flexibility indexes is the comparison between different system configurations or between the same configurations with different control strategies, so that there will always be more than one value to analyze.

For a better understanding two practical case studies are discussed in detail in the following chapters. In these case studies the flexibility index problem will be solved for a given unit design and the corresponding equipment oversizing will be assessed in order to evaluate the additional investment costs required to ensure a flexible operation under uncertain operating conditions when accounting for process dynamics.

3 Dynamic CSTR case study

Let us consider first the simple case study shown in Figure 8.3 consisting of a CSTR unit where a simple first order irreversible exothermic reaction:



Tab. 8.1: CSTR process parameters

Process variable	Symbol	Value	Unit
Inlet concentration	$C_{A,in}$	0.5	mol/L
Inlet flowrate	F_{in}	40	L/h
Inlet temperature	T_{in}	530	K
Reactor volume	V	48	L
Pre-exponential factor	k_0	$2.55 \cdot 10^{14}$	$1/h$
Activation energy	E_{att}	$3 \cdot 10^4$	J/mol
Reaction enthalpy	ΔH_r	$-3 \cdot 10^4$	J/mol
Heat transfer coefficient	U	150	$W/(m^2 \cdot K)$
Coolant inlet temperature	$T_{j,in}$	530	K

occurs and whose process variables are listed in Table 8.1.

The dynamic mass and energy balances are modeled by the following ODE system:

$$\left\{ \begin{array}{l}
 \text{Overall mass balance} \\
 \text{Component A mass balance} \\
 \text{Component B mass balance} \\
 \text{CSTR energy balance} \\
 \text{Jacket energy balance}
 \end{array} \right. \begin{array}{l}
 \frac{dV}{dt} = \frac{F_{in} - F_{out}}{\rho} \\
 \frac{dC_A}{dt} = \frac{F_{in} \cdot C_{A,in} - F_{out} \cdot C_A}{V} - k_0 \cdot \exp\left(\frac{-E_{att}}{R \cdot T_r}\right) \cdot C_A \\
 \frac{dC_B}{dt} = -\frac{F_{out} \cdot C_B}{V} + k_0 \cdot e^{\frac{-E_{att}}{R \cdot T_r}} \cdot C_A \\
 \frac{dT_r}{dt} = \frac{F_{in} \cdot T_{in} - F_{out} \cdot T_r}{V} - \frac{k_0 \cdot e^{\frac{-E_{att}}{R \cdot T_r}} \cdot C_A \cdot \Delta H_r}{\rho \cdot c_P} + \frac{4}{D_r} \cdot \frac{U \cdot (T_j - T_r)}{\rho \cdot c_P} \\
 \frac{dT_j}{dt} = \frac{F_j \cdot (T_{in,j} - T_j)}{V_j} - \frac{4 \cdot V}{D_r} \cdot \frac{U \cdot (T_j - T_r)}{V_j \cdot \rho_w \cdot c_{P,w}}
 \end{array} \quad (3.2)$$

The liquid level and the outlet composition are controlled by manipulating the outlet stream and the coolant flowrate respectively.

The inlet composition has been selected as uncertain variable while the design variable we want to monitor is the heat transfer surface required to remove the reaction heat and ensure the stability of the process by avoiding reaction runaway. According to this uncertain variable choice, level control can be considered of minor relevance while the composition controller needs to be accurately designed.

The control loop design has been performed both with a classical PID controller and with a Model Predictive Control strategy.

The PID controllers are modeled by means of the equations:

$$\left\{ \begin{array}{l}
 \text{Level} \\
 \text{Composition}
 \end{array} \right. \begin{array}{l}
 F_{out}(t) = F_{in} + K_L \cdot (e_L(t) + \frac{1}{\tau_{I,L}} \cdot \int_0^t e_L(\tau) \cdot dt) \\
 F_j(t) = F_{j,ss} - K_C \cdot (e_C(t) + \frac{1}{\tau_{I,C}} \cdot \int_0^t e_C(\tau) \cdot dt + \tau_{D,C} \cdot \frac{de_C(t)}{dt})
 \end{array} \quad (3.3)$$

As already anticipated, since no flowrate perturbations are accounted for, the level controller is present but it doesn't really operate during the flexibility assessment.

The performances of the PID controller are strictly related to the controller parameters, that's why they should be properly tuned. The proportional gain,

Tab. 8.2: Composition controller tuning parameters

Parameter	Symbol	ZN	TL	Unit
Ultimate gain	$K_{C,u}$	19.3		$(kg \cdot L)/(h \cdot mol)$
Ultimate oscillation period	τ_u	2		h
Proportional constant	K_C	11.353	8.773	$(kg \cdot L)/(h \cdot mol)$
Integral time	τ_I	1	4.4	h
Derivative time	τ_D	0.25	0.3175	h

the reset time and the derivative time constant have been then selected according to the two most spread tuning methodologies, namely the Ziegler-Nichols second method[38] and the Tyreus-Luyben method[39]. The obtained tuning parameters for the composition controller are listed in Table 8.2 according to the employed tuning methodologies. The use of more than one tuning methodology allows to assess the impact of two different sets of parameters on the same physical system with the same control philosophy.

After that, the same control loop has been designed based on a MPC strategy by means of Simulink[®] Model Predictive Control toolbox[™]. According to the available MPC rules of thumb[40], the control horizon was chosen as $HC = HP/5$ and the sample time has been selected in order to ensure the system stability according to the conditions assessed by Garcia and Morari (1982)[41].

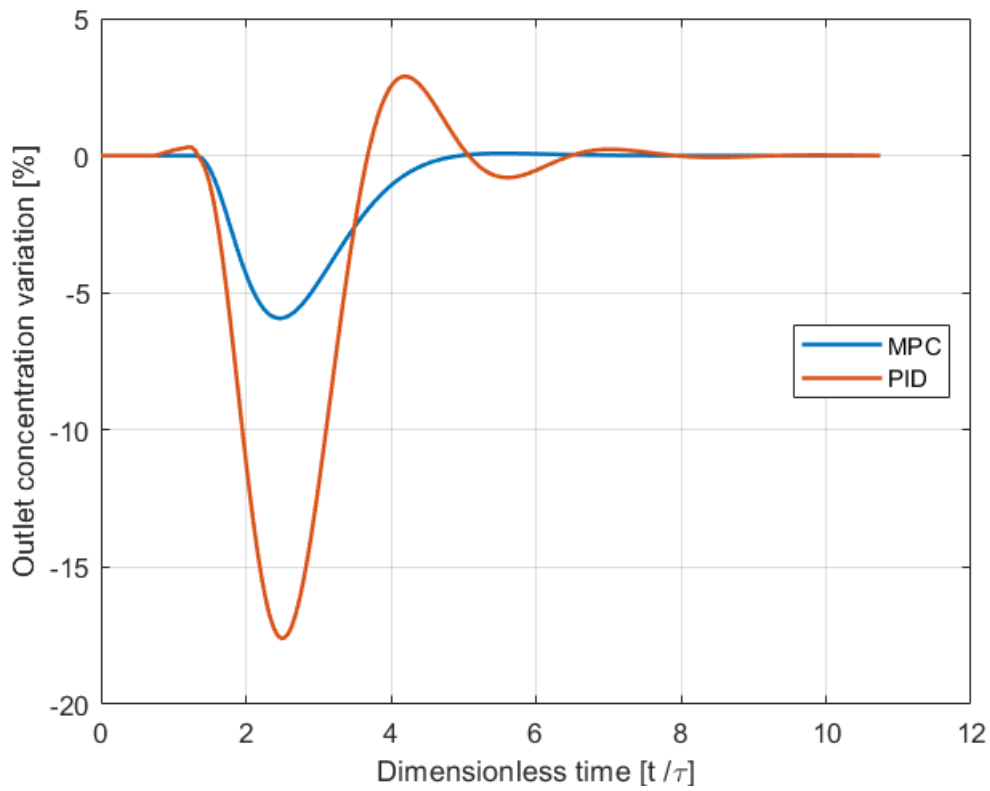
The objective function to be minimized has been defined as the sum of the controlled variables squared offsets and the square control moves on the HC sampling times to prevent too rapid control actions (i.e. “ringing effect”):

$$f_{obj} = \omega_1 \cdot \sum_{i=1}^{HP} (L_i - L^{SP})^2 + \omega_2 \cdot \sum_{i=1}^{HP} (C_{A,i} - C_A^{SP})^2 + \omega_3 \cdot \sum_{i=1}^{HC} \Delta F_{out,i}^2 + \omega_4 \cdot \sum_{i=1}^{HC} \Delta F_{j,i}^2 \quad (3.4)$$

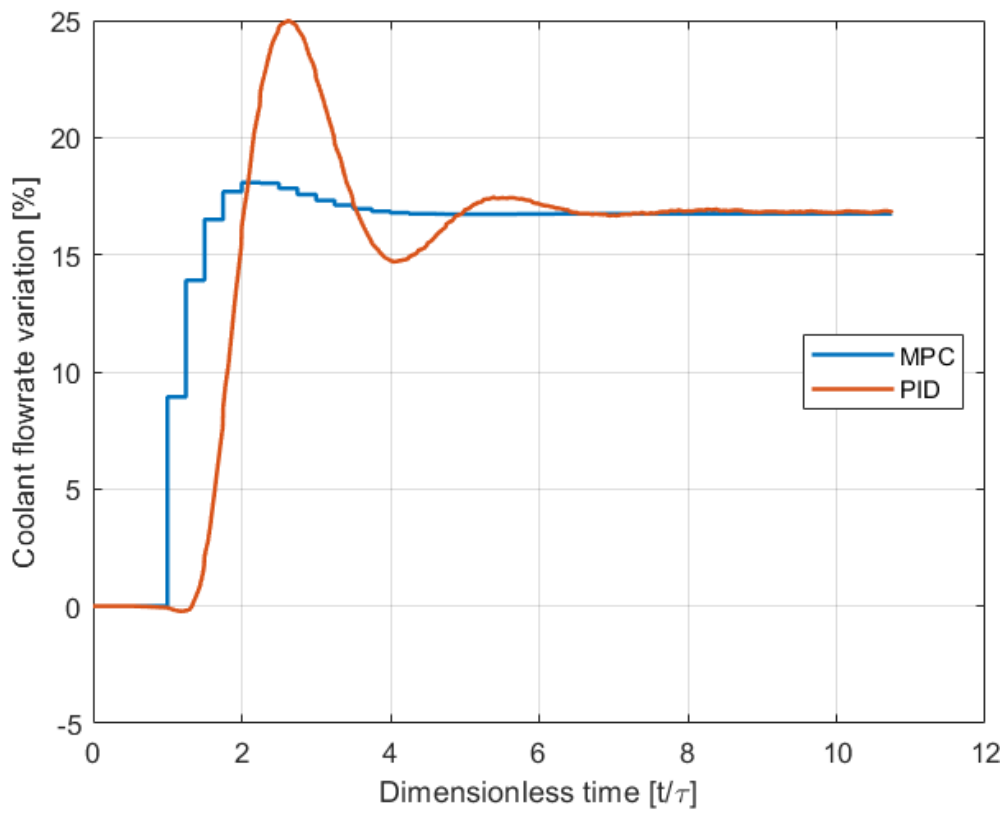
The system response as well as the control actions for a 10% deviation of the inlet concentration are reported in Figures 8.4a and 8.4b respectively as a function of time normalized with respect to the reactor residence time. As expected the MPC shows better performances than PID feedback controllers and considerably reduces both the overshoot and the settling time.

The heat transfer surface area between the process and the cooling sides has been assessed for a deviation range $[0, 30]\%$. The results for each control strategy are shown in Figure 8.5 normalized with respect to the nominal operating conditions. The “Flexibility” axis refers to the F_{SG} index for the steady state trends while, for the dynamic behaviour, it represents the DF index. The y axis refers to the heat transfer surface oversizing related to the previously defined reactor design in order to manage the operating conditions uncertainty.

On the one hand, the two PID feedback controller tuning methods perform similarly. The required additional heat transfer surface area is small for small disturbances due to the negligible overshoot while it increases when a more sub-



(a) Outlet concentration response



(b) Control action on the coolant flowrate

Fig. 8.4: Closed-loop dynamic response

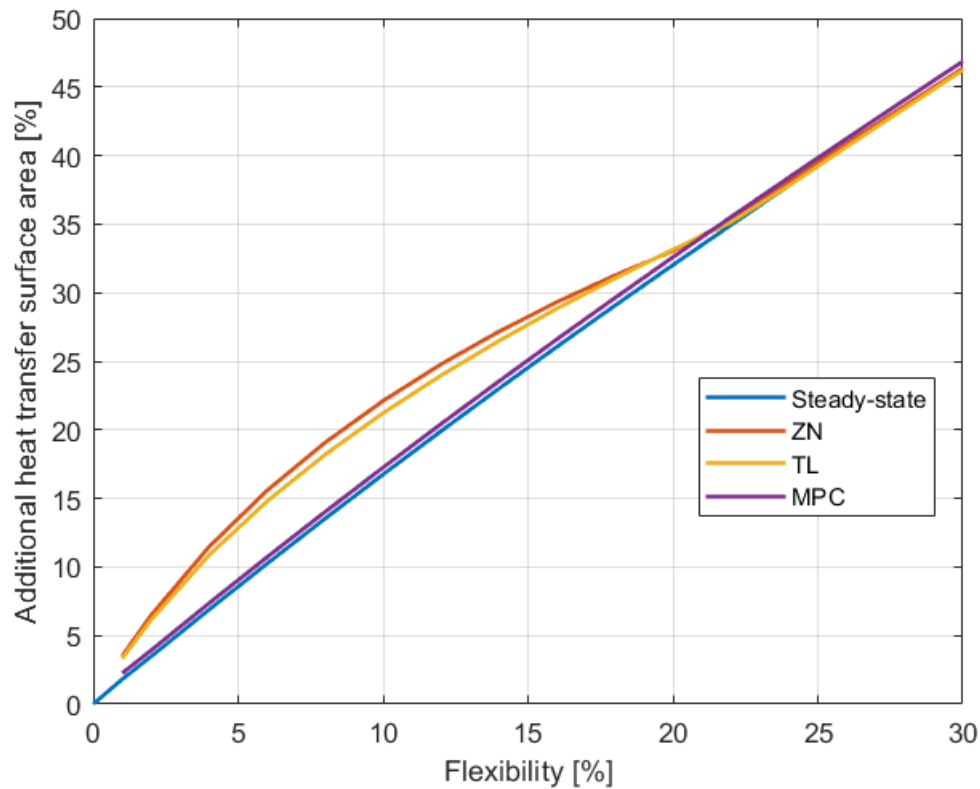


Fig. 8.5: Jacket heat transfer surface area

stantial deviation should be handled.

On the other hand the MPC shows a much smaller but constant overshoot almost independent on the deviation magnitude.

A more detailed discussion is worth to be done about the “high deviation” range, i.e. the right side of the graph. The definition of flexibility indeed associates a given design to the maximum external load that can be withstood. As already discussed, the main response parameter to be considered in a dynamic flexibility assessment is the overshoot. However, PID tuning methods and MPC optimal configuration aim to optimize some performance indicators such as decay ratio, ISE, IAE, ITAE that don’t necessarily minimize the overshoot.

For an external disturbance higher than about 10% indeed the PID strategy appears to better perform than for lower deviations since it starts approaching again the steady state trend until the dynamic and steady state values are the same (i.e. $SI = 1$). However, this smaller oversizing, i.e. lower additional investment, is obtained at the cost of reduced control quality due to the controller sluggish response, i.e. at the cost of the process productivity. That’s why, during the decision-making phase, in case of process design based of multiple criteria, both the OPEX and incomes flexibility assessment should be integrated to the CAPEX one as discussed by Di Pretoro et al. (2020)[7].

On the other hand, in this research study, the switchability assessment and the corresponding oversizing are performed on systems that were optimized with

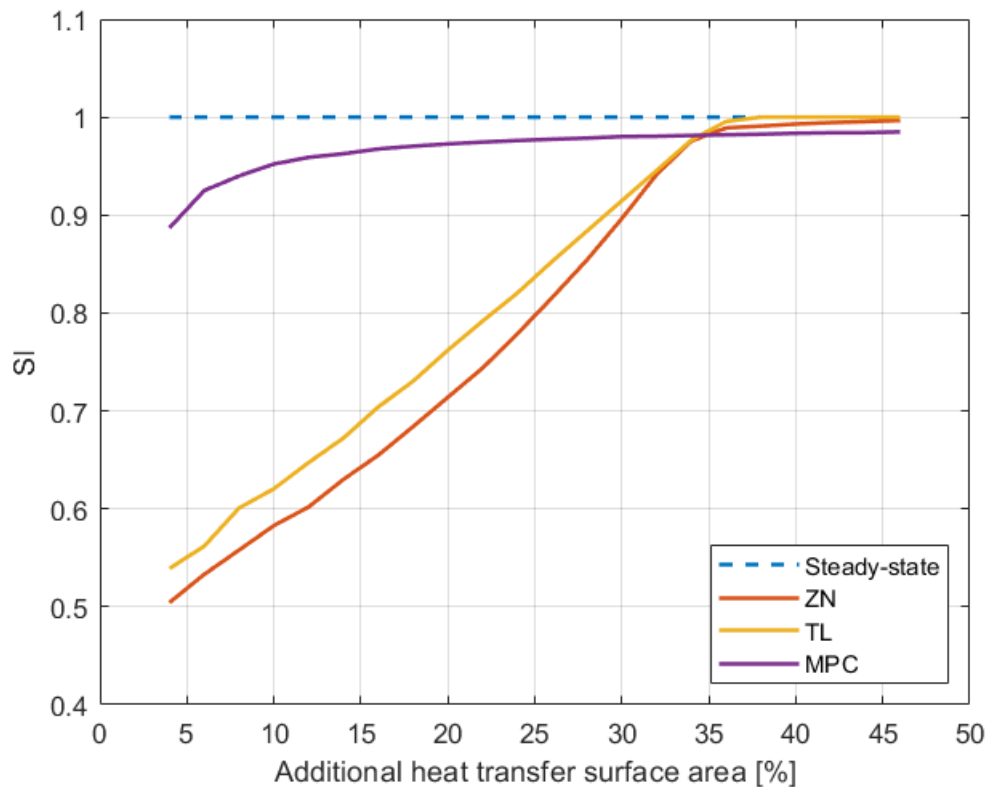


Fig. 8.6: Switchability vs design plot

respect to the steady state nominal operating conditions in order to highlight the drawbacks of such a procedure. Therefore, capital expenses are the cost item mainly accounted for.

The dynamic flexibility related remarks can be finally condensed in just one number by means of the switchability index SI . Let us consider an original plot, shown in Figure 8.6, representing the switchability index as a function of the process design that, in this case, is described by means of the additional heat transfer surface area required. For a 20 % oversizing the switchability indexes associated to each control configuration indicate similar performances between Ziegler-Nichols and Tyreus-Luyben tuned PID controller with an appreciable difference with respect to the steady state flexibility. On the other hand the MPC performs better than the PID and the system dynamic flexibility only slightly deviates from the steady state value.

For a 40 % additional surface area all the control strategies have good performances $SI > 0.98$ and the PID controllers are only marginally better than the MPC but they result in a relevant process productivity loss as previously discussed.

In conclusion, for this particular case study, it can be stated that the Model Predictive Control strategy exhibits better performances as expected and that it can be used as reference control configuration to assess the CSTR system switchability.

However, PID controllers are still the most used control strategy in the indus-

Tab. 8.3: Design data and process specifications

	Variable	Symbol	Value	Unit
<i>Design</i>				
	Number of stages (Feed)	N	20 (9)	/
	Top pressure	P_{top}	4	bar
<i>Feed</i>				
	Propylene	$F_{3=}$	0.055	mol/s
	Propane	F_3	0.053	mol/s
	n-Butane (lk)	F_4	6.863	mol/s
	n-Pentane (hk)	F_5	2.743	mol/s
<i>Specifications</i>				
	n-Butane fraction (bottom)	x_4^B	0.018	mol/mol
	n-Pentane recovery (bottom)	R_5^B	0.97	mol/mol

trial practice and are worth to be explored from a flexibility point of view as well. Two different tuning methodologies show similar results than can differ each other according to the deviation range, thus a dynamic flexibility analysis could help for a correct system design and a correct tuning method choice. For these reasons, a further comparison related to PID controllers is carried out in the following chapter.

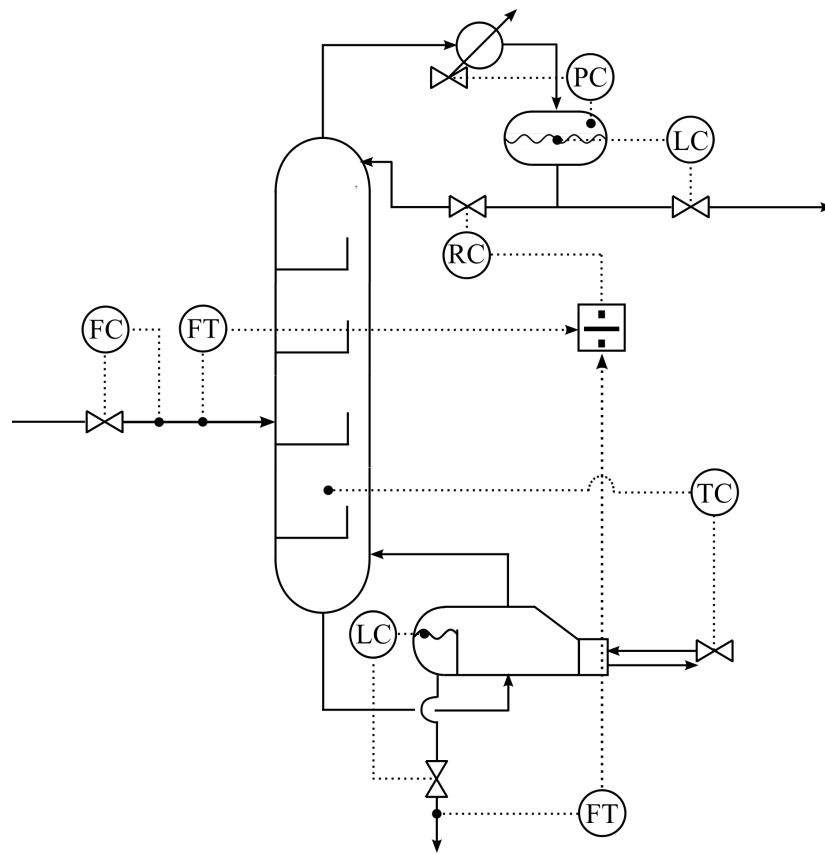
4 Distillation column case study

Distillation is by far one of the most common unit operations in chemical industry. It is a complex multistage operation made of several trays connected in series. Due to its importance, it is worth to be discussed in detail in order to compare different control strategies. A debutanizer distillation column based on the example presented by Di Pretoro et al. (2019)[37] and whose steady state results have already been discussed in previous research works[1, 2] is thoroughly analyzed here below.

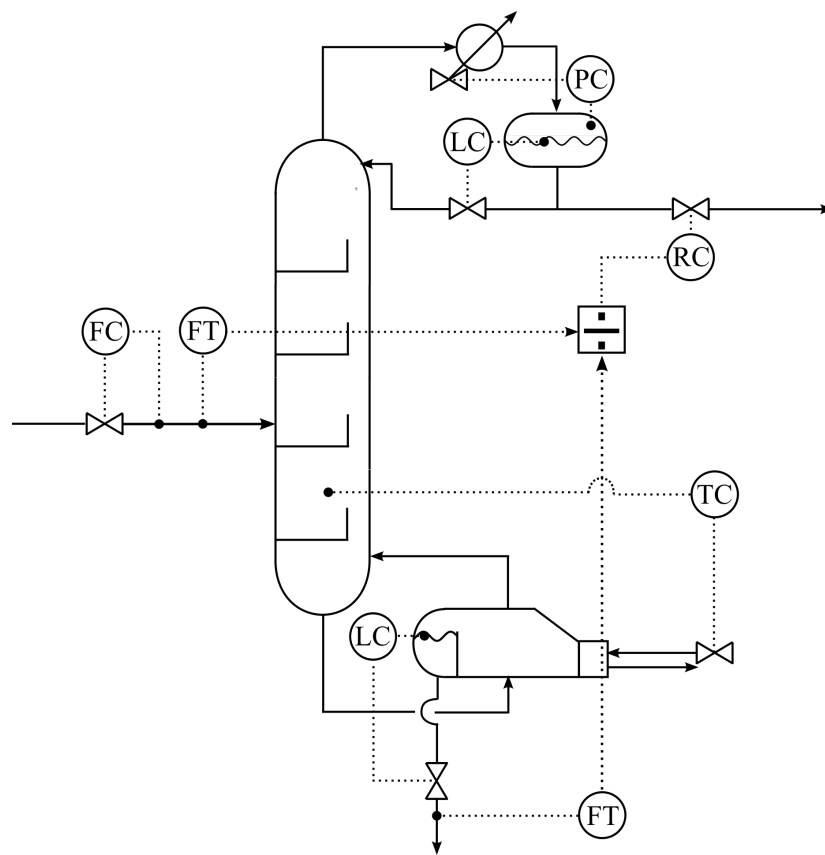
Design data and process specifications related to the column under analysis are listed in Table 8.3 while the uncertain parameters and their corresponding expected deviation range are presented in Table 8.4. Butane purity is controlled by means of a temperature controller located in correspondence of the most sensitive column stage.

The selection of an appropriate control structure is undoubtedly one of the most important tasks in the design of distillation control systems. The most common control practice in industrial applications for distillation columns is still the employment of PID controllers, that's why, even though it has been proved that the more general SI definition can be associated to an optimal control system, different PID control configurations are worth to be discussed and compared on a flexibility basis.

The two design solutions employed in this study are reported in Figures 8.7a



(a) LV control structure



(b) DV control structure

Fig. 8.7: Debutanizer control configurations

Tab. 8.4: Uncertain variables and expected deviations

Uncertain variables	Symbol	Value	Expected deviation [15 %]	Unit
n-Butane flowrate	F_4	6.86	1.029	mol/s
n-Pentane flowrate	F_5	2.74	0.411	mol/s
Condenser heat transfer coefficient	U_{cond}	473.77	71.07	$W/(m^2 \cdot K)$
Cooling water temperature	T_w	20.00	3.00	$^{\circ}C$
Reboiler heat transfer coefficient	U_{reb}	552.90	82.94	$W/(m^2 \cdot K)$
Max vapor velocity	G_f	0.38	0.057	m/s
Min vapor velocity	G_w	0.13	0.0195	m/s

and 8.7b. The former is called LV structure while the latter is called DV structure and they are named after the manipulated variables designed to control the process specifications in a dual composition control system[42, 43].

In particular, in the LV structure, often denoted "energy balance" or "indirect material balance" structure[42], the reflux rate is used to control the overhead purity, while the vapor boilup rate (i.e. the heat supply to the reboiler) is used to control the bottoms composition or, in any case, the other variables associated to them[44, 45]. In this case study, being both the specifications referred to the bottom stream, the pentane recovery ratio reflects somehow the overhead purity and thus will be controlled by means of the reflux rate.

On the other hand, the DV control configuration, also defined as "material balance" structure together with the LB one[45], differs from the previous one because of a different control strategy in the top section of the distillation column. The overhead purity is indeed controlled by manipulating the distillate flowrate while the reflux rate is used to manage the reflux drum holdup.

Among the huge amount of possible control configurations deeply studied in literature, these classical layouts are part of those configurations resulted to best perform in avoiding the competitive behaviour between the two manipulated variables and the variable controlled by the other control loop[45].

The flexibility analysis results for each of the two control structures are presented here below. The analysis was carried out with the conventional definition of the DF index proposed by Dimitriatis and Pistikopoulos (1995)[36] based on

the steady state Swaney and Grossmann F_{SG} index[33]. The dynamic simulation was performed by means of AVEVA DynSim[®] dynamic process simulator with the equilibrium based dynamic column model and feedback controller modules. For level controllers a PI configuration is employed while for the other controlled variables the derivative term is included as well.

4.1 Flexible design

Part of the results of the dynamic flexibility assessment related to the LV configuration have been introduced by Di Pretoro et al. (2019)[37] and are updated with much more detail in this research work while the DV configuration is presented here below for the first time.

First of all it is worth remarking that, since the feasible domain for the debutanizer case study a convex space as already proved by Hoch et al.(1996)[6] and further confirmed Di Pretoro et al.(2019)[2], the solution of the flexibility problem lie on the vertices of the hyperrectangle as discussed by Hoch et al.[1, 6]. In particular, the most constraining conditions for each design variable have been experienced in correspondence of the vertices listed in Table 8.5 in analogy with the steady state results[2] as expected. For instance, the condenser heat transfer surface area maximum value is obtained for the positive deviation of butane and pentane flowrate as well as for the cooling water temperature and a negative deviation of the heat transfer coefficient while the other parameters do not affect this design variable. The outcome for the other columns can be interpreted analogously.

Moreover, since not all the variables depend on every uncertain parameter, the dimension of the optimization problem could be reduced and the optimization of the entire set of design parameters can be decomposed by decoupling some of them. For instance, the column minimum diameter does not depend on the reboiler and condenser uncertain parameters. Therefore the associated flexible design problem can be performed over a reduced $F_4x F_5x G_f$ uncertain domain instead of the 7 dimensional one to be globally considered.

This procedure allows then to considerably reduce the flexible design problem computational time, accounting for the results obtained in correspondence of these vertices only when calculating the design parameters associated to given flexibility (DF and F_{SG}), and thus switchability SI , indices.

Dynamic simulations were then performed and perturbed for both the control system configurations in order to assess the optimal equipment sizing for the given distillation column design corresponding to process parameters responses. It is then possible to associate an optimal equipment design to each flexibility value.

The condenser and reboiler heat transfer surface area have been assessed by

Tab. 8.5: Uncertain parameters critical deviations (positive + or negative -)

Parameter vs design variable	A_{cond}	A_{reb}	D_{min}	D_{max}
Butane flowrate	+	+	+	-
Pentane flowrate	+	+	+	-
U_{cond}	-			
T_w	+			
U_{reb}		-		
G_f			-	
G_w				+

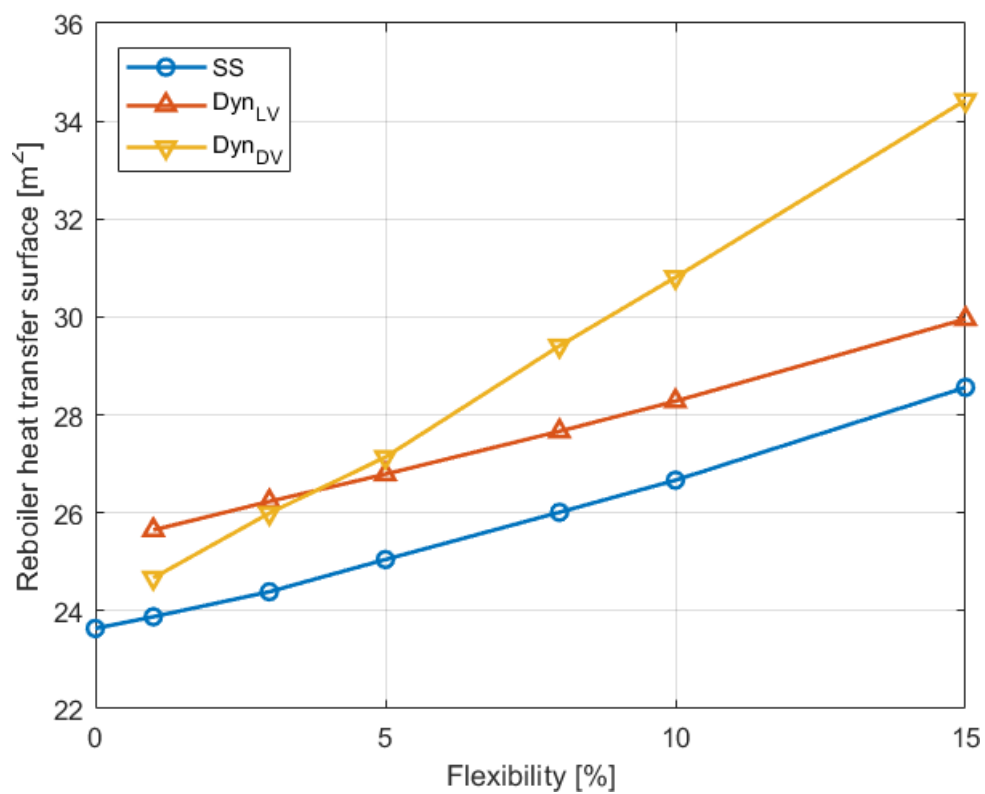


Fig. 8.8: Reboiler heat transfer surface area

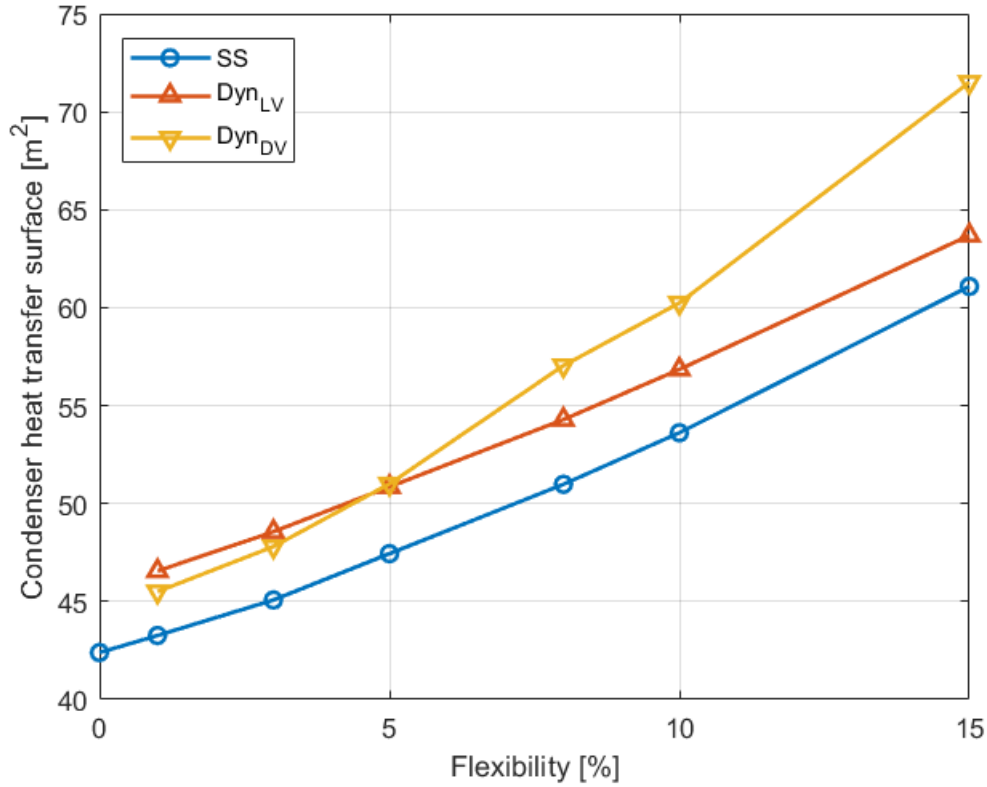


Fig. 8.9: Condenser heat transfer surface area

means of the heat exchanger characteristic equation:

$$Q_i = U_i \cdot A_i \cdot \Delta T_{lm,i} \quad (4.1)$$

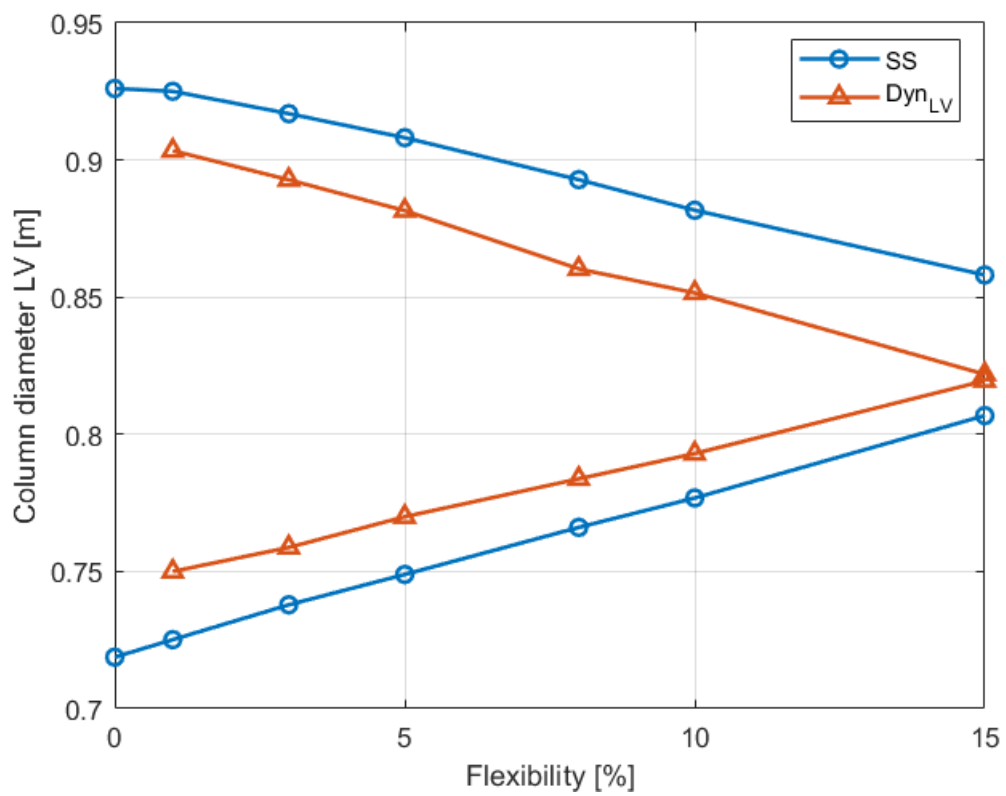
while the maximum and minimum column diameters have been designed at the 80% of the flooding and weeping conditions:

$$\pi \cdot \frac{D_{min}^2}{4} = \frac{F_V^{max}}{0.8 \cdot G_f} \quad (4.2)$$

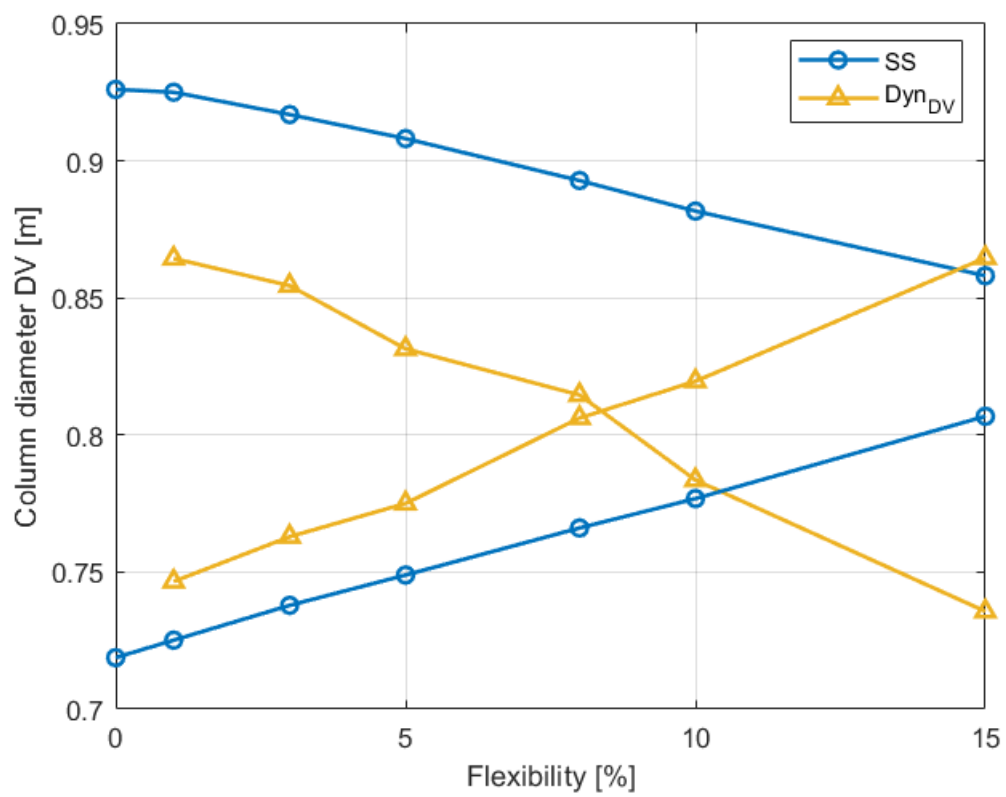
$$\pi \cdot \frac{D_{max}^2}{4} = \frac{0.8 \cdot F_V^{min}}{G_w} \quad (4.3)$$

where F_V^{max} and F_V^{min} are respectively the maximum and minimum vapor flowrates circulating along the column under the corresponding perturbed conditions.

The results concerning the equipment sizing are reported in Figures 8.8, 8.9 and 8.10 as a function of flexibility. Since the Swaney and Grossmann flexibility index was employed, a flexibility equal to 5%, for example, means that all the uncertain variables were perturbed by $\pm 5\%$ and the most constraining value of the design variables, e.g. highest heat transfer surface area, has been selected. The blue lines refer to steady state conditions and do not depend on the control strategy while red and yellow trends refer to LV and DV configurations respectively. All of them show an almost linear behaviour with respect to the flexibility index F_{SG}



(a) LV configuration



(b) DV configuration

Fig. 8.10: Column minimum and maximum diameter

with coefficients of determination R^2 in the range [0.987, 0.999]. This is a frequent trend when deterministic flexibility indexes are employed as already discussed in Di Pretoro et al. (2019)[2].

In both cases differences with respect to steady state value are appreciable and dynamics cannot be neglected. This could be due to non-optimal control strategies but, rather than that, a more relevant comparison between the LV and DV schemes is worth to be discussed. The DV line shows a higher slope with respect to the LV one and they cross each other at about $DF = 4 - 5\%$.

From a flexibility point of view, the optimal control structure depends then on the expected deviation. If the system is likely to undergo small perturbations the DV scheme results in a smaller oversizing while the LV is much more convenient for higher deviation values.

Moreover, referring to Figures 8.10a and 8.10b, there exists a certain flexibility index value for which the minimum and maximum diameters are the same. From a physical point of view, this is the maximum flexibility value attainable with a single diameter column. If higher flexibility is needed, a distillation column with different diameters for the rectifying and stripping sections should be employed with higher corresponding investment costs. In case only steady state is accounted for, this condition occurs at about $F_{SG} = 20\%$ while, taking into account dynamics, the infeasible condition is obtained at $DF = 15\%$ and $DF = 8.2\%$ for the LV and DV schemes respectively.

It can be then stated that a flexible design, neglecting the switchability assessment of a system, results in a considerable overestimation of the feasibility boundaries leading to wrong expectations about the process behaviour under uncertain operating conditions.

4.2 Economic assessment

Once the equipment design is available, the related costs can be estimated by means of the Guthrie-Ulrich-Navarrete correlations[46, 47, 48, 49] described in Appendix B. Figure 8.11 shows the additional costs related to the corresponding flexible design solutions normalized with respect to the nominal operating conditions.

These trends reflect the equipment sizing as expected. For small disturbances the design choice needed, in case a DV control scheme is used, results to be less expensive than the one required for a LV configuration. On the other hand, if deviations are more considerable, the DV configuration additional costs increase much faster than the LV related ones. In particular, if a flexibility value higher than $DF = 8.2\%$ is required, a distillation column with two different cross-sectional area should be employed in case of DV control structure.

However, in both cases the additional costs with respect to the steady state assessment result to be not negligible at all. This means that, for a given design,

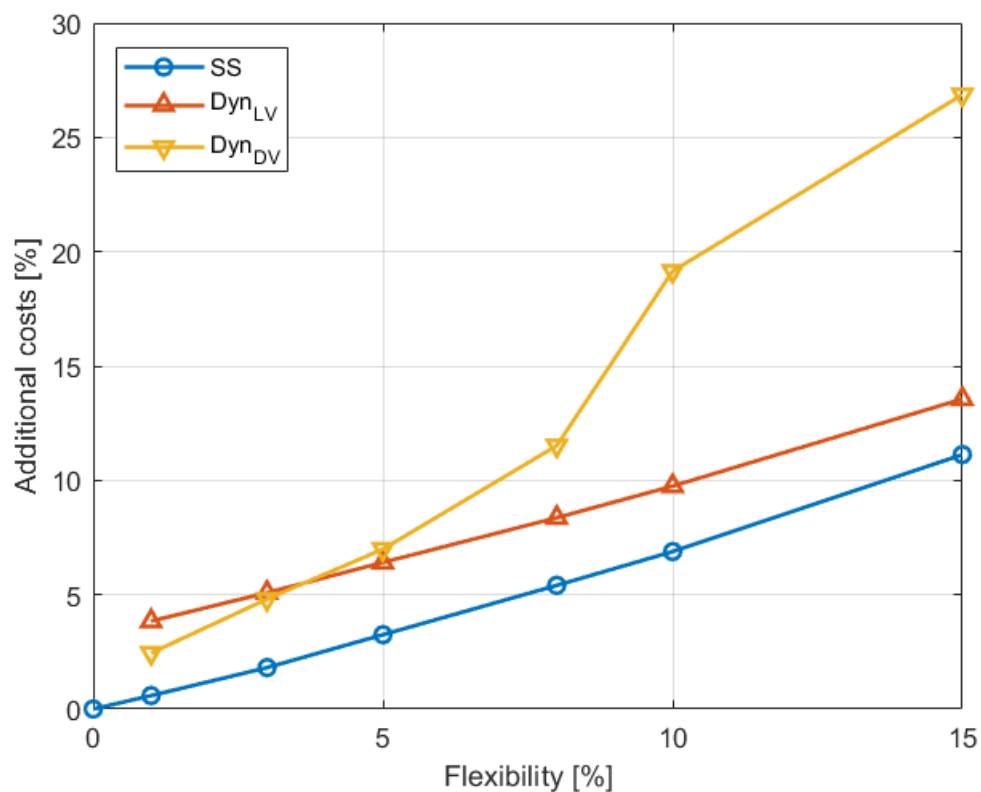


Fig. 8.11: Additional investment costs vs flexibility

steady state flexibility F_{SG} is an overestimation of the actual DF value. Inversely, for a given desired flexibility, the additional costs to be afforded are substantially underestimated.

Let us use the switchability index perspective to describe this behaviour. Two original switchability index plots can be outlined as a function of the additional costs, i.e. the column design, and the flexibility range respectively as shown in Figures 8.12a and 8.12b. With reference to Figure 8.12a it can be noticed that by investing 4% more $SI_{LV} = 0.27$ and $SI_{DV} = 0.45$ are obtained while for a 11% additional investment $SI_{LV} = 0.78$ and $SI_{DV} = 0.51$ are achieved. In the range [11.7 16.9]% a SI drop can be observed for the DV control structure since the dynamic flexibility is fixed at 8.2% due to the single column diameter constraint while the F_{SG} value keeps increasing. This behaviour can be better observed in Figure 8.12b where the switchability drop at the given flexibility value is even more evident. Moreover, Figure 8.12b allows a more immediate detection of the flexibility ranges where one control structure performs better than the other one

The dynamic flexibility indexes themselves could be used indeed to compare the two configurations but they provide no information about the difference between dynamics and steady state behaviours under uncertain conditions. On the contrary, the switchability index is able to condense both these properties.

It is worth observing that the considerable oversizing requirement related to this case study is due to the fact that the Swaney and Grossmann index F_{SG} was

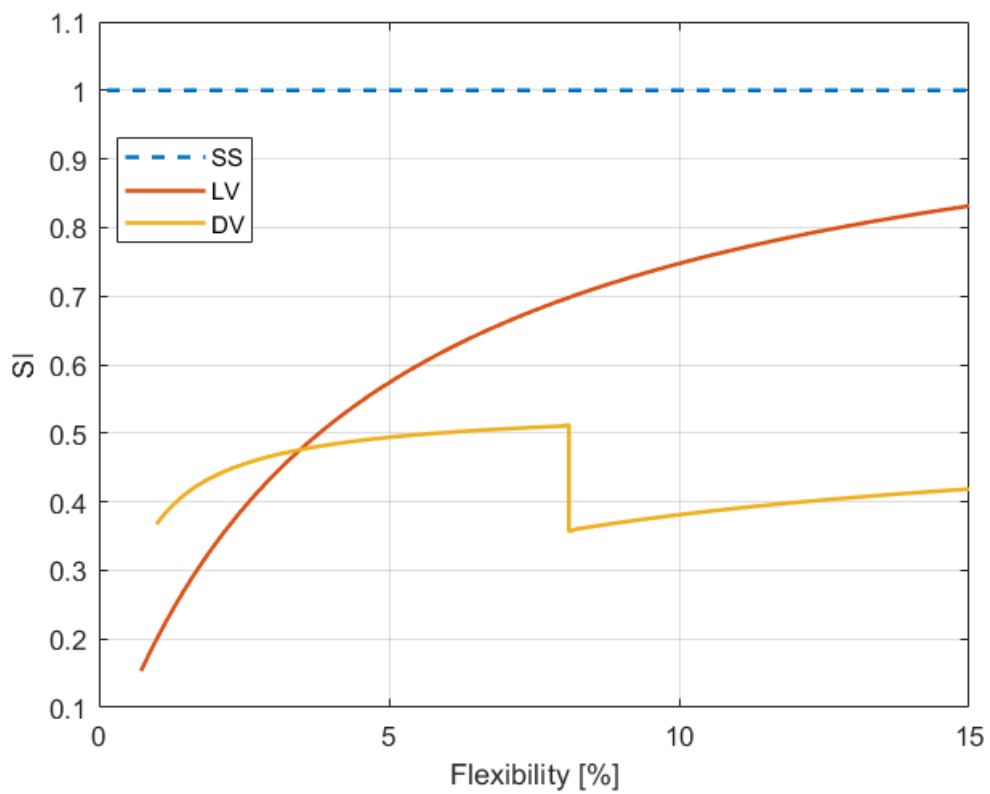
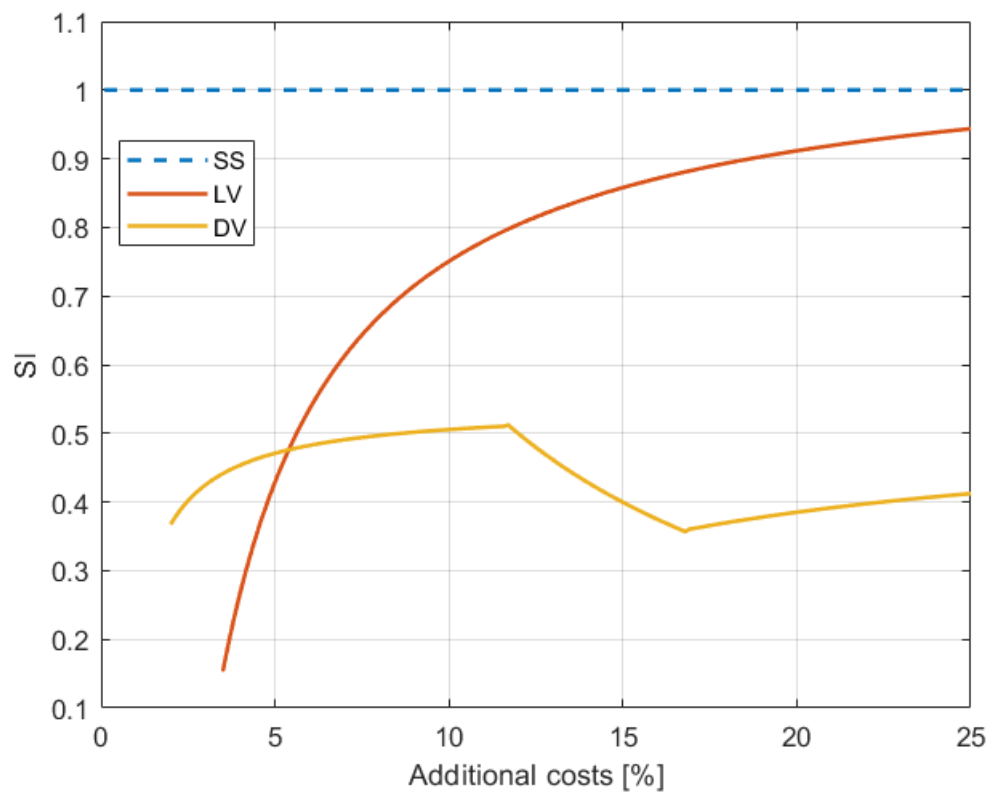


Fig. 8.12: Combined switchability and economic assessment chart

employed. This index indeed assesses the property of the system to withstand an F_{SG} deviation of all variables at the same time, i.e. it is very conservative. From a quantitative point of view, with flexibility indexes assessing less constraining properties more relaxed solutions would have been obtained.

Finally it is worth remarking that, in order to have flexible units, not only higher investments are required but they have to be exactly distributed according to the results obtained in the design phase as well. Otherwise, some units would be more constraining than others that, on the contrary, have been oversized in vain.

5 Conclusions

The first goal of this study is to emphasize the importance of the flexibility assessment integration during the design phase when process variables are likely to undergo external disturbances. In all these cases, the impact of process dynamics should be properly evaluated and, if transitions cannot be neglected, the conventional steady state flexibility analysis should be replaced by a dynamics based one.

A new switchability index SI has then been defined to quantify the impact of process dynamics from a flexibility point of view. As for the dynamic index, the switchability one resulted to be strictly related to the control loop as well. This correlation nevertheless allows the employment of this index for important comparisons between different design alternatives.

In particular, in this research work, three different classes of comparison are carried out from a switchability perspective, namely:

- Different control strategies: PID and MPC;
- Different tuning methods: Ziegler-Nichols and Tyreus-Luyben;
- Different PID control structures: LV and DV.

In the first case, the optimal control strategy showed a higher switchability index with respect to the classical PID feedback control one as expected. However, PID feedback controllers are still the most spread control tools in industrial applications and they are worth to be more deeply studied.

The two tuning methodologies exhibit slightly different trends with a relatively appreciable overshoot in both cases. The Tyreus-Luyben method results to better perform for the particular system under study. The SI index of the PID control structure approaches the value 1 for high flexibility requirement due to the sluggish system response and thus the absence of overshoot. The cost of the dynamically flexible design is paid then by the longer time required to suppress the perturbation, i.e. a higher productivity loss.

After that, two different control structures were analyzed on the same distillation column case study with interesting outcome. Although both of them resulted in relevant oversizing when accounting for dynamics, their additional costs vs flexibility trends have different slopes and cross each other. The flexible design with a DV control structure is indeed less profitable for higher flexibility requirement than LV and vice versa. The comparison between the two configurations could be easily performed by means of the newly defined switchability index SI .

Moreover, this case study highlights that neglecting process dynamics and control would have led to an overestimation of the feasible region with a standard distillation column. A two-diameter column is indeed required for $DF_{DV} = 8.2\%$ and $DF_{LV} = 15\%$ while the steady state value is about $F_{SG} = 20\%$.

In conclusion, dynamics resulted rarely negligible in all the case studies discussed in this paper. In particular, the importance of process dynamics from a flexibility point of view can be evaluated by means of the proposed switchability index that summarizes both the comparison between steady state and dynamic flexibility and the comparison between different control philosophies.

From a graphical point of view, two original switchability based plots, namely “switchability vs oversizing/additional costs” and “switchability vs flexibility”, have been proposed as a new tool to monitor and to have a more immediate insight about the switchability behaviour over different flexibility and cost ranges.

In addition, the results of this switchability assessment could be also further exploited to optimize different startup and (emergency) shutdown procedures and to compare different control configurations during unsteady state process operations.

A List of acronyms and symbols

Symbol	Definition	Unit
A	Characteristic dimension	m^n
A	Heat transfer surface area	m^2
C_i	i-th species concentration	mol/m^3
C_{BM}	Equipment bare module cost	\$
$c_{P,i}$	i-th species specific heat capacity	$J/kg/K$
C_p^0	Purchase equipment cost in base conditions	\$
$CAPEX$	CAPital EXPenses	$\$/y$
d	Design variable	Variable
D_r	Reactor diameter	m
DF	Dynamic Flexibility index	1
DV	Distillate-boilup control structure	/
e_i	Error of the i-th variable	mol/m^3 or m
E_{att}	Activation energy	J/mol
f	Constraint function	Function
F	Generic flexibility index	1
F_{BM}	Bare module factor	1
F_i	i-th flowrate	mol/s
F_M	Material factor	1
F_P	Pressure factor	1
F_q	Column trays factor	1
F_{SG}	Swaney and Grossmann flexibility index	1
G_f	Flooding velocity	m/s
G_w	Weeping velocity	m/s
HC	Control Horizon	s
HP	Prediction Horizon	s
ΔH_r	Reaction enthalpy	J/mol
IAE	Integral Absolute Error	Acronym
ISE	Integral Square Error	Acronym
$ITAE$	Integral Time Absolute Error	Acronym

Symbol	Definition	Unit
K	Proportional gain	$(kg \cdot L)/(h \cdot mol)$
k_0	Pre-exponential factor	$1/h$
L	Level	m
LV	Reflux-boilup control structure	/
$M\&S$	Marshall & Swift cost index	1
N	Number of stages	1
$OPEX$	OPERating EXpenses	$\$/y$
P	Pressure	bar
R_5^B	n-Pentane recovery ratio in the bottom	mol/mol
R^2	Coefficient of determination	1
SI	Switchability Index	1
t_i	Time at the i-th operating condition	s
T	Temperature	K
T_w	Cooling water temperature	$^\circ C$
U	Heat transfer coefficient	$W/(m^2 \cdot K)$
U_{cond}	Condenser heat transfer coefficient	$W/(m^2 \cdot K)$
U_{reb}	Reboiler heat transfer coefficient	$W/(m^2 \cdot K)$
V	Volume	m^3
x	Process variable	Variable
x_4^B	n-Butane molar fraction in the bottom	mol/mol
Z	Control domain	Function
z	Control variable	Variable
δ	Flexibility scale factor	1
Θ	Hyperrectangle	Function
θ_i	Uncertain parameters at the i-th operating condition	1
ρ_i	i-th species density	kg/m^3
τ	CSTR residence time	h
$\tau_{u,I,D}$	Ultimate/Integral/Derivative time	h
ω_i	Objective function i-th weight	1

Equipment	Typology	K_1	K_2	K_3	A
Heat exchanger	Fixed tubes	4.3247	-0.3030	0.1634	Heat transfer area [m^2]
	Kettle	4.4646	-0.5277	0.3955	Heat transfer area [m^2]
Columns (vessel)	Packed/tray	3.4974	0.4485	0.1074	Volume [m^3]
Trays	Sieved	2.9949	0.4465	0.3961	Cross sectional area [m^2]

Tab. 8.6: Equipment cost in base conditions parameters

B Capital costs estimations

In order to evaluate the investment required to build up a process plant or for whatever economic analysis and comparison related to process equipment, the cost of every single unit needs to be estimated.

For this purpose the Guthrie-Ulrich-Navarrete correlations described in the following paragraphs have been employed [46, 47, 48, 49].

B.1 Purchase equipment cost in base conditions

The purchase equipment cost in base conditions is obtained by means of the following equation:

$$\log_{10}(C_P^0[\$]) = K_1 + K_2 \cdot \log_{10}(A) + K_3 \cdot [\log_{10}(A)]^2 \quad (\text{B.1})$$

where A is the unit characteristic dimension and the K_i coefficients are relative to the equipment typology (cf. Table 8.6).

The provided coefficients refer to a Marshall & Swift equipment cost index equal to 1110. In order to update the cost estimations, a M&S index equal to 1638.2 will be used in order to refer the calculations to the year 2018 by means of the correlation:

$$C_{P,2}^0 = \frac{M\&S_2}{M\&S_1} \cdot C_{P,1}^0 \quad (\text{B.2})$$

B.2 Bare module cost

The equipment bare module cost can be calculated according to the following correlation:

$$C_{BM} = C_P^0 \cdot F_{BM} \quad (\text{B.3})$$

Equipment	Typology	B_1	B_2	F_M	F_P
Heat exchanger	Fixed tubes	1.63	1.66	1	1
	Kettle	1.63	1.66	1	$F_{P,Kettle}$
Columns/vessel	/	2.25	1.82	1	1
Pumps	Centrifugal	1.89	1.35	1.5	1

Tab. 8.7: Bare module parameters

where the bare module factor is given by:

$$F_{BM} = B_1 + B_2 \cdot F_M \cdot F_P \quad (\text{B.4})$$

The F_M and F_P factors refers to the actual constructions materials and operating pressure while the B_i coefficients refers to the equipment typology (cf. Table 8.7).

The $F_{P,Kettle}$ value is given by:

$$\log_{10}(F_P) = 0.03881 - 0.11272 \cdot \log_{10}(P) + 0.08183 \cdot [\log_{10}(P)]^2 \quad (\text{B.5})$$

where P is the relative pressure in *bar*.

For column trays bare module cost a slightly different correlation should be used:

$$C_{BM} = N \cdot C_P^0 \cdot F'_{BM} \cdot F_q \quad (\text{B.6})$$

where N is the real trays number, $F_{BM} = 1$ e F_q is given by:

$$\begin{cases} \log_{10}(F_q) = 0.4771 + 0.08561 \cdot \log_{10}(N) - 0.3473 \cdot [\log_{10}(N)]^2 & \text{if } N < 20 \\ F_q = 1 & \text{if } N \geq 20 \end{cases} \quad (\text{B.7})$$

References

- [1] Hoch, P.M., Eliceche, A.M., Grossmann, I.E., 1995. Evaluation of Design Flexibility in Distillation-Columns Using Rigorous Models. *Comput. Chem. Eng.* 19, S669–S674. [https://doi.org/10.1016/0098-1354\(95\)00137-Q](https://doi.org/10.1016/0098-1354(95)00137-Q)
- [2] Di Pretoro, A., Montastruc, L., Manenti, F., Joulia, X., 2019. Flexibility analysis of a distillation column: Indexes comparison and economic assessment. *Computers & Chemical Engineering* 124, 93–108. <https://doi.org/10.1016/j.compchemeng.2019.02.004>
- [3] Sudhoff, D., Leimbrink, M., Schleinitz, M., Górak, A., Lutze, P., 2015. Modelling, design and flexibility analysis of rotating packed beds for distillation. *Chemical Engineering Research and Design* 94, 72–89. <https://doi.org/10.1016/j.cherd.2014.11.015>
- [4] Adams II, T.A., Thatho, T., Le Feuvre, M.C., Swartz, C.L.E., 2018. The Optimal Design of a Distillation System for the Flexible Polygeneration of Dimethyl Ether and Methanol Under Uncertainty. *Front. Energy Res.* 6. <https://doi.org/10.3389/fenrg.2018.00041>
- [5] Saleh, J.H., Hastings, D.E., Newman, D.J., 2003. Flexibility in system design and implications for aerospace systems. *Acta Astronautica* 53, 927–944. [https://doi.org/10.1016/S0094-5765\(02\)00241-2](https://doi.org/10.1016/S0094-5765(02)00241-2)
- [6] Hoch, P.M., Eliceche, A.M., 1996. Flexibility analysis leads to a sizing strategy in distillation columns. *Comput. Chem. Eng.* 20, S139–S144. [https://doi.org/10.1016/0098-1354\(96\)00034-8](https://doi.org/10.1016/0098-1354(96)00034-8)
- [7] Di Pretoro, A., Montastruc, L., Manenti, F., Joulia, X., 2020. Optimal Design and Environmental Impact Assessment of Flexible Multistage Operations under Uncertain Conditions. *Ind. Eng. Chem. Res.*, UNDER REVIEW.
- [8] Stephanopoulos, G., 1983. *Chemical Process Control: An Introduction to Theory and Practice*, 1st edition. ed. Pearson College Div, Englewood Cliffs, N.J.
- [9] Luyben, M.L., Luyben, W.L., 1996. *Essentials of Process Control*. McGraw-Hill College, New York.
- [10] Seborg, D.E., Mellichamp, D.A., Edgar, T.F., III, F.J.D., 2010. *Process Dynamics and Control*, 3 edition. ed. Wiley, Hoboken, N.J.
- [11] O'Dwyer, A., 2009. *Handbook of PI and PID Controller Tuning Rules*, 3rd ed. edition. ed. Imperial College, London : Hackensack, NJ.

- [12] Howell, J.M., (1984). The effect of energy integration on the switchability of chemical processes. PhD thesis, University of London
- [13] Patil, B.P., Maia, E., Ricardez-Sandoval, L.A., 2015. Integration of scheduling, design, and control of multiproduct chemical processes under uncertainty. *AIChE Journal* 61, 2456–2470. <https://doi.org/10.1002/aic.14833>
- [14] Perkins, J.D., Walsh, S.P.K., 1994. Optimization as a tool for design/control integration. *IFAC Proceedings Volumes, IFAC Workshop on Integration of Process Design and Control (IPDC'94)*, Baltimore, USA, 27-28 June 27, 1–10. [https://doi.org/10.1016/S1474-6670\(17\)47956-0](https://doi.org/10.1016/S1474-6670(17)47956-0)
- [15] White, V., Perkins, J.D., Espie, D.M., 1996. Switchability analysis. *Computers & Chemical Engineering* 20, 469–474. [https://doi.org/10.1016/0098-1354\(95\)00037-2](https://doi.org/10.1016/0098-1354(95)00037-2)
- [16] Luo, A.C.J., 2008. A theory for flow switchability in discontinuous dynamical systems. *Nonlinear Analysis: Hybrid Systems* 2, 1030–1061. <https://doi.org/10.1016/j.nahs.2008.07.003>
- [17] Morari, M.; Grimm, W.; Oglesby, M.J.; Prosser, I.D. Design of resilient processing plants—VII. Design of energy management system for unstable reactors—New insights. *Chem. Eng. Sci.* 1985, 40, 187–198.
- [18] Palazoglu, A.; Manousiouthakis, B.; Arkun, Y. Design of chemical plants with improved dynamic operability in an environment of uncertainty. *Ind. Eng. Chem. Process Des. Dev.* 1985, 24, 802–813.
- [19] Skogestad, S.; Morari, M. Design of resilient processing plants-IX. Effect of model uncertainty on dynamic resilience. *Chem. Eng. Sci.* 1987, 42, 1765–1780.
- [20] Colberg, R.D.; Morari, M.; Townsend, D.W. A Resilience target for heat exchanger network synthesis. *Comput. Chem. Eng.* 1989, 13, 821–837.
- [21] Morari, M. Design of resilient processing plants—III: A general framework for the assessment of dynamic resilience. *Chem. Eng. Sci.* 1983, 38, 1881–1891.
- [22] Burnak, B.; Diangelakis, N.A.; Pistikopoulos, E.N. Towards the Grand Unification of Process Design, Scheduling, and Control—Utopia or Reality? *Processes* 2019, 7, 461.
- [23] Sargent, R.W.H. Integrated design and optimization of processes. *Chem. Eng. Prog.* 1967, 63, 71–78.
- [24] Perkins, J.D.; Wong, M.P.F. Assessing controllability of chemical plants. *Chem. Eng. Res. Des.* 1985, 63, 358–362.

- [25] Rosenbrock, H.H. *State-Space and Multivariable Theory*; Studies in Dynamical Systems Series; Wiley Interscience Division: Hoboken, NJ, USA, 1970.
- [26] Narraway, L.T.; Perkins, J.D.; Barton, G.W. Interaction between process design and process control: Economic analysis of process dynamics. *J. Process Control* 1991, 1, 243–250.
- [27] Narraway, L.; Perkins, J. Selection of process control structure based on economics. *Comput. Chem. Eng.* 1994, 18, S511–S515, doi:10.1016/0098-1354(94)80083-9.
- [28] Walsh, S.; Perkins, J. Application of integrated process and control system design to waste water neutralisation. *Comput. Chem. Eng.* 1994, 18, S183–S187, doi:10.1016/0098-1354(94)80031-6.
- [29] Narraway, L.T.; Perkins, J.D. Selection of process control structure based on linear dynamic economics. *Ind. Eng. Chem. Res.* 1993, 32, 2681–2692.
- [30] Sakizlis, V.; Perkins, J.D.; Pistikopoulos, E.N. Parametric Controllers in Simultaneous Process and Control Design Optimization. *Ind. Eng. Chem. Res.* 2003, 42, 4545–4563.
- [31] Diangelakis, N.A.; Pistikopoulos, E.N. A multi-scale energy systems engineering approach to residential combined heat and power systems. *Comput. Chem. Eng.* 2017, 102, 128–138.
- [32] Sanchez-Sanchez, K.B.; Ricardez-Sandoval, L.A. Simultaneous Design and Control under Uncertainty Using Model Predictive Control. *Ind. Eng. Chem. Res.* 2013, 52, 4815–4833.
- [33] Swaney, R.E., Grossmann, I.E., 1985. An index for operational flexibility in chemical process design. Part I: Formulation and theory. *AIChE J.* 31, 621–630. <https://doi.org/10.1002/aic.690310412>
- [34] Saboo, A.K., Morari, M., Woodcock, D., 1985. Design of Resilient Processing Plants .8. a Resilience Index for Heat-Exchanger Networks. *Chem. Eng. Sci.* 40, 1553–1565. [https://doi.org/10.1016/0009-2509\(85\)80097-X](https://doi.org/10.1016/0009-2509(85)80097-X)
- [35] Pistikopoulos, E.N., Mazzuchi, T.A., 1990. A Novel Flexibility Analysis Approach for Processes with Stochastic Parameters. *Comput. Chem. Eng.* 14, 991–1000. [https://doi.org/10.1016/0098-1354\(90\)87055-T](https://doi.org/10.1016/0098-1354(90)87055-T)
- [36] Dimitriadis V. D., Pistikopoulos E. N., 1995, Flexibility Analysis of Dynamic Systems, *Industrial & Engineering Chemistry Research*, 34.12, 4451–62.
- [37] Di Pretoro A., Montastruc L., Joulia X., Manenti F., 2019, Dynamic Flexibility Analysis of a Distillation Column, *Chemical Engineering Transactions*, 74, 703-708. <https://doi.org/10.3303/CET1974118>

- [38] Ziegler, J.G., Nichols, N.B., 1942, Optimum Settings for Automatic Controllers, *Trans. ASME*, 64, 759.
- [39] Tyreus, B.D., Luyben, W.L., 1992. Tuning PI controllers for integrator/dead time processes. *Ind. Eng. Chem. Res.* 31, 2625–2628. <https://doi.org/10.1021/ie00011a029>
- [40] Garriga, J.L., Soroush, M., 2010. Model Predictive Control Tuning Methods: A Review. *Ind. Eng. Chem. Res.* 49, 3505–3515. <https://doi.org/10.1021/ie900323c>
- [41] Garcia, C.E., Morari, M., 1982. Internal model control. A unifying review and some new results. *Ind. Eng. Chem. Proc. Des. Dev.* 21, 308–323. <https://doi.org/10.1021/i200017a016>
- [42] Skogestad, S., Lundström, P., Jacobsen, E.W., 1990. Selecting the best distillation control configuration. *AIChE Journal* 36, 753–764. <https://doi.org/10.1002/aic.690360512>
- [43] C.J. Ryskamp. New strategy improves dual composition control. *Hydrocarbon processing*, (6), 1980.
- [44] Barolo, M., Papini, C.A., 2000. Improving dual composition control in continuous distillation by a novel column design. *AIChE Journal* 46, 146–159. <https://doi.org/10.1002/aic.690460117>
- [45] Luyben, W.L., 1992. *Practical Distillation Control*. Springer US. <https://doi.org/10.1007/978-1-4757-0277-4>
- [46] Guthrie, K.M. , 1969. Capital cost estimating. *Chem. Eng.* 76 (3), 114–142 .
- [47] Guthrie, K.M. , 1974. *Process Plant Estimating, Evaluation, and Control*. Craftsman Book Company of America .
- [48] Ulrich G. D., 1984, ‘A Guide to Chemical Engineering Process Design and Economics’, Wiley.
- [49] Navarrete P. F. and Cole W. C., 2001, ‘Planning, Estimating, and Control of Chemical Construction Projects’, 2nd Edition, CRC Press.

Part IX. Conclusions and perspectives

1 Conclusions

After the thorough discussion of all the design procedure steps announced at the beginning of this thesis, some conclusions need to be drawn in order to make a meaningful summary of the achieved goals and the remaining challenges.

The main outcome of this thesis is the definition of a new and more complete design procedure able to deal with more aspects than the usual one, with a special focus on flexibility. We can describe the various steps of the newly defined process design algorithm by the block diagram shown in Figure 9.1.

Some of those steps were already present in the conventional algorithms for process design, however they are treated from a different perspective in order to be connected to the newly added ones.

The first modifications have been applied to the feasibility assessment. In general, the feasibility analysis of a process is carried out to verify its compliance to achieve the desired output for a given set of input parameters under nominal operating conditions. In a flexible design, this study must be performed from a quantitative perspective, not only to check whether the operation is feasible or not, but also to evaluate its feasibility boundaries with respect to certain variables deviations and, when possible, to outline the entire feasible space. In any case, if the operation is not feasible under nominal operating conditions, the selected process should be reconsidered.

The new approach to the feasibility assessment via Residue Curve Mapping mainly differs from the conventional one because it includes the recovery ratio, and thus the mass balances as process specifications while the usual methodology was based on product purities. Moreover, a flexibility index have been used to characterize the feasible domain that is conventionally outlined with a geometrical visualization. This tool allows to discuss feasible spaces even for a number of components higher than four (i.e. 3D space) [1].

As regards the particular case study, the Residue Curve Mapping procedure for distillation trains and DWC was investigated and analyzed in detail.

The “design” block is the one mainly affected by the proposed modifications. The three blocks representing “profitability”, “flexibility” and “environmental impact” are all connected to it at the same time. At each step of the design phase, the economic evaluation and the environmental impact assessment are carried out. The main difference with respect to the conventional procedure is that costs and emissions are calculated for a range of operating conditions and not only with respect to the nominal ones in order to be able to perform a flexibility assessment over the entire design alternatives domain and make a more conscious design choice accounting for uncertain operating conditions. As it can be noticed, in proposed methodology, flexibility is part of the design criteria and is taken into account during the design phase itself. On the contrary, the usual sensitivity analysis performed a posteriori with respect to the process design, has as main goal just to

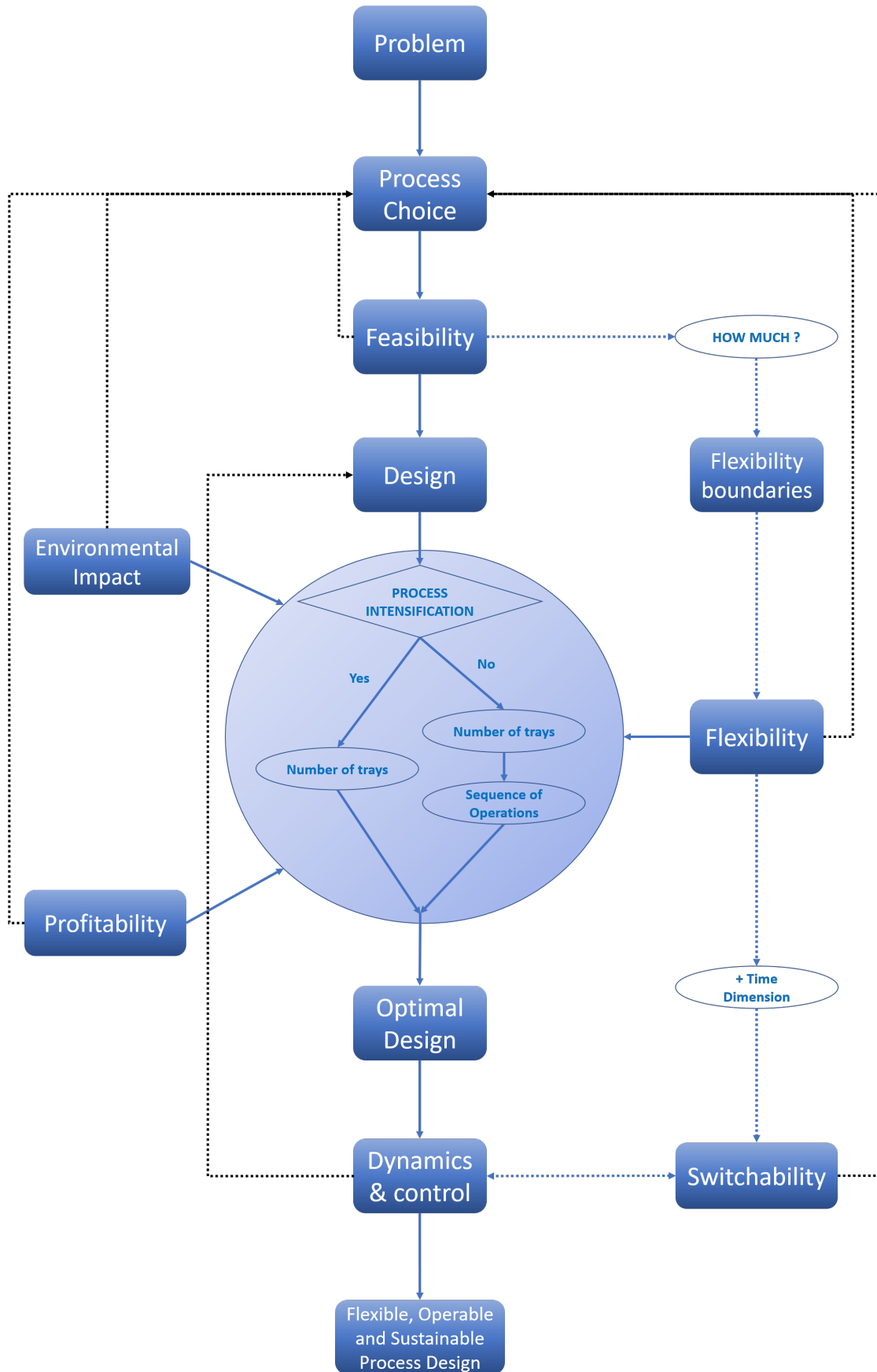


Fig. 9.1: New design procedure

test the feasibility range of a system/unit already optimized with respect to the nominal operating conditions only.

In case the requirements for one of these three aspects are not fulfilled, the selection of a different process/system aimed at solving the same problem could be considered. On the contrary, once the optimal design compromise is obtained, the multicriteria optimal design under uncertain conditions has been detected under steady state conditions.

This part of thesis work provided a literature review concerning flexibility indexes comparison that could not be found before in the scientific literature [2]. Moreover, the combined analysis of the aforementioned three aspects was proposed for the first time, resulting in the definition of an innovative graphical decisional tool allowing the decision maker to perform a more conscious design choice [3, 4].

In particular, the influence of the deviation probability distribution function on the economic and environmental aspects has been investigated in deep. This stochastic flexibility study allows to have some a priori general guidelines to define whether the external disturbances are likely to affect the optimal design or not from a flexibility perspective.

Inside the blue circle, the main features related to the specific system under analysis can be included. In this case, the selected case study being a separation process, the process intensification alternatives can be accounted for and compared to the conventional design solutions. In any case, all the steps contained in the “design” related circle, should be evaluated according to all the connected indicators, i.e. profitability, sustainability and flexibility.

The most relevant outcome of this thesis section is the definition of a rigorous procedure for the detection of the flexibility value beyond which the process intensifying solution becomes less profitable and sustainable than the conventional one.

Before the final validation, the system dynamics needs to be investigated. The flexibility assessment domain dimension increases due to the addition of the time semi-infinite axis and the switchability of the system between two transients can be analyzed according to different control configurations and strategies. This would allow to select the optimal control configuration not only on the basis of the usual indicators such as decay ratio, ISE, ITAE etc., but from a flexibility point of view as well.

In case of overshoot during the transients from one steady state to another, the process design could be reconsidered in the light of the obtained dynamic trajectories and the system/unit resized as a consequence. Moreover, in case the needed switchability could not be achieved, this could lead to a different process choice.

For this purpose, a new switchability index was conceived and its formulation defined in order to have a more suitable indicator to assess the properties discussed here above. Moreover, its application to chemical processes case studies provided

good feedbacks [5].

Once the selected process design has passed all the steps of the newly defined procedure, it can be identified as the best design compromise according to profitability, flexibility, sustainability and operability.

References

- [1] Di Pretoro, A., Montastruc, L., Manenti, F., Joulia, X., 2020a, Assessing Thermodynamic Flexibility Boundaries via Residue Curve Maps, 30th European Symposium on Computer Aided Chemical Engineering, Vol. 48
- [2] Di Pretoro, A., Montastruc, L., Manenti, F., Joulia, X., 2019a. Flexibility analysis of a distillation column: Indexes comparison and economic assessment. *Computers & Chemical Engineering* 124, 93–108. <https://doi.org/10.1016/j.compchemeng.2019.02.004>
- [3] Di Pretoro, A., Montastruc, L., Manenti, F., Joulia, X., 2019b. Flexibility Assessment of a Distillation Train: Nominal vs Perturbated Conditions Optimal Design, *Computer Aided Chemical Engineering*, 29 European Symposium on Computer Aided Process Engineering. Elsevier, pp. 667–672. <https://doi.org/10.1016/B978-0-12-818634-3.50112-0>
- [4] Di Pretoro, A., Montastruc, L., Manenti, F., Joulia, X., 2020b. Flexibility assessment of a biorefinery distillation train: Optimal design under uncertain conditions. *Computers & Chemical Engineering* 138, 106831. <https://doi.org/10.1016/j.compchemeng.2020.106831>
- [5] Di Pretoro, A., Montastruc, L., Joulia, X., Manenti, F., 2019c. Dynamic Flexibility Analysis of a Distillation Column. *Chemical Engineering Transactions*, 174, 703–708. <https://doi.org/10.3303/CET1974118>

2 Perspectives

Although this research work has provided the answers to the majority of the questions discussed in the introduction, some applications could be further explored and new questions have been raised. To be more precise, they can be classified into three main categories according to the expected required time to study them in deep.

Short-term perspectives, i.e. what I would have done if I have had six months more, could concern the finalization of the dynamic flexibility section. In particular, the application of the switchability index could be implemented first on the dynamic simulation of the ABE/W indirect distillation train. The series of two columns indeed could be simulated by means of AVEVA DynSim[®] dynamic process simulator and the system response to external perturbations could be compared to those already obtained under steady state conditions. Moreover, the Dividing Wall Column dynamic simulation could be set up as well in order to compare the dynamic flexibility performances of process integrated solutions and their feasibility limitations to the conventional design layouts.

In a mid-term perspective, all the aspects of the process design procedure could be discussed from a stochastic point of view. Although aleatory uncertainty and the corresponding probability distribution functions have already been included in part of the research studies, they were indeed estimated on the basis of physical considerations or process simulation. A more accurate assessment of the perturbations likelihood could be carried out by collecting and processing data from real plants and accounting for them when outlining the feasible domain and the likelihood of each perturbed condition.

Moreover, the same procedure concerning the input variable deviations could be extended to the market demand fluctuations in order to adjust the process operating conditions to meet the desired purity or component productivity according to the needs of the process industry.

In particular, it would be really interesting to discuss how to include the stochastic flexibility in the analysis of dynamic flexibility and switchability. Indeed since several possible design configurations can satisfy a given stochastic flexibility value, an optimization is required at each flexibility analysis step. Beside the difficulties in outlining all the possible design alternatives with the same dynamic flexibility value, the computational aspects will be nonetheless very challenging.

At last, the epistemic aspects of the uncertainty characterization, defined as a source of nondeterministic behavior deriving from some level of ignorance of the system or the environment, could be included in the process design procedure in order to complete the uncertainty overview.

In conclusion, from a long-term point of view, two main goals could be achieved. First of all the indicators discussed in the thesis associated respectively to flexibility, cost estimation, environmental impact and switchability can be integrated

into a comprehensive and unified design procedure. The optimization steps related to control, environmental impact and flexibility analysis should be performed at the same time and a rigorous algorithm as well as an associated graphical tool for a most comfortable results visualization can be outlined in order provide a more reliable comprehension of the design alternatives.

After that, the best computational approach to the optimization problem could be discussed to quantify the computational effort and find solutions to decouple the different optimization levels when possible in order to speed up the procedure.

At last, the outlined procedure could be extended and generalized to all those domains close but different from the process design. Having a deeper look to the newly defined design procedure in Figure 9.1, all its steps, excepted those included in the blue circle in the middle, have a general definition and could refer to any system and application.

The different features such as feasibility, cost estimation, flexibility, sustainability and switchability and their corresponding indexes can be used indeed to optimize any process not only in the chemical or process industry.

An example could be the detailed supply chain design and management under uncertainty. While their environmental and economic assessment are already part of the conventional procedure, flexibility in the supply chain domain could provide a non-negligible improvement in the view of the current needs for a flexible market and then a flexible industry. Moreover, it would allow to take into account the influence of some global phenomena, such as pandemics or financial crises, on the market demand, production changeover and raw materials supply.

On the other hand, the same remarks can be applied to supply chains dynamics. It would be really interesting indeed to analyze the system behaviour during the transient required to switch from a given supply chain layout to a new one. This would be of critical importance in order to have a more reliable estimation of the real efforts needed to sustain a flexible solution with respect to a fixed one. Moreover, it would allow to optimize the production changeover time by means of a better analysis during the early design phase rather than with a later and usually more expensive revamping.

The supply chain example was only one of the possible domains to apply such a general procedure for a flexible, profitable, operable and sustainable design. All those tools indeed can span over a wide range of applications for a given general formulation by modifying the design subsections inside the blue circle in Figure 9.1 according to the specific system case study.

All those perspectives will be further subjects of study during the next years.

Part X. Acknowledgements

Acknowledgements

I would like to express my deepest appreciation to you first, Ludovic. More, than a supervisor, more than a teacher, more than a friend, more than I could have ever expected. I can't find a way to express how grateful I am to have met you during my academic career.

I would also like to extend my deepest gratitude to you, Flavio, who believed in me since the very first moment, although I hadn't proved myself yet, and who introduced me in the inspiring process engineering domain and community. We still have plenty to do together.

My professional growth would not have been possible without your support and dedication, Xavier. After meeting you, I know which kind of person and professor I want to be when I grow up.

I'll be always in debt with my parents, who always let me free to choose my future and without whom I wouldn't be here today. I just hope to have fulfilled expectations at least comparable with the efforts you made for me.

My deepest gratitude goes also to my grandparents, who made everything to make me achieve my goals and who had not enough time to assist to the last steps of my success, of their success.

I am also grateful to all my friends at the Laboratoire de Génie Chimique who have made me feel a part of this big family since the first day I arrived and to all those former PhD students who shared with me part of this journey.

I couldn't have achieved this goals without all my friends of the SuPER team. I've never been so happy to come to Politecnico di Milano until I met you. Spending my days in the same office with you was so amazing that I can't really call it "working".

Finally, I'd like to acknowledge all those people who took part in my life during these three years and who made it joyful in a way or another.

Progettazione Ottimale di Processi Flessibili, Operabili e Sostenibili in Condizioni Operative Incerte : Applicazione alla Bioraffineria

La procedura convenzionale per il design dei processi è ben consolidata. Tuttavia la soluzione ottenuta è ottimale unicamente rispetto alle condizioni operative nominali e non tiene in conto le perturbazioni esterne. Lo scopo di questa tesi è quindi l'integrazione della flessibilità in tutte le sue tappe. A tal proposito è stato analizzato un processo di bioraffineria per la separazione di una miscela ABE/W. Dopo una dettagliata ricerca bibliografica, indici di tipo deterministico e stocastico sono stati individuati e paragonati su un semplice caso di distillazione. Gli aspetti economici ed ambientali sono stati quindi accoppiati in una procedura unificata al fine di definire il miglior compromesso tra sovradimensionamento delle apparecchiature e fabbisogno energetico necessario per compensare i disturbi delle condizioni operative. A causa dell'elevata non idealità della miscela ABE/W, la flessibilità termodinamica è stata inizialmente valutata al fine di definire i limiti di fattibilità. Diverse configurazioni di treni di distillazione sono state progettate e confrontate tenendo conto di un'alimentazione variabile. Questi sono tuttavia considerati soluzioni superate per la separazione multicomponente. Pertanto una colonna a parete separatrice è stata progettata tramite una procedura basata su cammini fattibili. Un'analisi di flessibilità sulla DWC ottenuta ha messo in risalto i benefici e gli inconvenienti legati all'intensificazione di processo. Per avere una visione più completa, anche la dinamica di processo è stata valutata. Un nuovo indice di "switchabilità" è stato definito correlando le prestazioni in dinamico ed in stazionario dal punto di vista della flessibilità. Il risultato finale di questa tesi è quindi la definizione di un approccio multi criterio per il design delle operazioni unitarie in condizioni di incertezza e l'analisi delle criticità associate. I criteri considerati sono l'aspetto economico, la flessibilità, la controllabilità e la sostenibilità.

Parole chiave : Flessibilità, Dinamica, Ottimizzazione, Sostenibilità, Bioraffineria

Résumé

Conception Optimale de Procédés Flexibles, Opérationnels et Durables dans un Environnement Incertain: Application à la Bioraffinerie

L'optimalité de la solution de la démarche conventionnelle pour le design des procédés est uniquement associée aux conditions opératoires nominales et néglige les perturbations externes. L'objectif de cette thèse est la prise en compte de la flexibilité à chaque étape de la démarche de conception des procédés. À ce propos un cas d'étude concernant une opération de séparation ABE/W a été choisi. Après une recherche bibliographique détaillée, des indices de flexibilité déterministes et stochastiques ont été trouvés et comparés. Les aspects économique et environnemental ont été couplés dans une procédure unifiée pour évaluer le meilleur compromis entre surdimensionnement des équipements et demande d'utilités externes nécessaires pour compenser les perturbations. À cause de la non-idéalité de la mélange ABE/W, la flexibilité thermodynamique a été analysée pour définir les limites physiques du domaine faisable. Différentes configurations pour des trains de distillation ont été conçues et comparées en prenant en compte les perturbations de l'alimentation. Cependant les trains de distillation sont considérés une solution obsolète pour la purification des mélanges multi-constituant. Le design d'une colonne à paroi séparatrice (DWC) a été donc mis en place avec une méthode à chemin réalisable et une analyse de flexibilité a été réalisée pour mettre en évidence les bénéfices et les inconvénients des procédés intensifiés. Finalement, la dynamique des procédés a été aussi analysée. Un nouveau index de «switchabilité» a été défini grâce à la corrélation entre les prestations du système en régime permanent et dynamique dans un point de vue de flexibilité. Le résultat final de ce travail de thèse est donc la définition d'une approche globale pour une conception multiobjectif des opérations unitaires dans des conditions opératoires incertaines et l'analyse de criticités associées. Ces critères sont notamment analyse économique, flexibilité, contrôlabilité et durabilité.

Mots clefs : Flexibilité, Dynamique, Optimisation, Durabilité, Bioraffinerie

Abstract

Optimal Design of Flexible, Operable and Sustainable Processes under Uncertainty : Biorefinery Applications

The conventional process design procedure is a well-established standard in process engineering. However, the optimality of the solution is strictly related to nominal operating conditions and doesn't account for external perturbations. The purpose of this PhD thesis is to include flexibility in every step of this procedure. An ABE biorefinery separation case study was selected for this purpose. After a detailed literature research about flexibility, both deterministic and stochastic flexibility indexes have been found and compared on a simple distillation column case study. The economic and environmental aspects were then coupled in a unified procedure in order to assess the best compromise between units oversizing and external duty demand required to compensate operating conditions perturbations. Due to the highly non-ideal behaviour of the ABE/W mixture, the thermodynamic flexibility was assessed to outline the uncertain domain feasible boundaries. Different configurations for the corresponding distillation column train have been designed and compared accounting for feed composition uncertainty. However, distillation trains are considered an outdated solution for multicomponent mixtures purification. A Dividing Wall Column was then designed by mean of a feasible path based methodology. A flexibility assessment was performed on the DWC as well highlighting both benefits and drawbacks of the employment of a process intensifying equipment. In order to have a more complete overview, process dynamics was investigated as well. A new "switchability" index has been defined by correlating the dynamic and steady state performances under a flexibility point of view. The final outcome of this thesis work is then the definition of a comprehensive approach for multicriteria design of unit operations under uncertain conditions and the investigation of the associated criticalities. Those criteria are respectively economics, flexibility, controllability and sustainability.

Keywords : Flexibility, Dynamics, Optimization, Sustainability, Biorefinery